VNIVERSITAT DE VALÈNCIA

Doctoral Program in Physiology
Department of Physiology
Faculty of Medicine and Odontology

STUDY OF THE ROLE OF BCL-XL IN HEALTHY AGING AND FRAILTY PREVENTION

International Doctoral Thesis presented by

Aurora Román Domínguez

Supervised by

Prof. Dr. Consuelo Borrás Blasco

Dr. Cristina Mas Bargues

Prof. Dr. José Viña Ribes

Valencia, October 2022

Prof. Dra. **Consuelo Borrás Blasco**, Catedrática del Dpto. de Fisiología de la Universitat de València.

Dra. **Cristina Mas Bargues**, Profesora Ayudante Doctor del Dpto. de Fisiología de la Universitat de València.

Prof. Dr. **José Viña Ribes**, Catedrático del Dpto. de Fisiología de la Universitat de València.

CERTIFICAN:

Que la presente memoria, titulada "**Study of the role of BCL-XL in healthy aging and frailty prevention**", corresponde al trabajo realizado bajo su dirección por la doctoranda **Aurora Román Domínguez**, para su presentación como Tesis Doctoral en el Programa de Doctorado en Fisiología de la Universitat de València.

Y para que conste firman el presente certificado en Valencia, a **22 de octubre de 2022**.

CONSUELO| BORRAS| BLASCO Firmado digitalmente por CONSUELO| BORRAS|BLASCO Fecha: 2022.11.02 11:46:53 +01'00'

Fdo. Consuelo Borrás Blasco

CRISTINA| MAS| BARGUES Firmado digitalmente por CRISTINA|MAS| BARGUES Fecha: 2022.11.02 11:52:09 +01'00'

Fdo. Cristina Mas Bargues

JOSE VIÑA RIBES - NIF:19454510Y Firmado digitalmente por JOSE VIÑA RIBES - NIF:19454510Y Fecha: 2022.11.08 01:42:54 +01'00'

Fdo. José Viña Ribes

TO ALL MICE USED FOR SCIENCE

GENERAL INDEX

ACKNOWLEDGMENTS ..... **XV**

FUNDINGS ..... **XXI**

PERSONAL FUNDINGS ..... **XXIII**

PROJECT FUNDINGS ..... **XXIV**

ABSTRACT ..... **XXV**

RESUMEN ..... **XLIX**

I. INTRODUCTION **1**

1. THE AGING PROCESS **1**
1.1. Definition of aging 1
1.2. Theories of aging 1
1.2.1. Longevity genes theory of aging 2
1.2.2. Immunological theory of aging 3
1.2.3. Rate-of-living theory of aging 5
1.2.4. Free radicals and the mitochondrial theory of aging 6
1.3. The aging phenotype 7
1.3.1. Poor physical health status 9
1.3.1.1. Decreased physical activity 9
1.3.1.2. Physical performance decline 10
1.3.1.3. Frailty 11
1.3.2. Metabolic deregulation 13
1.3.2.1. Changes in body composition 13
1.3.2.2. Impaired respiratory metabolism 14
1.3.2.3. Glucose intolerance 15
1.3.3. Compromised cellular function 15
1.3.3.1. Impaired response to stress 15
1.3.3.1.1. Autophagy 17
1.3.3.1.2. Senescence 18
1.3.3.1.3. Apoptosis 19
1.3.3.2. Mitochondrial dysfunction 20

2. THE BCL-XL PROTEIN 21
2.1. BCL-XL encoding gene 21
2.2. BCL-XL structure and location 22
2.3. BCL-XL protein functions 24
2.3.1. BCL-XL in apoptosis 24
2.3.2. BCL-XL in autophagy 26
2.3.3. BCL-XL in senescence 27
2.3.4. BCL-XL in mitochondrial function 29

3. INTERVENTIONS TO PROMOTE HEALTHY AGING: THE ROLE OF BCL-XL 32
3.1. Normal aging *versus* healthy aging 32
3.2. The importance of promoting healthy aging 32
3.3. Centenarians as models of healthy aging 33
3.4. BCL-XL's role in healthy aging 35

II. HYPOTHESIS AND AIMS 39

1. HYPOTHESIS 41

2. AIMS 41

III. MATERIAL AND METHODS 43

1. EXPERIMENTAL ANIMALS 45
1.1. Colony formation and housing conditions 45
1.2. Mice sacrifice and sample collection 46

2. MATERIAL 47
2.1. Equipment 47
2.2. Reagents 49
2.3. Additional supplies 52

3. METHODS 54
3.1. Experimental design 54
3.2. *In vivo* assays 55
3.2.1. Bodyweight 55
3.2.2. Grip strength test 56
3.2.3. Rotarod test 58
3.2.4. Treadmill incremental test 60
3.2.5. Assessment of frailty 62
3.2.6. Metabolic monitoring 63

3.2.6.1. Respiratory metabolism 64
3.2.6.2. Spontaneous locomotor activity 65
3.2.6.3. Intake 65
3.2.7. Body composition 65
3.2.8. Glucose tolerance test 66
3.3. *Ex vivo* assays 67
3.3.1. Mice genotype determination 67
3.3.2. BCL-XL expression levels 69
3.3.2.1. Organ homogenization 69
3.3.2.2. Protein quantification by Lowry-Folin 70
3.3.2.3. Western blot 72
3.3.3. T cell isolation and cell count 75
3.4. *In vitro* assays 78
3.4.1. T cell culture 78
3.4.2. Flow cytometry 78
3.4.2.1. T cell purity 80
3.4.2.2. Apoptosis 80
3.4.2.3. Senescence 82
3.4.2.4. Autophagy 83
3.4.2.5. Mitochondrial membrane potential and ROS 85
3.4.3. Seahorse 86
3.5. Data analysis 91
3.5.1. Software and programming language 91
3.5.2. Packages and functions 91
3.5.3. Outliers 92
3.5.4. Normality 92
3.5.5. Homoscedasticity 93
3.5.6. Statistical tests 93

IV. RESULTS 95

1. CHARACTERIZATION OF EXPERIMENTAL ANIMALS 97
1.1. Human BCL-XL transgene is present in Lck^{pr}-Bcl-X_L mice but not in B6 mice 97
1.2. BCL-XL protein is overexpressed in thymus, spleen, and splenic T cells from Lck^{pr}-Bcl-X_L mice 98

2. PHYSICAL HEALTH STATUS 100
2.1. Age-related performance decline is attenuated in Lck^{pr}-Bcl-X_L mice compared to B6 mice 100
2.1.1. Body weight gain 100
2.1.2. Grip strength loss 102

2.1.3. Motor coordination loss 103
2.1.4. Exercise endurance loss 104
2.2. Spontaneous activity is slightly increased in Lck^{pr}-Bcl-X$_L$ mice compared to B6 mice 105
2.2.1. Activity 105
2.2.2. Rearing 107
2.3. Frailty is prevented in aged Lck^{pr}-Bcl-X$_L$ mice compared to B6 mice 109
2.3.1. Prevalence of frailty 109
2.3.2. Valencia Frailty Score 111

3. METABOLISM-RELATED PARAMETERS 113
3.1. Body composition is maintained with the age in Lck^{pr}-Bcl-X$_L$ mice but not in B6 mice 113
3.1.1. Total body mass 114
3.1.2. Lean mass 115
3.1.3. Fat content 116
3.2. Energy metabolism referred as intake, RQ and EE is similar in B6 and Lck^{pr}-Bcl-X$_L$ mice 117
3.2.1. Intake 117
3.2.2. Respiratory quotient 118
3.2.3. Energy expenditure 120
3.3. Glucose tolerance is improved in aged Lck^{pr}-Bcl-X$_L$ mice compared to B6 mice 122

4. T CELL FUNCTION 124
4.1. Characterization of B6 and Lck^{pr}-Bcl-X$_L$ mice-derived T cells isolated from spleen 124
4.1.1. T cell purity, size, and shape 124
4.1.2. T cell number 126
4.2. Cell survival mechanisms are enhanced in Lck^{pr}-Bcl-X$_L$ mice-derived T cells under stressful conditions 128
4.2.1. Apoptosis 129
4.2.1.1. Apoptosis under physiological conditions 129
4.2.1.2. Apoptosis under stressful conditions 130
4.2.2. Autophagic response to starvation 132
4.2.3. Cellular senescence 133
4.3. Mitochondrial respiration efficiency is improved in Lck^{pr}-Bcl-X$_L$ mice-derived T cells 135
4.3.1. Basal respiration 136
4.3.2. Non-mitochondrial oxygen consumption 138
4.3.3. Proton leak 139

V. DISCUSSION 141

1. PHYSICAL HEALTH STATUS 143
1.1. Physical decline during aging: Lck^{pr}-Bcl-X$_L$ mice have an attenuated physical decline compared to B6 mice 143
1.1.1. Body weight gain is attenuated in Lck^{pr}-Bcl-X$_L$ mice at 8-11 and 17-20 months of age 143
1.1.2. Grip strength loss is attenuated in Lck^{pr}-Bcl-X$_L$ mice at 8-11 months of age with no differences in lean mass 144
1.1.3. Motor coordination loss is attenuated in Lck^{pr}-Bcl-X$_L$ mice at 8-11 and 17-20 months of age 145
1.1.4. Exercise endurance loss is attenuated in Lck^{pr}-Bcl-X$_L$ mice at 8-11 months of age 146
1.2. Spontaneous activity: Lck^{pr}-Bcl-X$_L$ mice exhibit increased rearing behaviour compared to B6 mice 147
1.3. Frailty: Lck^{pr}-Bcl-X$_L$ mice prevent frailty at very old ages in comparison to B6 mice 148

2. METABOLISM-RELATED PARAMETERS 148
2.1. Body composition: Lck^{pr}-Bcl-X$_L$ mice preserve a youthful body composition during aging 149
2.2. Energy metabolism: Lck^{pr}-Bcl-X$_L$ mice do not show differences in intake, RQ or EE compared to B6 mice 149
2.3. Glucose tolerance: Lck^{pr}-Bcl-X$_L$ mice prevent age-related glucose tolerance impairment 150

3. T CELL CHARACTERIZATION 152
3.1. Lymphocyte count: Lck^{pr}-Bcl-X$_L$ mice-derived splenic T cells are higher in number, with no differences in the total amount of splenic white cells 152
3.2. Cell survival pathways: Lck^{pr}-Bcl-X$_L$ mice-derived T cells exhibit improved cell survival and stress response 153
3.2.1. Apoptosis is differently modulated in Lck^{pr}-Bcl-X$_L$ mice-derived T cells in physiological and stressful conditions 154
3.2.2. Autophagic response to starvation is enhanced in Lck^{pr}-Bcl-X$_L$ mice-derived T cells 155
3.2.3. Senescence is not altered in Lck^{pr}-Bcl-X$_L$ mice 156
3.3. Mitochondrial function: Lck^{pr}-Bcl-X$_L$ mice-derived T cells have reduced mitochondrial respiration levels and improved proton leak 158

4. GENERAL PERSPECTIVE: BCL-XL AS A GENE IMPLICATED IN HEALTHY AGING 160

5. STUDY LIMITATIONS....163

VI. CONCLUSIONS....165

REFERENCES....169

ANNEXES....223

1. ANNEX I: ETHICAL COMMITTEES....225
1.1. Authorization for the creation and maintenance of the colony....225
1.2. Authorization for animal experimentation....226

2. ANNEX II: SUPPLEMENTARY DATA....227

ABBREVIATIONS AND SYMBOLS

Abbreviation	Definition
ACTB	Beta-actin
ANOVA	Analysis of variance
APS	Ammonium persulfate
ARDs	Age-related diseases
AUC	Area under the curve
B6	C57bl/6j
BB	Binding buffer
BCL2L1	BCL-2-Like protein 1
BCL-XL	B-cell lymphoma-extra large
BH	Bcl-2 homology
BSA	Bovine serum albumin
CD3	Cluster of differentiation 3
CTL	Control
DXA	Dual Energy X-ray Absorptiometry
DXM	Dexamethasone
ECAR	Extracellular acidification rate
EE	Energy expenditure
ER	Endoplasmic reticulum
ETC	Electron transport chain
FBS	Foetal bovine serum
FCCP	Carbonyl cyanide-4-(trifluoromethoxy) phenylhydrazone
FDG	Fluorescein di-β-D-galactopyranoside

GTT	Glucose tolerance test
H_2O_2	Hydrogen peroxide
HO·	Hydroxyl
IP_3R_3	Inositol 1,4,5-trisphosphate receptor
IQR	Interquartile range
LC3B	Microtubule-associated protein 1A/1B light chain 3B
Lck^{pr}	Lymphocyte protein tyrosine kinase proximal promoter
Lck^{pr}-Bcl-X_L	B6.Cg-Tg(lckprbcl2l1)12Sjk/J
MDA	Malondialdehyde
MEFs	Mouse embryo fibroblasts
MitoPY1	Mitochondria peroxy yellow 1
mo	Months old
MOMP	Mitochondrial outer membrane permeabilization
mRNAs	Messenger RNAs
mtDNA	Mitochondrial DNA
mTOR	Mammalian target of rapamycin
NAD	Nicotinamide adenine dinucleotide
NMOC	Non-mitochondrial oxygen consumption
O/N	Overnight
$\cdot O^{2-}$	Superoxide
OCR	Oxygen consumption rate
P/S	Penicillin/streptomycin
PBMCs	Peripheral blood mononuclear cells
PBS	Phosphate buffered saline
PFA	Paraformaldehyde

PH3	Phosphohistone H3
PI	Propidium iodide
PS	Phosphatidylserine
Q1	First quartile
Q3	Third quartile
RM	Recommended medium
ROS	Radical oxygen species
RQ	Respiratory quotient
RT	Room temperature
SASP	Senescence-associated secretory phenotype
SA-β-GAL	Senescence-associated β-galactosidase
SDS	Sodium dodecyl sulfate
SDS-PAGE	Sodium dodecyl sulfate-polyacrylamide gel electrophoresis
SM	Staining medium
TAE	Tris-acetate-EDTA
TCR	T cell receptors
TEMED	N,N,N′,N′-Tetramethylethylenediamine
TMRM	Tetramethylrodamine methyl ester
Tris	Trizma base
UCIM	Central Unit for Research in Medicine
Δψm	Mitochondrial membrane potential

FIGURE INDEX

I. INTRODUCTION

Figure 1. Major immunological alterations observed during immunosenescence. 5
Figure 2. Features of the aging phenotype based on this study. 8
Figure 3. A hierarchical, multiscale representation of the physiological dysregulation and likely biological drivers of physical frailty. 12
Figure 4. Mechanisms of the cellular stress response. 16
Figure 5. Mitochondrial dysfunction. 21
Figure 6. Genomic location of human BCL2L1 gene. 22
Figure 7. BCL-XL protein structure. 23
Figure 8. BCL-XL role in apoptosis. 25
Figure 9. BCL-XL role in autophagy. 27
Figure 10. BCL-XL role in apoptosis, autophagy, and senescence. 29
Figure 11. Schematic representation of ER to mitochondria Ca^{2+} regulation by Bcl-2 proteins. 31
Figure 12. Increasing healthspan to promote healthy aging. 33

III. MATERIAL AND METHODS

Figure 13. Experimental design. 55
Figure 14. Grip strength test. 57
Figure 15. Rotarod test. 59
Figure 16. Treadmill incremental test. 61
Figure 17. OxyletPro home cage. 64
Figure 18. Mice genotype determination. 69

Figure 19. Western blot procedure. 74
Figure 20. T cell isolation procedure. 77
Figure 21. Apoptosis detection by flow cytometry. 81
Figure 22. Autophagy mechanism and LC3. 83
Figure 23. Cell Mito Stress Test. 87
Figure 24. Electron transport chain modulators of the Cell Mito Stress Test 88

IV. RESULTS

Figure 25. Gel image of mice genotype. 97
Figure 26. BCL-XL expression in the thymus 98
Figure 27. BCL-XL expression in the spleen 99
Figure 28. BCL-XL expression in T cells 99
Figure 29. Body weight gain in B6 and Lck^{pr}-Bcl-X_L mice. 101
Figure 30. Grip strength loss in B6 and Lck^{pr}-Bcl-X_L mice. 102
Figure 31. Motor coordination loss in B6 and Lck^{pr}-Bcl-X_L mice 103
Figure 32. Exercise endurance loss in B6 and Lck^{pr}-Bcl-X_L mice 104
Figure 33. Spontaneous activity in 8-11 mo B6 and Lck^{pr}-Bcl-X_L mice. 106
Figure 34. Rearing events in 8-11 mo B6 and Lck^{pr}-Bcl-X_L mice. 108
Figure 35. Prevalence of frailty in 24-26 mo B6 and Lck^{pr}-Bcl-X_L mice. 111
Figure 36. Valencia frailty score in 24-26 mo B6 and Lck^{pr}-Bcl-X_L mice. 112
Figure 37. Total body mass correlation with age in B6 and Lck^{pr}-Bcl-X_L mice 114
Figure 38. Lean mass correlation with age in B6 and Lck^{pr}-Bcl-X_L mice. 115

Figure 39. Fat percentage correlation with age in B6 and Lck^{pr}-Bcl-X_L mice....116
Figure 40. Intake in 8-11 mo B6 and Lck^{pr}-Bcl-X_L mice. 118
Figure 41. The respiratory quotient in 8-11 mo B6 and Lck^{pr}-Bcl-X_L mice. 119
Figure 42. Energy expenditure in 8-11 mo B6 and Lck^{pr}-Bcl-X_L mice...121
Figure 43. Glucose tolerance test in Lck^{pr}-Bcl-X_L and B6 mice....123
Figure 44. Purity of isolated T cells from the spleen.....125
Figure 45. Shape and size of isolated T cell from the spleen....126
Figure 46. Spleen cell count from B6 and Lck^{pr}-Bcl-X_L mice. 127
Figure 47. Apoptosis in freshly isolated T cells from B6 and Lck^{pr}-Bcl-X_L mice....130
Figure 48. Apoptosis in cultured T cells from B6 and Lck^{pr}-Bcl-X_L mice. 131
Figure 49. Autophagy response in T cells from aged B6 and Lck^{pr}-Bcl-X_L mice....133
Figure 50. Senescence in T cells from B6 and Lck^{pr}-Bcl-X_L mice. 134
Figure 51. Seahorse Mito Stress Test OCR profiles in T cells.....136
Figure 52. Basal respiration in T cells from B6 and Lck^{pr}-Bcl-X_L mice. 137
Figure 53. Non-mitochondrial oxygen consumption in T cells from B6 and Lck^{pr}-Bcl-X_L mice....139
Figure 54. Proton leak in T cells from B6 and Lck^{pr}-Bcl-X_L mice.....140

V. DISCUSSION

Figure 55. BCL-XL's role in physical health, metabolism, and cellular function. 162
Figure 56. Thesis background and results summary. 163

TABLE INDEX

III. MATERIAL AND METHODS

Table 1. Frailty criteria and cut-off values..... 63
Table 2. Primers used for mice genotype determination..... 67
Table 3. Cycling procedure for DNA sequence amplification. 68
Table 4. Fluorescent markers used for flow cytometry. 79
Table 5. Compounds preparation and loading in the injection ports..... 89
Table 6. Packages used in R. 91

IV. RESULTS

Table 7. Cut-off values calculated for aged Lck^{pr}-Bcl-X_L and B6 mice. ..110

ACKNOWLEDGMENTS

Because most of the people I mention here are native Spanish speakers, please allow me to write this section in Spanish.

En primer lugar, quisiera agradecer a mis directores José Viña, Consuelo Borrás y Cristina Mas.

Al Prof. José Viña, querido Pepe, mi primer y único jefe que he tenido hasta ahora. Estoy convencida de que me encontraré a pocos tan buenos como tú. Recuerdo que al principio me atemorizaba estar en la misma sala que tú, y más aún dirigirte la palabra. Con cada reunión, eso ha cambiado, y el hecho de que me sienta cómoda y a gusto contándote mis cosas de laboratorio es la prueba de que has hecho una gran labor. Muchas gracias por tu amabilidad y dedicación.

Profa. Consuelo Borrás, Chelo, siempre me ha sorprendido tu capacidad de llevar conjuntamente una vida familiar y científica, lo cual me parece todo un desafío. Esta dualidad que admiro también se aprecia en tu manera de trabajar, que es dulce y firme al mismo tiempo. Hasta la biología nos demuestra que la clave de todo está en el equilibrio. He aprendido muchísimo estando bajo tu tutela, y por ello te doy las gracias.

Dra. Cristina Mas, Cris, desde el primer día has sido la persona que me ha educado en todo lo referente al laboratorio, estando día tras día conmigo, explicándome una y otra vez las cosas que tanto me han costado de entender. De ser una inculta aprendiz siguiéndote por los pasillos con cara de no saber dónde estoy, he pasado a ser una compañera meticulosa trabajando contigo mano a mano, y esa transición ha sido en gran parte gracias a ti y tu infinita paciencia.

En segundo lugar, quisiera agradecer al resto del equipo.

A Mar Dromant, la madre del laboratorio que, junto con Cris y Chelo, conforma la columna vertebral de nuestro mini grupo de envejecimiento. Tu experiencia y sabiduría son el mayor nutriente que tenemos los estudiantes. Incluso siendo ya seniors, seguimos buscando tu consejo. Muchas gracias por estar siempre ahí para nosotros.

A Jorge Sanz, el que me introdujo en este mundillo como hizo el cerebrito de Rick con el ignorante de Morty, con mucho humor y ganas de descubrir cosas nuevas. He disfrutado mucho de tu compañía y tu contagiable pasión por la ciencia, y por todo ello te doy las gracias.

Al resto del equipo, que siendo muchos para mencionar, todos me habéis ayudado de alguna manera a seguir caminando por esta montaña escarpada que es el doctorado. Atesoraré las divertidas conversaciones, los coros musicales y los chistes, tanto los malos como los buenos. Muchas gracias a todos por apreciarme tal y como soy, con mis rarezas y defectos.

También quisiera agradecer a las veterinarias Ana Díaz y Eva Blanch, y al resto del equipo del animalario por su magnífica labor y asesoramiento. Sin vosotros este trabajo hubiera sido imposible de realizar.

En tercer lugar, quisiera agradecer a mis amigos y seres queridos.

A mis amigos, un grupo muy variopinto de personas que ha enriquecido muchísimo mi visión del mundo. Todos habéis formado parte de esta etapa, ya sea acompañándome en mi ritual de comer ramen, formando equipo en la grieta o liándola parda en nuestras aventuras de dragones y mazmorras. Muchas gracias por los buenos momentos compartidos.

A Karina Formoso, que además de amiga también ha sido mi compañera de laboratorio durante mi estancia en el extranjero. Me has guiado tanto en lo profesional como en lo personal con honestidad, positivismo y muy buen humor. Siempre me he considerado una persona afortunada, y conocerte ha sido, sin duda, una suerte.

A Eduardo García Terrádez, Edu, mi compañero en esta gran aventura que es la vida. Durante toda esta etapa has sido mi ancla cuando mi barco se iba a la deriva. Has soportado mi mal humor y consolado mis mayores angustias en los peores momentos. Sin embargo, parece que los días buenos te han compensado los malos dado que, después de todo, aún sigues a mi lado. Gracias por hacer de mí una persona más completa y una mejor científica. Con mucho amor y cariño: gracias por todo lo dicho y por todo lo que me quedaría por decir.

Por último, quisiera agradecer a mis padres.

Charo Domínguez y Julio Román, para los que no los conozcáis. Papá, mamá, ¿qué puedo deciros? Me entran ganas de llorar de felicidad mientras escribo estas líneas. No sólo os agradezco la vida, sino también el cariño y el amor incondicional que me habéis entregado desde que era una criatura inconsciente en el útero de mamá. Haga lo que haga, siempre estáis orgullosos de mí, y por mucho que yo insista en mi mediocridad, siempre me ponéis en un pedestal. Pero qué más da si soy mediocre o excelente, ya que haceros felices es lo que me llena. Y podría enrollarme más, pero tengo que ofrecer al lector una tesis y no un texto bíblico de agradecimientos. Así que sólo me queda deciros una cosa: os quiero.

FUNDINGS

PERSONAL FUNDINGS

The investigations included in this doctoral thesis were made possible by financial contributions obtained by the doctoral student which are presented below in chronological order.

- Grant of a scholarship for the contract of staff in predoctoral training within the program I+D+i *"Subvenciones para la contratación de personal investigador de carácter predoctoral"* (Ref. ACIF/2019/164) from the *Generalitat* and the European Social Fund. This contract, assigned to the Department of Physiology of the University of Valencia, with a total duration of 3 years from 01/09/2019 to 08/31/2022.

- Grant of a scholarship for the stay of staff in predoctoral training in centers outside the Valencian Community within the program I+D+I *"Subvenciones para estancias de contratados predoctorales en centros de investigación fuera de la Comunitat Valenciana"* (Ref. BEFPI/2021/078) from the *Generalitat* and the European Social Fund. This stay with a total duration of 3 months was performed in the Institute of Metabolic and Cardiovascular Diseases (I2MC) located in Toulouse (France) from 9/8/2021 to 9/11/2021.

PROJECT FUNDINGS

The investigations included in this doctoral thesis were carried out as part of research projects which are presented below in chronological order.

- Grant for research initiatives within the program I+D+i *"Subvenciones del Programa para la promoción de la investigación científica, el desarrollo tecnológico y la innovación en la Comunitat Valenciana"* (Ref. GV/2019/092) from the Department of Education, Research, Culture and Sport. This grant was assigned to the project entitled *"Papel de Bcl-xL en el envejecimiento saludable y la prevención de la fragilidad"* with a start date on 01/01/2019 and end date on 31/12/2019.

- Grant for conducting research projects within the program *"XX Concurso Nacional para la adjudicación de Ayudas a la Investigación en Ciencias de la Vida y de la Materia"* from the *Fundación Ramón Areces*. This grant was assigned to the project entitled "Role of mitochondrial dysfunction in the energy collapse associated to aging and frailty. Basic and translational aspects" with a start date of 12/05/2021 and an end date of 12/05/2023.

ABSTRACT

STUDY OF THE ROLE OF BCL-XL IN HEALTHY AGING AND FRAILTY PREVENTION

INTRODUCTION

Aging is defined as an intrinsic, progressive, deleterious, and inevitable multifactorial phenomenon that occurs because of the gradual accumulation of damage at cellular and molecular levels. The biological process of aging is accompanied by a loss of homeostasis, which is the condition of stability required for the minimal functionality of the different systems of our body. Consequently, aging is the major risk factor for several pathologies, including cardiovascular diseases, cancer, and neurodegenerative diseases.

Many aging theories have been described to date. The longevity genes, the immunological, the rate of living, and the free radical theories of aging are among them. The longevity genes theory of aging states that aging can be controlled genetically as single genetic mutations in genes that play important roles in metabolic control and stress resistance such as mTOR. This theory is supported by the evidence of genetically mutated animal models which exhibit increased lifespans. The immunological theory places the immune system decline that occurs at advanced ages, also known as immunosenescence, as the major driver of aging, which leads to increased inflammation and vulnerability to infection. According to the rate-of-living theory of aging, lifespan is determined by oxygen consumption, being animals with a greater rate of oxygen consumption than ones with a shorter lifespan. Although this theory fails to explain the aging process in some taxa, it explains the effect of caloric restriction.

Ultimately, the free radical theory of aging postulates that highly reactive molecular species with impaired electrons accumulate in aged cells, causing cellular damage which would eventually lead to organism malfunction. Later, this theory was updated as the mitochondrial free radical theory of aging, which considers mitochondria as the main source of intracellular radical oxygen species. Thus, the accumulation of these species leads to mitochondrial DNA mutations. Nowadays, this theory is one of the most popular, although it fails to fully explain the aging process as oxidative damage is not the only type of damage that accumulates with age.

Although none of these aging theories can fully explain aging, all of them describe a possible mechanism, and more importantly, these theories are not mutually exclusive. Hence, aging could be explained by a combination of these theories, like pieces of a puzzle put together to see the big picture.

Regardless of the cause, the process of aging produces a specific phenotype that has been widely described. The most relevant hallmarks of aging include senescence, loss of proteostasis, deregulated nutrient sensing, and mitochondrial dysfunction, among others. The interaction of these changes at the cellular level results in changes at the organism level such as physical and cognitive decline, inflammation, immunodeficiency, and frailty. For this thesis, the most relevant features of the aging phenotype are 1) poor physical health, 2) metabolic deregulation, and 3) compromised cellular function. On the one hand, poor physical health in old age can be attributed to decreased physical activity and is associated with a physical performance decline and frailty. On the other hand, metabolic deregulation is accompanied by changes in body composition,

diminished energetic metabolism, and glucose intolerance. Ultimately, compromised cellular function can be caused by a poor stress response and mitochondrial dysfunction.

In the last decades, the human lifespan has increased globally across countries. However, not everyone exhibits the same aging phenotype as they get older. Indeed, the aging process occurs at a different rate at different times and in different regions. To explain this heterogeneity among the elderly population, a distinction between normal aging and healthy aging has been proposed. Healthy aging refers to elderly people with improved cognitive and physical function compared to people of the same age.

Centenarians are individuals who live extremely long lives, delaying or even escaping the onset of major age-related diseases, including cancer and cardiovascular diseases. When compared to their contemporaries who died at younger ages, centenarians exhibit lower hospitalization rates, decreased length of stays in hospitals, and fewer comorbidities. Indeed, they maintain such remarkable health until their later years that their healthspan is comparable to their lifespan. For this reason, centenarians have been proposed as a model of healthy aging, and researchers across the globe have been testing different approaches to decipher the biology of these exceptional human beings.

Previous studies performed by our group showed that BCL-XL protein is involved in extreme longevity as it is upregulated in peripheral blood mononuclear cells from centenarians when compared to octogenarians. BCL-XL protein belongs to the BCL-2 protein family, whose members are commonly classified into three main categories: the anti-apoptotic

proteins (e.g., BCL-2, BCL-XL, BCL-W, A1, and MCL1), pro-apoptotic proteins (e.g., BAX, BAK, and BOK/MTD) and BH3-only proteins (e.g., BID, BIM/BOD, BAD, PUMA/BBC and NOXA). BCL-XL was initially reported to be in the outer mitochondrial membrane, and later on in the inner membrane too, anchored by their hydrophobic c-terminal membrane domain. BCL-XL can also be found in the endoplasmic reticulum and as a soluble form in the cytosol.

The first role described for the BCL-XL protein was the inhibition of cell death in absence of growth factors in an IL-3-dependenT cell line. BCL-XL regulates the intrinsic apoptotic pathway along with the other BCL-2 family proteins in the mitochondria. When anti-apoptotic proteins are neutralized by BH3 domain-only proteins, BAX and BAK are free to bind to the outer mitochondrial membrane where they form pores that cause permeabilization. This causes the release of apoptosis activators from the mitochondria (e.g., cytochrome c, SMAC, and DIABLO). In the cytosol, cytochrome c forms the apoptosome along with APAF-1 and caspase-9 to initiate the caspase activation cascade. BCL-XL can repress this pathway by preventing the mitochondrial outer membrane permeabilization and the subsequent release of cytochrome c into the cytoplasm, which would eventually cause apoptosis. Moreover, apoptosis inhibition by BCL-XL is not solely due to its interaction with BAX and BAK, but also to the interception of upstream pro-apoptotic signals (e.g., BH3-only proteins and P53), its interaction with several mitochondrial outer membrane permeabilization promoters (e.g., the voltage-dependent anion channels), and the prevention of pro-apoptotic Ca^{2+} cytosolic signals generation.

In addition to apoptosis, BCL-XL is also able to regulate autophagy by direct interaction with the BH3 domain of BECLIN-1, preventing the formation of the BECLIN-1-VPS34 complex, which is essential for autophagosome formation. Thus, inhibiting the process of autophagy. In this sense, BH3-only proteins (e.g., BAD) and mimetic compounds (e.g., ABT-737) have been reported to induce autophagy by disrupting the interaction between BECLIN-1 and BCL-XL competitively. BCL-XL could also inhibit PINK1/PARKIN-dependent mitophagy by preventing the translocation of Parkin from the cytoplasm into mitochondria. Thus, BCL-XL is an important intermediary between autophagy and apoptosis, where both pathways converge.

In response to aggressive stimuli such as UV radiation, cells activate mechanisms of the stress response. Like apoptosis and autophagy, senescence is a cellular response to different stressors, and crosstalk between these three processes has been suggested by several authors. Even so, existing evidence describing BCL-XL function in cellular senescence is contradictory and not clearly understood. Given its ability to promote cell survival, BCL-XL is considered an oncogene. In this sense, several types of senescent cells exhibit high levels of BCL-XL, and the selective elimination of these cells has proven to have a wide range of beneficial effects. This is the case of senolytic drugs targeting BCL-XL and other anti-apoptotic BCL-2 family members, such as ABT-263, ABT-737, and TW-37.

In contrast, there is also evidence suggesting a protective role of BCL-XL against cellular senescence. In this regard, overexpression of BCL-XL decreases several markers of senescence, including $P16^{INK4a}$, $P19^{ARF}$,

$P21^{CIP1}$, and senescence-associated β-galactosidase activity in mouse embryo fibroblasts and primary human lymphocytes. BCL-XL has also been found to inhibit P53-induced irreversible growth arrest in human bladder cancer cells by preventing reactive oxygen species generation. Similarly, up-regulation of BCL-XL expression has been shown to reduce senescence in pancreatic neoplasia and during megakaryocyte differentiation. Thus, BCL-XL can prevent mitochondrial-dependent apoptosis, suppress BECLIN-1-dependent autophagy, and promote or suppress cellular senescence. Therefore, BCL-XL could be considered a key regulator of cellular response to stress and cell survival.

BCL-XL has been demonstrated to play a major role in other mitochondrial functions that would ultimately promote cell survival. In this regard, there is evidence suggesting that BCL-XL reduces futile ion flux across the inner mitochondrial membrane, thus, preventing a wasteful drain of cellular resources and energetic crisis during stress. Moreover, several studies indicate that BCL-XL interacts directly with the β-subunit of the F_1F_0 ATP synthase, decreasing ion leak and thereby increasing net transport of H^+ during complex V activity. However, the role of BCL-XL in aging is not fully understood and further studies are needed to determine if BCL-XL overexpression in centenarians is a consequence or a cause of the aging process in these models of healthy aging. Given the major role of BCL-XL in several functions associated with healthy aging, we set out to investigate the effect of BCL-XL overexpression during aging in a murine model.

HYPOTHESIS AND AIMS

Due to the recent discovery of BCL-XL being overexpressed in peripheral blood mononuclear cells from centenarians, a new approach has emerged to investigate the BCL-XL function in healthy aging. The BCL-XL ortholog for *Caenorhabditis elegans* Ced-9 proved its contribution to exceptional longevity by increasing the mean and maximum lifespan of this species. In *Drosophila melanogaster*, BCL-XL overexpression also increased lifespan with a complementary improvement of locomotor behaviour. Moreover, BCL-XL is known to regulate mitochondrial metabolic efficiency in neurons and improve plasticity in the brain. A protective role of BCL-XL against oxidative stress has also been described in vascular endothelial cells and fibroblasts. Additionally, BCL-XL overexpression reduces *in vitro* senescence and improves immune function in primary cells. Altogether, these data suggest a beneficial role of BCL-XL in aging. Thus, we hypothesize that transgenic mice overexpressing BCL-XL would exhibit improved health parameters, preserved mitochondrial function, and reduced frailty at advanced ages.

The major goal of this thesis is to study the role of BCL-XL in frailty and healthy aging in transgenic mice overexpressing a human form of BCL-XL in T cells. To accomplish this, we set the following specific aims: 1) To determine the effect of BCL-XL on the physical health status in terms of physical performance, spontaneous activity, and frailty in mice overexpressing BCL-XL and wild-type mice; 2) To study the effect of BCL-XL in metabolic-related parameters in terms of body composition, intake, energetic metabolism, and glucose tolerance in mice overexpressing BCL-XL and wild-type mice; 3) To characterize T cells isolated from mice

overexpressing BCL-XL and wild-type mice in terms of cell survival mechanisms, including apoptosis, senescence and autophagy, and mitochondrial function.

MATERIAL AND METHODS

In this study, heterozygous transgenic mice from Cg-Tg(LCKprBCL2L1)12Sjk/J strain purchased from The Jackson Laboratory were used. These transgenic mice express the human *BCL-XL* cDNA sequence under the control of a mouse lymphocyte protein tyrosine kinase proximal promoter, which drives BCL-XL expression in all thymocyte subsets.

To establish the colony, transgenic mice were bred with C57BL/6J inbred mice. We used C57BL/6J as a wild-type or control for our experiments. Mice were housed in the animal center of the Central Unit for Research in Medicine of the Faculty of Medicine and Odontology of the University of Valencia. Animals were kept in the facility at 22 ± 2˚C, with a relative humidity of 60% under 12-12h of dark-light cycles and with access to food and water *ad libitum*.

We defined four age groups to study the effect of BCL-XL overexpression in mice during aging, considering 2-5-month-old mice as young, 8-11 as adults, 17-20 as old, and 24-26-month-old mice as very old. First, we followed up an initial cohort of 144 transgenic and wild-type mice, with females and males in similar proportions.

When mice reached each age group respectively, physical performance assays were performed. Frailty was determined only at advanced ages, in 17-20 and 24-26-month-old mice. In parallel, approximately 36 animals were sacrificed in each age group for T isolation to determine T cell number and function. Finally, body composition, metabolic monitoring, and glucose tolerance test were performed cross-sectionally in young adult and old adult mice. More specifically, 8-11 and 17-20-month-old mice were used for metabolic monitoring, whereas the glucose tolerance test was performed in mice from 6 up to 23 months of age.

In vivo, we measured body weight with a precision balance, grip strength with a dynamometer, motor coordination as latency time to fall from a rotating rod using a rotarod apparatus, and physical endurance with the treadmill by forcing animals to run until exhaustion. Then, we determined body weight gain, grip strength loss, motor coordination loss, and physical endurance loss for each mouse individually at each age group. To assess frailty, we used the criteria of body weight, grip strength, motor coordination, and physical endurance following cut-off values of upper 20% for body weight and the lowest 20% for the other frailty criteria. Respiratory metabolism (i.e., respiratory quotient and energy expenditure), spontaneous locomotor activity, and intake were monitored for approximately 45 hours using metabolic cages. For the duration of the experiment, the 12 hours light-dark cycle was maintained to ensure a normal circadian rhythm. Body composition in terms of total mass, fat mass, and lean mass were evaluated using dual-energy x-ray absorptiometry. Finally, the glucose tolerance test was performed in 12 hours fasted mice following an intraperitoneal injection of 2g/kg glucose.

In ex vivo, we determined mice genotype and BCL-XL protein expression levels. Mice genotype was assessed by tissue digestion, control and transgene sequence amplification, electrophoresis, and gel visualization. BCL-XL expression was assessed by western blot in homogenized organs and isolated splenic T cells. Additionally, we counted the number of white splenic cells, and T cells isolated from the spleen.

In vitro, we measured T cell purity, cellular senescence, apoptosis, autophagy, cell death, and mitochondrial membrane potential by flow cytometry. When required, cells were cultured in RPMI 1640 medium supplemented with glutamine, 1% penicillin-streptomycin, and 10% foetal bovine serum, in a heat gas incubator at 5% CO_2. The markers used were cluster of differentiation 3 for T cell purity, microtubule-associated protein 1A/1B light chain 3B for autophagic activity, β-galactosidase activity for cellular senescence, Annexin V for apoptosis, propidium iodide for cell death and tetramethylrhodamine methyl ester for mitochondrial membrane potential. Additionally, mitochondrial respiration in isolated T cells was assessed by an extracellular flux analyser.

Data analysis was performed with RStudio, a free software environment for R, which is a programming language for statistical computing and graphics. For numerical variables, we first identified outliers for each variable in our sample. Then, we assessed normality and homoscedasticity. Depending on the variable type (numerical or categorical) and whether the data meet the assumptions of the parametric tests, we performed different statistical tests.

RESULTS

For easier comprehension, we divided our results into three main sections in association with the three main features of the aging phenotype previously described. These sections are 1) physical health status, 2) metabolism-related parameters, and 3) T cell characterization. First, BCL-XL overexpression was confirmed in the thymus, spleen, and T cells from transgenic animals by western blot. To evaluate overall physical health, we determined physical performance decline with age, spontaneous locomotor activity, and frailty in transgenic and wild-type mice. To evaluate metabolism-related parameters, we also determined body composition, respiratory metabolism, and glucose tolerance. Finally, T cell characterization was assessed by T cell count, T cell survival mechanisms, and mitochondrial function.

In the study of physical health status, transgenic mice overexpressing BCL-XL exhibited a significant reduction of body weight gain and motor coordination loss at 8-11 and 17-20 months of age compared to wild-type mice. Similarly, grip strength loss and exercise endurance loss in transgenic mice were diminished at 8-11 months of age. Additionally, the frequency of rearing events was higher during the dark cycle in 8-11-month-old transgenic mice compared to wild-type, but no statistical differences were found in 17-20-month-old mice nor spontaneous ambulatory activity levels. Moreover, the proportion of animals identified as frail according to the number of criteria met was almost doubled in wild-type mice (11.59 %) compared to transgenic mice (6.12 %) at 17-20 months of age, but these differences were not statistically significant. At 24-26 months of age, 2 out of 17 wild-type mice were classified as frail,

whereas none of the transgenic mice were frail, and only one transgenic mouse was pre-frail compared to 6 pre-frail wild-type mice. Consequently, the prevalence of frailty was significantly reduced in 24-26-month-old transgenic mice. Similarly, the Valencia Frailty Score was lower in these mice compared to the wild-type, although no statistical differences were found at 17-20 months of age. Taken together, transgenic mice exhibit attenuated physical performance decline and improved activity which translates to reduced frailty at more advanced ages. Hence, our findings suggest that transgenic mice have a better physical health status during aging compared to wild-type mice.

In the study of metabolism-related parameters, mice's total body mass and body fat percentage were positively correlated with age in wild-type mice but not in transgenic mice. Thus, the gain of body weight with age in wild-type mice could be attributed to an increase in fat content. However, no differences in intake were observed between strains, indicating that these differences in body size and fat content may not be related to differences in food consumption. Moreover, no differences in respiratory quotient or energy expenditure were observed between wild-type and transgenic mice at 8-11 and 17-20 months of age that could further explain these differences. In addition, when measuring non-fat mass, no correlation was observed between lean mass and age as it remained relatively uniform across the different ages in both strains. Thus, suggesting that the age-related grip strength loss may not be caused by a loss of muscle mass.

Furthermore, glycemia profiles from 15-23-month-old wild-type mice exhibited increased glucose levels during the glucose tolerance test,

whereas transgenic mice of similar age showed similar profiles to those of young mice at 6-14 months of age. These differences were confirmed whit the area under curve analysis, showing a statistical reduction of glucose intolerance in 15-23-month-old transgenic mice. Hence, BCL-XL overexpression prevents glucose tolerance impairment associated with aging.

In the study of T cell characterization, the total number of splenic white cells obtained from wild-type and transgenic mice were similar, between 50 and 150 million cells. However, the number of splenic T cells obtained from transgenic mice was significantly higher at 2-5, 8-11, and 17-20 months of age compared to the number of T cells obtained from wild-type mice. Interestingly, no significant differences were found in older mice. Altogether, BCL-XL overexpression increases the splenic T cell population without altering the total number of white cells, and these differences fade with increasing age.

When analysing the cellular stress response, no differences in cellular senescence were found in T cells, but an increased autophagic response to starvation was observed in old transgenic mice-derived T cells compared to wild-type-derived T cells. Regarding programmed cell death, apoptosis was increased in transgenic mice-derived T cells at 17-20 months of age under physiological conditions (freshly isolated cells). These results indicate that BCL-XL is not acting as an anti-apoptotic protein under these conditions, but rather as a pro-apoptotic one. On the contrary, apoptosis was reduced in transgenic mice-derived T cells at 2-5 and 8-11 months of age under more hostile conditions (cultured cells), both in the absence and in presence of the apoptotic inducer

dexamethasone. These results indicate that the anti-apoptotic function of BCL-XL is induced in response to stress.

When evaluating the mitochondrial function of these T cells, we observed a significant reduction of oxygen consumption rate and proton leak under basal conditions in 2-5 and 8-11-month-old transgenic mice-derived T cells compared to wild-type mice-derived T cells. Curiously, as we previously observed when measuring apoptosis, these differences decay with age as no effect was observed at 17-20 months of age. Additionally, no differences were observed in ATP-linked respiration, maximal respiration, and spare respiratory capacity. Taken together, our data suggest that BCL-XL could be enhancing oxidative phosphorylation efficiency in transgenic mice-derived T cells by maintaining the same metabolic demands with lower oxygen consumption, and consequently minimizing both proton leak and oxygen reactive species production.

DISCUSSION

The decline in physical function is associated with increased susceptibility to several age-related diseases (e.g., cardiovascular disease, hypertension, type 2 diabetes, and stroke) and reduced longevity in both rodents and humans. In rodents, body weight normally increases with age. We found that body weight gain was significantly lower in 8-11 and 17-20 months old transgenic mice compared to wild-type, but no differences were found at older ages. Given that BCL-XL seems to be strongly linked to longevity, and that reduced body weight in mice is associated with increased lifespans, we considered that the prevention of

body weight gain in transgenic mice in the middle ages is a desirable trait during aging. Grip strength is also reported to decrease in C57BL/6 old mice compared to young mice. In this thesis, we found that grip strength loss was also attenuated in 8-11 months old transgenic mice compared to wild-type, but again, no differences were found at older ages. Although the loss of muscle strength has been classically linked to a loss of muscle mass in both human and murine models, we did not find changes in lean mass. However, this lack of relationship between muscle strength and muscle mass has also been described by other authors.

The progressive loss of motor control also occurs at advanced ages and these changes are caused not only by a loss of muscle function but also due to a decline in cognitive and neurological systems in the elderly. When assessing motor coordination in our mice cohort, we found that age-related coordination loss is attenuated in 8-11 and 17-20-month-old transgenic mice compared to wild-type. Thus, suggesting an improved physical and cognitive function at middle-old age. Similarly, endurance capacity is known to decline over time in the elderly. In our mice, the age-associated loss of physical endurance was attenuated in 8-11-month-old transgenic mice compared to wild-type, indicating an improved resistance to extenuating exercise. Several studies have suggested a positive association between exercise endurance and immune function. Thus, given that transgenic mice overexpress BCL-XL specifically in T cells, we believe that the improved endurance observed in these mice could be attributed to an enhanced T cell function.

The lack of physical activity may account for roughly half of the physical decline associated with human aging. We observed a non-significant

increase in spontaneous activity in 8-11 and 17-20-month-old transgenic mice, being more prominent in the 8-11 age group. Rearing events were also more frequent in transgenic mice, but this increase was only statistically significant in 8-11 months old mice during the dark cycle. This increase in transgenic mice activity, albeit minor, corresponds to our findings in physical performance, all of which point towards a better physical state in these mice.

As we previously discussed, a state of reduced physical performance will almost certainly evolve into frailty, and eventually, disability. A low activity level is, indeed, one of the criteria used to assess frailty in humans along with weight loss, exhaustion, slowness, and weakness. We found a significant reduction in the prevalence of frailty and Valencia Frailty Score in the transgenic mice at 24-26 months of age. These results can be explained by the attenuated physical decline and the higher activity found in transgenic mice at earlier ages. Taken together, our findings in physical health status show that transgenic mice exhibit increased activity, general protection against physical performance decline that occurs from 2-5 up to 17-20 months of age, and consequent prevention of frailty at 24-26 months of age. Hence, transgenic mice have improved physical health status during aging, which may be attributed to an enhanced immune function, and may be related to a better cognitive function.

A poor physical health status (e.g., muscle weakness, decreased endurance capacity, and increase fatigability) is known to alter several metabolic parameters, including body composition, energy expenditure, and insulin resistance. In humans and rodents, lean body mass decreases whereas fat mass increases in old subjects compared to young. In our

mice, total body mass and fat mass increased with increasing age in wild-type mice, whereas these parameters were maintained constant in transgenic mice. However, no differences were found in daily food and drink consumption rates. Thus, the increase in body weight in wild-type mice is due to an increased fat mass which may not be attributed to increased intake.

In humans, total energy expenditure decreases with age, in part due to changes in body composition. Curiously, no differences in energy expenditure were found between strains despite the differences observed in body composition and activity. Still, the values obtained were comparable to other studies in wild-type mice of similar age. In addition, no differences in respiratory quotient were found between transgenic and wild-type mice at 8-11 nor 17-20 months old either. Although differences were expected due to the dissimilarities in body fat, these results could be explained by the fact that both strains had the same feeding conditions and exhibited similar intake consumption rates.

Lastly, glucose tolerance is known to decrease with age. Moreover, body fat mass and distribution, and physical fitness can additionally account for the decline in glucose tolerance. We found an increased age-associated glucose intolerance in old wild-type mice compared to transgenic mice, which fits our previous findings in physical health status and body composition. Given the major role of BCL-XL in the survival of pancreatic progenitors and β-cells and the importance of T cells as mediators of β-cell apoptosis in insulin-dependent diabetes, we believed that the protection against age-related glucose intolerance observed in

transgenic mice may be attributed to better maintenance of pancreatic cells under the regulation of T cells overexpressing BCL-XL.

As we already mentioned, our mice overexpress BCL-XL specifically in T cells. These cells are major regulators of the immune response and contribute to maintain homeostasis. During aging, T cells undergo various changes that impair their function through the process known as immunosenescence. We found an increased number of T cells in 2-5, 8-11, and 17-20-month-old transgenic mice compared to wild-type mice. Given that T cell number and diversity normally decrease with age, BCL-XL overexpression seems to protect mice from this decline of immune function. This accumulation of T cells in the spleen could be attributed to the anti-apoptotic effect of BCL-XL promoting cell survival, although the reason why this effect is lost in 24-26-month-old mice remains a mystery.

Frailty has been associated with significantly reduced expression levels of several genes implicated in the cellular stress response. Apoptosis, autophagy, and senescence are well-known cellular mechanisms that are activated under stressful conditions. In old subjects, lymphocytes are more susceptible to apoptosis, and exercise interventions have been demonstrated to reduce apoptosis in peripheral blood mononuclear cells. Contrary to our expectations, increased levels of apoptosis were found in T cells from 17-20-month-old transgenic mice compared to T cells from wild-type mice. Thus, BCL-XL is not preventing apoptosis in freshly isolated T cells. Nonetheless, when cultured, T cells from 2-5 and 8-11-month-old transgenic mice were protected from programmed cell death even in the presence of an apoptosis inducer. These findings evidence that BCL-XL lacks an anti-apoptotic effect under physiological conditions

and only prevents T cell apoptosis under stressful circumstances in which this pathway is enhanced. Still, BCL-XL's role in cellular apoptosis is completely lost in old age even though its overexpression is still maintained during aging.

The process of aging is generally associated with a decline in autophagy. Although the mechanisms responsible are not yet understood, human and murine models have also shown decreased autophagy in aged T cells. In the present study, old-mice-derived T cells overexpressing BCL-XL exhibited an improved adaptation to starving conditions in comparison with wild-type-derived T cells. These results contradict the described function of BCL-XL as a suppressor of autophagy. Nevertheless, this contradictory effect of BCL-XL increasing autophagy has also been described in cancer cells and under certain conditions, such as in response to etoposide and staurosporine. A possible explanation is the disassociation of BCL-XL with BECLIN-1 and its translocation to the mitochondrial membrane to block transition membrane pore formation, which would promote autophagy and suppression of cell death. Hence, our findings suggest that BCL-XL is not suppressing autophagy because it is anchored to the mitochondrial outer membrane inhibiting apoptosis, thereby promoting cell survival.

Senescent cells accumulate in aged tissues from different species, secreting various inflammatory cytokines and chemokines, substantially affecting the organism's physiology. Despite the existing evidence of BCL-XL's role in cellular senescence, no differences were found in splenic T cells from wild-type and transgenic mice. This outcome could be due to a complete lack of BCL-XL effect or could be the result of two opposing

roles, induction and suppression, resulting in a compensatory effect. This dual role of BCL-XL has been previously reported with the use of senolytics and by studies performed in our group in which BCL-XL overexpression reduces markers of cellular senescence. In summary, although no effect was found in cellular senescence, BCL-XL overexpression enhances cell survival under hostile conditions by preventing apoptosis in cultured young and adult mice-derived splenic T cells and boosting autophagic response to starvation.

Mitochondrial dysfunction is a hallmark of aging in several cell types. Our results show that overall O_2 uptake by young transgenic mice-derived T cells was lower compared to wild-type-derived T cells under basal conditions. At the same time, ATP production, maximal respiration, and spare respiratory capacity were similar in T cells from both strains. Thus, BCL-XL overexpressing T cells can maintain a similar energy demand by consuming less oxygen. Hence, our findings suggest that transgenic mice-derived T cells have an enhanced respiratory efficiency, which according to the rate-of-living theory of aging, could explain the healthier physical state observed in these mice at advanced ages. This hypothesis is reinforced by the reduced levels of proton leak observed in transgenic mice-derived T cells. However, this effect is lost with increasing age, and the reason why this occurs is still unknown. Similar results have been seen in other cell types, such as neurons, in which BCL-XL has been reported to decrease mitochondrial oxygen consumption, indicating an enhanced and more efficient coupling of ATP production to oxygen uptake.

As a general background perspective, previous research performed by our group found that BCL-XL is physiologically upregulated in centenarians, considered models of healthy aging. We also studied BCL-XL overexpression in primary cells, nematodes, and flies. In the *in vitro* studies, BCL-XL decreased markers of cellular senescence and enhanced immune function. BCL-XL ortholog gene ced-9, increased mean and maximal lifespan in *Caenorhabditis elegans*. In *Drosophila melanogaster*, BCL-XL overexpression increased lifespan and enhanced locomotor behaviour. In the present thesis, we studied the effect of BCL-XL overexpression in the mouse *Mus musculus*. In summary, our findings show that mice overexpressing BCL-XL exhibit reduced frailty accompanied by an attenuated decline in physical performance and increased activity, maintain youthful body composition, and display an improved glucose tolerance at advanced ages. Given the correlation between good physical health status and immune function in older adults, we believe that these beneficial effects can be attributed to improved T cell function. According to our hypothesis, T cells from transgenic mice are more abundant, exhibit enhanced stress response, and display an improved mitochondrial respiratory efficiency.

Taking into account the theories of aging described in the introduction, our results indicate that the aging process can be modulated genetically by BCL-XL (longevity genes theory) by enhancing T cell immune function (immunological theory) in terms of improving respiratory efficiency by reducing oxygen consumption (rate-of-living theory), thereby minimizing the probability to generate reactive oxygen species (free radicals theory), while maintaining mitochondrial function

(mitochondrial theory). Hence, our findings suggest that BCL-XL overexpression in T cells could promote healthy aging in our mice model.

CONCLUSIONS

The general conclusion of this thesis is that BCL-XL prevents frailty and promotes healthy aging in transgenic mice overexpressing the human form of this protein in T cells.

The specific conclusions of the study are: 1) Mice overexpressing BCL-XL exhibit improved physical health status due to the attenuation of the physical performance decline with age, the increase in spontaneous activity, and preventing frailty compared to wild-type mice at advanced ages; 2) Mice overexpressing BCL-XL display improved metabolism-related parameters due to maintained body composition and enhanced glucose tolerance at old ages compared to wild-type mice, but show no differences in intake nor respiratory metabolism; 3) T cells isolated from mice overexpressing BCL-XL exhibit an enhanced cellular function by being more resistant to apoptosis under stressful conditions, showing an improved autophagic response to starvation and having a lower oxygen consumption and proton leak, with no differences in cellular senescence, mitochondrial membrane potential, ATP production, maximal respiration, and spare respiratory capacity compared to T cells isolated from wild-type mice.

RESUMEN

ESTUDO DEL PAPEL DE BCL-XL EN EL ENVEJECIMIENTO SALUDABLE Y EN LA PREVENCIÓN DE LA FRAGILIDAD

INTRODUCCIÓN

El envejecimiento se define como un fenómeno multifactorial, intrínseco, progresivo, deletéreo e inevitable que ocurre como resultado de la acumulación gradual de daño a nivel celular y molecular. El proceso biológico del envejecimiento va acompañado de una pérdida de homeostasis, la cual es la condición de estabilidad requerida para la mínima funcionalidad de los distintos sistemas de nuestro cuerpo. Consecuentemente, el envejecimiento es un factor de riesgo principal en varias patologías, incluyendo enfermedades cardiovasculares, cáncer y enfermedades neurodegenerativas.

Un gran número de teorías del envejecimiento se ha descrito hasta la fecha. Las teorías de los genes de la longevidad, la inmunológica, la *rate-of-living* y la de los radicales libres están entre ellas. La teoría del envejecimiento de los genes de la longevidad establece que el envejecimiento puede ser controlado genéticamente como mutaciones genéticas únicas en genes los cuales jueguen papeles importantes en el control metabólico y la resistencia al estrés como mTOR. Esta teoría está apoyada por la evidencia de animales mutados genéticamente los cuales exhiben esperanzas de vida incrementadas. La teoría inmunológica sitúa el declive del sistema inmune que tiene lugar a edades avanzadas, también conocido como inmunosenescencia, como el principal impulsor del envejecimiento, lo que conduce a una mayor inflamación y

vulnerabilidad a infección. De acuerdo con la teoría del envejecimiento de *rate-of-living*, la esperanza de vida está determinada por el consumo de oxígeno, siendo los animales con mayor tasa de consumo de oxígeno aquellos con esperanzas de vida más cortas. Aunque esta teoría falla en explicar el proceso de envejecimiento en varios taxones, explica el efecto de la restricción calórica. Por último, la teoría del envejecimiento de los radicales libres postula que especies moleculares altamente reactivas con electrones despareados se acumulan en células envejecidas, causando un daño celular que, eventualmente, conduce al mal funcionamiento del organismo. Más tarde, esta teoría fue actualizada como la teoría del envejecimiento de los radicales libres mitocondriales, la cual considera las mitocondrias como la principal fuente de especies reactivas del oxígeno intracelulares. Por tanto, la acumulación de estas especies conduce a mutaciones en el ADN mitocondrial. Hoy en día, esta teoría es una de las más populares, aunque falla en explicar completamente el proceso de envejecimiento ya que el daño oxidativo no es el único tipo de daño que se acumula con la edad.

Aunque ninguna de estas teorías del envejecimiento puede explicar por completo el proceso de envejecimiento, todas ellas describen un posible mecanismo, y más importante, estas teorías no son mutuamente excluyentes. Por lo tanto, el envejecimiento podría explicarse mediante una combinación de estas teorías, como piezas de un rompecabezas ensamblado para ver el panorama general.

Independientemente de la causa, el proceso de envejecimiento produce un fenotipo específico que ha sido ampliamente descrito. Los sellos distintivos más relevantes del envejecimiento incluyen la senescencia, la

pérdida de proteostasis, la desregulación de la detección de nutrientes y la disfunción mitocondrial, entre otros. La interacción de estos cambios a nivel celular resulta en cambios a nivel de organismo, como declive físico y cognitivo, inflamación, inmunodeficiencia y fragilidad. Para esta tesis, las características más relevantes del fenotipo de envejecimiento son: 1) mala salud física, 2) desregulación metabólica y 3) función celular comprometida. Por un lado, la mala salud física en la vejez puede atribuirse a una disminución de la actividad física y está asociada a un declive del rendimiento físico y la fragilidad. Por otro lado, la desregulación metabólica está acompañada por cambios en la composición corporal, una disminución del metabolismo energético y la intolerancia a la glucosa. Por último, una función celular comprometida puede ser causada por una mala respuesta al estrés y disfunción mitocondrial.

En las últimas décadas, la esperanza de vida humana se ha incrementado globalmente en todos los países. Sin embargo, no todo el mundo exhibe el mismo fenotipo de envejecimiento a medida que envejecen. De hecho, el proceso de envejecimiento ocurre a distintas tasas en diferentes épocas y en diferentes regiones. Para poder explicar esta heterogeneidad entre la población envejecida, se ha propuesto la distinción entre envejecimiento normal y envejecimiento saludable. El envejecimiento saludable hace referencia a personas de edad avanzada con una mejor función cognitiva y física en comparación con personas de su misma edad.

Los centenarios son individuos con vidas extremadamente longevas, retrasando o incluso escapando a la aparición de las principales enfermedades asociadas a la edad, incluyendo el cáncer y las

enfermedades cardiovasculares. Cuando los comparamos con sus contemporáneos que murieron a edades más jóvenes, los centenarios exhiben una menor tasa de hospitalización, menor duración de estancia en hospitales y menos comorbilidades. De hecho, mantienen una salud tan notable hasta sus últimos años que su esperanza de calidad de vida es comparable a su esperanza de vida. Por esta razón, los centenarios se han propuesto como modelos de envejecimiento saludable e investigadores de todo el globo han estado probando distintas aproximaciones para descifrar la biología de estos seres humanos tan excepcionales.

Estudios previos realizados por nuestro grupo mostraron que la proteína BCL-XL está involucrada en la longevidad extrema ya que se encuentra incrementada en células mononucleares de sangre periférica de centenarios en comparación con octogenarios. La proteína BCL-XL pertenece a la familia de proteínas BCL-2, cuyos miembros son comúnmente clasificados en tres grandes categorías: las proteínas anti-apoptóticas (e.g., BCL-2, BCL-XL, BCL-W, A1 y MCL1), pro-apoptóticas (e.g., BAX, BAK and BOK/MTD) y las proteínas solo BH3 (e.g., BID, BIM/BOD, BAD, PUMA/BBC and NOXA). Se reportó inicialmente que BCL-XL se encuentra en la membrana mitocondrial externa, y después en la membrana interna también, anclado por su dominio de membrana terminal-c hidrofóbico. BCL-XL también se puede encontrar en el retículo endoplásmico y como forma soluble en el citosol.

El primer papel descrito para la proteína BCL-XL fue la inhibición de muerte celular en ausencia de factores de crecimiento en una línea celular independiente de IL-3. BCL-XL regula la vía apoptótica intrínseca junto con otras proteínas de la familia BCL-2 en la mitocondria. Cuando las

proteínas anti-apoptóticas son neutralizadas por proteínas con dominio solo BH3, BAX y BAK son libres para unirse a la membrana mitocondrial externa, donde forman poros que causan permeabilización. Esto provoca la salida de activadores de apoptosis de la mitocondria (e.g., citocromo c, SMAC and DIABLO). En el citosol, el citocromo c forma el apoptosoma junto con APAF-1 y caspasa-9 para iniciar la cascada de activación de caspasas. BCL-XL es capaz de reprimir esta vía mediante la prevención de la permeabilización de la membrana mitocondrial externa y la subsecuente salida del citocromo c hacia el citoplasma, lo cual causaría eventualmente apoptosis. Además, la inhibición de apoptosis por BCL-XL no se debe solamente a su interacción con BAX y BAK, sino también a la intercepción de señales pro-apoptóticas aguas arriba (e.g., proteínas solo y P53), su interacción con diversos promotores de permeabilización de la membrana mitocondrial externa (e.g., los canales aniónicos dependientes de voltaje), y la prevención de la generación de señales de Ca^{2+} citosólico pro-apoptóticas.

Además de la apoptosis, BCL-XL también es capaz de regular la autofagia mediante la interacción con el dominio BH3 de BECLINA-1, previniendo la formación del complejo BECLINA-1-VPS34, el cual es esencial para la formación del autofagosoma. Por tanto, inhibiendo el proceso de autofagia. En este sentido, se ha reportado que las proteínas solo BH3 (e.g., BAD) y componentes miméticos (e.g., ABT-737) inducen autofagia mediante la disrupción de la interacción BECLINA-1 y BCL-XL de manera competitiva. BCL-XL podría también inhibir la mitofagia dependiente de PINK1/PARKIN mediante la prevención de la translación de PARKIN desde el citoplasma a la mitocondria. Por tanto, BCL-XL es un

intermediario importante entre autofagia y apoptosis, por el cual ambas vías convergen.

En respuesta a estímulos agresivos como la radiación UV, las células activan mecanismos de respuesta al estrés. De manera similar a la apoptosis y la autofagia, la senescencia es una respuesta celular frente a distintos estreses y se ha sugerido una interacción entre estos tres procesos por varios autores. Incluso así, la evidencia existente describiendo la función de BCL-XL en la senescencia celular es contradictoria y no se entiende claramente. Dada su capacidad de promover la supervivencia celular, BCL-XL se considera un oncogén. En este sentido, varios tipos de células senescentes muestran niveles elevados de BCL-XL, y la eliminación selectiva de estas células ha demostrado tener un amplio rango de efectos beneficiosos. Este es el caso de los fármacos senolíticos que tienen como diana BCL-XL y otros miembros anti-apoptóticos de la familia BCL-2, como ABT-263, ABT-737 y TW-37.

En contraste, también hay evidencias sugiriendo un papel protector de BCL-XL frente a la senescencia celular. En este aspecto, la sobreexpresión de BCL-XL disminuye diversos marcadores de senescencia, incluyendo $P16^{INK4a}$, $P19^{ARF}$, $P21^{CIP1}$ y actividad β-galactosidasa asociada a senescencia en fibroblastos embrionarios de ratón y linfocitos primarios humanos. También se ha encontrado que BCL-XL inhibe la detención del crecimiento irreversible inducida por P53 en células cancerígenas de vejiga mediante la prevención de la generación de especies reactivas de oxígeno. De manera similar, se ha demostrado que la sobrerregulación de la expresión de BCL-XL reduce la senescencia en neoplasia pancreática y

durante la diferenciación de megacariocitos. Por tanto, BCL-XL es capaz de prevenir la apoptosis dependiente de mitocondria, suprimir la autofagia dependiente de BECLINA-1, y promover o reprimir la senescencia celular. Así, BCL-XL podría considerarse un regulador clave de la respuesta celular al estrés y la supervivencia celular.

BCL-XL ha demostrado jugar un papel importante en otras funciones mitocondriales que en último lugar promueven supervivencia celular. En este aspecto, existen evidencias sugiriendo que BCL-XL reduce el flujo fútil de iones a través de la membrana mitocondrial interna y, por tanto, previniendo el gasto innecesario de recursos celulares y la crisis energética durante estrés. Además, varios estudios indican que BCL-XL interacciona directamente con la subunidad β de la F_1F_0 ATP sintasa, reduciendo la fuga de protones y así incrementando el transporte neto de H^+ durante la actividad del complejo V. Sin embargo, el papel de BCL-XL en el envejecimiento no se comprende por completo y estudios adicionales son necesarios para determinar si la sobreexpresión de BCL-XL en centenarios es una consecuencia o una causa del proceso de envejecimiento en estos modelos de envejecimiento saludable. Dado el importante papel de BCL-XL en distintas funciones asociadas al envejecimiento saludable, nos propusimos investigar el efecto de la sobreexpresión de BCL-XL durante el envejecimiento en un modelo murino.

HIPÓTESIS Y OBJETIVOS

Debido al reciente descubrimiento de que BCL-XL se encuentra sobreexpresado en células mononucleares de sangre periférica de centenarios, ha surgido un nuevo enfoque para investigar la función de BCL-XL en el envejecimiento saludable. El ortólogo de BCL-XL Ced-9 para *Caenorhabditis elegans* ha demostrado su contribución a la longevidad excepcional mediante el aumento de la esperanza de vida media y máxima en esta especie. En *Drosophila melanogaster*, la sobreexpresión de BCL-XL también incrementa la esperanza de vida con una mejora complementaria del comportamiento locomotor. Además, es conocido que BCL-XL regula la eficiencia metabólica mitocondrial en neuronas y mejora la plasticidad en el cerebro. También se ha descrito un papel protector de BCL-XL frente a estrés oxidativo en células endoteliales vasculares y fibroblastos. Adicionalmente, la sobreexpresión de BCL-XL reduce la senescencia *in vitro* y mejora la función inmune en células primarias. Con todo, estos datos sugieren un papel beneficioso de BCL-XL en el envejecimiento. Por tanto, hipotetizamos que el ratón transgénico que sobreexpresa BCL-XL podría mostrar parámetros de salud mejorados, función mitocondrial preservada y menor fragilidad a edades avanzadas.

El objetivo principal de esta tesis es estudiar el papel de BCL-XL en la fragilidad y el envejecimiento saludable en un ratón transgénico que sobreexpresa la forma humana de BCL-XL en células T. Para conseguirlo, nos propusimos los siguientes objetivos específicos: 1) Determinar el efecto de BCL-XL en el estado de salud físico en términos de rendimiento físico, actividad espontánea y fragilidad en ratones que sobreexpresan

BCL-XL y ratones de fenotipo salvaje; 2) Estudiar el efecto de BCL-XL en parámetros relacionados con el metabolismo en términos de composición corporal, ingesta, metabolismo energético y tolerancia a la glucosa en ratones que sobreexpresan BCL-XL y ratones de fenotipo salvaje; 3) Caracterizar las células T aisladas de ratones que sobreexpresan BCL-XL y ratones de fenotipo salvaje en términos de mecanismos de supervivencia mitocondrial, incluyendo apoptosis, senescencia y autofagia, y función mitocondrial.

MATERIAL Y MÉTODOS

En este estudio, empleamos ratones transgénicos heterocigotos de la cepa Cg-Tg(LCKprBCL2L1)12Sjk/J comprados en *The Jackson Laboratory*. Estos ratones transgénicos expresan la secuencia humana ADNc *BCL-XL* bajo el control de un promotor proximal de proteína tirosina quinasa de linfocito murino, el cual induce la expresión de BCL-XL en todos los subconjuntos de timocitos.

Para establecer la colonia, se cruzaron los ratones transgénicos con ratones endogámicos C57BL/6J. Usamos los ratones C57BL/6J como ratones control o de fenotipo salvaje para nuestros experimentos. Los ratones se estabularon en el animalario de la Unidad Central de Investigación de Medicina de la Facultad de Medicina y Odontología de la Universidad de Valencia. Los animales se mantuvieron en las instalaciones a 22 ± 2˚C, con una humedad relativa del 60% bajo un ciclo de luz-oscuridad de 12-12h y con acceso a comida y agua *ad libitum*.

Definimos cuatro grupos de edades para el estudio del efecto de la sobreexpresión de BCL-XL en ratones durante el envejecimiento, considerando ratones de 2-5 meses de edad como jóvenes, de 8-11 como adultos, de 17-20 como viejos, y de 24-26 meses de edad como muy viejos. En primer lugar, seguimos una cohorte inicial de 144 ratones transgénicos y de fenotipo salvaje, con hembras y machos en proporciones similares. Cuando los ratones alcanzaban cada grupo de edad respectivamente, se realizaron las pruebas de rendimiento físico. La fragilidad se determinó únicamente a edades avanzadas, en ratones de 17-20 y 24-26 meses de edad. En paralelo, aproximadamente 36 animales se sacrificaron a cada grupo de edad para el aislamiento de células T para determinar el número y función de estas células. Finalmente, la composición corporal, el monitoreo metabólico y el test de tolerancia a la glucosa fueron realizados transversalmente en ratones adultos jóvenes y adultos mayores. Específicamente, ratones de 8-11 y de 17-20 meses de edad fueron usados para el monitoreo metabólico, mientras que la glucemia durante el test de tolerancia a la glucosa y la composición corporal fueron medidas en ratones desde los 6 a los 23 meses de edad.

In vivo, medimos el peso corporal con una balanza de precisión, la fuerza de agarre con un dinamómetro, la coordinación motora como tiempo de latencia a caerse desde un cilindro rotante usando el aparato rotarod, y la resistencia física con la cinta de correr forzando a los ratones a correr hasta el agotamiento. Así, determinamos la ganancia de peso corporal, la pérdida de fuerza de agarre, la pérdida de coordinación motora, y la pérdida de resistencia física para cada ratón de manera individual a cada grupo de edad. Para determinar la fragilidad, usamos los criterios de peso corporal, fuerza de agarre, coordinación motora y resistencia física

siguiendo los valores de corte del 20% superior para el peso y el 20% inferior para el resto de los criterios de fragilidad. El metabolismo respiratorio (i.e., cociente respiratorio y gasto energético), actividad locomotora espontánea e ingesta fueron monitoreados durante aproximadamente 45 horas usando jaulas metabólicas. Durante la duración del experimento, el ciclo luz-oscuridad de 12 horas fue mantenido para asegurar un ritmo circadiano normal. La composición corporal, en términos de masa total, masa grasa y masa magra, fue evaluada usando la absorciometría de rayos X de energía dual. Finalmente, la prueba de tolerancia a la glucosa fue realizado en ratones con ayuno de 12 horas seguido de una inyección intraperitoneal de 2g/kg de glucosa.

Ex vivo, determinamos el genotipo de los ratones y los niveles de expresión de la proteína BCL-XL. El genotipo de los ratones se determinó mediante la digestión de tejido, la amplificación de una secuencia control y secuencia transgén, electroforesis y la visualización del gel. La expresión de BCL-XL fue determinada por *western blot* en órganos homogeneizados y células T aisladas del bazo. Adicionalmente, contamos el número de células blancas y células T aisladas del bazo.

In vitro, medimos la pureza de las células T, senescencia celular, apoptosis, autofagia, muerte celular y potencial de membrana mitocondrial por citometría de flujo. Cuando se requería, las células fueron cultivadas en medio RPMI 1640 suplementado con glutamina, penicilina y estreptomicina al 1% y suero bovino fetal al 10%, en un incubador de gas con CO_2 al 5%. Los marcadores usados fueron el grupo de diferenciación 3 para la pureza de células T, la proteína asociada a

microtúbulos 1A/1B cadena ligera 3B para actividad autofágica, actividad β-galactosidasa para la senescencia celular, Anexina V para apoptosis, ioduro de propidio para muerte celular y éster metílico de tetrametilrodamina para el potencial de membrana mitocondrial. Adicionalmente, se determinó la respiración mitocondrial en células T aisladas mediante un analizador de flujo extracelular.

El análisis de los datos se realizó mediante RStudio, un entorno de software gratuito para R, que es un lenguaje de programación para computación estadística y gráficos. Para las variables numéricas, primero identificamos los *outliers* para cada una de las variables de nuestra muestra. Luego, evaluamos la normalidad y la homocedasticidad. Dependiendo del tipo de variable (numérica o categórica) y si los datos cumplían o no las asunciones de los test paramétricos, realizamos distintos test estadísticos.

RESULTADOS

Para una comprensión más sencilla, dividimos nuestros resultados en tres secciones principales en asociación con los tres rasgos más importantes del fenotipo asociado al envejecimiento descritos anteriormente. Estas secciones son 1) estado de salud físico, 2) parámetros relacionados con el metabolismo y 3) caracterización de células T. Primero, la sobreexpresión de BCL-XL fue confirmada en timo, bazo y células T de ratones transgénicos por *western blot*. Para evaluar el estado de salud físico general, determinamos el declive del rendimiento físico con la edad, la actividad locomotora espontánea y la fragilidad en

ratones transgénicos y de fenotipo salvaje. Para evaluar parámetros relacionados con el metabolismo, también determinamos composición corporal, metabolismo respiratorio y tolerancia a la glucosa. Por último, la caracterización de células T se determinó mediante el conteo de células T, los mecanismos de supervivencia celulares y la función mitocondrial.

En el estudio del estado de salud físico, los ratones transgénicos que sobreexpresan BCL-XL mostraron una reducción significativa de ganancia de peso y pérdida de coordinación a los 8-11 y a los 17-20 meses de edad en comparación con los ratones de fenotipo salvaje. De manera similar, la pérdida de fuerza de agarre y de resistencia al ejercicio se redujeron en los ratones transgénicos a los 8-11 meses de edad. Adicionalmente, la frecuencia de eventos de alzamiento sobre las patas traseras fue mayor durante el ciclo de oscuridad en ratones transgénicos de 8-11 meses en comparación con los ratones de fenotipo salvaje, pero no se observaron diferencias significativas en ratones de 17-20 meses, ni tampoco en los niveles actividad espontánea ambulatoria. Además, la proporción de ratones identificados como frágiles según el número de criterios de fragilidad cumplidos era casi el doble en ratones de fenotipo salvaje (11,59%) en comparación con los ratones transgénicos (6,12%) a 17-20 meses de edad, pero estas diferencias no eran estadísticamente significativas. A los 24-26 meses de edad, 2 de los 17 ratones de fenotipo salvaje se clasificaron como frágiles, mientras que ninguno de los ratones transgénicos era frágil, y sólo un ratón era pre-frágil en comparación con los 6 ratones pre-frágiles de fenotipo salvaje. Consecuentemente, la prevalencia de fragilidad se redujo significativamente en ratones transgénicos de 24-26 meses de edad. De manera similar, la Puntuación de Fragilidad Valenciana fue menor en estos ratones en comparación con

los de fenotipo salvaje, aunque tampoco se encontraron diferencias a los 17-20 meses de edad. En conjunto, los ratones transgénicos exhiben una atenuación del declive del rendimiento físico y una mejor actividad, que se traducen en una menor fragilidad a edades más avanzadas. Por tanto, nuestros hallazgos sugieren que el ratón transgénico tiene un mejor estado de salud físico durante el envejecimiento en comparación con el ratón de fenotipo salvaje.

En el estudio de parámetros relacionados con el metabolismo, la masa corporal total y el porcentaje de grasa corporal estaban positivamente correlacionados con la edad en ratones de fenotipo salvaje pero no en ratones transgénicos. Por tanto, la ganancia de peso corporal con la edad en los ratones de fenotipo salvaje podría atribuirse a un incremento del contenido graso. Sin embargo, no se observaron diferencias en la ingesta entre las cepas, indicando que estas diferencias de tamaño corporal y contenido graso puede que no estén asociadas a diferencias en el consumo de comida. Además, no se observaron diferencias en el cociente respiratorio ni en el gasto energético entre los ratones de fenotipo salvaje y los transgénicos a 8-11 ni a 17-20 meses de edad que puedan explicar estas diferencias. Asimismo, cuando medimos la masa no grasa, no observamos ninguna correlación entre este parámetro y la edad ya que se mantuvo relativamente uniforme a lo largo de las distintas edades en ambas cepas. Por tanto, esto sugiere que la pérdida de fuerza de agarre asociada a la edad podría no estar causada por una pérdida de masa muscular.

Por otra parte, los perfiles glucémicos de los ratones de fenotipo salvaje de 15-23 meses de edad mostraron niveles de glucosa incrementados

durante la prueba de tolerancia a la glucosa, mientras que los ratones transgénicos de edad similar mostraron perfiles parecidos a los de ratones jóvenes de 6-14 meses de edad. Estas diferencias se confirmaron con el análisis del área bajo la curva, mostrando una reducción significativa de la intolerancia a la glucosa en ratones transgénicos de 15-23 meses de edad. Por tanto, la sobreexpresión de BCL-XL previene el deterioro de la tolerancia a la glucosa asociado al envejecimiento.

En el estudio de la caracterización de células T, el número total de células blancas del bazo obtenidas de ratones transgénicos y de fenotipo salvaje era similar, entre 50 y 150 millones de células. Sin embargo, el número de células T del bazo obtenidas de ratones transgénicos era significativamente mayor a los 2-5, 8-11 y 17-20 meses de edad en comparación con el número de células T obtenidas de ratones de fenotipo salvaje. Curiosamente, no se observaron diferencias in ratones más mayores. En conjunto, la sobreexpresión de BCL-XL incrementa la población de células T del bazo sin alterar el número total de células blancas, y estas diferencias van desapareciendo con la edad.

Cuando analizamos la respuesta celular al estrés, no se encontraron diferencias en la senescencia de células T, pero se observó una mayor respuesta autofágica a la inanición en células T de ratones transgénicos viejos en comparación con células T de ratones de fenotipo salvaje. En cuanto a la muerte celular programada, la apoptosis estaba incrementada en células T de ratones transgénicos de 17-20 meses de edad en condiciones fisiológicas (células recién asiladas). Estos resultados indican que BCL-XL no está actuando como una proteína anti-apoptótica en estas condiciones, sino más bien como pro-apoptótica. Por el

contrario, la apoptosis estaba disminuida en células T de ratones transgénicos de 2-5 y de 8-11 meses de edad en condiciones más hostiles (células cultivadas), tanto en ausencia como en presencia del inductor de apoptosis dexametasona. Estos resultados indican que la función anti-apoptótica de BCL-XL está inducida en respuesta al estrés.

Evaluando la función mitocondrial de estas células T, observamos una disminución significativa en la tasa de consumo de oxígeno y la fuga de protones en condiciones basales en células T de ratones transgénicos de 2-5 y 8-11 meses de edad en comparación con células T de ratones de fenotipo salvaje. Curiosamente, como se observó con anterioridad cuando se midió apoptosis, estas diferencias decaen con la edad, ya que no se observa ningún efecto a los 17-20 meses de edad. Adicionalmente, no se observan en la respiración asociada a ATP, respiración máxima y capacidad respiratoria de reserva. En conjunto, nuestros datos sugieren que BCL-XL podría estar mejorando la eficiencia de la fosforilación oxidativa en las células T de ratones transgénicos manteniendo una misma demanda metabólica con un menor consumo de oxígeno, y consecuentemente minimizando la fuga de protones y la producción de especies reactivas del oxígeno.

DISCUSIÓN

El declive de la función física está asociado a un incremento de la susceptibilidad a distintas enfermedades asociadas a la edad (e.g., enfermedades cardiovasculares, hipertensión, diabetes de tipo 2 e infarto) y una longevidad reducida tanto en roedores como humanos. En

roedores, el peso corporal se incrementa normalmente con la edad. Nosotros vimos que la ganancia de peso corporal era significativamente menor en ratones transgénicos de 8-11 y de 17-20 meses de edad en comparación con los de fenotipo salvaje, pero no observamos diferencias a edades más avanzadas. Dado que BCL-XL parece estar estrechamente asociado a la longevidad, y que un menor peso corporal en ratones se asocia a esperanzas de vida incrementadas, consideramos que la prevención de la ganancia de peso en el ratón transgénico a mediana edad es un rasgo deseable durante el envejecimiento. La fuerza de agarre también se ha reportado que disminuye en ratones viejos de la cepa C57BL/6J en comparación con ratones jóvenes. En esta tesis, vimos que la pérdida de fuerza de agarre también se atenuaba en ratones transgénicos de 8-11 meses de edad en comparación con los de fenotipo salvaje, pero de nuevo, no observamos diferencias a mayor edad. Aunque la pérdida de fuerza muscular se ha asociado clásicamente a una pérdida de la masa muscular en modelos humanos y murinos, no observamos cambios en la masa magra. Sin embargo, esta falta de relación entre fuerza y masa musculares también ha sido descrita por otros autores.

La pérdida progresiva de coordinación motora también tiene lugar a edades avanzadas y estos cambios son causados no sólo por una pérdida de la función muscular, sino también por un declive de los sistemas cognitivo y neurológico en las personas mayores. Cuando evaluamos la coordinación motora en nuestra cohorte de ratones, vimos que la pérdida de coordinación asociada a la edad estaba atenuada en ratones transgénicos de 8-11 y 17-20 meses de edad en comparación con los ratones de fenotipo salvaje. Por tanto, sugiriendo una mejora función física y cognitiva a edad media-avanzada. De manera similar, se conoce

que la capacidad de resistencia disminuye con el tiempo en personas mayores. En nuestros ratones, la pérdida de resistencia física asociada a la edad estaba atenuada en ratones transgénicos de 8-11 meses de edad en comparación con los ratones de fenotipo salvaje, indicando una mejor resistencia al ejercicio extenuante. Varios estudios han propuesto una asociación positiva entre resistencia al ejercicio y función inmune. Por tanto, dado que el ratón transgénico sobreexpresa BCL-XL específicamente en células T, creemos que la mejora en resistencia observada en estos ratones podría ser atribuida a una mejor función de células T.

La falta de actividad física puede explicar aproximadamente la mitad del deterioro físico asociado al envejecimiento humano. Nosotros hemos observado un incremento no significativo en la actividad espontánea de ratones transgénicos de 8-11 y 17-20 meses de edad, siendo más prominente en el grupo de edad de 8-11 meses. Los alzamientos fueron también más frecuentes en ratones transgénicos, pero este incremento fue estadísticamente significativo únicamente en ratones de 8-11 meses de edad durante el ciclo de oscuridad. Este incremento en la actividad de los ratones transgénicos, aunque menor, se corresponde con nuestros hallazgos de rendimiento físico, y todo ello indica un mejor estado físico en estos ratones.

Como ya hemos discutido previamente, un estado de rendimiento físico reducido va a evolucionar, casi con total certeza, a fragilidad, y eventualmente a discapacidad. Niveles de baja actividad son, de hecho, uno de los criterios usados para determinar fragilidad en humanos junto con pérdida de peso, cansancio, lentitud y debilidad. Nosotros hemos

visto una reducción significativa de la prevalencia de fragilidad y de la Puntuación Valenciana de Fragilidad en ratones transgénicos de 24-26 meses de edad. Estos resultados pueden explicarse por el atenuado declive y la mayor actividad observada en ratones transgénicos a edades previas. En conjunto, nuestros descubrimientos en el estado de salud física muestran que los ratones transgénicos muestran una mayor actividad, una protección general frente al declive del rendimiento físico que ocurre desde los 2-5 meses hasta los 17-20 meses de edad, y una consecuente prevención de fragilidad a los 24-26 meses de edad. Por tanto, los ratones transgénicos tienen un mejor estado de salud físico durante el envejecimiento, que podría atribuirse a una mejor función inmune, y que podría estar relacionada con una mejor función cognitiva.

Se sabe que un peor estado de salud física (e.g., debilidad muscular, capacidad de resistencia disminuida y mayor fatigabilidad) altera distintos parámetros metabólicos, incluyendo la composición corporal, el gasto energético y la resistencia a insulina. En humanos y roedores, la masa magra disminuye mientras que la masa grasa aumenta en sujetos ancianos en comparación con los jóvenes. En nuestros ratones, la masa total y la masa grasa se vieron incrementadas con la edad en ratones de fenotipo salvaje, mientras que estos parámetros se mantuvieron constantes en ratones transgénicos. Sin embargo, no se encontraron diferencias en la tasa de consumo de comida y bebida diarias. Por tanto, el incremento del peso corporal en ratones de fenotipo salvaje se debe a un incremento de masa grasa la cual podría no estar atribuida a una mayor ingesta.

En humanos, el gasto energético total disminuye con la edad, en parte debido a cambios en la composición corporal. Curiosamente, no observamos diferencias en gasto energético entre las cepas a pesar de las diferencias observadas en composición corporal y actividad. Aun así, los valores obtenidos eran comparables a otros estudios de ratones de fenotipo salvaje de edades similares. Adicionalmente, no se encontraron diferencias en el cociente respiratorio entre ratones transgénicos y ratones de fenotipo salvaje a 8-11 ni a 17-20 meses de edad. Aunque se esperaban diferencias debido a las diferencias de grasa corporal, estos resultados pueden ser explicados por el hecho de que ambas cepas tenían exactamente las mismas condiciones de alimentación y exhibían tasas de consumo de ingesta similares.

Por último, se conoce que la tolerancia a la glucosa disminuye con la edad. Además, la masa y distribución de grasa corporal, y la forma física pueden explicar también la disminución de tolerancia a la glucosa. Nosotros vimos una mayor intolerancia a la glucosa asociada a la edad en ratones de fenotipo salvaje en comparación con los transgénicos, lo cual encaja con nuestros descubrimientos anteriores en el estado de salud física y composición corporal. Dado el importante papel de BCL-XL en la supervivencia de progenitores pancreáticos y células β, y la importancia de las células T como mediadores de la apoptosis de células β en la diabetes dependiente de insulina, creemos que la protección frente a la intolerancia a la glucosa asociada a la edad que observamos en ratones transgénicos podría atribuirse a una mejor manutención de las células pancreáticas bajo la regulación de células T sobreexpresando BCL-XL.

Como ya hemos mencionado anteriormente, nuestros ratones sobreexpresan BCL-XL específicamente en células T. Estas células son importantes reguladores de la respuesta inmune y ayudan a mantener la homeostasis. Durante el envejecimiento, las células T sufren una serie de cambios que alteran su funcionamiento en un proceso conocido como la inmunosenescencia. Nosotros vimos un mayor número de células T en ratones transgénicos de 2-5, 8-11 y 17-20 meses de edad en comparación con ratones de fenotipo salvaje. Dado que el número de células T y su diversidad disminuyen normalmente con la edad, la sobreexpresión de BCL-XL parece proteger a los ratones de este declive de la función inmune. Esta acumulación de células T en el bazo podría atribuirse al efecto anti-apoptótico de BCL-XL promoviendo la supervivencia celular, aunque la razón por la que este efecto desaparece en ratones de 24-26 meses de edad sigue siendo un misterio.

La fragilidad se ha asociado con una reducción significativa de los niveles de expresión de varios genes implicados en la respuesta celular al estrés. La apoptosis, la autofagia y la senescencia son mecanismos celulares conocidos que se activan bajo condiciones estresantes. En sujetos mayores, los linfocitos son más susceptibles a apoptosis, y las intervenciones con ejercicio han demostrado reducir la apoptosis en células mononucleares de sangre periférica. Contrariamente a nuestras expectativas, encontramos mayores niveles de apoptosis en células T de ratones transgénicos de 17-20 meses en comparación con células T de ratones de fenotipo salvaje. Por tanto, BCL-XL no previene la apoptosis en células recién aisladas. Sin embargo, cuando las cultivamos, las células T de ratones transgénicos de 2-5 y de 8-11 meses de edad estaban protegidas frente a la muerte celular programada incluso en presencia de

un inductor de apoptosis. Estos hallazgos evidencian que BCL-XL carece de efecto anti-apoptótico bajo condiciones fisiológicas y que sólo previene la apoptosis de células T bajo circunstancias estresantes en las cuales esta vía está aumentada. Aun así, el papel de BCL-XL en apoptosis celular se pierde completamente a edades avanzadas a pesar de que su sobreexpresión se mantiene durante el envejecimiento.

El proceso de envejecimiento está generalmente asociado a un declive en la autofagia. Aunque los mecanismos responsables no se comprenden aún, los humanos y los modelos murinos también han mostrado una menor autofagia en células T envejecidas. En el presente estudio, células T de ratones viejos que sobreexpresan BCL-XL muestran una mejor adaptación a las condiciones de inanición en comparación con células T de ratones de fenotipo salvaje. Estos resultados contradicen la función descrita previamente de BCL-XL como supresor de autofagia. Sin embargo, este efecto contradictorio de BCL-XL incrementando la autofagia también se ha descrito en células cancerígenas y bajo ciertas condiciones, como en respuesta a etopósido y estaurosporina. Una posible explicación es la disociación de BCL-XL con BECLINA-1 y su translocación a la membrana mitocondrial para bloquear la formación del poro de transición, lo cual promovería la autofagia y suprimiría la muerte celular. Por tanto, nuestros descubrimientos sugieren que BCL-XL no está suprimiendo la autofagia porque se encuentra anclado a la membrana externa mitocondrial inhibiendo apoptosis, y por tanto, promoviendo la supervivencia celular.

Las células senescentes se acumulan en tejidos envejecidos de diferentes especies, secretando diversas citoquinas y quimiocinas inflamatorias,

afectando substancialmente la fisiología del organismo. A pesar de la evidencia existente sobre el papel de BCL-XL en la senescencia celular, no encontramos diferencias en células T del bazo de ratones de fenotipo salvaje y transgénicos. Este resultado podría deberse a una total falta de efecto por parte de BCL-XL, o podría ser el resultado de dos fuerzas opuestas, de inducción y supresión, resultando en un efecto compensatorio. Este papel dual de BCL-XL ha sido descrito previamente con el uso de los senolíticos y con estudios realizados por nuestro grupo en los cuales la sobreexpresión de BCL-XL reduce marcadores de senescencia celular. En resumen, aunque no observamos diferencias en senescencia celular, la sobreexpresión de BCL-XL mejora la supervivencia celular bajo condiciones hostiles mediante la prevención de apoptosis en células T de ratones jóvenes y adultos en cultivo y aumentando la respuesta autofágica a la inanición.

La disfunción mitocondrial es un rasgo distintivo del envejecimiento en un gran número de tipos celulares. Nuestros resultados muestran que el gasto general de oxígeno por parte de células T de ratones transgénicos es menor en comparación con las células T de ratones de fenotipo salvaje en condiciones basales. Al mismo tiempo, la producción de ATP, la respiración máxima y la capacidad respiratoria de reserva eran similares en células T de ambas cepas. Por tanto, las células T que sobreexpresan BCL-XL son capaces de mantener una demanda energética similar mediante el consumo de menos oxígeno. Por tanto, nuestros hallazgos sugieren que las células T de ratones transgénicos tienen una mejor eficiencia respiratoria, lo cual, de acuerdo con la teoría del envejecimiento *rate-of-living*, podría explicar el estado físico más saludable observado en estos ratones a edades avanzadas. Esta hipótesis

está reforzada por los menores niveles de fuga de protones observados en células T de ratones transgénicos. Sin embargo, este efecto se pierde con el aumento de la edad, y la razón por la cual esto ocurre aún se desconoce. Resultados similares se han observado en otros tipos celulares, como neuronas, en las cuales se ha reportado que BCL-XL disminuye el consumo de oxígeno mitocondrial, indicando un acoplamiento mejor y más eficiente de la producción de ATP a la toma de oxígeno.

Como perspectiva general de los antecedentes, en estudios previos realizados por nuestro grupo se descubrió que BCL-XL se encuentra regulado al alza fisiológicamente en centenarios, los cuales se consideran modelos de envejecimiento saludable. También estudiamos la sobreexpresión de BCL-XL en células primarias, nematodos y moscas. En los estudios *in vitro*, BCL-XL disminuía la senescencia celular y mejoraba la función inmune. El gen ortólogo de BCL-XL, ced-9, incrementaba la esperanza de vida media y máxima en *Caenorhabditis elegans*. En *Drosophila melanogaster*, la sobreexpresión de BCL-XL incrementaba la esperanza de vida y mejoraba el comportamiento locomotor. En la presente tesis, estudiamos el efecto de la sobreexpresión de BCL-XL en el ratón *Mus musculus*. En resumen, nuestros hallazgos muestran que los ratones que sobreexpresan BCL-XL exhiben menor fragilidad acompañada de un menor declive del rendimiento físico y una mayor actividad, mantienen una composición corporal juvenil, y muestran una mejor tolerancia a la glucosa a edades avanzadas. Dada la correlación entre un buen estado de salud físico y la función inmune en adultos mayores, creemos que este efecto beneficioso podría atribuirse a una mejor función de las células T. Acorde con nuestra hipótesis, las células T

de ratones transgénicos son más abundantes, exhiben una mejor respuesta al estrés y muestran una mejor eficiencia respiratoria mitocondrial.

Teniendo en cuenta las teorías del envejecimiento descritas en la introducción, nuestros resultados indican que el proceso de envejecimiento puede ser modulado genéticamente por BCL-XL (teoría de los genes de la longevidad) mediante la mejora de la función inmune de las células T (teoría inmunológica) en términos de mejorar la eficiencia respiratoria por la reducción del consumo de oxígeno (teoría *rate-of-living*), y por tanto minimizando la probabilidad de generar especies reactivas del oxígeno (teoría de los radicales libres), mientras se mantiene la función mitocondrial (teoría mitocondrial). Por tanto, nuestros hallazgos sugieren que la sobreexpresión de BCL-XL en células T podría promover el envejecimiento saludable en nuestro modelo de ratón.

CONCLUSIONES

La conclusión general de esta tesis es que BCL-XL previene la fragilidad y promueve el envejecimiento saludable en ratones transgénicos que sobreexpresan la forma humana de esta proteína en células T.

Las conclusiones específicas del estudio son: 1) Los ratones que sobreexpresan BCL-XL muestran un mejor estado de salud física debido a la atenuación del declive del rendimiento físico con la edad, el incremento de la actividad espontánea y la prevención de fragilidad en

comparación con ratones de fenotipo salvaje a edades avanzadas; 2) Los ratones que sobreexpresan BCL-XL exhiben parámetros relacionados con el metabolismo mejorados debido a la mantención de la composición corporal y la mejor tolerancia a la glucosa a edades avanzadas en comparación con ratones de fenotipo salvaje, pero no muestran diferencias de ingesta o metabolismo respiratorio; 3) Las células T aisladas de ratones que sobreexpresan BCL-XL exhiben una función celular mejorada siendo más resistentes a la apoptosis bajo condiciones estresantes, mostrando una mejor respuesta autofágica a la inanición y teniendo menor consumo de oxígeno y fuga de protones, sin diferencias en la senescencia celular, potencial de membrana mitocondrial, producción de ATP, respiración máxima y capacidad respiratoria de reserva en comparación con células T aisladas de ratones de fenotipo salvaje.

I. INTRODUCTION

1. THE AGING PROCESS

1.1. Definition of aging

Aging is an inevitable, intrinsic, progressive, and deleterious multifactorial phenomenon that refers to the progressive loss of an individual's physical, mental and cognitive health throughout life, leading to impaired physiological functions and increased vulnerability to morbidity and mortality (Viña, Borrás and Miquel, 2007; López-Otín *et al.*, 2013; Chang *et al.*, 2019). This biological process is accompanied by a loss of homeostasis, which is the condition of stability required for the minimal functionality of the different systems of our body (Rodrigues *et al.*, 2021).

The process of aging is considered the result of the gradual accumulation of damage at the cellular and molecular levels and is also the major risk factor for several pathologies, including cardiovascular diseases, cancer, diabetes, and neurodegenerative diseases (López-Otín *et al.*, 2013; Chang *et al.*, 2019). These diseases that accumulate with increasing age are defined as age-related diseases (ARDs). Although aging has been a subject of study for several decades, it is still one of the less-known biological processes due to its complexity.

1.2. Theories of aging

A large number of aging theories have been described to date, and the number continues to grow as new advances in the field are made (Viña *et al.*, 2013; Borrás, 2021). In addition, several authors have proposed integrated theories by connecting other existing theories (Carpenter,

1968). Nonetheless, neither of them appears to fully explain the aging process as some pieces of the aging puzzle are still missing (Troen, 2003; Jin, 2010). In this section, we will summarise the theories of aging that are most relevant to this thesis.

1.2.1. Longevity genes theory of aging

Several studies in nematodes, fruit flies, and mice have demonstrated that maximal lifespan can be controlled genetically as single genetic mutations can significantly change the aging rate (Troen, 2003). These gene products have a variety of functions, including modulating stress response, sensing nutritional status, increasing metabolic capacity, and silencing genes that promote aging.

The first longevity gene that greatly increased lifespan (i.e., age-1) was discovered in mutants of the worm *Caenorhabditis elegans* (Friedman and Johnson, 1988). Many other genes (daf-2, daf-12, daf-18, daf-23) were discovered over the next decade that, when mutated, increased the worm's mean and maximum life span (Jazwinski, 1996; Brys, Vanfleteren and Braeckman, 2007). These genes are major players in the physiological process of metabolic control and stress resistance. Moreover, many of these genes participate in the evolutionarily conserved insulin-IGF-1 signalling pathway, which regulates glucose and insulin homeostasis and plays a pivotal role in aging and longevity (Anisimov and Bartke, 2013; Sasako and Ueki, 2016).

Recently, more genes have been related to aging and ARDs, such as P66Shc, the mammalian target of rapamycin (mTOR), sirtuins, and BECLIN-1 (Liberale *et al.*, 2020). For instance, mice lacking cardiac-

specific mTOR developed fatal cardiomyopathy with apoptosis and premature death (Mazelin *et al.*, 2016). Sirtuins, on the other hand, are a highly conserved family of proteins implicated in nicotinamide adenine dinucleotide (NAD)-dependent reactions that regulate cell function and responses to stressors (Kida and Goligorsky, 2016). These proteins have been shown to play important roles in the modulation of oxidative stress, inflammation, autophagy, cellular senescence, and apoptosis (Favero *et al.*, 2015) through the regulation of the AKT signalling pathway (Pillai, Sundaresan and Gupta, 2014). Finally, the deletion of BECLIN-1, a protein implicated in macroautophagy, has been associated with defective autophagy and shortened lifespan (Meléndez *et al.*, 2003).

1.2.2. Immunological theory of aging

The immunological theory of aging states that the immune system deteriorates progressively over time, increasing vulnerability to infections, several types of cancer, and, as a result, aging and death (Jin, 2010). This theory was first described by Roy L. Walford in the 60s and postulates that the aging phenomenon is the result of auto-immune reactions caused by a loss of recognition patterns due to increased immunogenetic diversification (Walford, 1964). This diversification, which occurs progressively with age, could be the result of spontaneous somatic mutations or aggressions in the immunological tolerance homeostatic control.

This theory has been constantly updated with scientific advances in the field. The decline in the immune system with age was later associated with replicative senescence (Effros, 2005). Human immune cells, and more specifically, T cells, undergo replicative senescence in cell culture

(Perillo *et al.*, 1989, 1993) and show increased cell cycle inhibitor proteins, reduced response to stress, telomere shortening, and resistance to apoptosis (Guimarães *et al.*, 2021). The absolute number of T cells decreases with age as well as T cell activation by macrophages (Castelo-Branco and Soveral, 2013). In addition, the T cell function is altered in old compared to young individuals from different species (Pawelec *et al.*, 2002). Furthermore, a large body of evidence suggests that decreased $CD4^+$ and $CD8^+$ T cell function contributes significantly to the immune system senescence associated with aging (Gruver, Hudson and Sempowski, 2007).

The role of the immune system in various ARDs has been widely described. Moreover, the immune response decline contributes to an increase in the prevalence of various chronic diseases with a low-grade inflammatory activity at advanced ages (i.e. inflammaging) (Pawelec *et al.*, 2002; Fulop *et al.*, 2014; Franceschi *et al.*, 2017). The concept of immunosenescence has been recently coined as the process by which the immune system deteriorates over time, leading to increased inflammation and vulnerability to infectious diseases (Figure 1) (Castelo-Branco and Soveral, 2013; Lian *et al.*, 2020).

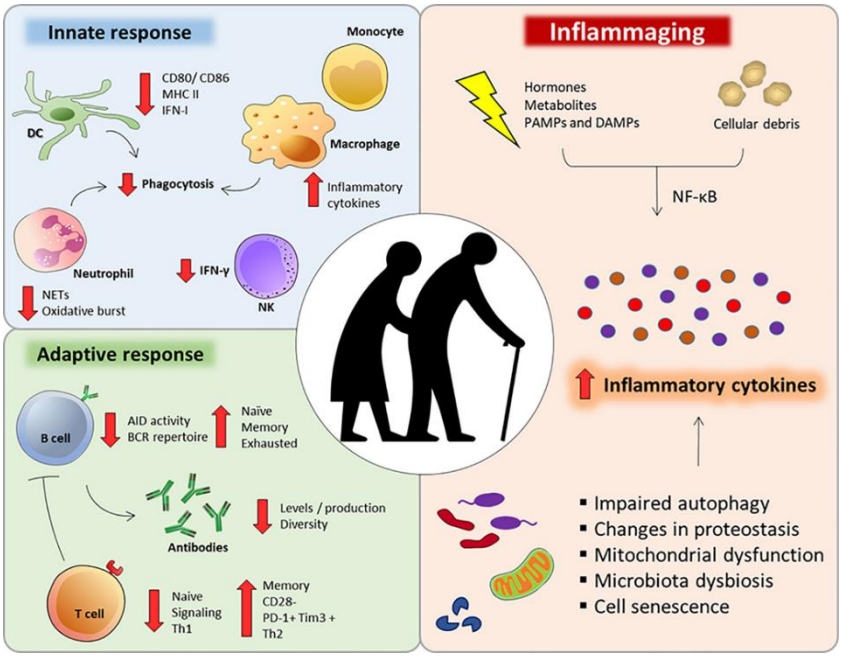

Figure 1. Major immunological alterations observed during immunosenescence. From (Pietrobon, Teixeira and Sato, 2020).

1.2.3. Rate-of-living theory of aging

The rate of living theory of aging states that the lifespan of a living being is determined by oxygen consumption, being animals with a greater rate of oxygen consumption the ones with a shorter life span (Jin, 2010). This theory was first postulated by Rubner & Pearl in the early 21st century (Pearl, 1928). The authors saw that the average mass-specific metabolic rate was inversely proportional to lifespan by comparing different species of mammals. Both man and mouse expend approximately 700 calories per gram of tissue throughout their lives; however, the mouse expends its energy at roughly thirty times the rate that man does, and thus lives a correspondingly shorter time (Carpenter, 1968).

Some authors have linked the idea of Hayflick's replicative senescence with the rate-of-living hypothesis since there may be a limit to how many times a stem cell can divide (Krishnamurthy and Sharpless, 2007). This theory has been also linked with caloric restriction studies, which is one of the few interventions to date that appears to successfully result in increased lifespan (Speakman *et al.*, 2002). Caloric restriction reduces energy intake, total daily energy demands, and body mass; thus, producing an overall reduction in metabolism. Consequently, it is easy to assume that the effect of caloric restriction in aging is due to, to some extent, a reduction of the metabolic rate. However, this theory fails to explain the aging process in animals of the same size but in different taxa that exhibit higher metabolic rates and yet, live longer (e.g., birds) (Vaanholt *et al.*, 2015).

1.2.4. Free radicals and the mitochondrial theory of aging

This theory was originally described by Dr. Gerschman in 1954 but was later developed by Dr. Denham Harman (Harman, 1956). In brief, the free radical theory of aging states that highly reactive molecular species with impaired electrons (i.e., free radicals) accumulate in cells, causing damage to the macromolecular components of the cell and leading to organism malfunction (Jin, 2010).

Our cells produce superoxide anion ($\cdot O^{2-}$) and hydrogen peroxide (H_2O_2) during aerobic metabolism, which are radical oxygen species (ROS) that can, in turn, form the extremely reactive hydroxyl radical ($HO\cdot$) (Fridovich, 1978; Troen, 2003). Although these radicals at low concentrations play important roles in several physiological processes (e.g., the regulation of gene expression, cell division and differentiation,

apoptosis, and cell death), they accumulate with age, causing oxidative stress in our cells and eventually, leading to oxidative damage, cell malfunction and organ failure.

Later on, this theory was updated as the mitochondrial free radical theory of aging, which postulates that mitochondria are the main source of intracellular ROS and the accumulation of these species leads to mitochondrial DNA mutations (Cui, Kong and Zhang, 2012). Electrons that leak from the electron transport chain (ETC) can produce short-lived radicals as $\cdot O^{2-}$ which can be later converted to more stable forms like H_2O_2, which is permeable to the membrane and can easily diffuse within the cell, causing cellular damage outside the mitochondria. Although this theory is still one of the most popular ones, it fails to fully explain the aging process as oxidative damage is not the only type of damage that accumulates with age (Gladyshev, 2014).

1.3. The aging phenotype

The aging phenotype is the result of a variety of stochastic, environmental, and molecular events that negatively affect our bodies throughout our lives (Colloca *et al.*, 2020). These negative effects, widely known as hallmarks of aging, are manifested at different levels of the organism and are commonly quantified to evaluate interventions aiming to prevent ARDs and promote lifespan. Several hallmarks of aging have been described in different cell types, organs, and the overall organism (Rebelo-Marques *et al.*, 2018; Picca *et al.*, 2019). The most relevant hallmarks of aging were described by López-Otín in 2013 and include senescence, loss of proteostasis, deregulated nutrient sensing, and

mitochondrial dysfunction, among others (López-Otín *et al.*, 2013). The interaction of these changes at the cellular level results in changes at the organism level such as physical and cognitive decline, inflammation, immunodeficiency, and frailty (Fulop *et al.*, 2010; Pera *et al.*, 2019). Figure 2 shows features of the aging phenotype which are most relevant based on this study. The following sections provide greater detail about these features.

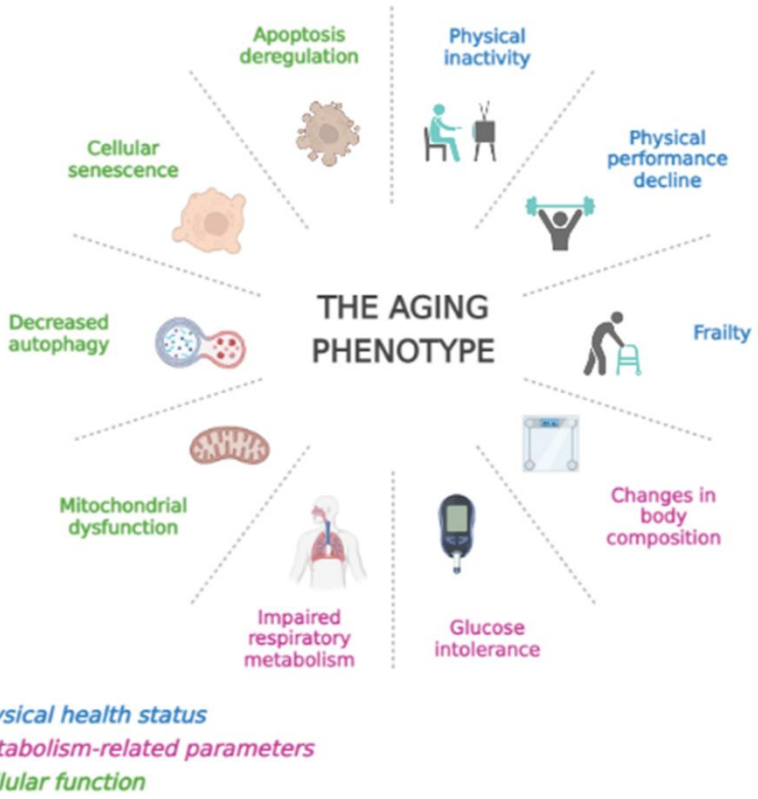

Figure 2. Features of the aging phenotype based on this study.
Created with BioRender.com.

1.3.1. Poor physical health status

1.3.1.1. Decreased physical activity

Physical activity refers to any movement produced by skeletal muscles that require energy expenditure during an individual's daily life (e.g., movement performed during leisure time, to move between places, or as part of a person's work) (Caspersen, Powell and Christenson, 1985). Physical activity is classically assessed with self-report questionnaires (Bondarev *et al.*, 2021), but more recent studies use accelerometers that enable physical activity monitoring for multiple days (Portegijs *et al.*, 2019).

Physical inactivity is known to be an important risk factor for chronic diseases, morbidity, and ultimately, mortality during aging. The prevalence of high-intensity activities decreases with age in adults, whereas the prevalence of reported inactivity increases with age (DiPietro, 2001; Milanović *et al.*, 2013). Moreover, physical activity decline is also observed in other species, including rodents, which decrease their overall activity levels by approximately 50% after the adult age range (Sallis, 1999). Similarly, increased physical activity has been associated with a lower incidence of several chronic ARDs and has been demonstrated to prevent overweight, bone loss, falls, and hip fracture.

1.3.1.2. Physical performance decline

In contrast to physical activity, which is related to the movement that an individual performs daily, we refer to physical performance as a set of athletic capabilities and health-related components including muscular strength, exercise endurance, balance, and coordination (Caspersen, Powell and Christenson, 1985; Pate, 1988). Physical performance is frequently measured as walking speed, muscle strength, and aerobic capacity in older humans (Portegijs *et al.*, 2019; Bondarev *et al.*, 2021). Similar methods are also used in experimental animals using treadmills, dynamometers, and other apparels adapted for each species.

Several studies demonstrate the association of decreased physical performance with aging in a variety of species, including worms (Hahm *et al.*, 2015), flies (Moretti *et al.*, 2020), mice (Ge *et al.*, 2016; Bartling *et al.*, 2017; Muhammad and Allam, 2018) and humans (Herndon *et al.*, 2002; Hollmann *et al.*, 2007; Hebert *et al.*, 2015). Lower muscle strength, running speed, and endurance (or aerobic capacity) are also associated with several age-related pathologies (Berthelot *et al.*, 2019; Grevendonk *et al.*, 2021). This is the case for cognitive-related diseases, such as dementia (Bullain *et al.*, 2013), dyspnea (de Fátima Ribeiro Silva *et al.*, 2020), and type 2 diabetes (Gregg, Engelgau and Narayan, 2002).

1.3.1.3. Frailty

Physical frailty (hereafter referred to as frailty) is defined as a clinical syndrome with a distinct phenotype associated with a decreased reserve and high vulnerability to stressors, as well as a risk of adverse outcomes, including death (Fried *et al.*, 2021). The frailty phenotype was first described in 2001 by L. Fried and colleagues with five parameters: 1) unintentional weight loss, 2) self-reported exhaustion, 3) low energy expenditure, 4) slow gait speed, and 5) weak grip strength (Fried *et al.*, 2001). Since then, several different definitions and indexes have been developed including different symptoms and deficits to assess frailty in humans (Mitnitski, Mogilner and Rockwood, 2001; Rockwood and Mitnitski, 2007; Leng, Chen and Mao, 2014; Antoch *et al.*, 2017) and rodents (Liu *et al.*, 2014; Howlett, 2015; Gomez-Cabrera *et al.*, 2017; Bisset and Howlett, 2019; Heinze-Milne, Banga and Howlett, 2019; Baumann, Kwak and Thompson, 2020).

Frailty emerges as a result of cumulative declines in multiple systems, including stress response systems, energy metabolism (e.g., glucose intolerance and insulin resistance), and musculoskeletal function (e.g., energy utilization efficiency and mitochondrial function), as well as underlying biological drivers (Clegg *et al.*, 2013; Colloca *et al.*, 2020; Fried *et al.*, 2021) (Figure 3). Most importantly, frailty is a reversible condition (Viña, *et al.*, 2016; Chen, Gan and How, 2018; García-Giménez *et al.*, 2021). Nowadays, the L. Fried criteria for frailty are still the most frequently used and its prognostic capacity has been extensively validated (Viña, *et al.*, 2016).

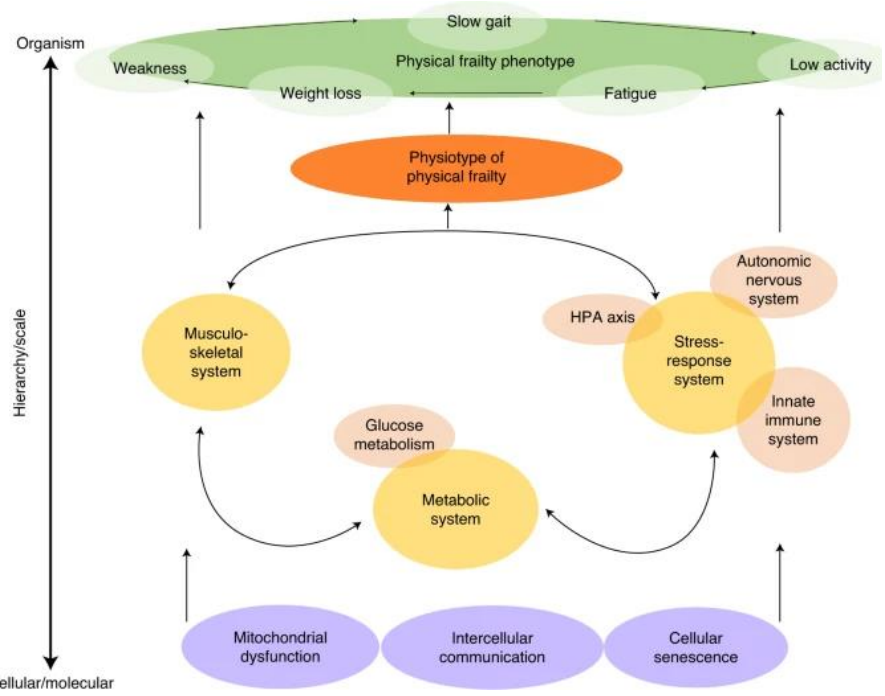

Figure 3. A hierarchical, multiscale representation of the physiological dysregulation and likely biological drivers of physical frailty.
From (Fried *et al.*, 2021).

Altogether, physical inactivity, performance decline, and frailty have been widely associated with ARDs, adverse clinical outcomes, and death (Fried *et al.*, 2001; Jones, Song and Rockwood, 2004; Fulop *et al.*, 2010; Schultz *et al.*, 2020). Moreover, these parameters seem to predict lifespan (i.e. amount of time an individual lives) and, more importantly, healthspan (i.e. amount of time an individual lives without disease) (Ingram, 2000; Palliyaguru *et al.*, 2019). Similarly, interventions with physical exercise have shown many beneficial effects in several pathological conditions affecting the elderly (Viña, *et al.*, 2016; Rebelo-Marques *et al.*, 2018), including chronic inflammation (Nicklas and Brinkley, 2009) and cognitive impairment (Tarazona-Santabalbina *et al.*, 2016). Indeed,

exercise has proven to be an efficient and cost-effective method to prevent the functional capacity decline in older people (Cvecka *et al.*, 2015). Hence, physical inactivity, physical performance decline, and frailty can be considered key features of the aging phenotype.

1.3.2. Metabolic deregulation

1.3.2.1. Changes in body composition

Body composition is a very well-known factor that influences organism metabolism as it provides information about the human body's nutritional status as well as its functional capacity. Changes in body composition occur when there is an imbalance between nutrient intake and energetic requirement (Kuriyan, 2018), with a positive energy balance leading to weight gain while a negative one results in weight loss (St-Onge and Gallagher, 2010).

Total body mass is observed to decrease with increasing age in humans (Manini, 2010), although this relationship seems to be inverted in rodents (Glatt *et al.*, 2009; McDonald *et al.*, 2011). Nonetheless, body composition changes during aging are well documented even in the absence of changes in total body weight (St-Onge and Gallagher, 2010). As a general rule observed in mammals, lean body mass decreases with age, whereas fat body mass increases (Vaughan, Zurlo and Ravussin, 1991; Speakman, Acker and Harper, 2003; St-Onge and Gallagher, 2010; Reynolds *et al.*, 2019). In humans, loss of muscle mass (i.e. sarcopenia) and excessive fat accumulation (i.e. obesity) are major causes of functional decline and disability in older adults (Evans and Campbell, 1993; Walston, 2012;

Mesinovic *et al.*, 2019). Still, some studies have observed no significant variation through lifespan (O'Connor *et al.*, 2002).

1.3.2.2. Impaired respiratory metabolism

In addition to changes in body composition, alterations in respiratory quotient (RQ) and energy expenditure (EE) also occur as we grow older, although the underlying mechanisms are less understood (Rizzo *et al.*, 2005; Bartke *et al.*, 2021). On the one hand, RQ is defined as a dimensionless number calculated as the volume of released carbon dioxide divided by the volume of absorbed oxygen during respiration and is used as an indirect estimation of the EE (Patel, Kerndt and Bhardwaj, 2022). On the other hand, total EE is comprised of three major components: i) resting (i.e., basal) metabolic rate, which is affected by body composition, sex, and age; ii) the thermic effect of food, which refers to the energy consumed for food intake, digestion, absorption and nutrient storage; and iii) the EE associated to physical activity, which can vary significantly between individuals (Lam and Ravussin, 2016).

Changes in body composition are normally associated with changes in food intake and energy homeostasis. Lower EE and intake are observed with age in humans (Das *et al.*, 2001; Westerterp and Meijer, 2001; St-Onge and Gallagher, 2010) and mice (Joly-Amado *et al.*, 2016; Azzu and Valencak, 2017). Additionally, previous studies have shown that old C57BL/6J mice have higher RQ levels than young mice, indicating a preference for carbohydrate rather than fat utilization at advanced ages (Arc-Chagnaud *et al.*, 2021).

1.3.2.3. Glucose intolerance

Glucose metabolism is also altered during aging. In that regard, glucose tolerance is known to decline with age (de Fronzo, 1981), leading to type 2 diabetes mellitus and increased risk of cardiovascular diseases (Chia, Egan and Ferrucci, 2018). The primary cause of glucose intolerance in the elderly is a decreased insulin effect in the tissues mainly due to diminished insulin secretion and increased cellular resistance to insulin (Basu *et al.*, 2003). A similar decline is seen in rodents, exhibiting decreased glucose tolerance, and increased fasting glycemia in aged animals (Ueda *et al.*, 2000; Reynolds *et al.*, 2019).

Age-related changes in glucose metabolism are commonly accompanied by changes in body composition and energy metabolism. Moreover, these changes are closely related to the individual's physical activity (Vaughan, Zurlo and Ravussin, 1991; Westerterp and Meijer, 2001). In this sense, exercise training interventions have been shown to prevent age-related metabolism changes (Grevendonk *et al.*, 2021). Thus, studying these parameters along with the physical fitness parameters simultaneously allows for a comprehensive understanding of other organisms' overall health.

1.3.3. Compromised cellular function

1.3.3.1. Impaired response to stress

The inability to cope with stress is one of the most important aspects that contribute to the aging phenotype. Cells rely on several response mechanisms when damage is accumulated inside them (Vicencio *et al.*,

2008). They can degrade damaged subcellular components (i.e., autophagy), enter a permanent state of growth arrest (i.e., senescence), or trigger a cell death program (i.e., apoptosis) (Figure 4). These mechanisms can be activated in response to different stressors, including fasting, oxidative stress, DNA damage, and mitochondrial damage (Di Micco *et al.*, no date; Campisi and D'Adda Di Fagagna, 2007; Galluzzi *et al.*, 2008; Childs *et al.*, 2014).

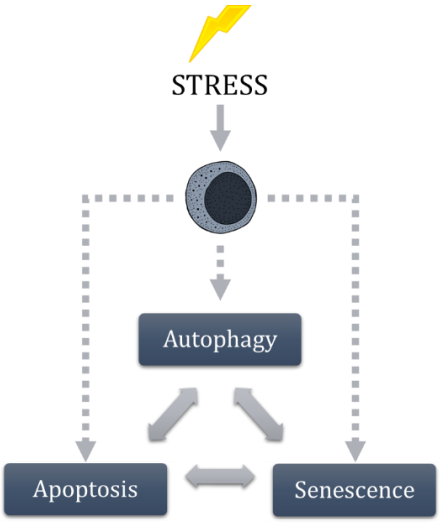

Figure 4. Mechanisms of the cellular stress response.

Although the interplay between autophagy, apoptosis, and senescence is not fully understood (Pawlowska *et al.*, 2018), several studies have suggested a cross-talk between the tumor suppressor P53 and the AKT/mTOR pathway that would eventually decide cell fate (Vicencio *et al.*, 2008; Strozyk and Kulms, 2013; Li *et al.*, 2016). Ultimately, these mechanisms are well-described cellular survival pathways that are found altered in aged individuals and are frequently used as markers of the aging phenotype.

1.3.3.1.1. Autophagy

Autophagy involves lysosomes for the degradation and recycling of cytoplasmic components by three described routes: macroautophagy, chaperone-mediated autophagy, and microautophagy. In this thesis, we focus on macroautophagy (hereafter referred to as autophagy), a process in which a double membrane vesicle (i.e., autophagosome) engulfs macromolecules in bulk (e.g., portions of the cytoplasm, organelles, and proteins) and fuses with lysosomes to form autolysosomes, where the content is ultimately degraded and recycled (Rubinsztein, Mariño and Kroemer, 2011; Cheon *et al.*, 2019). Autophagy is normally maintained at low levels under physiological conditions and increases in response to a wide range of stress stimuli (Russo, Bono and Ghigo, 2021).

During aging, a diminished autophagic activity is observed (Cheon *et al.*, 2019; Wong *et al.*, 2020) accompanied by the accumulation of autophagosomes and defective vesicular trafficking (Kaushik *et al.*, 2021). The decline of autophagic activity in aged cells is likely to compromise the ability of cells to degrade aberrant proteins, aggregates, or defective organelles (Escobar *et al.*, 2019); thus, contributing to a progressive accumulation of cellular waste that could ultimately lead to loss of cellular function, senescence or even cell death. Indeed, autophagy dysfunction is known to shorten lifespan, whereas autophagy restoration contributes to lifespan and healthspan in several animal models (Aman *et al.*, 2021). Similarly, interventions to attenuate the aging phenotype in different experimental models have been demonstrated to also stimulate autophagy (Cuervo *et al.*, 2005).

1.3.3.1.2. Senescence

Cellular senescence refers to the permanent and irreversible state of cell cycle arrest characterized by the increase of the senescence-associated β-galactosidase (SA-β-GAL) enzymatic activity, resistance to apoptosis, and the activation of the senescence-associated secretory phenotype (SASP) (Van Deursen, Deursen and Van Deursen, 2014; Childs *et al.*, 2015). The secretion of SASP has been identified as a major effector of the senescent cells as it contains several molecules (e.g., inflammatory cytokines, chemokines, and growth factors) that may spread senescence to neighboring cells (Di Micco *et al.*, no date; Herranz and Gil, 2018).

In physiological conditions, senescent cells contribute to the organism's development and survival by maintaining tissue homeostasis and limiting tumor progression (Kumari and Jat, 2021). However, these cells can accumulate in aged tissues, causing a variety of deleterious effects (e.g. chronic inflammation and stem cell exhaustion) and contributing to the aging process *per se* (Campisi and D'Adda Di Fagagna, 2007; Vicencio *et al.*, 2008; Kumari and Jat, 2021). Consequently, the selective elimination of senescent cells has been found to delay age-related dysfunction and extend lifespan.

1.3.3.1.3. Apoptosis

Apoptosis is a process of programmed cell death that serves to eliminate unwanted cells and regulate cell populations (Carthy *et al.*, 2003). Two major apoptotic pathways have been described to date: the death receptor pathway (i.e. extrinsic), and the mitochondrial pathway (i.e. intrinsic) (Zhang and Herman, 2002; Elmore, 2007). Although triggered by different signals, both pathways converge in the activation of caspase 3, which activates a cascade of molecular events that will eventually result in chromatic and cytoplasmic condensation, nuclear fragmentation, the formation of the apoptotic bodies and, consequently, cell death.

Apoptosis is deregulated during aging (Lu *et al.*, 2012), and is a determining factor in several ARDs such as neurodegenerative diseases (Zhang and Herman, 2002; Tower, 2015). On the one hand, accumulating evidence suggests that apoptosis is upregulated in aged tissues and organs (Muradian and Schachtschabel, 2001; Tower, 2015). On the other hand, increased resistance to apoptosis has been shown in cancer and senescent cells, contributing to the aging process (Salminen, Ojala and Kaarniranta, 2010). Moreover, several studies have found a reduced apoptotic response to different stressors in aged cells (Polyak *et al.*, 1997; Suh *et al.*, 2002). Thus, the mechanism by which apoptosis contributes to the aging process remains controversial.

1.3.3.2. Mitochondrial dysfunction

Mitochondrial dysfunction is commonly thought to be caused by oxidative damage, which causes flaws in the ETC (Conley, Marcinek and Villarin, 2007). In physiological conditions, the electron transfer is coupled with the proton transfer across the inner mitochondrial membrane to generate the mitochondrial membrane potential ($\Delta\psi m$) required for ATP synthesis (Moro, 2019). However, electron leakage can occur in dysfunctional mitochondria, resulting in the production of ROS. With age, mitochondrial DNA (mtDNA) mutations and deletions accumulate whereas mtDNA abundance declines, leading to mitochondrial dysfunction (Cui, Kong and Zhang, 2012). Moreover, increased mitochondrial uncoupling (i.e., lower ATP produced per O_2 uptake) is observed in human cells long before the accumulation of irreversible DNA damage (Conley, Marcinek and Villarin, 2007).

Mitochondria play an important role in ARDs, particularly in neurodegenerative diseases (e.g., Alzheimer's disease, Parkinson's disease, and Huntington's disease), associated with an increase in oxidative damage (Cui, Kong and Zhang, 2012). Additionally, mitochondria are major regulators of intrinsic apoptosis as it is dependent on the permeability transition pore formation, which allows cytochrome c release towards the cytosol (Sastre *et al.*, 2002). Thus, dysfunctional mitochondria exhibit a lower $\Delta\psi m$ and a diminished respiratory capacity and are more likely to produce more ROS, which leads to decreased ATP production and the release of pro-apoptotic factors such as cytochrome c (Figure 5).

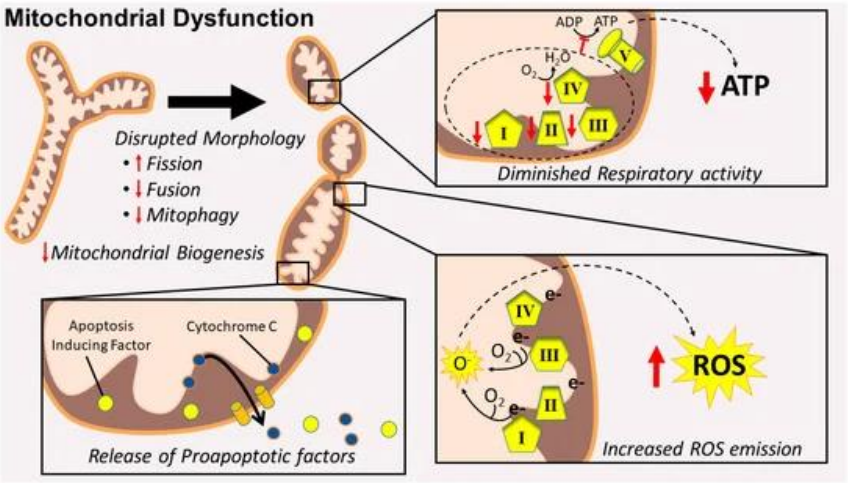

Figure 5. Mitochondrial dysfunction.
From (Hyatt and Powers, 2021).

2. THE BCL-XL PROTEIN

2.1. BCL-XL encoding gene

B-cell lymphoma-extra large (BCL-XL) protein belongs to the BCL-2 protein family and is encoded by the human *BCL-2-Like protein 1* (*BCL2L1*) gene. This gene was first identified in 1993 as a BCL-2-independent regulator of apoptotic cell death (Boise *et al.*, 1993), and is located in chromosome 20 (20q11.21) (Borrás *et al.*, 2020) (Figure 6). In mice, the ortholog of this gene is in chromosome 2. BCL-2 family members are commonly classified into three main categories: the anti-apoptotic proteins (e.g., BCL-2, BCL-XL, BCL-W, A1, and MCL1), pro-apoptotic proteins (e.g., BAX, BAK, and BOK/MTD) and BH3-only proteins (e.g., BID, BIM/BOD, BAD, PUMA/BBC and NOXA) (Chipuk *et al.*, 2010; Banjara *et al.*, 2020).

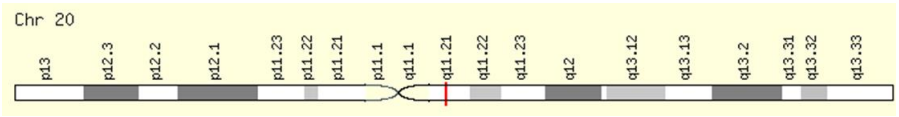

Figure 6. Genomic location of human BCL2L1 gene.
From GeneCards.

The *BCL2L1* gene encodes two known messenger RNAs (mRNAs) by alternative splicing of BCL-X: BCL-XL (anti-apoptotic), which is the larger and more abundant form, and BCL-XS (pro-apoptotic), which is the shorter form (Boise *et al.*, 1993; Stevens and Oltean, 2019). Interestingly, BCL-XS is not detected in murine T cells (Sevilla *et al.*, 2001). More information about the *BCL2L1* gene can be found on the GeneCards® website (https://www.genecards.org).

2.2. BCL-XL structure and location

The human BCL-XL protein contains a hydrophobic C-terminal region and four BCL-2 Homology (BH) motifs (BH1-BH4), which are conserved regions of sequence homology (Lee and Douglas Fairlie, 2019; Banjara *et al.*, 2020; Borrás *et al.*, 2020). These domains are arranged in a total of eight alpha-helical regions (α1- α8), two of which (α5 and α6) constitute an inner hydrophobic nucleus flanked by the other amphipathic helices (α3 and α4 on one side, and by α1, α2 and α8 on the other side) (Muchmore *et al.*, 1996; Warren, Wong-Brown and Bowden, 2019). Figure 7 shows BCL-XL primary, secondary and tertiary structures.

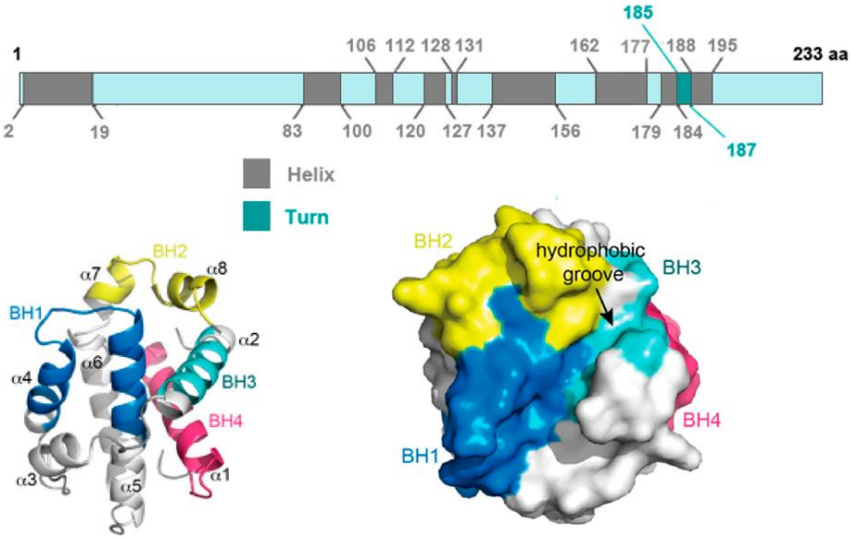

Figure 7. BCL-XL protein structure.

Adapted from (Borrás et al., 2020; Lee & Douglas Fairlie, 2019).

BCL-XL was initially reported to be located in the outer mitochondrial membrane, and later on, in the inner membrane too (Belzacq *et al.*, 2003; Borrás *et al.*, 2020), anchored by their hydrophobic C-terminal membrane domain (Zhou, Yang and Xing, 2011). BCL-XL can also be found in the endoplasmic reticulum (ER) (Popgeorgiev, Jabbour and Gillet, 2018) and as a soluble form in the cytosol (Jia *et al.*, 1999). According to the Genecards database, BCL-XL may locate in the mitochondrial matrix, different parts of the cytoskeleton, several types of vesicles, and the nucleus membrane as well.

2.3. BCL-XL protein functions

BCL-XL functions have traditionally been related to cell fate and survival. Apoptosis, senescence, and autophagy are well-known cell survival mechanisms. Although apoptosis suppression was the first identified BCL-XL function, recent evidence indicates a major role in autophagy and senescence pathways as well. The following sections go into greater detail about the role of BCL-XL in these cell survival pathways.

2.3.1. BCL-XL in apoptosis

The first role described by the BCL-XL protein was the inhibition of cell death in absence of a growth factor in an IL-3-dependent cell line (Boise *et al.*, 1993). This is the most well-known function of BCL-XL to date. BCL-XL regulates the intrinsic apoptotic pathway along with the other BCL-2 family proteins in the mitochondria (Tsujimoto, 1998; Huska, Lamb and Hardwick, 2019). Following the death signal, intrinsic apoptosis is regulated by the interaction between pro-apoptotic (e.g., BAK, BAX, and BOC) and anti-apoptotic (e.g., BCL-2, BCL-XL, and A1) (Burlacu, 2003; Singh, Letai and Sarosiek, 2019; Dou *et al.*, 2021).

Following an apoptosis induction signal, the anti-apoptotic proteins are neutralized by BH3 domain-only proteins, and BAX and BAK are free to bind to the outer mitochondrial membrane where they form pores that cause permeabilization. This leads to the release of apoptosis activators from the mitochondria (e.g., cytochrome c, SMAC, and DIABLO) (Ola, Nawaz and Ahsan, 2011). In the cytosol, cytochrome c forms the apoptosome along with APAF-1 and caspase-9 to initiate caspase activation (Borrás *et al.*, 2020). BCL-XL can repress this pathway by

preventing the mitochondrial outer membrane permeabilization (MOMP) and the subsequent release of cytochrome c into the cytoplasm, which would eventually cause apoptosis (Breckenridge and Xue, 2004; Jacotot *et al.*, 2006; Billen *et al.*, 2008; Stevens and Oltean, 2019) (Figure 8). Moreover, apoptosis inhibition by BCL-XL is not solely due to its interaction with BAX and BAK, but also to the interception of upstream pro-apoptotic signals (e.g., BH3 only proteins and P53), its interaction with several MOMP promoters (e.g., the voltage-dependent anion channels), and the prevention of pro-apoptotic Ca^{2+} cytosolic signals generation (Michels *et al.*, 2013).

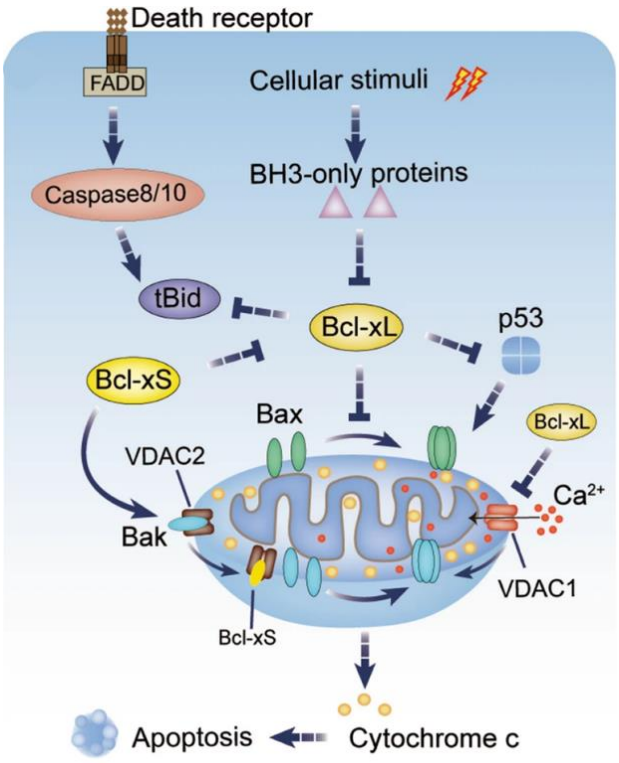

Figure 8. BCL-XL role in apoptosis.

Adapted from (Dou *et al.*, 2021).

2.3.2. BCL-XL in autophagy

Many signalling pathways that regulate apoptosis also regulate autophagy (Doherty and Baehrecke, 2018). Several molecular regulators of both pathways (e.g., Agt5 and Ca^{2+} signals) are interconnected by BCL-XL to eventually activate or suppress them (Zhou, Yang and Xing, 2011). BECLIN-1 is a key regulator of the lysosomal degradation pathway as it is essential during autophagosome formation. During the initial steps of autophagy, activation of class III PI3K regulators (e.g., hVPS34) by BECLIN-1 is required for the membrane elongation of the autophagosome precursor (Zhou, Yang and Xing, 2011).

In addition to apoptosis, BCL-XL is also able to regulate autophagy (Kim *et al.*, 2014) by direct interaction with the BH3 domain of BECLIN-1, preventing the formation of BECLIN-1-hVPS34 complex, thus, inhibiting autophagy (Pimkina *et al.*, 2009; Li *et al.*, 2020; Dou *et al.*, 2021) (Figure 9). In this sense, BH3-only proteins (e.g., BAD) and mimetic compounds (e.g., ABT-737) have been reported to induce autophagy by disrupting the interaction between BECLIN-1 and BCL-XL in a competitive manner (Maiuri *et al.*, 2007; Tian *et al.*, 2010). BCL-XL could also inhibit PINK1/PARKIN-dependent mitophagy by preventing the translocation of PARKIN from the cytoplasm into mitochondria.

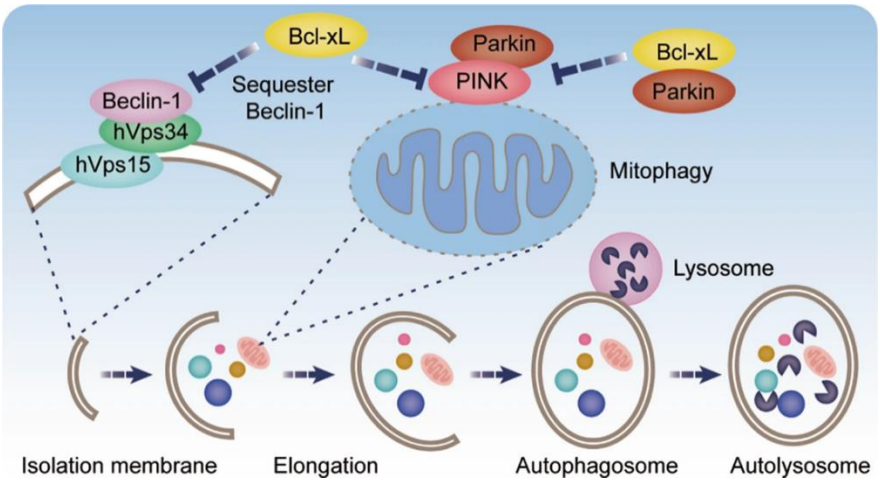

Figure 9. BCL-XL role in autophagy.
Adapted from (Dou *et al.*, 2021).

2.3.3. BCL-XL in senescence

Like apoptosis and autophagy, senescence is a cellular response to different stressors, and crosstalk between these three processes has been suggested by several authors. Even so, existing evidence describing BCL-XL function in cellular senescence is contradictory and not clearly understood. Given its ability to promote cell survival, BCL-XL is considered an oncogene (Adams and Cory, 2007). In this sense, several types of senescent cells exhibit high levels of BCL-XL, and the selective elimination of these cells has proven to have a wide range of beneficial effects (Zhu *et al.*, 2017; Mas-Bargues *et al.*, 2020; Robbins *et al.*, 2021). This is the case of the senolytic drugs targeting BCL-XL and other anti-apoptotic BCL-2 family members, such as ABT-263, ABT-737, and TW-37, which not only have proven to clear senescent cells (Zhu *et al.*, 2016; Fan *et al.*, 2020) but also reverse ARDs in murine models (Pan *et al.*, 2017).

In contrast with this data, there is also evidence suggesting a protective role of BCL-XL againsT cellular senescence. Overexpression of BCL-XL decreases several markers of senescence, including $P16^{INK4a}$, $P19^{Arf}$, $P21^{CIP}$, and SA-β-GAL, in mouse embryo fibroblasts (MEFs) and primary human lymphocytes (Borrás *et al.*, 2016). BCL-XL has also been found to inhibit P53-induced irreversible growth arrest in human bladder cancer cells by preventing ROS generation (Jung *et al.*, 2004). Similarly, up-regulation of BCL-XL expression has been shown to reduce senescence during megakaryocyte differentiation (Sanz *et al.*, 2001), and in pancreatic neoplasia (Ikezawa *et al.*, 2017). Thus, BCL-XL is likely to do both: promote and suppress cellular senescence.

In summary, BCL-XL can prevent mitochondrial-dependent apoptosis, suppress BECLIN-1-dependent autophagy, and promote or suppress cellular senescence depending on the cell type and physiological conditions (Figure 10). Therefore, BCL-XL could be considered a key regulator of cellular response to stress and cell survival mechanisms.

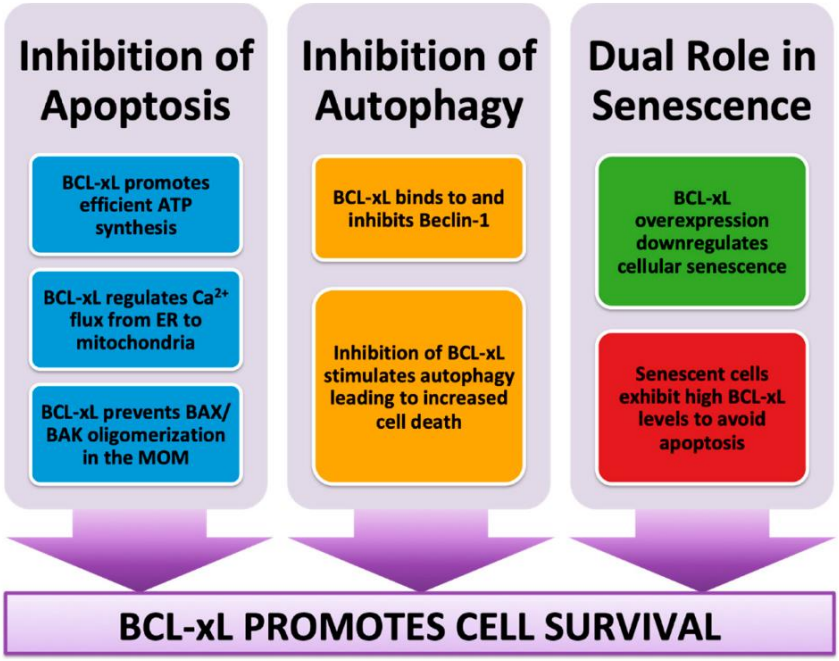

Figure 10. BCL-XL role in apoptosis, autophagy, and senescence.
From (Borrás *et al.*, 2020).

2.3.4. BCL-XL in mitochondrial function

In addition, to regulate mitochondrial-dependent apoptosis, BCL-XL has been demonstrated to play a major role in other mitochondrial functions that would ultimately promote cell survival. First, the mTOR signalling pathway is thought to regulate mitochondrial glycolytic and respiratory metabolism in a BCL-XL-dependent manner (Ramanathan and Schreiber, 2009). Second, BCL-XL is required for membrane potential stabilization across the inner mitochondrial membrane. In this regard, there is evidence suggesting that BCL-XL reduces futile ion flux across the inner mitochondrial membrane, thus, preventing a wasteful drain of cellular resources and energetic crisis during stress (Chen *et al.*, 2011).

Third, studies in rat hippocampal neurons indicate that BCL-XL interacts directly with the β-subunit of the F_1F_0 ATP synthase, decreasing ion leak and thereby increasing net transport of H^+ during F_1F_0 ATPase activity (Alavian *et al.*, 2011). Moreover, BCL-XL also proved to increase ATP synthesis under highly demanding energy conditions, and its effect was prevented after adding the BCL-XL inhibitor ABT-737.

Lastly, overexpression of anti-apoptotic proteins such as BCL-2 and BCL-XL prevents Ca^{2+} transfer from the endoplasmic reticulum (ER) to the mitochondria, promoting cell survival (Kaufman and Malhotra, 2014). Indeed, BCL-XL has been shown to enhance bioenergetics driven by inositol 1,4,5-trisphosphate receptor (IP_3R_3)-mediated Ca^{2+} signalling (Williams *et al.*, 2016). This emerging role of BCL-2 family proteins as major regulators of Ca^{2+} homeostasis gives a new approach to study BCL-XL as a key regulator of cell survival decision (Morris *et al.*, 2021) (Figure 11). Taken together, these data suggest an important role of BCL-XL in overall mitochondrial energetic efficiency and cell fate.

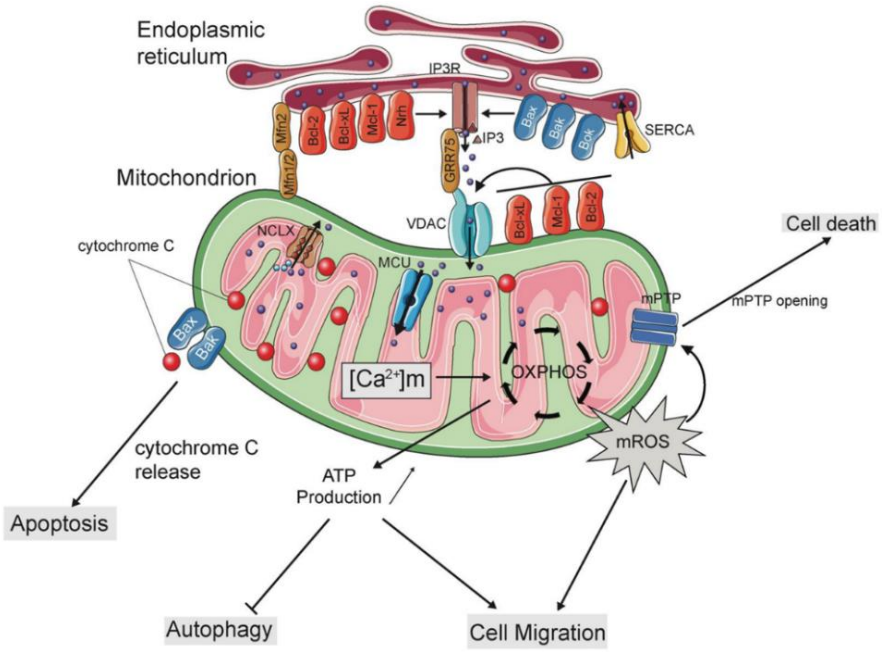

Figure 11. Schematic representation of ER to mitochondria Ca^{2+} regulation by Bcl-2 proteins.

From (Morris *et al.*, 2021).

3. INTERVENTIONS TO PROMOTE HEALTHY AGING: THE ROLE OF BCL-XL

3.1. Normal aging *versus* healthy aging

The aging process occurs at a different rate at different times and in different regions. To explain this heterogeneity among the elderly population, Rowe and Kahn proposed the distinction between normal aging and healthy aging (also known as successful aging) in 1987 (Rowe and Kahn, 1987). Hence, the concept of healthy aging emerges to identify elderly people with improved cognitive and physical function compared to healthy people of the same age. The definition of healthy aging has been revised by several authors, introducing new assessment methods (Li *et al.*, 2006; Michel and Sadana, 2017). However, there is no agreement on the definition of healthy aging nor standardized criteria for its evaluation.

3.2. The importance of promoting healthy aging

In the last century, the proportion of the elderly population has increased steadily and with that, the number of ARDs and disabilities have risen alarmingly, jeopardizing the sustainability of economic, social, and healthcare systems (Mas-Bargues, Borrás and Viña, 2021). The scenario described can be attributed to increased lifespans without a complementary delayed onset of ARDs, which implies more years of illness before death (Khaw, 1997). This dilemma has impulsed the focus on healthspan rather than lifespan in the research community (Seals, Justice and Larocca, 2016; Olshansky, 2018; Wickramasinghe *et al.*, 2020).

Understanding the biological mechanisms of aging would allow the development of effective interventions to slow the biological process of aging, and thus delay the aging phenotype (e.g., frailty, mitochondrial dysfunction, and impaired metabolism) and the onset of ARDs (Figure 12). These interventions would reduce the medical and social impact and improve the economic system. Hence, healthspan rather than lifespan has become the focus of study in gerontology.

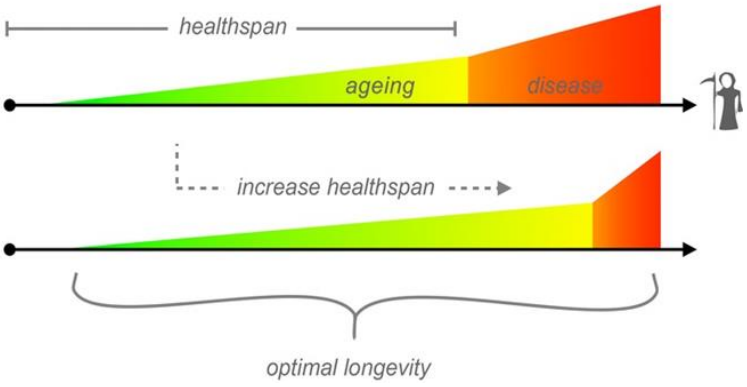

Figure 12. Increasing healthspan to promote healthy aging.
Adapted from (Seals, Justice and Larocca, 2016).

3.3. Centenarians as models of healthy aging

Centenarians are individuals who live extremely long lives, delaying or even escaping the onset of major ARDs. When compared to their contemporaries who died at younger ages, centenarians exhibit lower hospitalization rates, decreased length of stays in hospitals, and fewer comorbidities (Engberg *et al.*, 2009; Gellert *et al.*, 2018). Indeed, they maintain such remarkable health until their later years so that their

healthspan is comparable to their lifespan (Andersen *et al.*, 2012; C. Borrás *et al.*, 2020). For this reason, centenarians have been proposed as models of healthy aging (Franceschi *et al.*, 2017), and researchers across the globe have been testing different approaches to decipher the biology of these exceptional human beings.

Specific genetic variants associated with longevity have been identified in centenarians. One example is the variant of apolipoprotein E APOE4, which is hardly found in centenarians (Sebastiani and Perls, 2012). Additionally, they have been shown to overexpress pluripotency-related genes, including Yamanaka factors (i.e., OCT3/4, SOX2, C-MYC, KLF4) and other stemness-related genes, which may contribute to their longevity (Inglés *et al.*, 2019). Given the growing evidence of the genetic component of centenarians, it has been suggested that exceptional longevity is a hereditable trait (Caruso *et al.*, 2019).

Studies in centenarians have revealed unique features in immunological and endocrine functions as well (Franceschi and Bonafè, 2003; Borrás *et al.*, 2015). In this regard, neutrophil function (e.g., adherence, chemotaxis, phagocytosis) is enhanced in centenarians compared to the middle-aged group and similar to that of young adults (Alonso-Fernández *et al.*, 2008). Indeed, their particular immunological profile has been proposed to exert anti-inflammatory protection against inflammaging (Franceschi *et al.*, 2017). Regarding the endocrine system, centenarians seem to have well-maintained glucose homeostasis and insulin sensitivity, although the underlying mechanisms of these preserved functions are still controversial (Vitale *et al.*, 2017).

Studies performed by our group revealed that the miRNA and mRNA profiles of centenarians and young people were more similar to those of octogenarians (Borrás *et al.*, 2016). Furthermore, when compared to young people, lymphocyte function was found to be impaired in septuagenarians but preserved in centenarians. These results suggest that centenarians have improved homeostasis control and are more resistant to oxidative damage, which was confirmed by lower plasma levels of carbonylated proteins (Inglés *et al.*, 2018) and lipid peroxidation (Pradas *et al.*, 2019) in centenarians compared to control groups (Borrás *et al.*, 2016).

3.4. BCL-XL's role in healthy aging

Previous studies performed by our group showed that BCL-XL is involved in extreme longevity as it is upregulated in peripheral blood mononuclear cells (PBMCs) from centenarians, which are considered examples of healthy aging (Borrás *et al.*, 2016). The fact that centenarians overexpress this protein, as well as FAS and FAS-L, suggests that apoptosis is tightly controlled in these individuals. Indeed, well-balanced modulation of apoptosis may be useful to expand lifespan and attenuate ARDs (Ginaldi *et al.*, 2004).

To further understand the role of BCL-XL in healthy aging, we transduced MEFs with a plasmid encoding BCL-XL (Borrás *et al.*, 2016). MEFs overexpressing BCL-XL exhibit decreased markers of cellular senescence ($P16^{INK4a}$, $P19^{Arf}$, and $P21^{CIP}$ and SA-β-GAL), increased proliferation measured as phosphohistone H3 (PH3), and lower levels of lipid peroxidation determined as malondialdehyde (MDA). In addition, the

overexpression of the human BCL-XL ortholog, Ced-9, has been shown to expand the lifespan in *C. elegans*, suggesting an important role of BCL-XL in the aging process.

Given the importance of apoptosis in the immune system, the anti-apoptotic protein BCL-XL has also been linked to immunity. BCL-XL is important for the development of several immune cell lines such as B cells and CD4 Treg cells and has been found highly expressed in $CD4^+$ and $CD8^+$ thymocytes (Li *et al.*, 2020). Transgenic mice overexpressing BCL-XL in the T lineage are protected from collagen-induced arthritis (Chen *et al.*, 2002). More evidence suggesting a protective role of BCL-XL in aging has been reported in the brain. BCL-XL expression remains constant in the adult brain whereas the expression of other BCL-2 family members decreases significantly during the development (Borrás *et al.*, 2020). Additionally, BCL-XL has also been found to regulate neuronal growth and synaptic plasticity and to confer neuroprotection (Park *et al.*, 2018; Li *et al.*, 2020). During the neuronal activity, BCL-XL improves mitochondrial bioenergetic efficiency and vesicle trafficking, promoting neuronal function (Jonas, Porter and Alavian, 2014).

However, the role of BCL-XL in aging remains controversial since drugs targeting BCL-XL that selectively delete senescent cells (i.e., senolytics), have also demonstrated a wide range of positive effects both *in vivo* and *in vitro* (Song *et al.*, 2020; Robbins *et al.*, 2021; Tarantini *et al.*, 2021). Enhanced cardiovascular function, increased physical endurance, and reduced frailty during aging are the most remarkable (Zhu *et al.*, 2015; Soto-Gamez and Demaria, 2017).

This dual role of BCL-XL gets us to a paradox by which BCL-XL is increased in senescent cells and the deletion of these cells results in several beneficial effects, whereas BCL-XL overexpression reduces senescence in other cells as well (Borrás *et al.*, 2020). Hence, BCL-XL function remains debatable: on one hand, BCL-XL may promote cell survival by improving the cell's ability to restore homeostasis after a stressful stimulus; on the other hand, it may allow the survival of malignant cells with accumulated damage, the presence of which may pose a threat to the organism. The goal of this thesis is to investigate the role of BCL-XL in a murine model overexpressing this protein to better understand its role in the aging process.

II. HYPOTHESIS AND AIMS

1. HYPOTHESIS

The recent discovery of BCL-XL being overexpressed in PBMCs from centenarians (Borrás *et al.*, 2016) has emerged as a new approach to investigate the BCL-XL function in healthy aging. BCL-XL overexpression proved its contribution to exceptional longevity by increasing the mean and maximum lifespan in nematodes (Borrás *et al.*, 2016) and flies (Gimeno-Mallench *et al.*, 2021). In addition, BCL-XL is known to regulate mitochondrial metabolic efficiency in neurons and improve plasticity in the brain (Chen *et al.*, 2011; Jonas, Porter and Alavian, 2014). Moreover, BCL-XL has a protective role against oxidative stress in vascular endothelial cells (Ni *et al.*, 2013) and fibroblasts (Pfeiffer *et al.*, 2017). Altogether, these data suggest a beneficial role for BCL-XL in aging. Thus, we hypothesize that transgenic mice overexpressing BCL-XL would exhibit improved health-related parameters, including enhanced mitochondrial function and reduced frailty at advanced ages.

2. AIMS

The major goal of this thesis is to study the role of BCL-XL in frailty and healthy aging in a transgenic mouse model overexpressing a human form of this protein in T cells.

To accomplish this, we set the following specific aims:

1) Characterize experimental animals by genotyping and BCL-XL quantification in thymus, spleen, and T cells from transgenic and wild-type mice.

2) Study the effect of BCL-XL on physical health status.
    a. Determine physical performance decline in mice overexpressing BCL-XL and wild-type mice during aging.
    b. Determine spontaneous activity in mice overexpressing BCL-XL and wild-type mice in middle age.
    c. Determine frailty in mice overexpressing BCL-XL and wild-type mice in old age.

3) Study the effect of BCL-XL on metabolism-related parameters.
    a. Determine body composition changes with age in mice overexpressing BCL-XL and wild-type mice.
    b. Determine respiratory metabolism and daily intake rates in mice overexpressing BCL-XL and wild-type mice.
    c. Determine glucose tolerance in mice overexpressing BCL-XL and wild-type mice.

4) Study the effect of BCL-XL on T cell function.
    a. Characterize purity and number of splenic T cells isolated from mice overexpressing BCL-XL and wild-type mice.
    b. Determine stress response and survival-related mechanisms in T cells isolated from mice overexpressing BCL-XL and wild-type mice.
    c. Determine mitochondrial function in T cells isolated from mice overexpressing BCL-XL and wild-type mice.

III. MATERIAL AND METHODS

1. EXPERIMENTAL ANIMALS

In this study, heterozygous mice from the B6.Cg-Tg(LCKprBCL2L1)12Sjk/J (Lck^{pr}-Bcl-X$_L$) strain purchased from The Jackson Laboratory (Stock Number 013738) were used. These mice express the human *BCL-XL* cDNA sequence under the control of a mouse lymphocyte protein tyrosine kinase proximal promoter (*Lck^{pr}*). This promoter drives BCL-XL expression in all thymocyte subsets.

All the experiments performed on these animals have been authorized by the Animal Experimentation and Welfare Committee of the University of Valencia and by the *Consellería d'Agrigultura, Medi Ambient, Canvi Climàtic I Desenvolupament Rural* of the *Generalitat Valenciana*. The corresponding authorized projects for colony formation and maintenance and the experimental procedures are shown in COMMITTEES.

1.1. Colony formation and housing conditions

Lck^{pr}-Bcl-X$_L$ mice were bred with C57BL/6J (B6) inbred mice to establish the colony. We used B6 mice as wild-type or control for our experiments. Mice were housed in the animal center of the Central Unit for Research in Medicine (UCIM, by its acronym in Spanish) of the Faculty of Medicine and Odontology of the University of Valencia. Animals were kept in the facility at 22 ± 2°C, with a relative humidity of 60% under 12-12h of dark-light cycles and with access to food and water *ad libitum*.

1.2. Mice sacrifice and sample collection

Ex vivo and *in vitro* experiments required animal sacrifice to obtain tissues, organs, and T cells from the spleen. Animals were sacrificed in the morning from 9:00 to 11:00h by cervical dislocation followed by decapitation. Troncular blood was collected immediately in a 1.5 ml tube with 10 µl heparin. Blood samples were processed for plasma obtention and stored at -80˚C for future measurements. For each mouse, half brain, cerebellum, heart, lungs, gastrocnemius, liver, kidney, aorta, and thymus were freeze-clamped and stored at -80˚. In parallel, spleens were removed from mice for immediate T cell isolation.

2. MATERIAL

2.1. Equipment

The infrastructure and laboratory equipment required to complete the work presented in this thesis belongs to the research team co-directed by Prof. José Viña Ribes and Prof. Consuelo Borrás Blasco. The laboratory is located in the Department of Physiology at the Faculty of Medicine and Odontology (University of Valencia). Furthermore, the use of the equipment and various services provided by the UCIM were also needed. The equipment used is described in detail below.

Genotyping:

- T100™ Thermal Cycler (Bio-Rad)
- Thermomixer compact (Eppendorf)
- GT Mini Gel casting system (Bio-Rad, 1704422)

Physical performance test:

- Precision balance (Gram precision, STZ-1000, BAL 66-0002)
- Grip Strength Test (BIOSEB, BIO-GS3)
- Rotarod Panlab (Harvard Apparatus, LE8505)
- Treadmill LE8710MTS and treadmill control LE8710 (Panlab, Harvard Apparatus)

Body composition:

- Dual Energy X-ray Absorptiometry (DXA) InAlyzer (Medikors. Inc, 12100)
- Isoflurane vaporizer Panlab (Harvard Apparatus)

Metabolic monitoring:

- OxyletPro Physiocage (Panlab, REF LE405 76-0810)

Tissue homogenization:

- Precellys® Evolution homogenizer (Bertin technologies)

T cell isolation and culture:

- Centrifuge MPW-352R (MPW Med. Instruments)
- EasySepTM Magnet (Stemcell, #18000)
- Automated Cell Counter TC20 (Bio-Rad, #1450102)
- Cell culture hood Cultair BC 100
- Heat CO_2 incubator NU-5700E (Nuaire)
- Water bath P Selecta (Preciseterm)

Protein quantification:

- Spectrophotometer 7315 (Jenway)

Western blot:

- Mini-PROTEAN Tetra Handcast Systems (Bio-Rad)
- Mini Trans-Blot® Electrophoretic Transfer Cell (Bio-Rad)

Flow cytometry:

- FACSVerse™ flow cytometer (BD, Biosciences)

Seahorse:

- Seahorse XFe96 Analyzer (Agilent)
- Centrifuge 5430 (Eppendorf)

General equipment:

- ImageQuant™ LAS 4000 imaging system (GE Healthcare, Biosciences)
- Ductless Fume Hood Model 1100-G A (CRUMA)
- Precision balance 6110 Tecator (Sartorius)
- WB01 Thermostatic water bath (Ibx instruments, Labbox)
- Inverted microscope Oxion Inverso (Euromex, OX.2053-PL)
- Microliter centrifuge Mikro 220 R (Hettich, 2205)
- Centrifuge 1-14 D3752-0 (Sigma)

- pH meter pH 50 (Instruments XS)
- Hotplate stirrer SB 162-3 (Stuart)
- -80˚C freezer Evolution BM EVO 690 L (Froilabo)
- -20 ˚C freezer Liebherr (Comfort Nofrost)
- 2-4˚C refrigerator Lynx

2.2. Reagents

The reagents used in this study, including kits and culture media, as well as buffer and solutions prepared in the laboratory, are described in detail below.

Genotyping:

- KAPA HotStart Mouse Genotyping Kit (Kapa Biosystems, KK7352)
- Agarose (OmniPur®, 2120)
- Tris-acetate-EDTA (TAE) 50x (242g TRIS, 57g glacial acetic acid, 100ml sodic EDTA 0.5M)
- RedSafe™ Nucleic Acid Staining Solution 20000x (iNtRON Biotechnology, 21141)
- GeneRuler 100 bp DNA Ladder (Thermo Fisher, SM0241)
- DNA Gel Loading Dye (6X) (Thermo Fisher, R0611)

T cell isolation and culture :

- Lysis Buffer, 100 ml 10X (BD Pharm Lyse™, 555899)
- EasySep™ Mouse T cell Isolation Kit (Stemcell Technologies, #19851)
- Inactivated Foetal Bovine Serum (FBS) (Invitrogen)

- Recommended medium (RM) 50 ml (0.0184 EDTA K_2, 49 ml Dulbecco's Phosphate Buffered Saline (PBS), and 1ml FBS)
- RPMI 1640 w/ stable Glutamine (Biowest, L0498-500)
- Penicillin/Streptomycin (P/S) 10,000 U/mL (GIBCO)

Protein quantification:

- Trizma base (Tris) (Sigma, T6066-1KG)
- Sodium dodecyl sulfate (SDS) (Sigma, L3771-500G)
- Glycerol (Fisher Scientific, G/0650/17)
- Tris-SDS-Glycerol lysis buffer (Tris, 10% glycerol and 2% SDS)
- Protease Inhibitor Cocktail (Sigma, P8340-5ML)
- Sodium orthovanadate (Sigma-Aldrich, S6508)
- Lowry Reagent Powder (Sigma, L3540-1VL)
- Folin & Ciocalteu's Phenol Reagent (Merck Millipore, F9252-500ml)

Western blot:

- PBS-T (PBS, pH 7.2-7.5, 0.05% Tween 20)
- Bovine Serum Albumin (BSA) (Albumin Fraction V, Pancreac, A1391,0500)
- Acrylamide/Bis Solution, 29:1 (40% w/v), 3.3% C 500 ml (Serva, 10680.01)
- SDS (Sigma, L3771-500G) diluted with distilled water at 12% and 10%
- Ammonium persulfate (APS) (Sigma, A3678-100G) at 10 %
- N,N,N′,N′-Tetramethylethylenediamine (TEMED) (Sigma, T9281-50ML)
- PageRuler Plus Prestained Protein Ladder (Thermo scientific, 26620)

- Running Buffer 10x (0.25 M Tris, 2 M Glycine and 1% SDS dissolved in distilled H2O)
- Transfer Buffer 1x (25mM Tris, 0.2 M Glycine, and 20% Methanol dissolved in distilled H_2O)
- Ponceau S for electrophoresis abs (Panreac, 517-523) (prepared at 5% with 1% acetic acid, dilute with distilled H20)
- Luminata™ Classico Western HRP Substrate (Millipore, 140935)
- Restore Western blot stripping buffer (Thermo Scientific, 21059)
- BCL-XL Rabbit antibody (Cell Signaling Technology, #2762S)
- Anti-GAPDH antibody produced in rabbit (Sigma, G9545-100UL)
- Anti-β-Actin antibody, mouse monoclonal (Sigma, A1978-100UL)
- Anti-rabbit IgG HRP linked (Cell Signaling, 70745)

Flow cytometry:

- APC anti-mouse CD3ε Antibody (Biolegend, #100312)
- Annexin V CF-Blue apoptosis detection kit (Immunostep, ANXVCFB-200T)
- FluoReporter™ *lacZ* Flow Cytometry Kit (Molecular probes, #F-1930)
- Propidium iodide (PI) (Molecular Probes, F-1930)
- HEPES Buffer (Gibco, 15630-049)
- Staining Medium (SM) (PBS with 4% foetal calf serum, 10 mM HEPES, pH 7.2)
- MitoPY1 (Bio-Techne R&D Systems, 4428)
- Tetramethylrodamine methyl ester (TMRM) (Thermo Fisher Scientific, T668)
- DAPI (SIGMA Aldrich, D9542)
- Anti-Human-Mouse INTRACELL (Immunostep, INTRA-100)
- LC3B (D11) XP® Rabbit mAb (Cell signaling, #3868)

- Anti-Rabbit IgG (H+L), F(ab')2 Fragment Alexa Fluor® 488 Conjugate (Cell signaling, #4412)
- Flow cytometry buffer (Thermo Fisher Scientific, 00-4222-26)

Seahorse:

- XF Cell Mito Stress Test Kit (Agilent Technologies, 103015-100)
- XF Base Medium Minimal DMEM Seahorse XF 1L (Agilent Technologies, 102353-100)
- D-(+)-Glucose, 99.5% (glucose) (Sigma, G7528-250G)
- L-Glutamine (glutamine) (Sigma, G3126-100G)
- Sodium pyruvate, >=99% (pyruvate) (Sigma, P5280-25G)

General reagents:

- Sodium heparin ROVI 5000 U.l./1ml (ROVI, G23942N)
- PBS pH 7.4 (GIBCO)
- Alcohol 96˚

2.3. Additional supplies

Specific supplies:

- Precellys Lysing Kit (Bertin Technologies, P000945-LYSK0-A.0)
- Bulk bead for 500 preps (P000927-LYSK0-A.0)
- Amersham™ Hybond™ 0.2 µm PVDF blotting membrane (GE Healthcare, 10600021)
- Seahorse XFe96 FluxPak mini (Agilent Technologies, 102601-100)
- Dual-Chamber Cell Counting Sliders (BIO-RAD, 1450011)
- Sterile cell strainer 70 µm Nylon Mesh (Fisher brand, 22363548)
- Glucometer Accu-Check Guide Me (Accu-Chek)
- Test strips Accu-Chek Guide (Accu-Chek, 07453736)

- Culture plates TC Surface (Thermo scientific, 140675)
- Brand Cuvettes semi-micro, 1.5 ml (Fisher Brand, 14955127)

General stock:

- Surgical instruments
- Microtubes for 0.2, 0.5, 1.5 and 2 ml
- Tubes for 15 and 50 ml
- Pipettes and tips for different volumes
- Multichannel pipettes
- Glass pipettes and pipettors
- Syringes and nylon membrane filters 0.2 μm
- Petri dishes
- Cytometry tubes
- Gloves and lab coat
- Surgical instruments
- Liquid N_2
- Normal and dry ice

3. METHODS

3.1. Experimental design

We divided our mice into four age groups to study the effect of BCL-XL overexpression during aging, considering 2-5-month-old (mo) mice as young, 8-11 mo as adults, 17-20 mo as old, and 24-26 mo as very old.

First, we followed up an initial cohort of 144 Lck^{pr}-Bcl-X_L and B6 mice, with females and males in similar proportions. When mice reached each age group respectively, blood, urine, and feces were collected, and physical performance assays were performed longitudinally. Frailty was determined only at advanced ages, in 17-20 and 24-26 mo mice.

In parallel, approximately 36 animals (~18 Lck^{pr}-Bcl-X_L and ~18 B6) were sacrificed in each age group for *ex vivo* and *in vitro* experiments. Blood, tissue, and organs were collected and stored, and T cells from the spleen were immediately isolated to determine T cell count, apoptosis, autophagy, and mitochondrial function.

Finally, body composition, metabolic monitoring, and the glucose tolerance test (GTT) were performed cross-sectionally in young-adult and old-adult mice. More specifically, 8-11 and 17-20 mo mice were used for metabolic monitoring, whereas glycemia during GTT and body composition were determined in mice from 6 up to 23 months of age. Figure 13 summarises the experimental design throughout the different age groups.

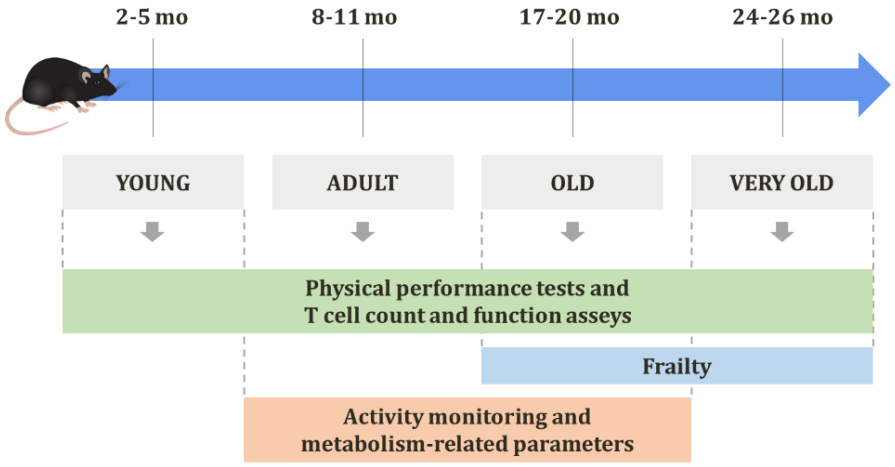

Figure 13. Experimental design.

Four age groups were defined to study the effect of BCL-XL overexpression in mice during aging: 2-5 (young), 8-11 (adult), 17-20 (old), and 24-26 mo (very old). We first evaluated the physical performance in a longitudinal cohort, from which several animals were sacrificed for the *ex vivo* and *in vivo* experiments (green box). Frailty was assessed only in the aged mice of this cohort at 17-20 and 24-26 mo (blue box). Additionally, body composition, metabolic monitoring, and glucose tolerance were evaluated in a cross-sectional cohort with mice from 5 to 24 months of age (orange box).

3.2. *In vivo* assays

In this section, we describe the *in vivo* assays performed in this study, which include all experiments realized in living mice.

3.2.1. Bodyweight

Mice's body weight was measured with the precision balance. Three measurements of body weight were assessed on day 0 (before the physical performance assays), day 7 (on the de first day of the assays), and day 14 (after the assays). The mean was calculated for each mouse in

each age group. Then, to determine individual body weight gain, the percentage of increment was defined for each mouse from a young age (2-5 mo) to 8-11, 17-20, and 24-26 mo.

Thereby, bodyweight gain for a mouse given a specific age group is:

$$\text{Body weight gain (\%)} = \frac{(BW_X - BW_{2\text{-}5\ mo})}{BW_{2\text{-}5\ mo}} * 100$$

Where *BW* is the bodyweight value, and *X* denotes each age group (2-5, 8-11, 17-20, or 24-26 mo). Acknowledge that the percentage of body weight gain at young (2-5 mo) age will always be 0%.

3.2.2. Grip strength test

The grip strength test is commonly used to assess neuromuscular function as maximal peak force developed by rodents (Ackert-Bicknell *et al.*, 2015; Graber *et al.*, 2021). We performed the grip strength test to determine the mice's forelimb grip strength using the dynamometer Grip Strength Test. The procedure used is as follows:

1) Remove the mouse from its home cage by gripping the base of the tail between the thumb and the forefinger.
2) Lower the mouse over the dynamometer until it grasps the metallic bars with its forelimbs.
3) Gently, pull back the mouse by its tail, ensuring the animal grips the metallic bars and its torso remains horizontal.
4) Return the mouse to its home cage and record the maximal grip strength value displayed on the screen of the dynamometer.

5) Repeat this procedure twice leaving 10 minutes of rest between each attempt to obtain a total of three measurements of forelimb grip strength.
6) Divide the highest grip strength value obtained by the mouse bodyweight to assess the relative mice's grip strength.

Figure 14 summarizes the grip strength test procedure.

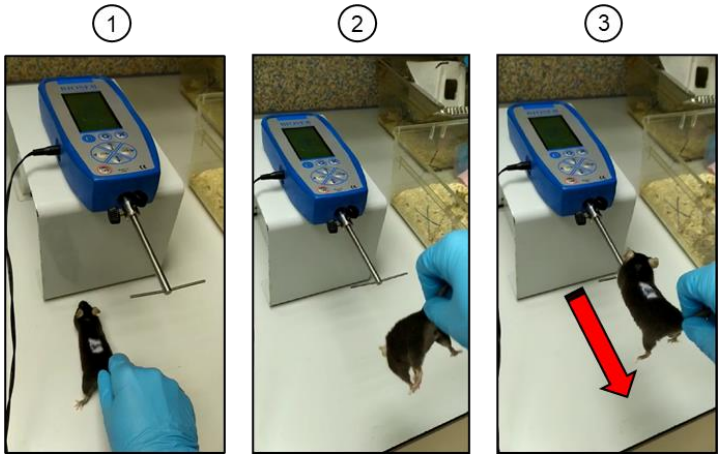

Figure 14. Grip strength test.

Steps to perform the grip strength test in mice. (1) Hold the mouse by griping the base of its tail, (2) lower the mouse until it grasps the bar, and (3) pull back gently to register maximal strength.

This procedure was performed twice before the day of the test to ensure the adaptation of the animals to the evaluation process. Next, to determine grip strength loss, we defined the percentage of loss for each mouse from a young age (2-5 mo) to 8-11, 17-20, and 24-26 mo.

The grip strength loss for a mouse given a specific age group is:

$$\text{Grip strength loss (\%)} = \frac{(GS_{2\text{-}5\ mo} - GS_X)}{GS_{2\text{-}5\ mo}} * 100$$

Where *GS* is the grip strength value, and *X* denotes each age group (2-5, 8-11, 17-20, or 24-26 mo). Acknowledge that the percentage of grip strength loss at a young age will always be 0%.

3.2.3. Rotarod test

Motor coordination has traditionally been assessed by the rotarod test in rodents (Liu *et al.*, 2014; Shoji *et al.*, 2016; Graber *et al.*, 2021). In this test, the animal is placed on a horizontal rod that rotates about its long axis, and the animal is expected to walk forward to remain upright and not fall off. We assessed motor coordination using the Rotarod. The procedure used is as follows:

1) Turn on the Rotarod apparatus.
2) Set it to accelerating mode for 4 to 40 rpm in 300 sec. The rod will initially rotate at a 4-rpm constant speed to allow positioning of all the mice in their respective lanes and the screen will indicate “acceleration waiting” of 4 rpm constant speed.
3) Remove the mice from their home cage and place them on the lane.
4) Wait 10 sec while the mice placed on the rod walk forward to keep their balance.
5) Press the start button to initiate the acceleration from 4 rpm to 40 rpm in 300 sec. From this moment, the timer will start counting.

6) Record the latency at which each mouse falls off the rod (the value will be displayed on the screen for each lane) and place the mice back in their home cage.
7) Repeat this procedure twice, leaving 15 minutes of rest between each attempt to obtain a total of 3 latency measurements.
8) Use the maximal latency value obtained to assess motor coordination.

Figure 15 shows a summary of the Rotarod test procedure.

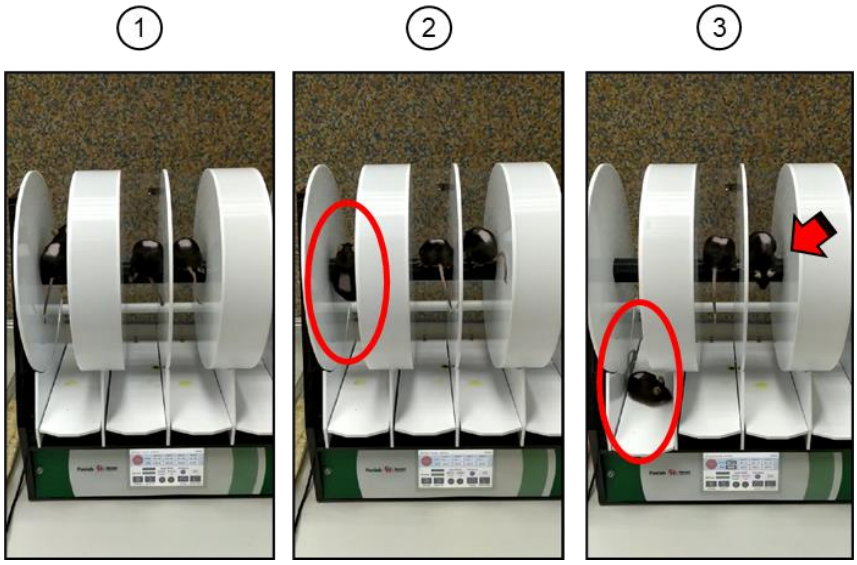

Figure 15. Rotarod test.

Images from the rotarod test while assessing motor coordination. (1) Usually, all mice can keep their balance at the beginning of the test. (2) Over time, one mouse (marked with a red circle) loses its balance, but it is holding to the rod by its forelimbs; (3) however, it will eventually fall off the rod and the timer for that lane will stop. The arrow points to a mouse walking backward.

This procedure is performed three times before the day of the test to ensure the adaptation of the animals to the evaluation process. Mice that fall off the rod during the first 10 sec of the test (when the timer is not counting yet) are identified as animals unable to do the test, thus will automatically fail the test. Also, be aware of mice that turn themselves and start working backward, like the mice shown in the figure in step 3. If this happens and the mouse falls off the rod before turning around again, the measurement is invalid, and the test must be repeated.

Finally, to determine motor coordination loss, we defined the percentage of latency time loss for each mouse from a young age (2-5 mo) to 8-11, 17-20, and 24-26 mo.

The motor coordination loss for a mouse given a specific age group is:

$$\text{Motor coordination loss } (\%) = \frac{(MC_{2\text{-}5\ mo} - MC_X)}{MC_{2\text{-}5\ mo}} * 100$$

Where *MC* is the motor coordination value (latency time), and *X* denotes each age group (2-5, 8-11, 17-20 or 24-26 mo). Be aware that the percentage of latency time loss at a young age will be 0% for all mice.

3.2.4. Treadmill incremental test

Physical endurance is a type of moderate-intensity aerobic exercise that has traditionally been used to assess the physical function of rodents. The treadmill incremental test is widely used to assess mice endurance by allowing animals to run on the treadmill until exhaustion while monitoring their running duration (Marcaletti, Thomas and Feige, 2011; Gomez-Cabrera *et al.*, 2017; Graber *et al.*, 2021).

We determined physical endurance with the incremental treadmill test using the treadmill apparatus. The procedure used is as follows:

1) Set the treadmill to an uphill inclination angle of 5%.
2) Insert the lane dividers into the slots of the treadmill.
3) Switch on the treadmill.
4) Adjust the electric shock intensity to 0.2-0.4 mA.
5) Remove the mice from their home cage and place them on the lane.
6) Adjust the belt speed to 10 cm/s.
7) Allow mice to run for 4 min at a constant velocity of 10 cm/s.
8) Increase the speed by 4 cm/s every 2 min until exhaustion.
9) When a mouse becomes exhausted, return the mouse to its home cage and record the time displayed at that moment on the screen.

The treadmill incremental test procedure is exemplified in Figure 16.

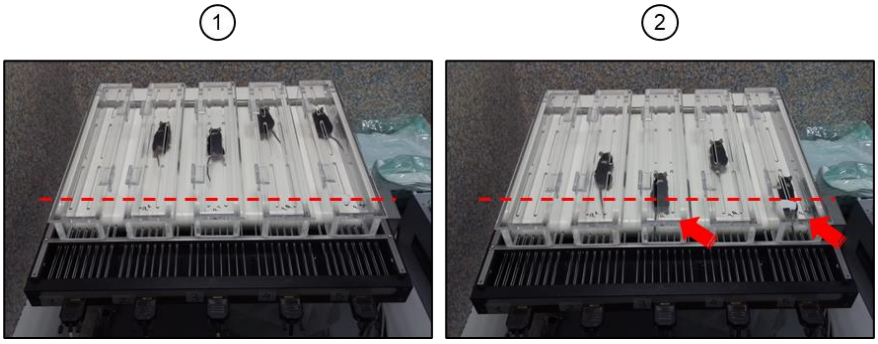

Figure 16. Treadmill incremental test.

Images from the treadmill incremental test while assessing physical endurance. (1) At the beginning of the test, mice run in the upper part of the treadmill; (2) however, as time passes, animals tend to run closer to the shock grid (pointed with arrows) until they eventually touch it continuously due to exhaustion.

A 10 min for acclimatization to the test is performed twice before the day of the assay to ensure adaptation of the animals to the treadmill apparatus. For the acclimatization, follow the previous protocol until step 6, then allow mice to run 6 min, increase speed to 14 cm/s, and allow them to run 4 min more. Mice that become exhausted during step 7 are counted as unable to do the test and will automatically fail the test. Lastly, to assess physical endurance loss, we defined the percentage of running time loss for each mouse from young age (2-5 mo) to 8-11, 17-20, and 24-26 mo.

The physical endurance loss for a mouse given a specific age group is:

$$\text{Physical endurance loss (\%)} = \frac{(PE_{2\text{-}5\ mo} - PE_X)}{PE_{2\text{-}5\ mo}} * 100$$

Where *PE* is the physical endurance value (running time), and *X* denotes each age group (2-5, 8-11, 17-20, or 24-26). Acknowledge that the percentage of running time loss at a young age will be 0%.

3.2.5. Assessment of frailty

Frailty phenotype in mice is commonly characterized as poor physical performance and is used as a relevant predictor of lifespan (Huffman *et al.*, 2016; Heinze-Milne, Banga and Howlett, 2019). To identify frail mice, we used a combination of the frailty criteria used by Baumann et al. (Baumann, Kwak and Thompson, 2018) and a modified version of the Valencia Score for Frailty developed by our group (Gomez-Cabrera *et al.*, 2017). The mentioned criteria are based on the frailty score used in humans (Fried *et al.*, 2001) but adapted to experimental animals.

We assessed frailty in 17-20 and 24-26 mo mice using the frailty criteria and cut-off values described in Table 1. According to the number of criteria met, mice were classified as frail (> 2), pre-frail (= 2), and non-frail (< 2).

Table 1. Frailty criteria and cut-off values.

	Test	Frailty criteria	Cut-off values
	Body weight	Body weight	Upper 20%
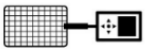	Grip strength test	Grip strength	Lower 20%
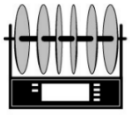	Rotarod test	Motor coordination (latency time)	Lower 20%
	Treadmill incremental test	Physical endurance (running time)	Lower 20%

3.2.6. Metabolic monitoring

The metabolic phenotype has been traditionally studied in animal models of aging (Harman, 1981; Houtkooper *et al.*, 2011; Folgueras *et al.*, 2018). We determined the *in vivo* metabolic phenotype from 8-11 and 17-20 mo mice by monitoring with the OxyletPro Physiocage (Figure 17). This flexible system integrates the evaluation of respiratory metabolism, food, and drink intake, as well as spontaneous locomotor activity that allows the determination of overall metabolic function in rodents.

Figure 17. OxyletPro home cage.

Mice were removed from their home cage, weighted, and placed individually in the metabolic cages for approximately 45 h. For the duration of the experiment, the 12 h light/dark cycle was maintained to ensure a normal circadian rhythm. Before the analysis of the results, the first 3 h of registration in which animals adapt to the new environment were discarded from the study. The procedures used to determine each parameter are described below.

3.2.6.1. Respiratory metabolism

RQ and EE were measured by indirect calorimetry to assess respiratory metabolism. Oxygen consumption and carbon dioxide production values used to calculate these parameters were recorded every 5 min for each mouse. For statistical analysis, mean RQ and EE values for dark and light cycles were calculated. Additionally, the total area under the curve (AUC) for both parameters was also computed for each mouse individually for statistical analysis.

3.2.6.2. Spontaneous locomotor activity

Overall spontaneous locomotor activity was evaluated by horizontal (activity) and vertical activity (rearing). Activity is detected by the sensor platform located in the metabolic cage and is commonly used to identify circadian patterns and activity levels. Additionally, infrared sensor bars detect the occurrence and duration of rearing events. Both activity and rearing values were recorded every minute for each mouse. Mean values of activity and rearing were calculated for dark and light cycles. Additionally, individual AUCs for both parameters were also computed for statistical analysis.

3.2.6.3. Intake

Food and drink consumption rates were registered from the weight changes in the food and drink dispensers. Both parameters are recorded every minute for each mouse to assess food and drink intake. First, we observed individual intake values over time during the 45 h of monitoring. Then, daily food and drink consumption rates were calculated by assessing hourly consumption rates and multiplying by 24.

3.2.7. Body composition

Dual Energy X-ray Absorptiometry (DXA) is an imaging modality to measure body composition in which the whole body can be scanned by exposing the patient to a very small dose of ionizing radiation (Shepherd *et al.*, 2017). This system has been recently used to measure total, lean and fat mass in humans (Kyrana *et al.*, 2022) and mice (Powell *et al.*, 2022).

We evaluated body composition using the DXA analyser for laboratory animals. Mice were anesthetized with the Isoflurane vaporizer before and during the measurement. To ensure a better image resolution, we immobilized the anesthetized animal using adhesive tape to restrain its limbs and tail. Mice's total mass, fat mass, and lean mass were analysed among other parameters. As a reference, the mice's body weight was registered with the precision balance to check if the DXA registration was correct.

3.2.8. Glucose tolerance test

The GTT is a standard procedure used in humans and rodents to measure changes in blood glucose concentration (i.e., glycemia) following the administration of a high concentration of glucose (Pedro, Tsakmaki and Bewick, 2020; Eyth, Basit and Smith, 2022). It is widely used to identify individuals with impaired glucose tolerance (Stevic *et al.*, 2007; Kmetová *et al.*, 2022; Rostagno *et al.*, 2022; Rouabhi, Guo and Rahmouni, 2022).

For our study, glycemia was measured in blood drops from the saphenous vein before (min 0) and after (min 15, 30, 60, 120, and 180) the intraperitoneal injection of 2g/kg glucose in 12 h fasted mice. The glucometer Accu-Check Guide Me and the corresponding test strips were used for this test.

3.3. *Ex vivo* assays

In this section, we describe *ex vivo* assays, which include all experiments performed outside the organism, in absence of a culture medium; thus, experiments performed in organs, tissues, and cells extracted from the mice with no further treatments.

3.3.1. Mice genotype determination

Genotype was determined in recently born animals after being separated from their progenitor cage to identify B6 and Lck^{pr}-Bcl-X_L mice. To that aim, we amplified two DNA sequences: one corresponding to the *BCL2L1* transgene (400 bp) and the internal positive control (200 bp) (Table 2).

Table 2. Primers used for mice genotype determination.

Primer label	Sequence 5' → 3'
Transgene BCL-XL (forward)	GCA TTC AGT GAC CTG ACA TC
Transgene BCL-XL (reverse)	CTG AAG AGT GAG CCC AGC AGA ACC
Control (forward)	CAA ATG TTG CTT GTC TGG TG
Control (reverse)	GTC AGT CGA GTG CAC AGT TT

The procedure used for genotyping is as follows:

1) Digest the tissue with Kit Kapa. We used ear tissue that is removed from animals when marked for individual identification.
2) Amplify transgene and control DNA sequences with Kit Kapa using the cycling procedure in Table 3.

Table 3. Cycling procedure for DNA sequence amplification.

Step	Temp (˚C)	Time	Note
1	94	2 min	
2	94	20 sec	
3	65	15 sec	-0.5˚C per cycle decrease
4	68	10 sec	
5			Repeat steps 2-4 for 10 cycles
6	94	15 sec	
7	60	15 sec	
8	72	10 sec	
9			Repeat steps 6-8 for 28 cycles
10	72	2 min	
11	10		Hold

3) Load 5 µl of sample in a well within an agarose gel. To prepare the gel, weigh 0.6 g of agarose, add 15 mL TAE 1x, and heat until agarose is diluted. Then, add 4 µl of Red Safe and let the solution gel in the mold.
4) Run electrophoresis in TAE 1x buffer at 100 V for 20-30 min to separate the different DNA fragments amplified in step 2.
5) Obtain gel image by exposing stained samples with a UV transilluminator (312 nm). We used the ImageQuant LAS 4000 camera system.

Lck^{pr}-Bcl-X_L mice are identified by exhibiting both bands, at 400 bp (transgene) and 200 bp (internal positive control), whereas B6 mice samples show only the control band at 200 bp. Figure 18 summarizes the genotype determination procedure.

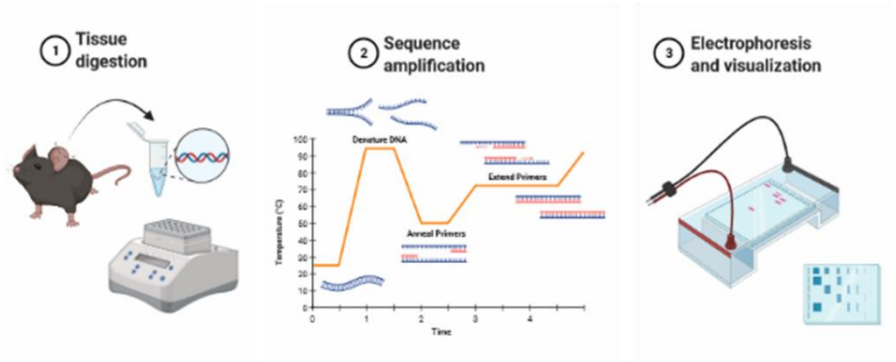

Figure 18. Mice genotype determination.
Created with BioRender.com.

3.3.2. BCL-XL expression levels

We determined BCL-XL expression levels in the thymus, spleen, and splenic T cells from B6 and Lck^{pr}-Bcl-X_L mice. To determine protein expression levels in cells, we isolated and lyse T cells from the spleen with Tris-SDS-Glycerol lysis buffer. For the thymus and spleen, a homogenization protocol was performed before BCL-XL protein quantification. Once we obtained homogenous samples, total protein content was quantified by the Lowry-Folin technique and BCL-XL protein levels were determined by western blot. The methods used are described in detail in the following sections.

3.3.2.1. Organ homogenization

The isolation of intracellular content, such as proteins, lipids, and genetic material, requires an efficient disruption method, and one of the most widely used is homogenization (Simpson, 2010). There are several types of homogenization techniques, including mechanical, sonication, bead

beating, and enzymatic processes. Selecting the homogenization technique depends significantly on the tissue type, size, and stiffness, but also the characteristics of the biomolecule of interest. To analyse protein content, we homogenised the thymus and spleen with the Precellys® Evolution homogenizer.

The procedure used is as follows:

1) Prepare 2 ml precellys tubes with ~0.65 g of bulk beads.
2) Weight a piece of ~50 mg of freeze-clamped tissue.
3) Add 1/10 (w/v) µl of Tris-SDS-Glycerol lysis buffer supplemented with 1% of protease inhibitor cocktail and phosphatase inhibitors.
4) Homogenize samples at 6800 rpm at 4˚C in 3 cycles of 20 s each, with pauses of 30 s between cycles (soft pre-set protocol).
5) Centrifuge at 1500 g for 5 min at 4˚C and transfer supernatant to 1.5 ml tubes.
6) Store samples at -20˚C until use.

During this procedure, is important to keep samples at 4°C to avoid sample degradation. We used sodium orthovanadate as an inhibitor of protein phosphatases.

3.3.2.2. Protein quantification by Lowry-Folin

The Lowry-Folin protein assay to quantify protein content is based on the combination of two different reactions: the Biuret reaction and the Folin-Ciocalteu reaction (Layne, 1957; Waterborg and Matthews, 1994). During the first one, Cu^{2+} ions chelate between the nitrogen of peptide bonds

(Shen, 2019). During the second one, phenols reduce phosphomolybdic phosphotungstic acid to heteropolymolybendum blue, which gives the sample the characteristic blue colour that gets darker in high protein content samples (Lowry and Randall, 1951).

Total protein content was quantified by the Lowry-Folin method. The procedure used is as follows:

1) Prepare the stock BSA solution and dilutions for the standard curve. We used 10, 8, 5, 2.5, 1.25 and 0.625 mg/ml.
2) Add 250 µl of distilled H_2O in 1.5 ml tubes for each sample/dilution or standard.
3) Add 10 µl of sample/dilution or standard. For the thymus and spleen samples, we used a 1:10 dilution.
4) Add 500 µl of Lowry reagent.
5) Mix with vortex and incubate for 20 min in dark.
6) Add 250 µl of Folin & Ciocalteu's phenol reagent (dilution 1:6).
7) Mix with vortex and incubate for 30 min in dark.
8) Measure absorbance at 660 nm in the spectrophotometer. Always run a blank as the first sample of the standard curve.

To estimate sample protein concentration, create a standard plot with BSA concentration values on the X-axis and absorbance values on the Y-axis. Then, calculate the equation and the R^2 value of a linear trendline. For a reliable measurement, an $R^2 > 0.98$ is expected.

3.3.2.3. Western blot

Western blot is an extensively used technique in molecular biology to semi-quantify specific proteins from a complex mixture of proteins extracted from organs, tissues, biological fluids, or cells (Mahmood and Yang, 2012). This method is based on three steps. First, proteins are separated by size during electrophoresis. Then, proteins are transferred to a solid support, typically a nitrocellulose or PVDF membrane. Finally, proteins of interest are identified by specific antibodies, which in turn are marked by secondary antibodies for visualization by chemiluminescence.

We determined BCL-XL protein levels in tissue and cell-derived samples in Tris-SDS-Glycerol lysis buffer by sodium dodecyl sulfate-polyacrylamide gel electrophoresis (SDS-PAGE) western blot using the procedure described below.

Sample and gel preparation:

1) Prepare gels with 1.5 mm of thickness and at 12.5% of acrylamide/bisacrylamide (40% w/v, 29:1) (0.5 M Tris at pH 6.8, 1.5 M Tris at pH 8.8, Milli-Q water, 10% SDS, 10% APS and TEMED).
2) Place the gel in the tank.
3) Add 1x Running Buffer until the gel is completely covered.
4) Load 30 ug of total protein samples per well.
5) Load 4 µl of protein ladder in a well.

Electrophoresis:

6) Run electrophoresis at 100 V for approx. 90 min (or until the sample front reaches the bottom of the gel).

Transfer to membrane:

7) Transfer proteins to PVDF membrane by tank transfer using cold 1x Transfer Buffer at 170 mA per membrane. Avoid voltages over 100 V that could burn the membrane.
8) Check protein transfer efficiency by staining total protein with Red ponceau.

Antibody incubation:

9) Block nonspecific sites by incubating the membrane with blocking buffer (PBS-T 1% BSA) for 1 h with gentle shaking.
10) Incubate the membrane with primary antibody BCL-XL Rabbit antibody diluted 1:1000 with blocking buffer overnight at 4°C with gentle shaking.
11) Wash membrane for 15 min with 1x PBS-T with gentle agitation. Repeat twice.
12) Incubate the membrane with the secondary antibody anti-rabbit IgG HRP linked diluted 1:2000 with blocking buffer for 3 h at room temperature (RT) and gentle shaking.
13) Repeat the wash step.

Protein detection:

14) Drain the excess buffer from the membrane and place it, protein side up, over a plastic sheet.
15) Add 1 ml of chemiluminescent reagent (luminol) over the membrane.
16) Incubate for 1 min in the dark to start the enzyme-substrate chemiluminescent reaction.

17) Detect protein of interest by digital imaging with ImageQuantTM LAS 4000 imaging system.

Figure 19 summarizes the western blot procedure.

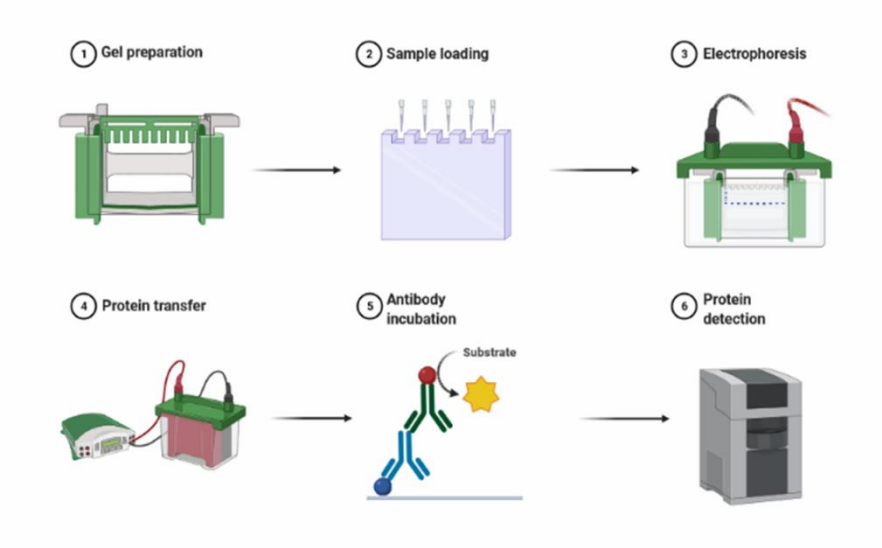

Figure 19. Western blot procedure.
Created with BioRender.com.

To relativize BCL-XL (30 kDa) optical density value to a housekeeping protein, incubate the membrane with Restore Western blot stripping buffer and repeat the immunodetection steps using the antibody of the housekeeping protein. For thymus and spleen samples, an anti-GAPDH antibody produced in rabbits was used to detect the housekeeping GAPDH protein (36 kDa). For T cells, an anti-β-actin antibody, mouse monoclonal to detect beta-actin (ACTB) (42 kDa) was used instead.

3.3.3. T cell isolation and cell count

T cells were obtained from the spleen with the EasySepTM Mouse T cell Isolation Kit. This kit isolates T cells from single-cell suspensions of splenocytes or other tissues by negative selection. Thus, unwanted cells are labelled with biotinylated antibodies and streptavidin-coated magnetic particles and separated using the EasySepTM Magnet. The procedure used is as follows:

Part 1. Spleen white cells isolation:

1) Sacrifice the mouse by cervical dislocation.
2) Extract the spleen from the thorax and transfer it to a sterile Petri plate.
3) Add 1 ml of Lysis Buffer 1x.
4) Homogenize the organ with the plunger of a syringe until the tissue becomes a uniform mixture.
5) Filter the homogenate with a sterile cell strainer 70 μm nylon mesh into a new tube.
6) Incubate for 10 min at RT.
7) Centrifuge at 300 g for 10 min at RT.
8) Discard the supernatant and resuspend the pellet with RM.
9) Load 10 μl of cell suspensions in the counting slides and counT cell number with the Automated Cell Counter TC20.

Part 2. T cell purification:

1) Prepare a tube with 100 million cells in 1 ml of RM.
2) Add 50 µl of Rat Serum and 50 ul isolation cocktail (provided by the EasySepTM Mouse T cell Isolation Kit).
3) Mix and incubate for 10 min at RT.
4) Add 75 µl of Spheres (provided by the EasySepTM Mouse T cell Isolation Kit) previously mixed with vortex for 15 s.
5) Mix and incubate for 5 min at RT.
6) Add 1.5 ml of RM for an approximate final volume of 2.5 ml and place the tube in the magnet.
7) Incubate for 5 min at RT.
8) Gently transfer the supernatant into a new tube and centrifuge at 180 g for 5 min at RT.
9) Discard the supernatant and resuspend the pellet with 1 ml of RM and count the number of cells with the Automated Cell Counter.

Figure 20 summarizes the T cell isolation procedure. For optimal results, it is precise to work under sterile conditions and with disinfected or autoclaved material. The T cell count was determined by the TC20 automated cell counter and the corresponding counting slides. The number of T cells obtained for each mouse is relative to 100 million white cells.

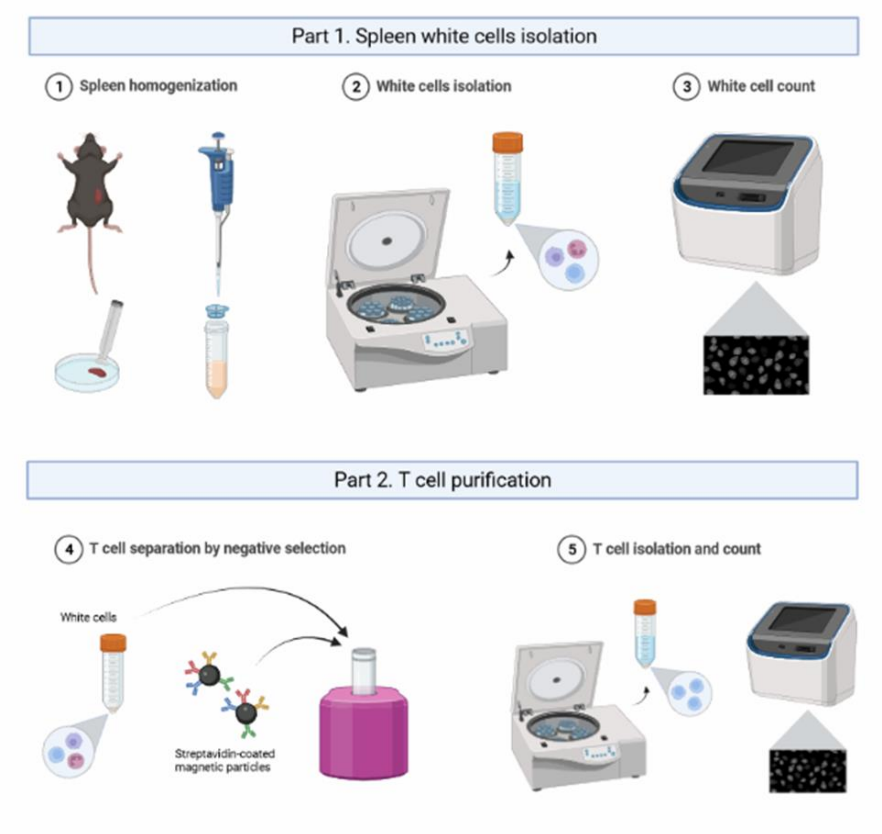

Figure 20. T cell isolation procedure.

Created with BioRender.com.

3.4. *In vitro* assays

In this section, we describe *in vitro* assays, which include all experiments performed in isolated T cells that required a culture medium.

3.4.1. T cell culture

Cell culture is the process of extracting cells from an animal and growing them in a controlled environment. For the experiments that require cell culture, 1 million freshly isolated T cells were seeded per well in the culture plates with 0.5 ml RPMI 1640 medium supplemented with glutamine, 1% P/S, and 10% FBS, in a heat gas incubator at 5% CO_2. For the study of apoptosis in cultured cells, we used dexamethasone with a final concentration of 100 nM.

3.4.2. Flow cytometry

Flow cytometers are sophisticated instruments that measure the optical properties of particles such as cells in a flow system. Because particles must pass through the instrument one by one to be analyzed, they must be prepared as a single-particle suspension and free of aggregates (Ormerod and Imrie, 1990). The characteristics of a cell that can be measured using flow cytometry are referred to as parameters. Some parameters, such as cell size (forward scatter) or cell granularity (side scatter), can be measured without the use of a special reagent. Additional parameters can also be determined but require the use of fluorescent reagents, including fluorescently conjugated antibodies, nucleic acid binding dyes, viability dyes, ion indicator dyes, and fluorescent expression proteins (McKinnon, 2018).

We used the fluorescent markers described in Table 4 to evaluate cellular parameters, including senescence, apoptosis, and autophagy, by flow cytometry.

Table 4. Fluorescent markers used for flow cytometry.

Parameter	Marker	Excitation (λ)	Emission (λ)
T cell purity	Anti-CD3ε	633 nm (red)	723 nm
Senescence	FDG	490 nm (blue)	514 nm
Apoptosis	Annexin V	405 nm (violet)	450 nm
Cell death	PI	535 nm (green)	615 nm
Mitochondrial H_2O_2	MitoPY1	510 (green)	528 nm
Δψm	TMRM	488 nm (blue)	570 nm
Cell nucleus	DAPI	340 nm (ultraviolet)	488 nm

The first time a fluorescent marker is used, measure the sample cells' autofluorescence without staining for the gating. Remember to bring all mediums and reagents to 37˚C (except for the SM) before starting with the procedure. Although it is not strictly required, aseptic conditions are recommended to minimize sample contamination. The procedures used are described in detail in the following sections.

3.4.2.1. T cell purity

T cell markers are needed to validate the efficiency of the isolation method used to obtain these cells. The cluster of differentiation 3 (CD3) is a multimeric protein complex present within all blood T cell subsets, including T-γδ, T-αβ (DN, $CD4^+$, and $CD8^+$), and NK-T cells (Mousset *et al.*, 2019; Weiss *et al.*, 2021). Consequently, CD3 is commonly used to assess T cell purity. Similarly, positive sorting with anti-CD3 antibody-coated beads is employed to isolate T cells (Pedini *et al.*, 2019).

We used the anti-mouse CD3ε antibody conjugated with APC fluorochrome to identify T cells so that we could evaluate the efficiency of the T cell isolation protocol used. Briefly, we added 5 µl of APC anti-mouse CD3ε in aliquots with 0.5-1 million T cells suspended in 200 µl of RM. After a 10 min incubation at RT, we adjusted volumes to 500 µl with RM and measured APC fluorescence by flow cytometry.

3.4.2.2. Apoptosis

Cellular apoptosis, also known as programmed cell death, refers to a cell deletion mechanism that differs from necrosis in terms of morphology and molecular pathways. The expression of phosphatidylserine (PS) at the cell surface is a well-known alteration that accompanies apoptosis and is crucial for the recognition and removal of apoptotic cells by the immune system (Koopman *et al.*, 1994). In this sense, Annexin V is a binding protein widely used as an apoptotic cell marker due to its high affinity to PS (Pellicciari, Bottone and Biggiogera, 1997). Apoptotic cells that have not been removed by phagocytic cells will eventually undergo secondary necrosis, also known as late apoptosis (Strzyz, 2017).

By taking advantage of these mechanisms, we used Annexin V conjugated with CF-Blue fluorochrome to identify apoptotic T cells (Figure 21). Cells undergoing late apoptosis were also detected by PI staining, a fluorescent intercalating dye that binds to DNA in cells with damaged plasmatic and nucleolar membranes.

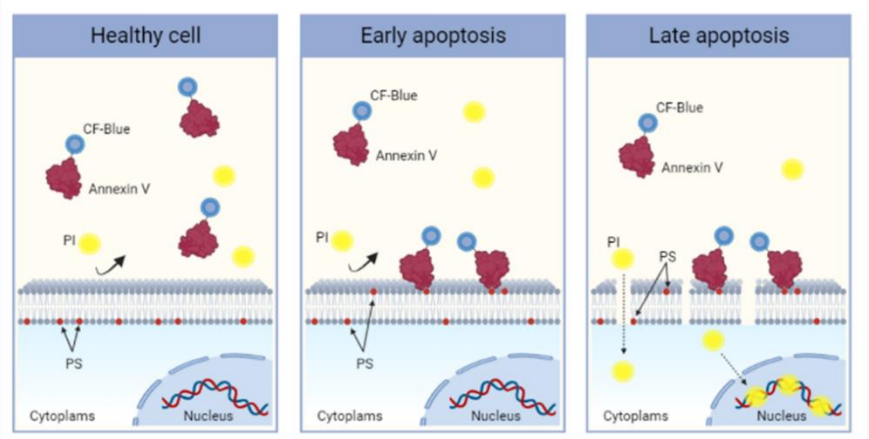

Figure 21. Apoptosis detection by flow cytometry.

In healthy cells, Annexin V is not able to bind phosphatidylserine (PS) and the propidium iodide (PI) is not permeable. During the early stages of apoptosis, PS residues are exposed to the surface of the cell, allowing the adherence of the Annexin V conjugate. In the late stages of apoptosis (secondary necrosis) the cell and nucleus membranes are compromised, allowing the entrance of PI. Created with BioRender.com.

The procedure followed is described below:

1) Prepare aliquots with 0.5-1 million T cells in 100 µl of RM.
2) Add 100 µl of 1x Binding Buffer (BB, provided by the apoptosis detection kit).
3) Add 5 µl of CF-Blue Annexin V.
4) Incubate aliquots for 10 min at 37˚C in the dark.
5) Add 300 µl of PI (1:100) diluted in SM.
6) Keep samples in ice until measurements.

3.4.2.3. Senescence

Senescence refers to a cellular state of permanent detention of the cellular cycle characterized by morphological and functional changes (Rufini *et al.*, 2013; Yeh, 2016). The SA-β-GAL activity was one of the first markers described, and soon became widely used to identify cells with a senescence phenotype (Di Micco *et al.*, no date).

To identify senescent cells, we used the FluoReporterTM lacZ Flow Cytometry Kit. This kit allows the quantification of SA-β-GAL activity with the substrate fluorescein di-β-D-galactopyranoside (FDG), which is hydrolysed to highly fluorescent fluorescein that can be easily detected by flow cytometry. To allow FDG entrance into the cells, we provoke a hypotonic shock at 37˚C.

The procedure followed is described below:

1) Prepare aliquots with 0.5-1 million T cells in 100 µl of RM.
2) Add 50 µl of RM/BB.
3) Add 50 µl of FDG (dilution 1:10).
4) Incubate for 1 min in the dark at 37˚C.
5) Add 300 µl of PI (1:100) diluted in cold SM.
6) Keep samples in ice until measurements.

Note that, in practice, we measured T cell purity (CD3), apoptosis (Annexin V), and senescence (FDG, PI) simultaneously in the same aliquot.

3.4.2.4. Autophagy

Autophagy is the major degradation mechanism of intracellular structures that involves double-membrane vesicles known as autophagosomes. Microtubule-associated protein 1A/1B light chain 3B (LC3B) is a central protein in the autophagy pathway and is widely used as an autophagosome marker (Tanida, Ueno and Kominami, 2008; Tian *et al.*, 2013; Warnes, 2014). When autophagosomes engulf cytoplasmic components during autophagy, including unwanted or dysfunctional cytosolic proteins and organelles, a cytosolic LC3-I is conjugated to eventually form LC3-II which binds the autophagosome membrane (Tanida, Ueno and Kominami, 2008; Klionsky *et al.*, 2016) (Figure 22).

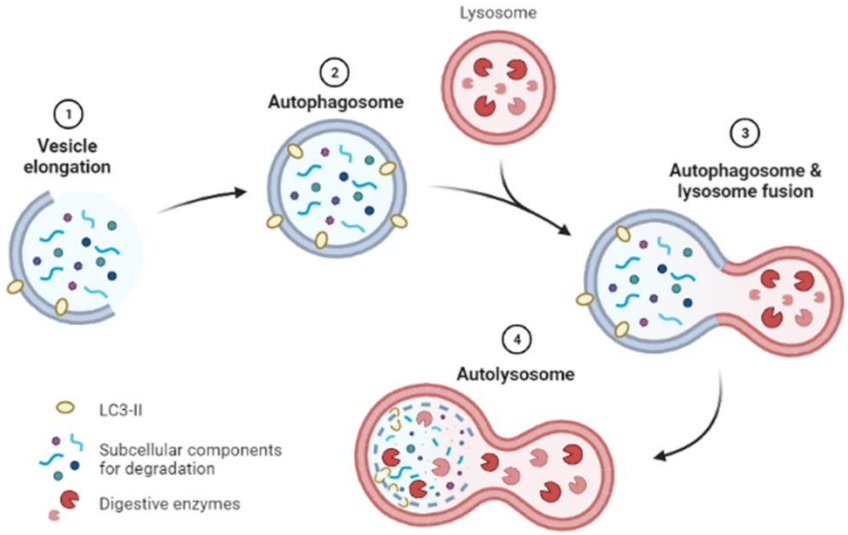

Figure 22. Autophagy mechanism and LC3.

During autophagy, autophagosomes engulf subcellular components for degradation and recruit LC3-II in their membranes. Eventually, the autophagosome fuses with the lysosome, forming the autolysosome and degrading LC3-II and the other components. Created with BioRender.com.

We cultured T cells in the presence and absence of FBS to induce starving conditions. After 4 h of culture, at the peak of macroautophagy activation (Kaushik *et al.*, 2008), cells were permeabilized and LC3-II protein was measured by flow cytometry to study T cell autophagic response to starvation. The Anti-Human/Mouse INTRACELL kit was used to permeabilize the cells. Additionally, the LC3B and the anti-rabbit IgG antibodies were used as indicators of autophagy.

The procedure used is as follows:

1) Culture cells as indicated in section 3.4.1 for 4 h.
2) Collect the cells and centrifuge at 300 g for 5 min at RT.
3) Carefully, discard the supernatant with a pipette.
4) Add 100 µl of Intracell Reagent A (fixative) (INTRA-100).
5) Incubate for 15 min at RT.
6) Wash cells by adding 2 ml of PBS, centrifuge at 300 g for 5 min at RT, and carefully, discard the supernatant with a pipette.
7) Add 100 µl of Intracell Reagent B (permeabilizer) (INTRA-100).
8) Incubate for 15 min at RT.
9) Repeat step wash from step 6.
10) Add 100 µl of LC3B (dilution 1:200, in PBS 2% BSA).
11) Incubate overnight (O/N) at 4˚C in the dark.
12) Repeat the wash from step 6.
13) Add 100 µl of anti-rabbit igG (dilution 1:4000, in PBS 1% BSA).
14) Incubate 1 h at RT in the dark.
15) Repeat step wash from step 6.
16) Adjust volume to 200 µl with flow cytometry buffer.
17) Keep samples in ice until measurements.

3.4.2.5. Mitochondrial membrane potential and ROS

Δψm and mitochondrial ROS are key parameters that allow for a general assessment of mitochondrial function, and which are disrupted in mitochondrial dysfunction (Bou-Teen *et al.*, 2021; Peng *et al.*, 2021; Teixeira *et al.*, 2021; Zupin *et al.*, 2021).

The Δψm is the primary driving force in the generation of ATP by the mitochondria and is composed of a proton gradient produced by the mitochondrial respiratory chain complexes I, III, and IV (Zorova *et al.*, 2018; Creed and McKenzie, 2019). Lipophilic cationic dyes, including the TMRM, are widely used for labelling and measuring the membrane potential of mitochondria in living cells (Chazotte, 2011).

In terms of ROS, mitochondria are considered major producers of these species which contribute to redox signalling. ROS production occurs normally in healthy cells during mitochondrial ATP synthesis; however, this process can be exacerbated by mitochondrial dysfunction, resulting in oxidative stress. H_2O_2 is one of the most studied ROS forms and is commonly detected by mitochondria peroxy yellow 1 (MitoPY1), a small-molecule fluorescent probe that selectively responds to mitochondrial H_2O_2 over other ROS types (Dickinson, Lin and Chang, 2013; Reula *et al.*, 2021).

We measured Δψm and mitochondrial H_2O_2 in freshly isolated T cells from the spleen by flow cytometry using the dyes TMRM and MitoPY1 respectively. Additionally, we used DAPI to mark dead cells.

The procedure used is as follows:

a) Prepare aliquots with 0.5-1 million cells in 200 µl RM.
b) Add 1 µl of MitoPY1.
c) Add 5 µl TMRM (dilution 1:100).
d) Incubate aliquots for 10 min at 37˚C in the dark.
e) Add 300 µl of warm RM.
f) Keep samples in ice until measurements.

3.4.3. Seahorse

The quantification of cellular respiration, together with ΔΨm and ROS production, is one of the most informative assays to determine energy metabolism and mitochondrial function (Brand and Nicholls, 2011; Yépez *et al.*, 2018). Recent advances in methodologies for assessing mitochondrial respiratory function allow the measurement of direct oxygen consumption in a limited number of cultured cells. This is the case with the Seahorse XF Extracellular Flux Analyzer, which allows simultaneous real-time measurements of the oxygen consumption rate (OCR) and extracellular acidification rates (ECAR) of living cells.

The Cell Mito Stress Test is a common method for measuring mitochondrial respiration in cultured cells. This assay determines key parameters using different modulators of the mitochondrial ETC in four different mitochondrial stages: (1) basal conditions, (2) first injection with oligomycin, (3) second injection with carbonyl cyanide-4-(trifluoromethoxy) phenylhydrazone (FCCP) and (4) third injection rotenone and antimycin A (Figure 23).

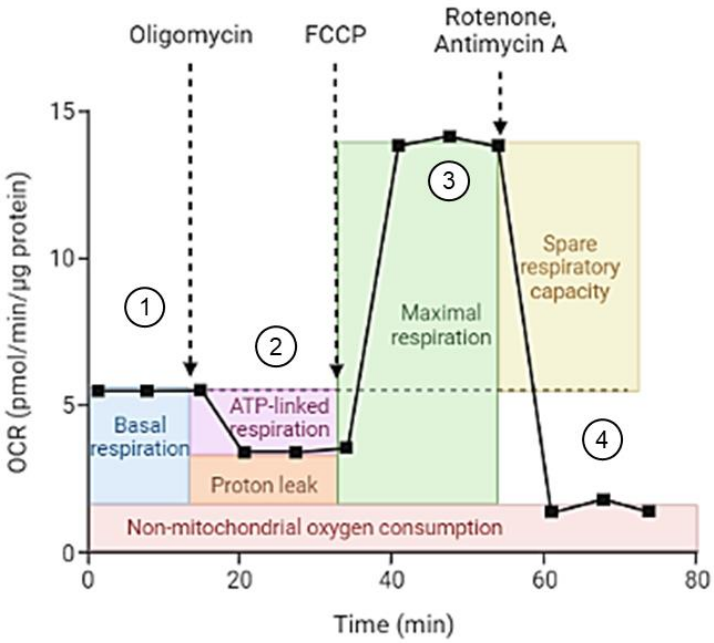

Figure 23. Cell Mito Stress Test.
Created with BioRender.com.

Under basal conditions, complex I, III, and IV pump protons across the inner mitochondrial membrane to generate the proton gradient used by complex V for ATP synthesis. In presence of oligomycin, an inhibitor of complex V, proton translocation towards the mitochondrial matrix is paused, resulting in an unexploited gradient and the halt of the ETC. The subsequent injection of the uncoupling agent FCCP causes the dissipation of the proton gradient and disruption of the ΔΨm. Consequently, the electron flow through the ETC is boosted, forcing cells into a stage of maximal oxygen consumption by complex IV. Finally, the administration of rotenone, an inhibitor of complex I, and antimycin A, an inhibitor of complex III, shuts down mitochondrial respiration, which reveals the non-mitochondrial respiration process outside the mitochondria.

Figure 24 summarizes the action mechanism of the compounds used in the Cell Mito Stress Test to modulate the ETC.

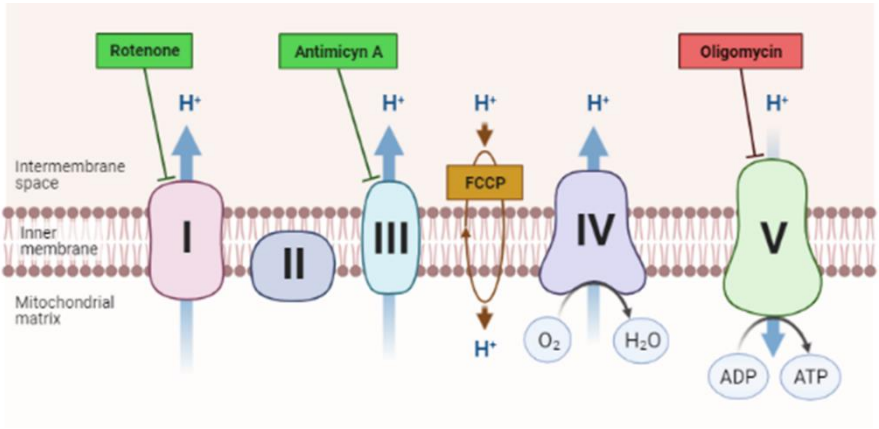

Figure 24. Electron transport chain modulators of the Cell Mito Stress Test.
Created with BioRender.com.

We determined mitochondrial respiratory function in T cells by Seahorse XFe96 Cell Mito Stress Test. XF DMEM medium pH 7.4 with 25 mM glucose, 2mM glutamine, and 1mM pyruvate was used for T cell culture during the assay. The final concentrations used for each compound are Oligomycin 1 µM, FCCP 1.5 µM, and Rotenone/Antimycin A 0.5 µM. The procedure used is as follows:

The day before assay:

1) Place the sensor cartridge upside down (avoid sensor contact).
2) Fill each well of the utility plate with 200 µl of Seahorse XF Calibrant.
3) Lower the sensor cartridge onto the utility plate, submerging the sensors in the calibrant.
4) Incubate the sensor cartridge and utility plate in a non-CO_2 incubator at 37˚C overnight.

5) Turn on the Seahorse XFe Analyzer and let it warm up overnight.

Day of Assay:

1) Prepare assay medium with 25 mM glucose, 2mM glutamine, and 1mM pyruvate, and adjust pH to 7.4 at 37˚C.
2) Seed 0.5 million cells in 180 µl in each well of the XFe96 cell culture microplate.
3) Incubate cells in a non-CO_2 incubator at 37˚C.
4) Prepare stock and working solutions for oligomycin, FCCP, and Rot/AA as shown in Table 5.
5) Remove the cartridge sensor and utility plate from the incubator and load working solutions in the injection ports of the sensor cartridge as shown in Table 5.

Table 5. Compounds preparation and loading in the injection ports.

	Stock solutions		**Working solutions**		**Sensor cartridge solutions**	
Compound	Vol. of assay medium	Stock conc.	Vol. of stock	Vol. of assay medium	Vol. added to port	Final conc. in well
Oligomycin (Port A)	630 µl	100 µM	300 µl	2.7 ml	20 µl	1.0 µM
FCCP (Port B)	720 µl	100 µM	450 µl	2.5 ml	22 µl	1.5 µM
Rot/AA (Port C)	540 µl	50 µM	300 µl	2.7 ml	25 µl	0.5 µM

6) Open Wave program in the computer assigned for the Seahorse XFe Analyzer and open the template file for the Cell Mito Stress Test.
7) Select the *Review and Run* tab, and then click *Start Run*.
8) Place the sensor cartridge and utility plate on the instrument tray, then click *I'm ready*.
9) Meanwhile, the calibration is in process (15-30 min), centrifuge the cell culture plate at 200 g for 1 min.
10) Examine the cells under a microscope to confirm confluence and adherence to the bottom of the plate.
11) Keep the cell plate in a non-CO2 incubator at 37˚C until the assay is ready to run.
12) Following calibration, replace the calibration plate with the cell culture microplate and click *I'm ready* to run the assay.

Isolate T cells the same day of the assay. Similarly, use the compounds on the same day that they are reconstituted and discard any remaining compound solution. Multichannel pipettes are recommended for this assay. Use a minimum of four replicates (wells) for T cells from the same mice. Mean values for each mouse were used for statistical analysis.

3.5. Data analysis

3.5.1. Software and programming language

Data analysis was performed with RStudio, a free software environment for R, which is a programming language for statistical computing and graphics.

3.5.2. Packages and functions

R packages used for data analysis are described in Table 6.

Table 6. Packages used in R.

Package	**Version**	**Description**
dplyr	1.0.7	A grammar of data manipulation
readxl	1.3.1	Import data from excel files into R
ggplot2	3.3.5	Grammar of graphics for data visualization
ggpubr	0.4.0	'ggplot2' based publication ready plots
rstatix	0.7.0	Pipe-friendly framework for basic statistical test
PK	1.3-5	Basic non-compartmental pharmacokinetics
tidyverse	1.3.1	A set of packages that share common data representations and application programming interface design
kableExtra	1.3.4	Construct complex table with 'kable' and pipe syntax
reshape2	1.4.4	Flexibly reshape data
tidyr	1.1.4	Tools to create tidy data
ggmosaic	0.3.3	Mosaic plots in the 'ggplot2' framework
lubridate	1.8.0	Functions to work with data-times
emmeans	1.7.2	Estimated marginal means for linear and mixed models

3.5.3. Outliers

Outliers are extremely distant values in each data set. Since outliers can significantly alter the distribution of the data, the detection of these values is important to assess some statistical tests (Coin, 2007; Osborne and Overbay, 2019). This is the case of correlation studies, regression, T-test, and analysis of variance (ANOVA), which assume a normal distribution of the data. Boxplots are particularly useful for the detection of outliers since display minimum and maximum, first and third quartiles, and the median. Additionally, any observation classified as a suspected outlier using the interquartile range (IQR) criterion is shown as individual points outside the box. According to the IQR criterion, all observations above the first quartile (Q1) or 1.5 times the IQR below the third quartile (Q3) are considered potential outliers (Cho and Eo, 2016; Jeong *et al.*, 2017). We considered outliers those values matching the IQR criterion that were visually identified as extreme for a specific variable.

3.5.4. Normality

As mentioned before, many statistical tests make assumptions about the data being studied. The assumption of normality is one of them and refers to the data following a normal or Gaussian distribution (Ghasemi and Zahediasl, 2012; Schmidt and Finan, 2018). Normality can be assessed by visual methods or normality test, or ideally by a combination of both (Das and Rahmatullah Imon, 2016).

We assessed normality by visualizing density plots and performing Shapiro-Wilk's test. For variables with more than 5000 observations (e.g., the *in vivo* monitoring data sets), the Kolmogorov-Smirnov test was used

instead. On one hand, density plots provide a visual judgment about whether the distribution is bell-shaped. On the other hand, normality tests compare the sample distribution to a normal one to ascertain whether data show a significant deviation from normality or not. The null hypothesis of these tests is that the sample distribution is normal.

3.5.5. Homoscedasticity

The assumption of homoscedasticity (or homogeneity of variances) assumes equal or similar variances in the different groups that are being compared. Similar to the assumption of normality, homoscedasticity is assumed in parametric statistical tests (Goldfeld and Quandt, 1965; Yang, Tu and Chen, 2019). The F-test was used to assess homoscedasticity for normally distributed data. Note that there is no need to perform a test of this assumption in non-normal data because a non-parametric test is used instead.

3.5.6. Statistical tests

Different statistical tests were performed depending on the variable type (numerical or categorical) and whether the data meet the assumptions of the corresponding tests. For variables meeting the assumptions of normality and homoscedasticity, a T-test was used for comparing two groups and linear regression was used to assess the correlation between two variables (Neideen and Brasel, 2007; Kim, 2015). If the assumptions were not met, the Wilcox test was used instead (Wilcox, 2016). For categorical variables, we created a contingency table and performed the Fisher's Exact Test (Fisher, 1992; Raymond and Rousset, 1995).

IV. RESULTS

1. CHARACTERIZATION OF EXPERIMENTAL ANIMALS

1.1. Human BCL-XL transgene is present in Lck^{pr}-Bcl-X$_L$ mice but not in B6 mice

When we obtained our first Lck^{pr}-Bcl-X$_L$ and B6 mice to establish the colony, we determined the presence or absence of the human BCL-XL transgene so that we could identify transgenic mice in recently born animals, which are phenotypically identical to wild-type mice. To determine animal genotype, we amplified two DNA sequences: the BCL-XL transgene (400 bp) and the internal positive control (200 bp). As a result, the presence of the BCL-XL transgene was confirmed in Lck^{pr}-Bcl-X$_L$ mice whereas the control sequence was present in both B6 and Lck^{pr}-Bcl-X$_L$ mice (Figure 25). Thus, we used genotyping to identify Lck^{pr}-Bcl-X$_L$ mice and B6 mice for our experimental purposes.

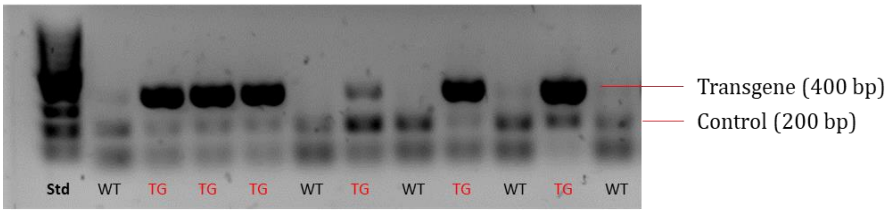

Figure 25. Gel image of mice genotype.

Example of a gel image obtained from genotyping B6 (WT) and Lck^{pr}-Bcl-X$_L$ (TG) mice. We used a gene ruler (Std) to identify transgene and control bands. Samples were obtained from ear tissue.

1.2. BCL-XL protein is overexpressed in thymus, spleen, and splenic T cells from Lck^{pr}-Bcl-X$_L$ mice

At the beginning of the study, we aimed to confirm BCL-XL overexpression in lymphoid organs and T cells from the Lck^{pr}-Bcl-X$_L$ mice born in our colony. First, we sacrificed 2-5 mo B6 and Lck^{pr}-Bcl-X$_L$ mice, to characterize BCL-XL expression in the thymus and spleen. Next, we determined BCL-XL expression levels in splenic isolated T cells from 17-20 and 24-26 mo mice to verify that BCL-XL overexpression is preserved at advanced ages. As a result, BCL-XL overexpression in Lck^{pr}-Bcl-X$_L$ mice compared to B6 mice was confirmed in the thymus (Figure 26), spleen (Figure 27), and T cells (Figure 28) by western blot.

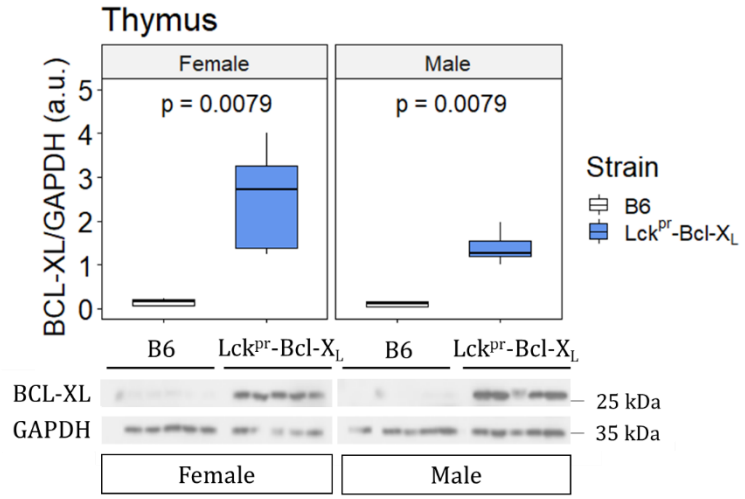

Figure 26. BCL-XL expression in the thymus.

BCL-XL expression relativized to GAPDH in the thymus from 2-5 mo male (n=10) and female (n=10) B6 and Lck^{pr}-Bcl-X$_L$ mice. Data are presented as box plots, and p values were calculated with the Wilcox test.

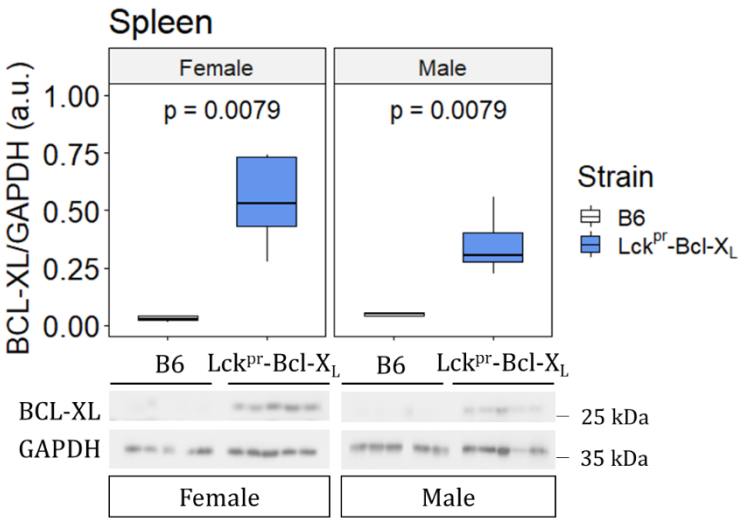

Figure 27. BCL-XL expression in the spleen.

BCL-XL expression relativized to GAPDH in spleen from 2-5 mo male (n=10) and female (n=10) B6 and Lck^{pr}-Bcl-X$_L$ mice. Data are presented as box plots, and p values were calculated with the Wilcox test.

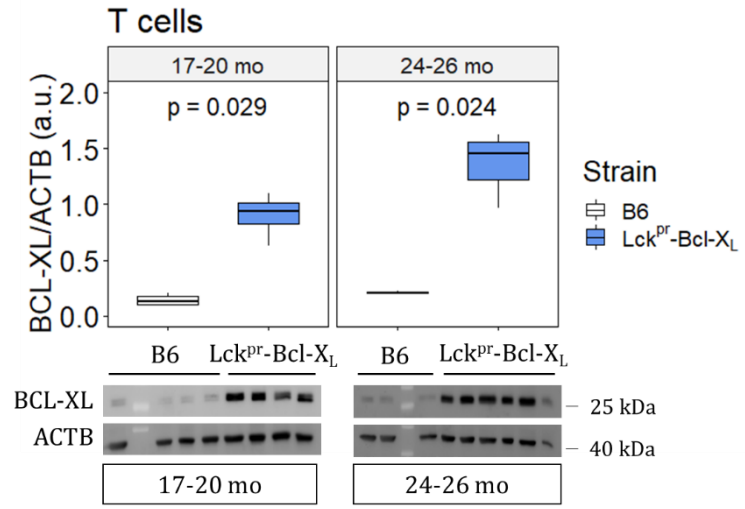

Figure 28. BCL-XL expression in T cells.

BCL-XL expression relativized to beta-actin (ACTB) in T cells from 17-20 (n=8) and 24-26 mo (n=9) B6 and Lck^{pr}-Bcl-X$_L$ mice of both sexes. Data are presented as box plots, and p values were calculated with the Wilcox test.

2. PHYSICAL HEALTH STATUS

2.1. Age-related performance decline is attenuated in Lck^{pr}-Bcl-X$_L$ mice compared to B6 mice

Physical performance declines with increasing age and is used as a predictor of clinical outcome, mortality, and longevity in humans (Guralnik *et al.*, 1994; Onder *et al.*, 2002; Hirsch *et al.*, 2012) and rodents (Carter *et al.*, 2002; Yanai and Endo, 2021). In an approach to measure healthy aging and frailty due to causes occurring early in life, we studied several parameters of physical performance in B6 and Lck^{pr}-Bcl-X$_L$ mice through their lifespan.

We measured mice's body weight, forelimb grip strength, latency time to fall from a rotating rod (as an indicator of motor coordination), and running time during an incremental treadmill test (as a parameter of exercise endurance) in an initial cohort of 142 young mice (2-5 mo). These tests were repeated at 8-11, 17-20, and 24-26 mo as the animals aged. Finally, we calculated the percentage of body weight gain, grip strength decline, latency time loss, and running time decrease for each mouse individually.

2.1.1. Body weight gain

B6 mice's body weight is known to increase with increasing age (Houtkooper *et al.*, 2011; Shoji *et al.*, 2016; Yanai and Endo, 2021). We measured the body weight of B6 and Lck^{pr}-Bcl-X$_L$ mice at different ages and computed the percentage of body weight gain from 2-5 months of age.

In our mice cohort, we observed a general increase of body weight gain above 25% in both strains at all age groups compared to the initial values corresponding to 2-5 months of age represented as a dashed red line (Figure 29). At 8-11 and 17-20 mo, Lck^{pr}-Bcl-X$_L$ mice showed significantly lower body weight gain compared to B6 mice. No differences were found between B6 and Lck^{pr}-Bcl-X$_L$ mice at 24-26 mo. Thus, the increase in body weight associated with aging is attenuated in Lck^{pr}-Bcl-X$_L$ mice, but this protective effect of BCL-XL is lost at very old age.

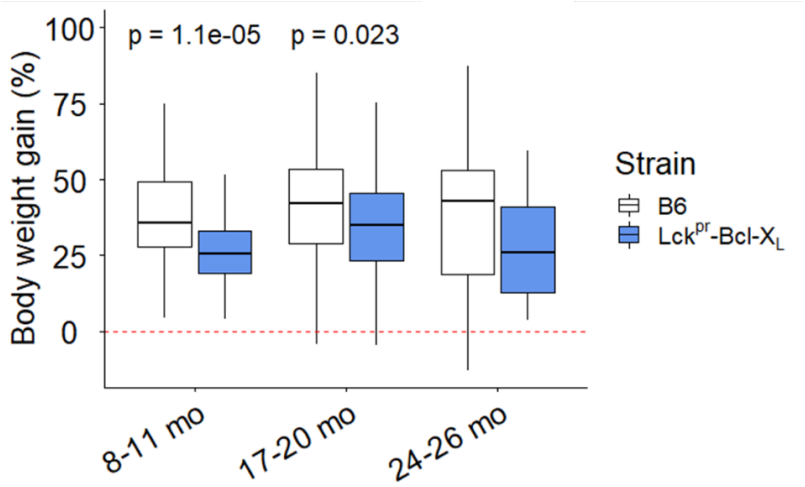

Figure 29. Body weight gain in B6 and Lck^{pr}-Bcl-X$_L$ mice.

Percentage of body weight gain in 8-11 (n=135), 17-20 (n=116) and 24-26 mo (n=34) B6 and Lck^{pr}-Bcl-X$_L$ mice. Reference values at 2-5 months of age (n=135) are represented as a dashed red line. Data are presented as median ± IQR, and p values were calculated with the Wilcox test.

2.1.2. Grip strength loss

The forelimb grip strength test is easy to perform and is used as a universal measurement to assess physical fitness in older adults. Several studies on the elderly have found that grip strength predicts all-cause mortality (Al Snih *et al.*, 2002; Gale *et al.*, 2007). In rodents, and specifically in B6 mice, grip strength decreases with age (Ge *et al.*, 2016; Yanai and Endo, 2021). We calculated the grip strength loss at different ages. As the animals grew older, we observed an increased percentage of grip strength loss in both strains (Figure 30). This increment was attenuated in 8-11 mo Lck^{pr}-Bcl-X$_L$ mice compared to wild-type and no differences were found between B6 and Lck^{pr}-Bcl-X$_L$ mice at older ages. We additionally observed reduced variability at older ages, probably due to smaller sample size.

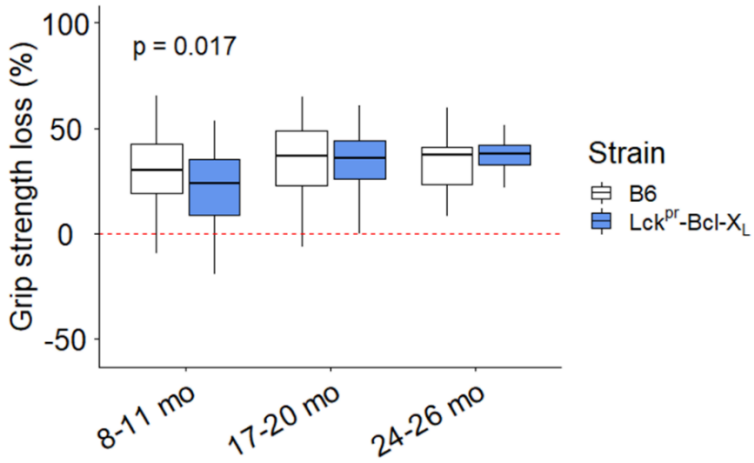

Figure 30. Grip strength loss in B6 and Lck^{pr}-Bcl-X$_L$ mice.

Percentage of grip strength loss in 8-11 (n=138), 17-20 (n=116) and 24-26 mo (n=32) B6 and Lck^{pr}-Bcl-X$_L$ mice. Reference values at 2-5 months of age (n=138) are represented as a dashed red line. Data are presented as median ± IQR, and p values were calculated with the Wilcox test.

2.1.3. Motor coordination loss

Several studies have reported a general motor coordination decline in mouse models of aging (Forster *et al.*, 1996; Allen and Cavanaugh, 2014; Justice *et al.*, 2014). In addition, motor coordination measured as latency to fall off a rotating rod during the rotarod test is known to decrease with age in B6 mice (Shoji *et al.*, 2016). We calculated the percentage of latency time loss at different ages. Compared to B6 mice, Lck^{pr}-Bcl-X$_L$ mice showed a reduced loss of latency time at 8-11 and 17-20 mo, maintaining similar values comparable to their youth (Figure 31). Once again, these data suggest that BCL-XL overexpression delays motor coordination decline in middle age although this protection is lost at very advanced ages.

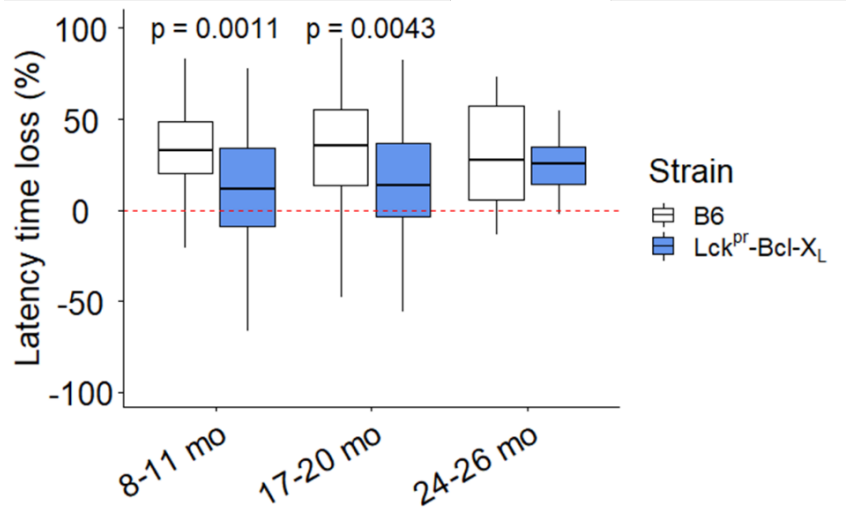

Figure 31. Motor coordination loss in B6 and Lck^{pr}-Bcl-X$_L$ mice.

Percentage of latency time loss indicating motor coordination in 8-11 (n=131), 17-20 (n=110) and 24-26 mo (n=31) B6 and Lck^{pr}-Bcl-X$_L$ mice. Reference values at 2-5 months of age (n=131) are represented as a dashed red line. Data are presented as median ± IQR, and p values were calculated with the Wilcox test.

2.1.4. Exercise endurance loss

Similar to the previous physical parameters, exercise endurance measured as running time declines with advancing age in humans (Tanaka and Seals, 2008; Lara, Salinero and Del Coso, 2014) and rodents (Graber *et al.*, 2021). We evaluated exercise endurance decline as running time decrease in B6 and Lck^{pr}-Bcl-X$_L$ mice at different ages. We found that the running times remained like values recorded at a young age until 24-26 mo when the loss of physical endurance is more noticeable. In addition, running time decrease at 8-11 mo was found attenuated in Lck^{pr}-Bcl-X$_L$ mice compared to B6 (Figure 32). No differences were found between B6 and Lck^{pr}-Bcl-X$_L$ mice at 17-20 and 24-26 mo, indicating a lack of protective role of BCL-XL at older ages.

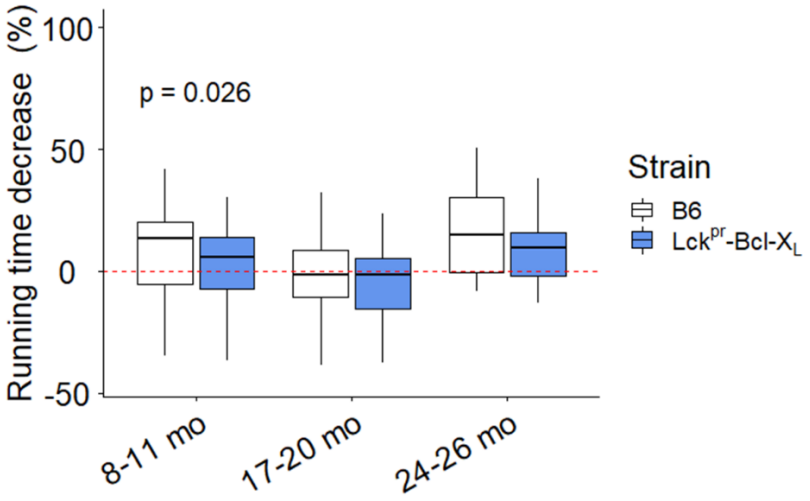

Figure 32. Exercise endurance loss in B6 and Lck^{pr}-Bcl-X$_L$ mice.

Percentage of running time decrease indicating physical endurance in 8-11 (n=133), 17-20 (n=106) and 24-26 mo (n=33) B6 and Lck^{pr}-Bcl-X$_L$ mice. Reference values at 2-5 mo (n=133) are represented as a dashed red line. Data are presented as median ± IQR and p values were calculated with the Wilcox test.

2.2. Spontaneous activity is slightly increased in Lck^{pr}-Bcl-X_L mice compared to B6 mice

Physical inactivity is a leading risk factor for overall morbidity and mortality worldwide (Thornton *et al.*, 2016) and is also well known to decrease with aging in both humans (Meijer *et al.*, 2001; Westerterp and Meijer, 2001; Milanović *et al.*, 2013; Ethisan *et al.*, 2017) and mice (Houtkooper *et al.*, 2011; Seldeen, Pang and Troen, 2015; Shoji *et al.*, 2016; Singhal *et al.*, 2020; Yanai and Endo, 2021). To find an explanation for the differences found in performance decline, we measured spontaneous locomotor activity at the ages where we found the most differences between strains, that is at 8-11 and 17-20 months of age. Thus, we analyzed activity and rearing events registered during *in vivo* metabolic monitoring in B6 and Lck^{pr}-Bcl-X_L mice in these groups of age.

2.2.1. Activity

Activity is a useful parameter reflecting the physical and mental status of experimental animals. After two hours of adaptation to the metabolic home cage, spontaneous activity was monitored for 42 h in 8-11 and 17-20 mo B6 and Lck^{pr}-Bcl-X_L mice.

At 8-11 months of age, activity profiles over time from Lck^{pr}-Bcl-X_L mice were slightly higher than B6 mice (Figure 33A). Mean values of activity were also more elevated in Lck^{pr}-Bcl-X_L, though no significant differences were found between strains (Figure 33B). Similar results were found in the activity AUC analysis (Figure 33C). Both strains exhibited a peak of activity during the dark cycles, as would be expected of nocturnal

animals. This analysis was also performed in 12-20 mo mice and no differences were found between strains (Supplementary figure 1).

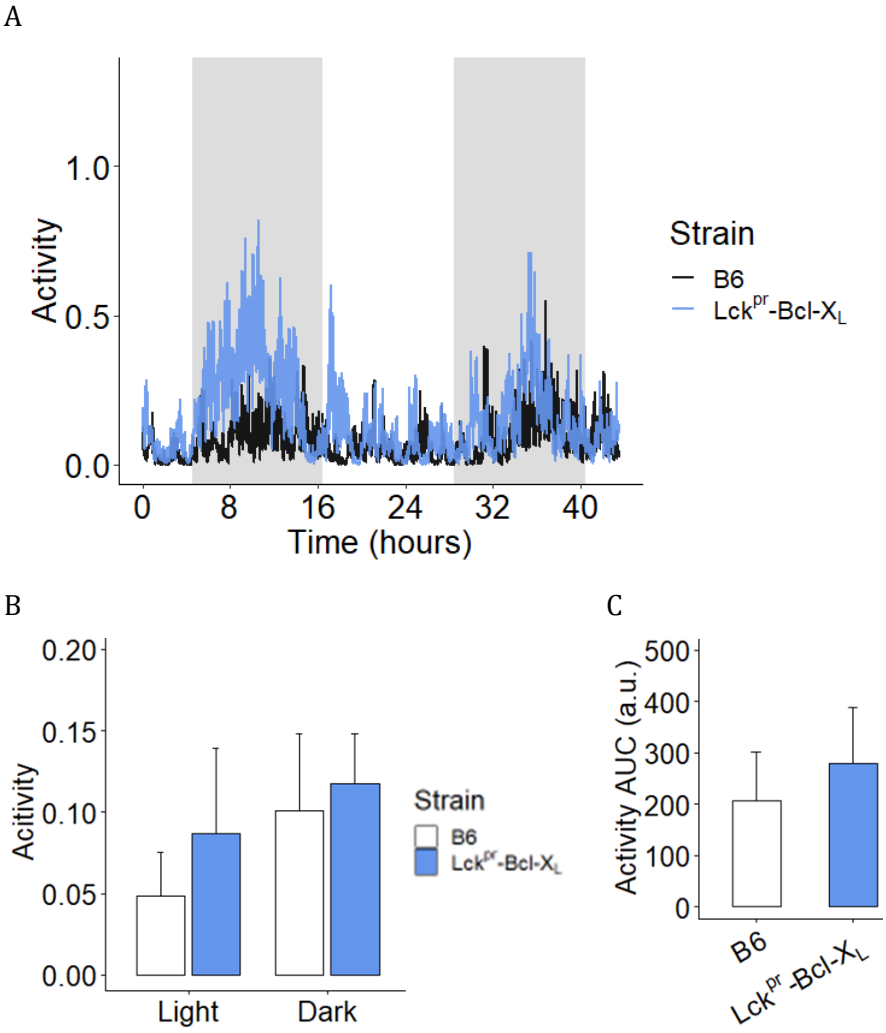

Figure 33. Spontaneous activity in 8-11 mo B6 and Lck^{pr}-Bcl-X$_L$ mice.

Activity measured as horizontal activity over 42 h (A), average data from the light and dark cycles (B), and area under curve (AUC) analysis (C) in 8-11 mo B6 (n=6) and Lck^{pr}-Bcl-X$_L$ (n=9) mice. Data are presented as mean ± sd, and p values were calculated with the T-test.

2.2.2. Rearing

Rearing occurs when rodents stand on their hind legs to explore. This behaviour was evaluated as a complementary parameter to activity to have a comprehensive analysis of the spontaneous locomotor activity. Rearing events were measured as vertical activity registered for 42 h after two hours of adaptation to the metabolic home cage in 8-11 and 17-20 mo B6 and Lck^{pr}-Bcl-X_L mice.

At 8-11 months of age, rearing profiles over time from Lck^{pr}-Bcl-X_L mice are slightly more frequent than in B6 mice (Figure 34A). Mean values of rearing events were slightly higher during the light cycle and significantly elevated during the dark cycle in Lck^{pr}-Bcl-X_L (Figure 34B). Although not statistically significant, transgenic mice exhibited an increased rearing AUC compared to B6 (Figure 34C). At 17-20 months of age, the frequency of rearing events was similar in both strains (Supplementary figure 2). Again, increased levels of rearing can be observed in both strains during the dark cycle, as would be expected of nocturnal animals.

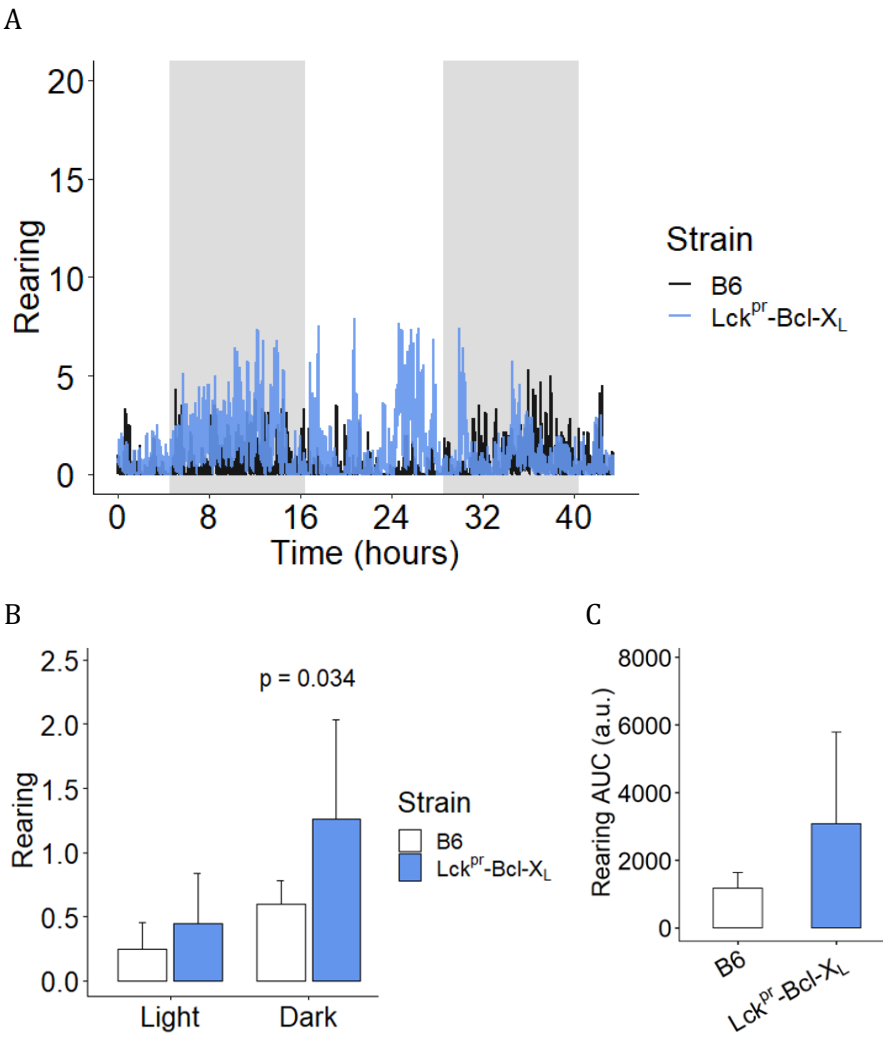

Figure 34. Rearing events in 8-11 mo B6 and Lck^{pr}-Bcl-X$_L$ mice.

Rearing measured as vertical activity over 42 h (A), average data from the light and dark cycles (B), and area under curve (AUC) analysis (C) in 8-11 mo B6 (n=6) and Lck^{pr}-Bcl-X$_L$ (n=9) mice. Data are presented as mean ± sd, and p values were calculated with the T-test.

2.3. Frailty is prevented in aged Lck^{pr}-Bcl-X$_L$ mice compared to B6 mice

Aging is characterized by a general decline of overall function from cellular to organismal levels. In terms of physical health, these changes will eventually lead to frailty, a state of physical vulnerability at advanced ages which compromises the ability to cope with stress (Fried *et al.*, 2001; Xue, 2011). Frailty determination is a potential tool to measure health parameters in aging populations (Whitehead *et al.*, 2014; von Zglinicki *et al.*, 2016; Baumann, Kwak and Thompson, 2018).

The major goal of our research was to assess whether BCL-XL overexpression affects frailty and healthy aging. To accomplish this, cut-off values of several physical tests (body weight, forelimb grip strength, latency time to fall from a rotating rod, and running time during incremental treadmill test) performed at 17-20 and 24-26 months of age were used to calculate the prevalence of frailty and the Valencia Frailty Score in these age groups. It is important to remark that frailty is a syndrome present only in aged individuals, thus, it only makes sense to assess this parameter in old mice.

2.3.1. Prevalence of frailty

Frailty research in human populations focuses on people over 65 years and reports a steady increase of frailty with age (Clegg *et al.*, 2013). The same is observed in mouse models, in which the onset of frailty has been reported to occur around 17 months of age using a frailty phenotype, which included criteria of body weight, walking speed, grip strength, exercise endurance, and physical activity (Kwak, Baumann and

Thompson, 2019). To evaluate the effect of BCL-XL on the prevalence of frailty, we categorized each mouse as non-frail, pre-frail, or frail, according to the number of met criteria. Table 7 shows the cut-off values calculated for 17-20 and 24-26 mo mice.

Table 7. Cut-off values calculated for aged B6 and Lck^{pr}-Bcl-X$_L$ mice.

	17-20 mo *(n=118)*	***24-26 mo*** *(n=35)*
Body weight (g)	37.88	32.16
Grip strength (g/g)	4.38	5.00
Motor coordination (s)	63.00	74.80
Exercise endurance (min)	21.96	15.45

At 17-20 months of age, the proportion of animals identified as frail was almost double in B6 mice (11.59 %) compared to Lck^{pr}-Bcl-X$_L$ mice (6.12 %), but no statistical differences were detected (Supplementary figure 3). At 24-26 months of age mice, 2 out of 17 B6 mice were classified as frail, whereas none of the Lck^{pr}-Bcl-X$_L$ mice were frail, and only one transgenic mouse was pre-frail compared to 6 pre-frail B6 mice (Figure 35). Moreover, the number of non-frail Lck^{pr}-Bcl-X$_L$ mice almost doubled the number of non-frail B6 mice. This frequency distribution resulted in statistically significant. Hence, BCL-XL overexpression prevents frailty in mice at very advanced ages.

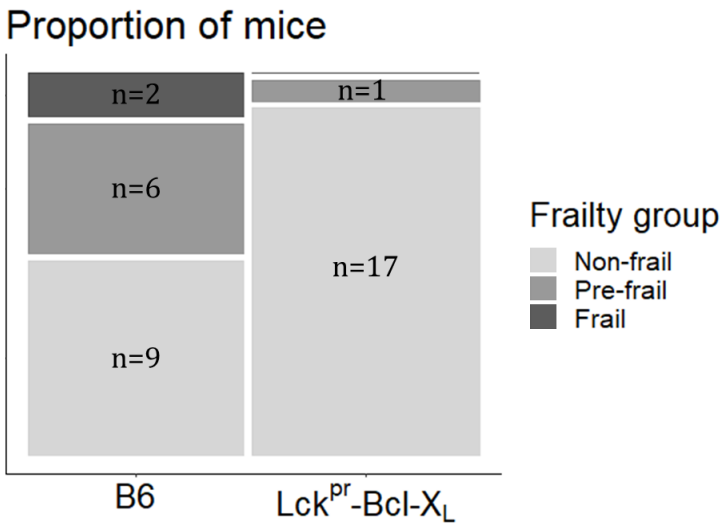

Figure 35. Prevalence of frailty in 24-26 mo B6 and Lck^{pr}-Bcl-X$_L$ mice.
Proportion of 24-26 mo B6 (n=17) and Lck^{pr}-Bcl-X$_L$ (n=18) mice for each frail group (non-frail, pre-frail, and frail). The number of mice is indicated for each group. Data are presented as mosaic plots and a p-value = 0.01244 was calculated with Fisher's exact test.

2.3.2. Valencia Frailty Score

The Valencia frailty score developed by Gómez-Cabrera and colleagues (Gomez-Cabrera *et al.*, 2017) is a simple tool to reflect with a numerical value how badly, rather well, did mice performed the different tests used to assess frailty. As we described in section III. *MATERIAL AND METHODS*, we evaluated frailty with a modified version of this criteria. Still, we were able to determine this score in aged B6 and Lck^{pr}-Bcl-X$_L$ mice following the same rules as described by the authors.

At 17-20 months of age, similar scores were observed in B6 (22.83%) and Lck^{pr}-Bcl-X$_L$ (19.39%) strains (Supplementary figure 4). On the contrary, Valencia Frailty Score was significantly lower in Lck^{pr}-Bcl-X$_L$ mice

(11.11%) compared to B6 mice (29.41%) at 24-26 months of age (Figure 36). To clarify, the higher the score, the worse the performance on the test. Hence, 24-26 mo Lck^{pr}-Bcl-X$_L$ mice displayed a better physical status than B6 of the same age. Thus, suggesting that Lck^{pr}-Bcl-X$_L$ mice are less likely to be frail than their wild-type homologs.

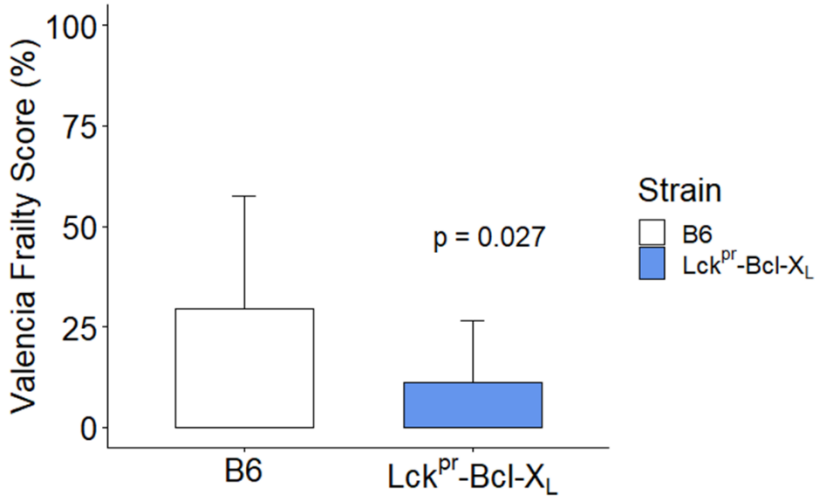

Figure 36. Valencia frailty score in 24-26 mo B6 and Lck^{pr}-Bcl-X$_L$ mice.
Valencia frailty score in 24-26 mo B6 (n=17) and Lck^{pr}-Bcl-X$_L$ (n=18). Data are presented as mean ± sd, and the p-value was calculated with the unpaired two-samples T-test.

3. METABOLISM-RELATED PARAMETERS

3.1. Body composition is maintained with the age in Lck^{pr}-Bcl-X$_L$ mice but not in B6 mice

Changes in body composition in old age are due to changes in the balance between energy intake and expenditure among other factors. In humans, it is generally accepted that as we age, fat mass increases while fat-free mass decreases (Pappas and Nagy, 2019). Similarly, different studies reported a gain in body mass and fat content and a decrease in lean mass in mice during aging (Zamboni *et al.*, 2005; St-Onge and Gallagher, 2010). In the same way, interventions to promote healthy aging have been reported to prevent gains in body mass and fat content (Colman *et al.*, 2007; McMullan *et al.*, 2016). To further clarify the influence of BCL-XL overexpression on mice's physical health, we determined body composition and daily energy intake in young-adult and older-adult B6 and Lck^{pr}-Bcl-X$_L$ mice.

3.1.1. Total body mass

Mice's total body mass was measured with the body composition analyzer DXA to confirm the increased body weight gain with age observed in the previous section (Figure 29). Thus, we expected to see a gain in body mass with age in both strains, but with an exacerbated increase in B6 mice. In agreement with the results described in the section on physical health, B6 exhibited a statistically significant correlation between total body mass and age. Surprisingly, this parameter remained stable throughout the life of Lck^{pr}-Bcl-X$_L$ mice (Figure 37).

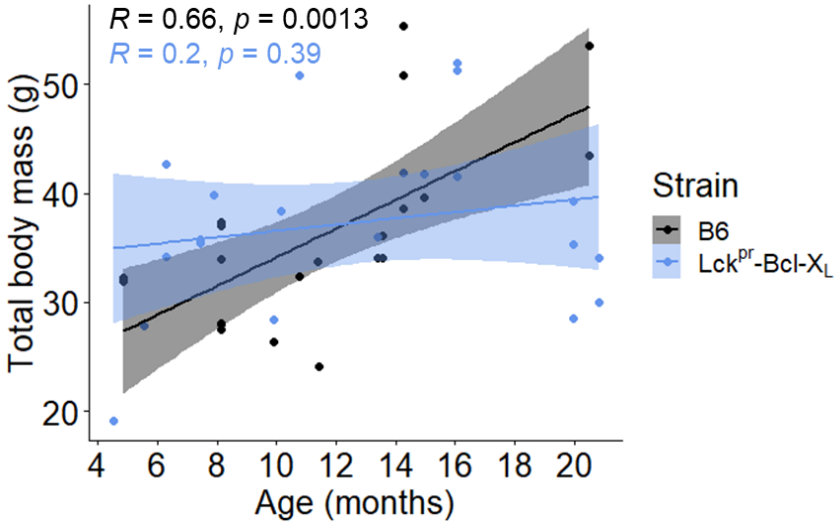

Figure 37. Total body mass correlation with age in B6 and Lck^{pr}-Bcl-X$_L$ mice.
Total body mass in B6 and Lck^{pr}-Bcl-X$_L$ mice of different ages. Data is represented as a scatter plot; dots represent individual values. Linear regression and correlation coefficients p values were calculated with a simple linear regression model.

3.1.2. Lean mass

Similar to total body mass, DXA was used to examine lean mass so that we could understand the differences found in muscle strength and the other physical performance parameters previously described. We did not find a relationship between lean mass and age in none of the strains (Figure 38). Moreover, lean mass is similar in both strains. These results indicate that loss of grip strength observed with age and the differences in strength loss found between strains may not be caused by a loss of muscle mass.

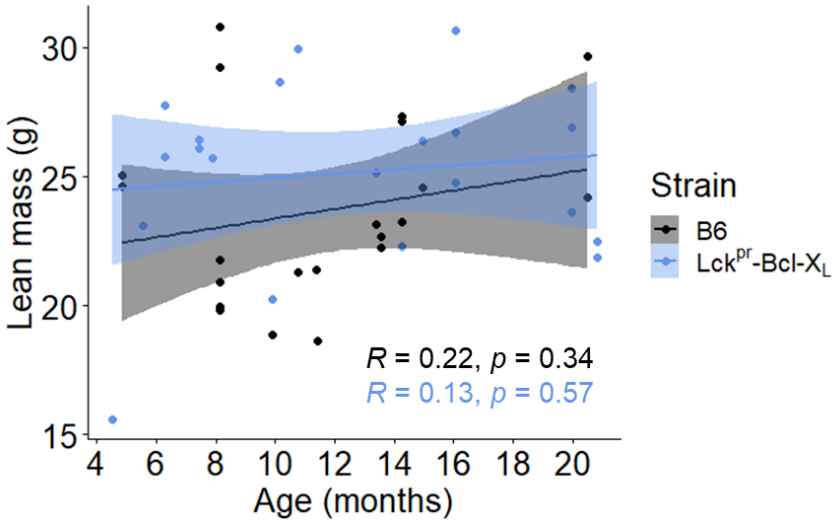

Figure 38. Lean mass correlation with age in B6 and Lck^{pr}-Bcl-X$_L$ mice.

Lean mass in B6 and Lckpr-Bcl-XL mice of different ages. Data is represented as a scatter plot; dots represent individual values. Linear regression and correlation coefficients p values were calculated with a simple linear regression model.

3.1.3. Fat content

In addition to total body mass and lean mass, we analyzed fat content to further investigate the age-related increase in body mass shown in the previous section. We found that body fat percentage, measured as fat mass divided by total body mass, was positively correlated with age in B6 but not Lck^{pr}-Bcl-X$_L$ mice (Figure 39). Thus, the gain of body mass with age in B6 mice could be attributed to an increase in fat content in these animals.

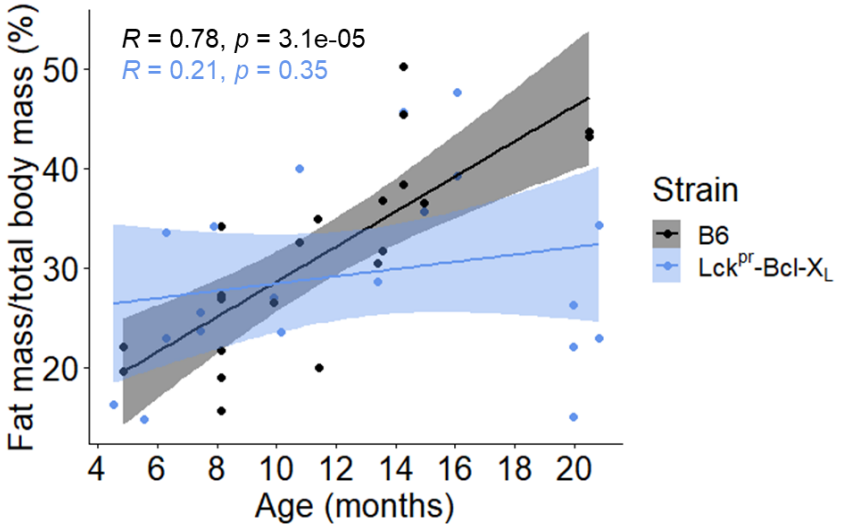

Figure 39. Fat percentage correlation with age in B6 and Lck^{pr}-Bcl-X$_L$ mice.
Percentage of fat body content measured as fat mass divided by total body mass in B6 and Lck^{pr}-Bcl-X$_L$ mice of different ages. Data is represented as a scatter plot; dots represent individual values. Linear regression and correlation coefficients p values were calculated with a simple linear regression model.

3.2. Energy metabolism referred as intake, RQ and EE is similar in B6 and Lck^{pr}-Bcl-X$_L$ mice

Energy homeostasis is critical for the organism's survival and the aging process. Changes in energy regulation contribute to aging-related changes in body composition (Roberts and Rosenberg, 2006). Although little is known about *in vivo* respiratory function during aging, recent studies suggest that age-related physical decline is usually accompanied by a change in the metabolic respiratory phenotype (Houtkooper *et al.*, 2011). We aimed to study the possible influence of BCL-XL overexpression on energy metabolism in adult and old mice to further clarify the differences observed in physical health and body composition. To accomplish this, we measured the RQ and total EE by indirect calorimetry in 8-11 and 17-20 mo B6 and Lck^{pr}-Bcl-X$_L$ mice.

3.2.1. Intake

Energy intake is commonly altered with aging, contributing to age-related changes in energy metabolism. Indeed, body weight maintenance requires energy intake to match EE (Galgani and Ravussin, 2008). Aged mice from several strains exhibit lower food consumption rates (Azzu and Valencak, 2017). In addition to food intake, water intake also decreases with age in rodents (McKinley *et al.*, 2006). The daily food consumption rate observed in our mice was between 0.15 and 0.20 g/g whereas the drink consumption rate was around 0.05 ml/g. However, no differences in daily intake were found between B6 and Lck^{pr}-Bcl-X$_L$ at 8-11 or 17-20 months of age (Figure 40). Hence, the positive correlation

observed in B6 mice of total body mass and fat content with age may not be related to increased consumption.

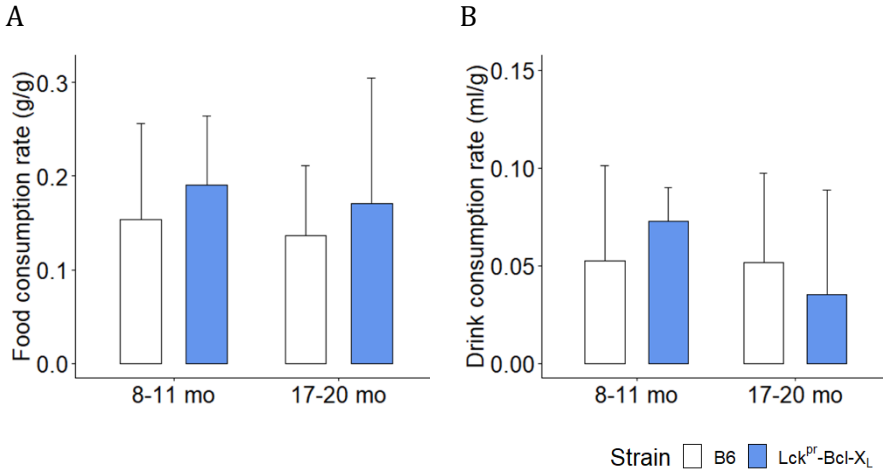

Figure 40. Intake in 8-11 mo B6 and Lck^{pr}-Bcl-X$_L$ mice.

Daily food (A) and drink (B) consumption rates normalized to body weight in 8-11 mo (n=15) and 17-20 (n=12) B6 and Lck^{pr}-Bcl-X$_L$ mice. Data are presented as mean ± sd, and p values were calculated with the unpaired two-samples T-test.

3.2.2. Respiratory quotient

The RQ calculated from the gas exchange by indirect calorimetry is used to investigate the relative contribution of various substrates to energy metabolism (Ferrannini, 1988; McClave *et al.*, 2003; Glass *et al.*, 2013). RQ has been reported to decrease with age in humans (Rizzo *et al.*, 2005) and mice (Houtkooper *et al.*, 2011). Moreover, low levels of RQ are linked to age-associated pathologies such as sarcopenia (Glass *et al.*, 2013). In our mice, we observed mean RQ values above 0.8, suggesting a predominant protein substrate utilization (Figure 41A). No differences in RQ were found between 8-11 mo B6 and Lck^{pr}-Bcl-X$_L$ mice (Figure 41B-C). Similar

results were observed in 17-20 mo mice, with no differences in RQ between strains (Supplementary figure 5).

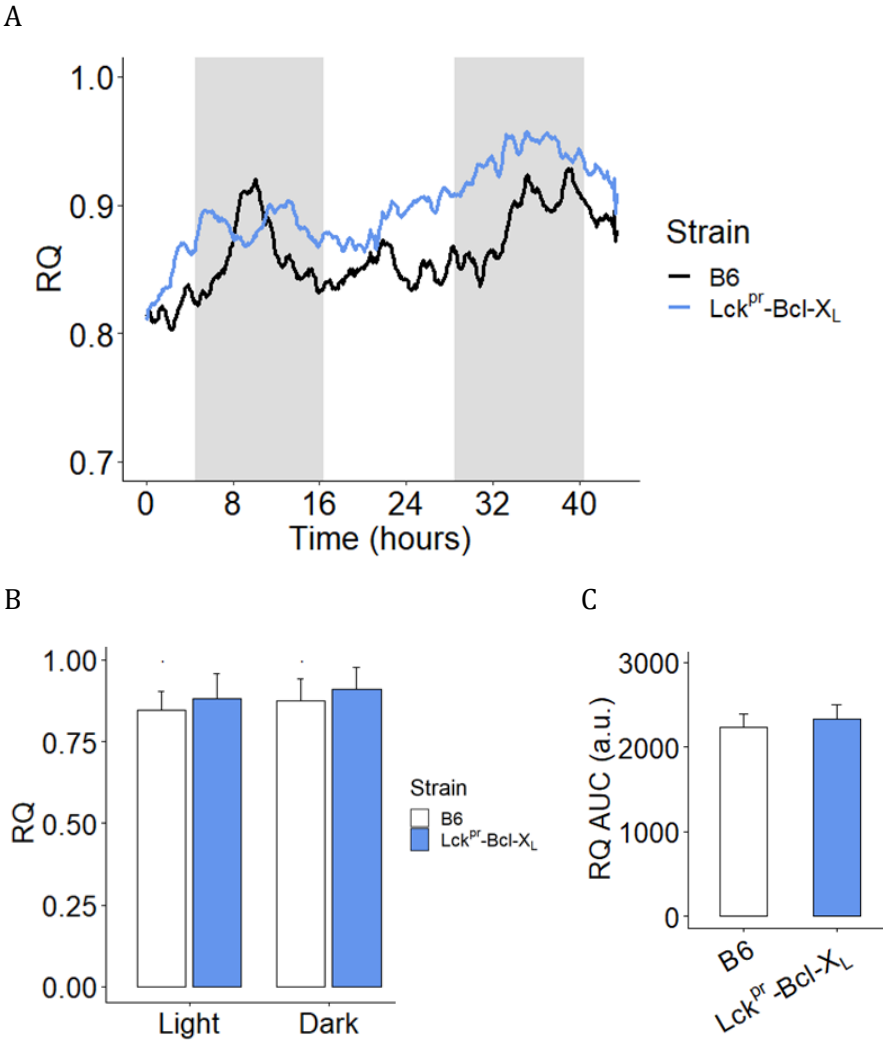

Figure 41. Respiratory quotient in 8-11 mo B6 and Lck^{pr}-Bcl-X$_L$ mice.

Respiratory quotient (RQ) over 42h (A), average data from the light and dark cycles (B), and area under curve (AUC) analysis (C) in 8-11 mo B6 (n=6) and Lck^{pr}-Bcl-X$_L$ (n=9) mice. Data are presented as mean ± sd, and p values were calculated with the unpaired two-samples T-test.

3.2.3. Energy expenditure

Total EE is the amount of energy expended to carry out everyday activities and is determined as the sum of basal metabolic rate, the thermic effect of food, and the activity thermogenesis (Manini, 2010; Levine, 2022). Several studies reported that an age-associated decrease in physical activity is accompanied by a progressive decline in total EE (Poehlman, 1992; Ritz and Berrut, 2005; Roberts and Rosenberg, 2006; Roberts, Dallal and Mayer, 2007). Indeed, all components of EE decrease with aging, particularly basal metabolic rate and EE due to physical activity (Roberts and Rosenberg, 2006; Azzu and Valencak, 2017).

We recorded mean EE values between 125 and 225 kcal/min/$kg^{0.75}$ in our mice, with discernible peaks during the night cycles probably due to increased activity (Figure 42A). Once more, no differences in EE were found between 8-11 mo B6 and Lck^{pr}-Bcl-X_L mice (Figure 42B-C). Similar results were observed in 17-20 mo mice (Supplementary figure 6).

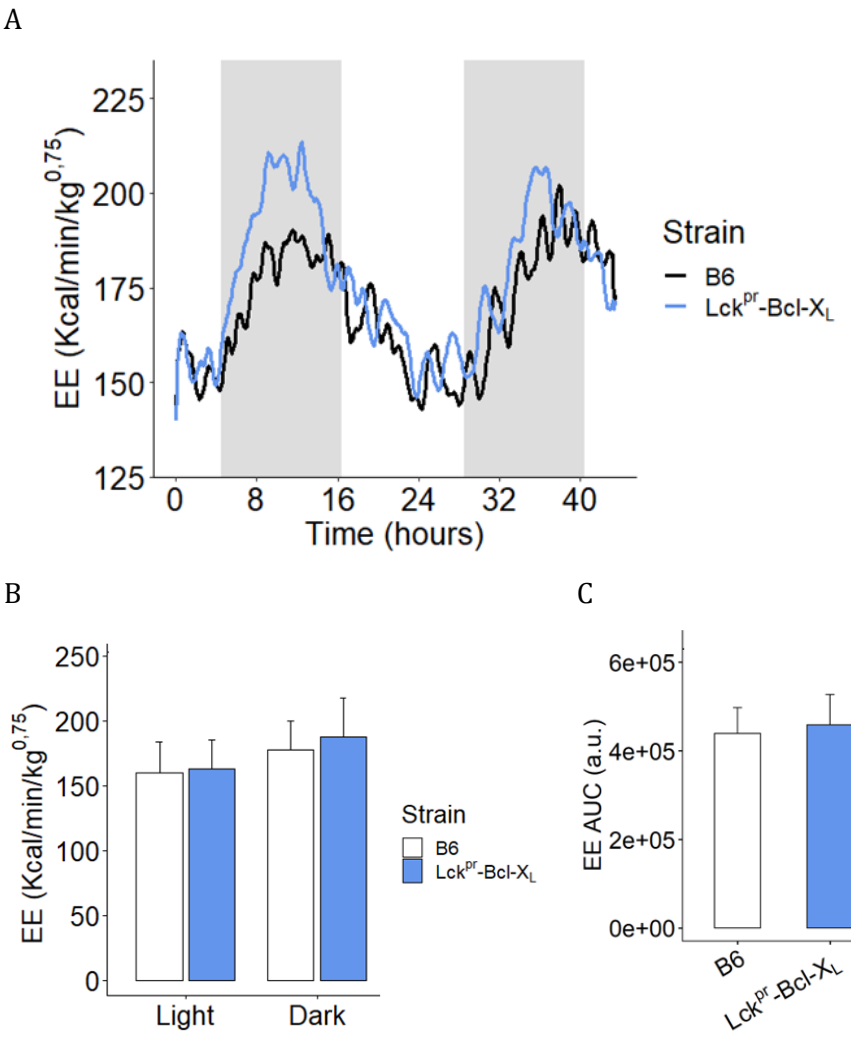

Figure 42. Energy expenditure in 8-11 mo B6 and Lck^{pr}-Bcl-X$_L$ mice.

Energy expenditure (EE) over 42 h (A), average data from the light and dark cycles (B), and area under curve (AUC) analysis (C) in 8-11 mo B6 (n=6) and Lck^{pr}-Bcl-X$_L$ (n=9) mice. Data are presented as mean ± sd, and p values were calculated with the unpaired two-samples T-test.

3.3. Glucose tolerance is improved in aged Lck^{pr}-Bcl-X$_L$ mice compared to B6 mice

The aging phenotype is accompanied by all sorts of pathological conditions, including metabolic dysfunction, that may contribute to reduce healthspan. Glucose tolerance is impaired in older adults, making it one of the major risk factors for diabetes mellitus (de Fronzo, 1981; Stevic *et al.*, 2007; Kalyani and Egan, 2013; Chia, Egan and Ferrucci, 2018). Similarly, several interventions to prevent the age-related phenotype, such as caloric restriction and exercise, also reported beneficial effects on glucose tolerance (Flack *et al.*, 2011; Mayurasakorn *et al.*, 2018). Although little is known about the effect of BCL-XL on glucose metabolism during aging, and considering the enhanced physical status observed in our transgenic mice, we decided to investigate glucose metabolism under the hypothesis that BCL-XL overexpression would also improve glucose tolerance.

In our mice, we registered basal blood glucose levels around 100 mg/dL and observed a pronounced peak at 15 and 30 min after the glucose intraperitoneal injection followed by a progressive decrease with time during the GTT (Figure 43A). Consistent with our hypothesis, similar profiles were observed in the 6-14 mo mice and 15-23 mo Lck^{pr}-Bcl-X$_L$ mice, whereas 15-23 mo B6 mice showed the highest values of glycemia during the recovery phase. The AUC analysis confirmed an improved glucose metabolism in aged Lck^{pr}-Bcl-X$_L$ mice compared to B6 mice of similar age (Figure 43B). Hence, BCL-XL overexpression prevents glucose tolerance impairment associated with aging.

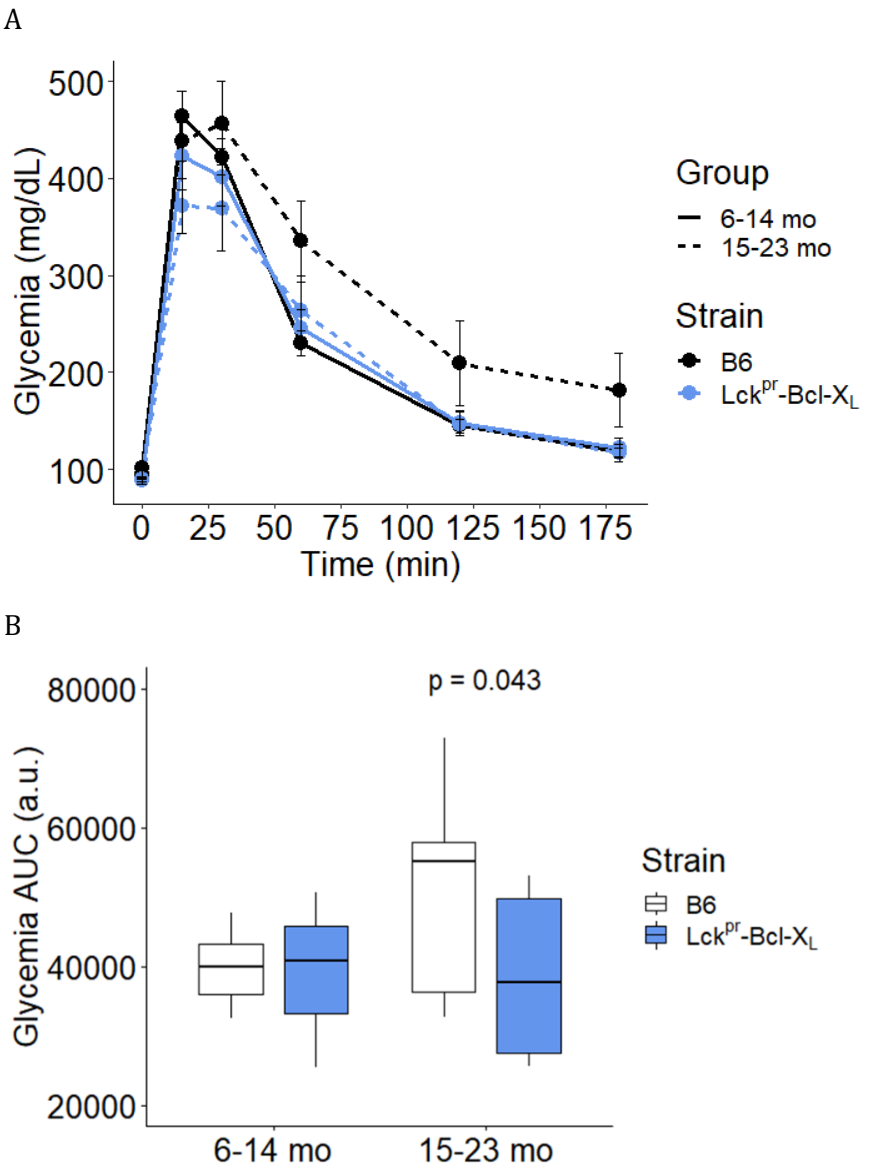

Figure 43. Glucose tolerance test in Lck^{pr}-Bcl-X$_L$ and B6 mice.

Glycemia evolution in 6-14 mo (n=20) and 15-23 mo (n=19) B6 and Lck^{pr}-Bcl-X$_L$ mice during GTT (A). Data are presented as mean ± sem. Glycemia was measured before (min 0) and after an intraperitoneal injection of glucose (2g/kg) in 12 h fasted mice. Glycemia area under curve (AUC) analysis (B). Data are presented as box plots and p values were calculated with the two-sample Wilcox test.

4. T CELL FUNCTION

4.1. Characterization of B6 and Lck^{pr}-Bcl-X$_L$ mice-derived T cells isolated from spleen

Because Lck^{pr}-Bcl-X$_L$ mice overexpress BCL-XL in T cells specifically, we wanted to study their phenotype. Thus, by understanding the specific characteristics of these transformed cells, we may be able to explain the differences found *in vivo* between B6 and Lck^{pr}-Bcl-X$_L$ mice. First, we wanted to investigate if the isolation method used to obtain splenic T cells was adequate. Second, we wanted to examine if the overexpression of BCL-XL affected the T cell population.

4.1.1. T cell purity, size, and shape

To verify whether the isolation method used to obtain T cells from the spleen was adequate for our experimental purposes, we quantified T cell purity as CD3-positive cells. We determined T cell purity in the cell suspension obtained after the T cell isolation protocol using mice of different age groups (2-5 mo, 8-11 mo, 17-20 mo, and 24-26 mo). As a result, all mice-derived cells had values of CD3-positive cells over 90%, and all experimental groups showed a median value of over 95% following T cell isolation (Figure 44). Hence, the isolation method used was, indeed, effective.

A

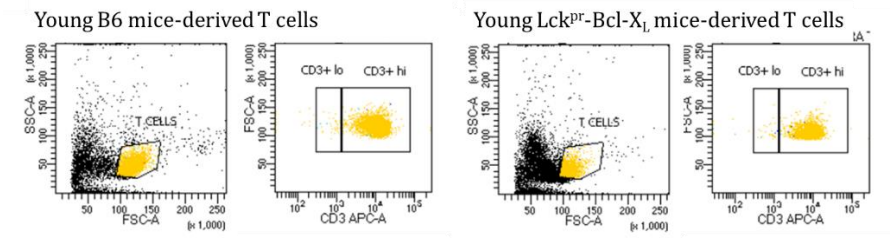

C

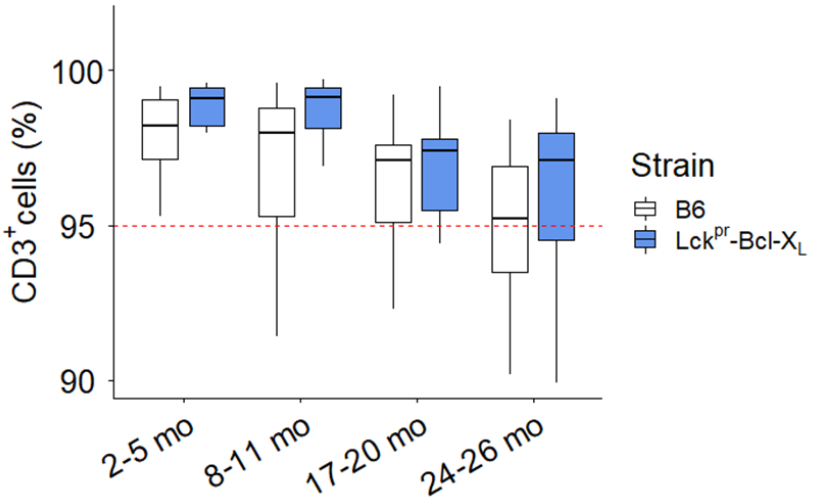

Figure 44. Purity of isolated T cells from the spleen.

Representative image showing T cell gating for side scatter (SSC), forward scatter (FSC), and CD3 (CD3+ lo and CD3+ hi) positive cells for young B6 and Lck^{pr}-Bcl-X$_L$ mice (A). T cell isolation efficiency measured as percentage of total CD3 positive events in freshly isolated T cells from 2-5 (n=27), 8-11 (n=28), 17-20 (n=29) and 24-26 mo (n=33) B6 and Lck^{pr}-Bcl-X$_L$ mice by flow cytometry (B). Data are presented as box plots, and p values were calculated with the Wilcox test.

Under normal circumstances, naïve T cells are spherical in shape and have an average size of 6.5 µm of diameter (Lin *et al.*, 2015; Tasnim *et al.*, 2018). We also confirmed T cell shape and size in a cell suspension of young mice-derived T cells under the microscope (Figure 45).

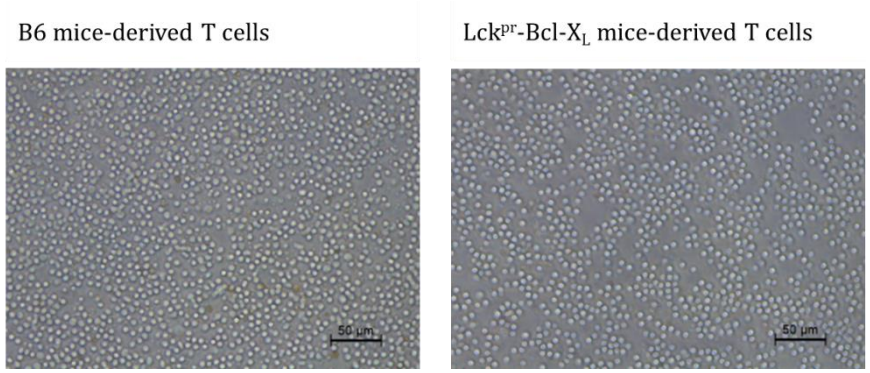

Figure 45. Shape and size of isolated T cell from the spleen.
Representative image of T cell shape and size isolated from young B6 (left) and Lck^{pr}-Bcl-X$_L$ mice (right) in culture under an optic microscope with a 20x objective.

4.1.2. T cell number

The first investigations using Lck^{pr}-Bcl-X$_L$ mice found that constitutive expression of BCL-XL in T cells resulted in an accumulation of thymocytes in lymphoid organs, as evidenced by an increase in total and splenic thymocytes when compared to wild-type mice (Chao *et al.*, 1995; Grillot, Merino and Nunez, 1995). To reproduce these experiments, we measured the number of total white cells and T cells isolated from mice spleens.

As a result, the total number of splenic white cells obtained from B6 and Lck^{pr}-Bcl-X$_L$ mice was similar, approximately between 50 and 150 million cells (Figure 46A). On the other hand, the number of splenic T cells per 100 million white cells obtained from was significantly higher in Lck^{pr}-Bcl-X$_L$ mice compared to B6 mice at 2-5, 8-11, and 17-20 months of age (Figure 46B). Interestingly, no significant differences were found in older mice. These results suggest that BCL-XL overexpression increases the T cell population without altering the total number of splenic white cells, and this effect is lost with age.

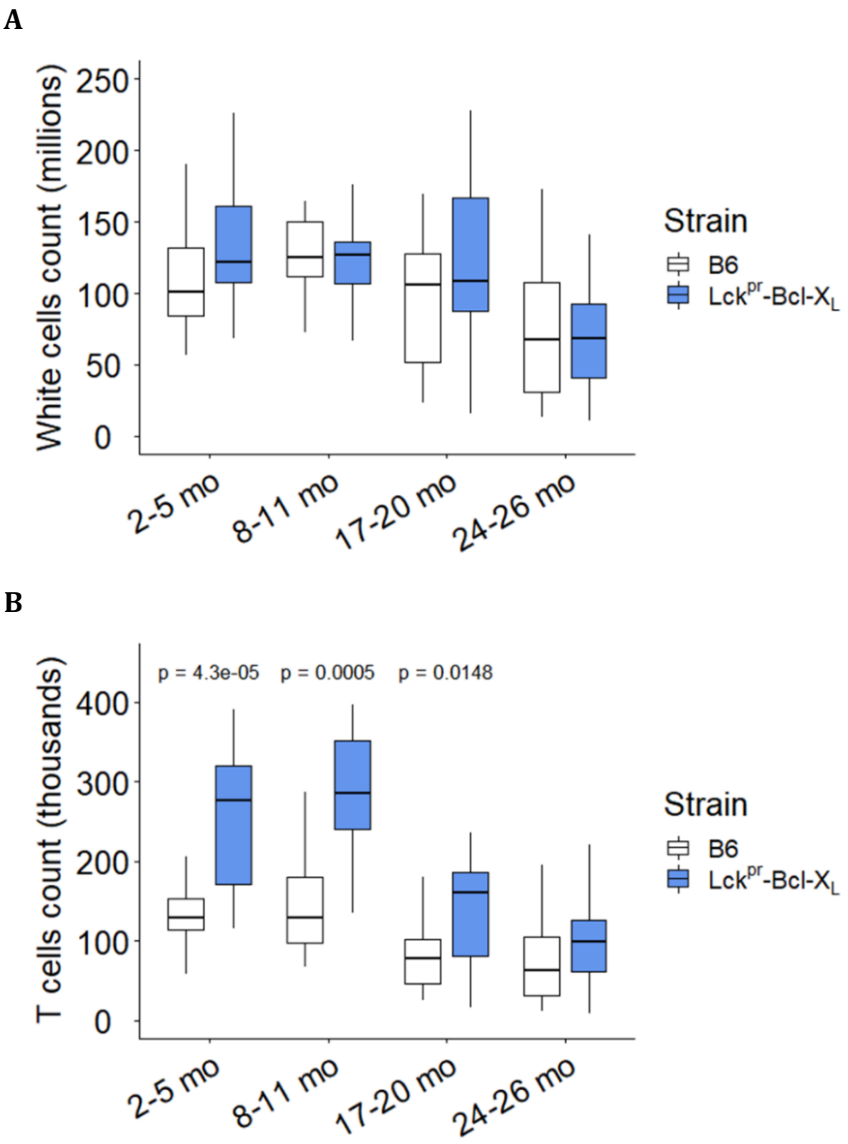

Figure 46. Spleen cell count from B6 and Lck^{pr}-Bcl-X$_L$ mice.

Number of splenic white cells and obtained from 2-5 (n=34), 8-11 (n=29), 17-20 (n=29) and 24-26 (n=34) mo B6 and Lck^{pr}-Bcl-X$_L$ mice (A). Number of splenic T cells per 100 million white cells obtained from 2-5 (n=39), 8-11 (n=28), 17-20 (n=32) and 24-26 (n=37) mo B6 and Lck^{pr}-Bcl-X$_L$ mice (B). Data are presented as box plots and p values were calculated with the two-sample Wilcox test.

4.2. Cell survival mechanisms are enhanced in Lck^{pr}-Bcl-X$_L$ mice-derived T cells under stressful conditions

Cellular apoptosis (i.e., self-killing pathway) and autophagy (i.e., self-eating pathway) are critical processes that help to maintain organismal and cellular homeostasis, but can also lead cells to commit suicide (Jin and El-Deiry, 2005; Fan and Zong, 2013). These processes are deeply intertwined at multiple levels, with complementary pathways involved in the activation and inhibition of both processes. Moreover, similar stimuli have been reported to be able to induce either of both (Galluzzi *et al.*, 2008; Fan and Zong, 2013).

BCL-XL role in cell survival is well characterized in both apoptosis and autophagy. In brief, BCL-XL promotes cell survival and inhibits cell death mechanisms by sequestering pro-apoptotic and pro-autophagic antagonists such as BAX/BAK and BECLIN-1, respectively (Galluzzi *et al.*, 2008; Michels *et al.*, 2013; Hatok and Racay, 2016). By blocking these pathways, we expected that BCL-XL would improve T cell survival, which in turn would explain why T cells accumulate in the spleen. To test this hypothesis, we investigated apoptosis and autophagy in fresh and cultured spleen-isolated T cells from B6 and Lck^{pr}-Bcl-X$_L$ mice by flow cytometry. Since BCL-XL overexpression has been shown to decrease senescence in lymphoid cells, we also would expect a reduction of senescence parameters.

4.2.1. Apoptosis

4.2.1.1. Apoptosis under physiological conditions

Apoptosis occurs during development and aging as a homeostatic mechanism to maintain cell populations in tissues. Under some circumstances (e.g. malignant or damaged cells, immunological responses), apoptosis is also a defence mechanism (Elmore, 2007). Inhibition of apoptosis was the first function described for BCL-XL protein (Chao *et al.*, 1995).

To assess cellular apoptosis in freshly isolated T cells from the spleen, we quantified the percentage of T cells positive for Annexin V (Wlodkowic, Skommer and Darzynkiewicz, 2009; Ni *et al.*, 2013). Contrary to our expectations, our results showed that 17-20 mo Lck^{pr}-Bcl-X_L mice-derived T cells had higher levels of apoptosis than T cells from B6 mice (Figure 47). These results indicate that BCL-XL is not acting as an anti-apoptotic protein under these conditions, but rather as a pro-apoptotic one.

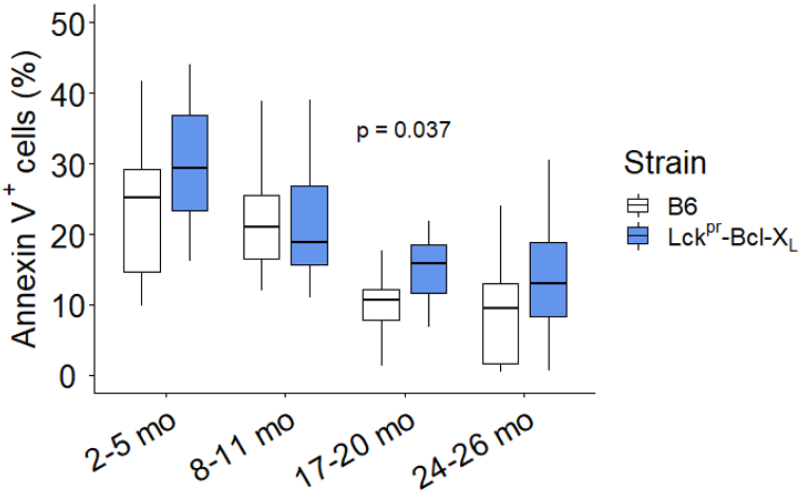

Figure 47. Apoptosis in freshly isolated T cells from B6 and Lck^{pr}-Bcl-X$_L$ mice.
Percentage of Annexin V positive events in freshly isolated T cells from 2-5 (n=23), 8-11 (n=28), 17-20 (n=32) and 24-26 mo (n=35) B6 and Lck^{pr}-Bcl-X$_L$ mice by flow cytometry. Data are represented as box plots and p values were calculated with the two-sample Wilcox test.

4.2.1.2. Apoptosis under stressful conditions

After observing a null anti-apoptotic effect of BCL-XL in T cells from Lck^{pr}-Bcl-X$_L$ mice (Figure 47), we wondered if this effect would be visible in a more hostile environment, in which apoptotic pathways would be greatly upregulated. Previous studies show that T cells commonly die after being isolated from animals and cultured without any further intervention such as T cell induction of T cell activation by cytokines (Vella *et al.*, 1998; Siemasko *et al.*, 2008; Mohtashami, Zarin and Zúñiga-Pflücker, 2016). Moreover, glucocorticoid dexamethasone has been found to induce apoptosis in T cells (Schmidt *et al.*, 2004; Orlikowsky *et al.*, 2005; Xing *et al.*, 2015). In this sense, it has been previously demonstrated that thymocytes overexpressing BCL-XL exhibited increased viability *in vitro*

and were resistant to apoptosis induced by dexamethasone (Grillot, Merino and Nunez, 1995). Thus, we determined apoptosis in control cultured T cells (CTL) and the presence of the T cell-apoptosis inductor dexamethasone (DXM) after 4, 24, and 48 hours of culture. As a result, a general decrease in apoptosis was observed in T cells from Lck^{pr}-Bcl-X$_L$ mice at 2-5 and 8-11 months of age compared to B6 mice (Figure 48). These results indicate an anti-apoptotic role of BCL-XL in cultured T cells early in life, but this protective effect fades with age. Curiously, no differences were found in cells from aged mice.

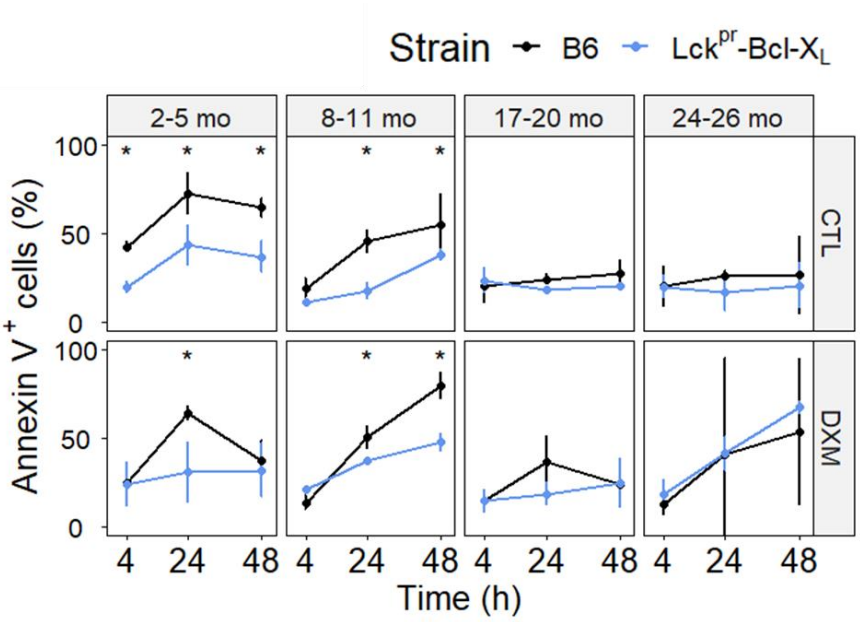

Figure 48. Apoptosis in cultured T cells from B6 and Lck^{pr}-Bcl-X$_L$ mice.

Percentage of Annexin V positive events in T cells from 2-5 (n=8), 8-11 (n=8), 17-20 (n=10) and 24-26 mo (n=9) B6 and Lck^{pr}-Bcl-X$_L$ mice by flow cytometry. Cells were cultured in the absence (CTL) and presence of dexamethasone (DXM) for 4, 24, and 48 h. Data are presented as median ± IQR and p values were calculated with the two-sample Wilcox test. We use the following convention for symbols indicating statistical significance: (*) $p \leq 0.05$.

4.2.2. Autophagic response to starvation

Autophagy is a catabolic pathway that promotes the lysosomal degradation of subcellular components such as cytoplasm portions, damaged proteins, and organelles (Galluzzi *et al.*, 2008). The most potent known physiological inducer of autophagy is starvation. In the absence of nutrition, autophagy may either lead to cell death or serve as a cellular defence against this stress (M.C. Maiuri, Criollo, *et al.*, 2007; M.C. Maiuri, LeToumelin, *et al.*, 2007). Several studies evidence the important role of BCL-XL in the regulation of autophagy by interacting with BECLIN-1 (Maiuri, *et al.*, 2007; Zhou, Yang and Xing, 2011; Lee and Douglas Fairlie, 2019; Li *et al.*, 2020); thus, preventing the formation of the autophagy-inducing BECLIN-1-VPS34 complex (Furuya *et al.*, 2005; He and Levine, 2010; Maejima *et al.*, 2013).

We determined autophagy in permeabilized T cells targeting LC3-II, a protein found in autophagosomes and autolysosomes (Tanida, Ueno and Kominami, 2008; Runwal *et al.*, 2019). First, LC3-II was determined in starved cells from B6 and Lck^{pr}-Bcl-X_L mice at different ages, but no differences were found between strains (Supplementary figure 7).

Then, we cultured T cells from aged mice in which LC3-II was more present and put them under fed and starving conditions to further explore autophagy response to starvation at advanced ages. Whereas no difference in LC3-II was observed in T cells from B6 mice when comparing fed and starved cells, a significant increase was found in cells from Lck^{pr}-Bcl-X_L mice at 17-20 and 24-26 mo (Figure 49). These results indicate an enhanced autophagic response in T cells from Lck^{pr}-Bcl-X_L mice compared to B6 mice. Additionally, these differences could be a

consequence of a preserved basal LC3-II signal in BCL-XL overexpressing T cells, whereas this parameter is already increased in B6-derived T cells.

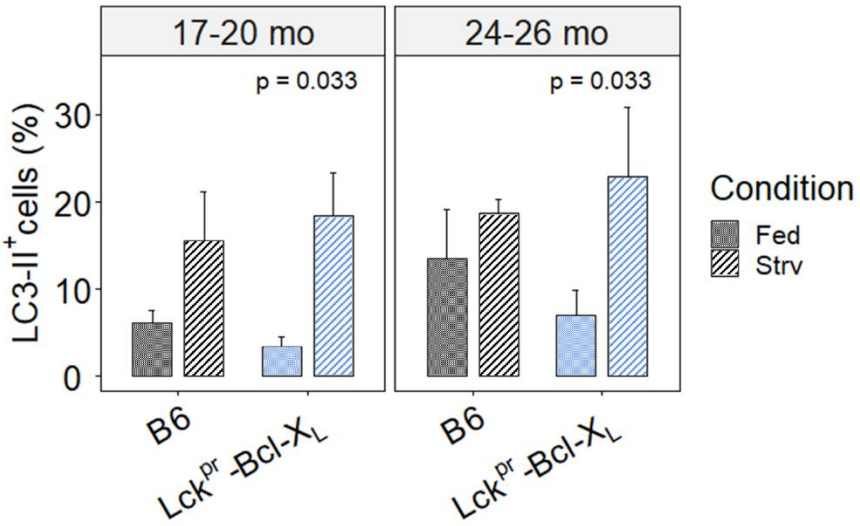

Figure 49. Autophagy response in T cells from aged B6 and Lck^{pr}-Bcl-X$_L$ mice.
Percentage of LC3-II positive T cells from 17-20 mo (n=12) and 24-26 mo (n=16) B6 and Lck^{pr}-Bcl-X$_L$ mice after 4 h of culture under control (Fed) and starving (Strv) conditions. Data are presented as mean ± sd and p values were calculated with the two-samples T-test.

4.2.3. Cellular senescence

Cellular senescence is critical for several biological processes, including tumorigenesis suppression (Van Deursen, Deursen and Van Deursen, 2014). Senescent cells accumulate in different tissues as we age (Dimri *et al.*, 1995; Jeyapalan *et al.*, 2007). On one hand, BCL-XL might be able to avoid an excessive burden of senescent cells by apoptosis regulation (Mas-Bargues, Borrás and Viña, 2021). On the other hand, an increased overexpression of BCL-XL cells has been observed in senescent cells

(Yosef *et al.*, 2016). We identified senescent cells with SA-β-GAL activity as the percentage of FDG-positive T cells from B6 and Lck^{pr}-Bcl-X$_L$ mice.

Even though no differences were found in the percentage of senescent cells, suggesting a lack of effect of BCL-XL, a remarkable increase was observed in 24-26 mo mice from both strains whereas this parameter remained below 10% at younger ages (Figure 50). Although it cannot be appreciated in the figure, this increment is due to the appearance of a new subpopulation of T cells with high levels of SA-β-GAL activity rather than an increase in the overall population.

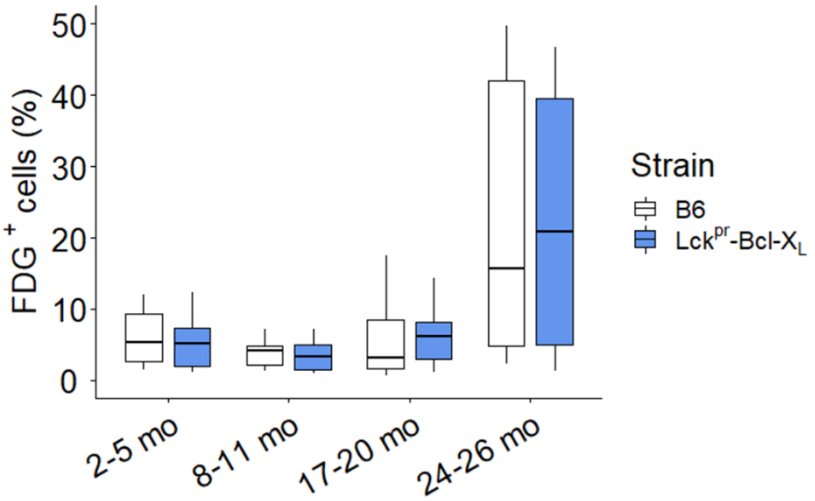

Figure 50. Senescence in T cells from B6 and Lck^{pr}-Bcl-X$_L$ mice.

Percentage of fluorescein di-β-D-galactopyranoside (FDG) positive events in freshly isolated T cells from 2-5 (n=29), 8-11 (n=29), 17-20 (n=32) and 24-26 mo (n=27) B6 and Lck^{pr}-Bcl-X$_L$ mice by flow cytometry. Data are represented as box plots and p values were calculated with the two-sample Wilcox test.

4.3. Mitochondrial respiration efficiency is improved in Lck^{pr}-Bcl-X$_L$ mice-derived T cells

Mitochondria is a key organelle during all stages of T cell adaptative immune response (Desdín-Micó, Soto-Heredero and Mittelbrunn, 2018). Although the BCL-2 family of proteins has been commonly characterized by their anti-apoptotic function, a large amount of evidence has revealed an important role in mitochondrial function as well (Hatok and Racay, 2016). In this regard, BCL-XL can stabilize mitochondrial membrane (Chen *et al.*, 2011), enhance Ca^{2+} flux (Tornero, Posadas and Ceña, 2011), regulate β-F_1F_0-ATP synthase (Veas-Perez de Tudela *et al.*, 2015) and improve overall energetic efficiency (Chen *et al.*, 2011). Similarly, BCL-XL dissociation from the β subunit of F_1F_0-ATP synthase or BCL-XL deficiency causes oxidative stress (Veas-Perez de Tudela *et al.*, 2015; Pfeiffer *et al.*, 2017).

Mitochondrial respiration maintains cellular homeostasis during the regulation of T cell function. Moreover, alterations in mitochondrial metabolism could lead to an increase in proinflammatory T cell response (Baixauli *et al.*, 2015). Aging has been shown to impair mitochondrial respiratory function in immune cells (Pence and Yarbro, 2018). To evaluate the mitochondrial function, we first examined Δψm and H_2O_2 to assess mitochondrial integrity. Next, we analyzed OCR during the Mito Stress Test in T cells derived from mice at different ages. An example of the OCR profile of T cells from 8-11 mo mice is shown below (Figure 51).

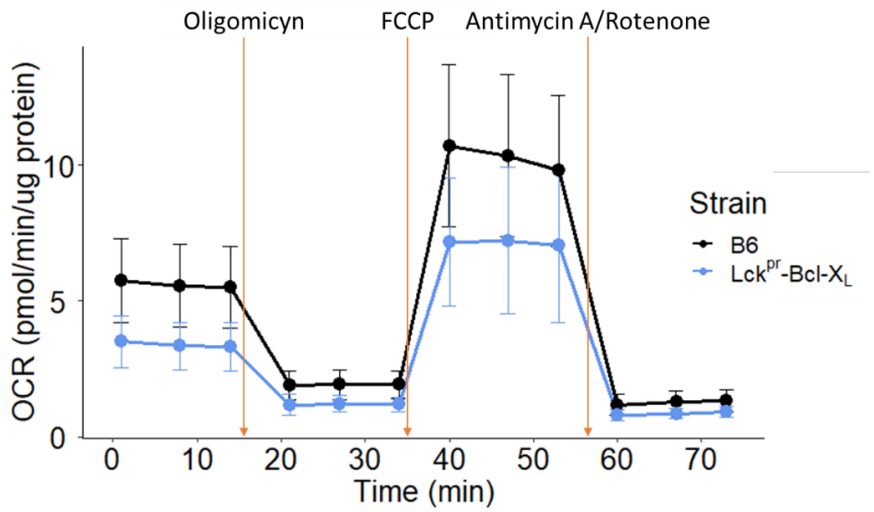

Figure 51. Seahorse Mito Stress Test OCR profiles in T cells.

Representative image of oxygen consumption rate (OCR) profile in T cells from adult B6 (n=2) and Lck^{pr}-Bcl-X_L (n=2) mice with the Mito Stress Test.

4.3.1. Basal respiration

Given the important role of BCL-XL in the mitochondria, we aimed to characterize T cells' mitochondrial integrity and respiratory function in basal conditions.

First, we measured ΔΨm (Supplementary figure 8) and H_2O_2 (Supplementary figure 9) as TMRM and MitoPY1 signals respectively by flow cytometry. However, no differences were found in these parameters between T cells from B6 and Lck^{pr}-Bcl-X_L mice. Thus, suggesting a lack of effect by BCL-XL in mitochondrial membrane integrity and H_2O_2 formation.

Then, we measured basal respiration in T cells from B6 and Lck^{pr}-Bcl-X$_L$ mice with an extracellular flux analyzer. Basal respiration was significantly lower in T cells from 2-5 mo Lck^{pr}-Bcl-X$_L$ compared to B6-derived T cells, with no differences in T cells from older mice (Figure 52). These results indicate that BCL-XL overexpression prevents excessive O_2 uptake by the cells early in life during physiological conditions and that this effect is lost with age.

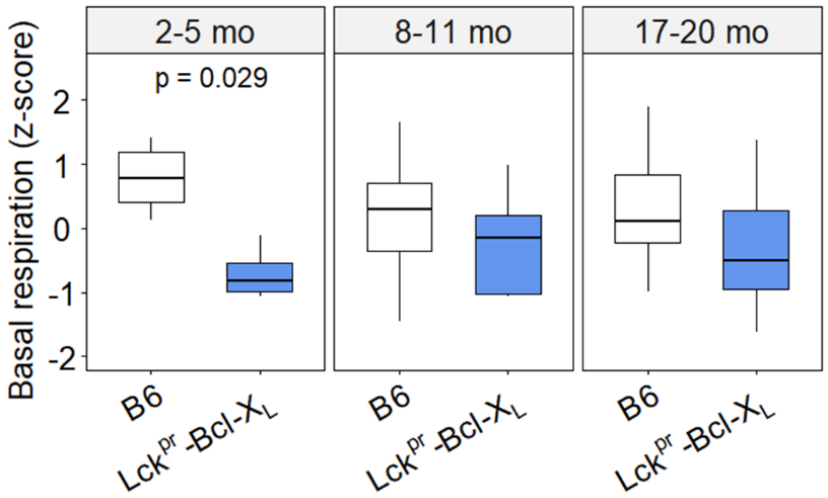

Figure 52. Basal respiration in T cells from B6 and Lck^{pr}-Bcl-X$_L$ mice.

Basal respiration measured as OCR in T cells from 2-5 (n=15), 8-11 (n=17) and 17-20 mo (n=22) B6 and Lck^{pr}-Bcl-X$_L$ mice. Data was relativized to total protein content and normalized with the z-score. Data is represented as boxplot and p values were calculated with the Wilcox t-test.

4.3.2. Non-mitochondrial oxygen consumption

Cell-surface oxygen consumption from ETC at the membrane (Herst and Berridge, 2007) and enzymatic ROS production (Manes and Lai, 1995; Starkov, 2008) are examples of non-mitochondrial oxygen consumption (NMOC) (Muller *et al.*, 2019). In this sense, cell-surface oxygen consumption has been shown to support tumor-like proliferating rates in cells with highly active glycolysis (Herst and Berridge, 2007). Furthermore, recent research has shown that T cells from older people produce more ROS than T cells from younger people (Bharath *et al.*, 2020). We measured NMOC in freshly isolated T cells from B6 and Lck^{pr}-Bcl-X_L mice during the Mito Stress Test after the third injection with a mix of rotenone and antimycin A, which completely shuts down mitochondrial respiration.

As a result, T cells from 2-5 mo Lck^{pr}-Bcl-X_L mice showed decreased levels of NMOC compared to B6-derived T cells, and no longer differences were observed at older ages (Figure 53). These reduced NMOC could be a consequence of a less oxidative environment in T cells overexpressing BCL-XL. As a result, these cells might be less likely to produce ROS and, consequently, less prone to endure oxidative stress. Once more, this protective effect of BCL-XL seems to decay with age.

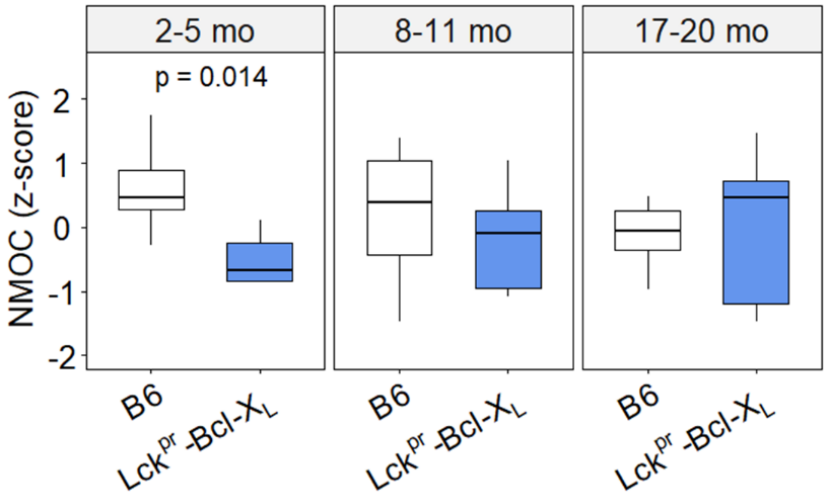

Figure 53. Non-mitochondrial oxygen consumption in T cells from B6 and Lck^{pr}-Bcl-X_L mice.

Non-mitochondrial oxygen consumption (NMOC) measured as OCR after rotenone/antimycin A injection by extracellular flux analyzer in T cells from 2-5 (n=15), 8-11 (n=17) and 17-20 mo (n=20) B6 and Lck^{pr}-Bcl-X_L mice. Data was relativized to total protein content and normalized with the z-score. Data is represented as boxplot and p values were calculated with the Wilcox t-test.

4.3.3. Proton leak

Proton leak is defined as the remaining basal respiration not coupled to ATP production. This parameter can be a sign of mitochondrial damage or can be used as a mechanism to regulate mitochondrial ATP production. Excessive proton leak has been described as a mechanism of age-related dysfunction in cardiomyocytes (Zhang *et al.*, 2020). Recently, T cells from old subjects have been shown to have increased proton leak compared to cells from young subjects (Bharath *et al.*, 2020). We calculated proton leak as the difference between OCR after oligomycin injection and NMOC in T cells isolated from B6 and Lck^{pr}-Bcl-X_L mice.

We found lower levels of proton leak in T cells from 2-5 and 8-11 mo Lck^{pr}-Bcl-X$_L$ mice (Figure 54). However, this beneficial effect of BCL-XL is lost one more time at older ages.

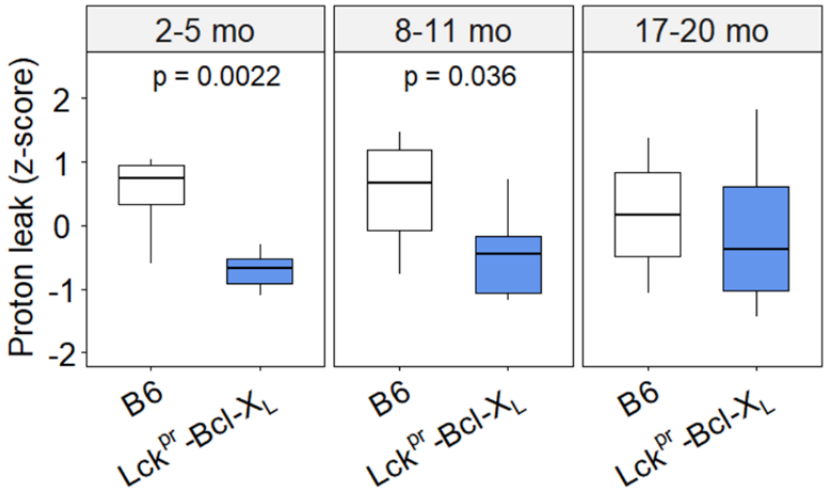

Figure 54. Proton leak in T cells from B6 and Lck^{pr}-Bcl-X$_L$ mice.

Proton leak measured by extracellular flux analyzer in T cells from 2-5 (n=15), 8-11 (n=17) and 17-20 mo (n=21) B6 and Lck^{pr}-Bcl-X$_L$ mice. Data was relativized to total protein content and normalized with the z-score. Data is represented as boxplot and p values were calculated with the Wilcox t-test.

Moreover, T cells from both strains exhibited similar levels of ATP-linked respiration (Supplementary figure 10), maximal respiration (Supplementary figure 11), and spare respiratory capacity (SRC) (Supplementary figure 12). Taken together, our results suggest that overexpression of BCL-XL could be enhancing oxidative phosphorylation efficiency in Lck^{pr}-Bcl-X$_L$ mice-derived T cells by maintaining the cellular respiratory demands, such as ATP production, with lower oxygen consumption, and consequently minimizing proton leak.

V. DISCUSSION

1. PHYSICAL HEALTH STATUS

The aging phenotype is characterized by poor physical health due to low activity levels, reduced physical performance, and an increased prevalence of frailty. This decline in physical function is associated with increased susceptibility to several ARDs (e.g., cardiovascular disease, hypertension, type 2 diabetes, and stroke) and reduced longevity in both rodents and humans (Warburton, Nicol and Bredin, 2006; Ludlow and Roth, 2011). Similarly, a physically active lifestyle is associated with a reduction in the negative impact of some ARDs, including Alzheimer's disease (Okonkwo *et al.*, 2014). Given that good physical health leads to improved health outcomes, physical health is a valuable parameter that should be taken into consideration in both clinical geriatrics and aging research (Guralnik *et al.*, 1989). In this thesis, physical health evaluation is the most important goal to achieve, specifically, in terms of frailty.

1.1. Physical decline during aging: Lck^{pr}-Bcl-X$_L$ mice have an attenuated physical decline compared to B6 mice

1.1.1. Body weight gain is attenuated in Lck^{pr}-Bcl-X$_L$ mice at 8-11 and 17-20 months of age

We found that body weight gain is significantly reduced in 8-11 and 17-20 mo Lck^{pr}-Bcl-X$_L$ compared to B6 mice, but no differences were found at older ages (24-26 mo). Jean Harper reviews body weight changes during aging in humans, dogs, and cats revealing an interesting trend. In humans, body weight is lower in elderly subjects compared to younger subjects (Steen, 1988; Harper, 1998). Studies in dogs revealed that total

body weight remains relatively constant, whereas the lean-fat ratio decreases with increasing age. This transition continues in rodents, in which body weight gain occurs with aging (Tamura *et al.*, 2021). Given that BCL-XL seems to be strongly linked to longevity (Borrás *et al.*, 2016; Borrás *et al.*, 2020), and that reduced body weight in mice is associated with increased lifespan (Kwak, Baumann and Thompson, 2019; Caristia *et al.*, 2020), we considered that the prevention of body weight gain in Lck^{pr}-Bcl-X$_L$ mice at middle-ages could be a favourable trait during aging. Indeed, several studies associate small body sizes, especially early in adult life, with long lifespans in rodents (Brown-Borg *et al.*, 1996; Miller, Chrisp and Atchley, 2000; Baumann, Kwak and Thompson, 2018). This is the case of the mutant dwarf mice, in which the differences in early and mid-life body weight seem to be under the control of polymorphic genes (Miller *et al.*, 2002). These results suggesting genes as regulators of lifespan support the longevity genes theory of aging.

1.1.2. Grip strength loss is attenuated in Lck^{pr}-Bcl-X$_L$ mice at 8-11 months of age with no differences in lean mass

In humans, grip strength is a long-term predictor of cardiovascular disease, cancer, and mortality (Gale *et al.*, 2007). Grip strength is also reported to decrease in B6 old mice compared to young mice (Takeshita *et al.*, 2017), with a gradual decline to 28 mo (Ge *et al.*, 2016). In our mice, we found that grip strength loss was attenuated in 8-11 mo Lck^{pr}-Bcl-X$_L$ compared to B6 mice, but again, no differences were found at older ages (17-20 and 24-26 mo). Although the loss of muscle strength has been classically linked to a loss of muscle mass in both humans and murine models (Zamboni *et al.*, 2005; Hamrick *et al.*, 2006; Bisset and Howlett,

2019; Xie *et al.*, 2021), we did not find changes in lean mass measured by DXA. This lack of relationship between muscle strength loss and muscle mass has also been described by other authors (Ge *et al.*, 2016; Sheth *et al.*, 2018). Interestingly, studies focusing on finding other explanations for age-related muscle loss revealed a determinant loss of motor unit number in hind limb muscles that occurs early in life (Sheth *et al.*, 2018).

1.1.3. Motor coordination loss is attenuated in Lck^{pr}-Bcl-X$_L$ mice at 8-11 and 17-20 months of age

It is common knowledge that a progressive loss of motor control and balance occurs at advanced ages and that these changes are caused not only by a loss of muscle function but also due to a decline in cognitive and neurological systems in the elderly (Camicioli, Panzer and Kaye, 1997; Matsumura and Ambrose, 2006; Seidler *et al.*, 2010). Indeed, reduced motor coordination and balance assessed by beam test and foot-printing analysis were associated with synaptic plasticity deficit and loss of noradrenergic modulation in a murine model of Alzheimer's disease (Russo *et al.*, 2018). When assessing motor coordination in our mice cohort, we found that age-related coordination loss was attenuated in 8-11 and 17-20 mo Lck^{pr}-Bcl-X$_L$ mice compared to B6. Thus, suggesting an improved physical and cognitive function. Nonetheless, the set speed rotarod appears to have some drawbacks, as animals with poor coordination will fall off at the start of the test, whereas in those who do stay, endurance rather than coordination is more likely to be measured (Deacon, 2013). Hence, a combination of tests including beam walking and footprint analysis (Carter, Morton and Dunnett, 2001), would be more precise in assessing motor coordination and balance in rodents.

1.1.4. Exercise endurance loss is attenuated in Lck^{pr}-Bcl-X$_L$ mice at 8-11 months of age

Cardiovascular performance is known to decline over time in the elderly (Cherubini *et al.*, 1998). While a considerable variation exists, an average decline in endurance capacity of 20% is observed between 40 and 60-year-old subjects. After the age of 60 years, a linear age-related decline has been reported in the total duration of exercise during the Bruce treadmill test (Mendonca *et al.*, 2017). In our mice, the age-associated loss of endurance was attenuated in 8-11 mo Lck^{pr}-Bcl-X$_L$ mice compared to B6, indicating an improved resistance to extenuating physical exercise.

Several studies have suggested a positive association between exercise endurance and immune function. For instance, old-aged individuals that habitually practice endurance exercise maintained an improved T cell function (e.g., increased levels of IL-2, IFN-gamma, and IL-4 production) compared to sedentary individuals of similar age (Shinkai *et al.*, 1995). Moreover, endurance exercise is associated with an improved immune response (Smith, Kennedy and Fleshner, 2004; Schlagheck *et al.*, 2020). Thus, given that Lck^{pr}-Bcl-X$_L$ mice overexpress BCL-XL specifically in T cells, we believe that the improvement observed in these mice could be attributed to an enhanced T cell function.

Taken together, our findings suggest that Lck^{pr}-Bcl-X$_L$ mice exhibit general protection against physical performance decline that occurs from 2-5 up to 17-20 months of age. Nonetheless, this protection is completely lost at 24-26 months of age, suggesting that the mechanisms occurring early in life that improve these physical attributes, decline with increasing age until the effect fades at advanced ages.

1.2. Spontaneous activity: Lck^{pr}-Bcl-X$_L$ mice exhibit increased rearing behaviour compared to B6 mice

Physical activity has numerous benefits for the elderly, including maintaining posture and gait stability, pain management, and preventing osteoporosis (Pedrinelli, Garcez-Leme and Nobre, 2009). Conversely, the lack of physical activity may account for roughly half of the physical decline associated with human aging. People over the age of 50 who do not engage in regular exercise may suffer from a variety of health problems, including reduced strength, physical endurance, coordination, and balance (McPhee *et al.*, 2016).

We observed a non-significant increase in spontaneous activity in 8-11 and 17-20 mo Lck^{pr}-Bcl-X$_L$ mice in comparison to B6 mice, being more prominent in the 8-11 age group. Rearing events were significantly more frequent and long-lasting in 8-11 mo Lck^{pr}-Bcl-X$_L$ mice during the dark cycle. This increase in Lck^{pr}-Bcl-X$_L$ mice activity, albeit minor, corresponds to our findings in physical performance, all of which point to a better physical status in these mice. Moreover, increased physical activity has been associated with improved cognitive function. In this sense, older subjects with great physical activity levels are less likely to experience motor (Buchman *et al.*, 2007) and cognitive decline (Yaffe *et al.*, 2001). This correlation can also be seen in other studies with B6 mice, which exhibit reduced locomotion accompanied by an enhanced anxiety-like behaviour at older ages compared to young mice (Singhal *et al.*, 2020). Therefore, these results suggest that Lck^{pr}-Bcl-X$_L$ mice may have an improved physical and cognitive function which may improve the quality of life during aging.

1.3. Frailty: Lck^{pr}-Bcl-X$_L$ mice prevent frailty at very old ages in comparison to B6 mice

As we discussed in the previous section, a state of reduced physical performance will almost certainly evolve into frailty, and eventually, disability. Low activity is, indeed, one of the criteria used to assess frailty in humans along with weight loss, exhaustion, slowness, and weakness (Fried *et al.*, 2001). We found a significant reduction in frail mice in the Lck^{pr}-Bcl-X$_L$ strain at 24-26 months of age. These results can be explained by the attenuated physical decline in middle-aged and the higher activity found in Lck^{pr}-Bcl-X$_L$ mice. Overall, our findings suggest that Lck^{pr}-Bcl-X$_L$ mice have improved age-associated physical health status, which may be attributed to an enhanced immune function, and may be related to a better cognitive function. Hence, Lck^{pr}-Bcl-X$_L$ mice have improved healthspan.

2. METABOLISM-RELATED PARAMETERS

Decreased physical health is known to alter several metabolic parameters, including body composition, EE, and insulin resistance (Stewart, 2006). Additionally, the prevalence of frailty has been linked with altered metabolism systems, such as glucose tolerance and energy metabolism (Fried *et al.*, 2021). Thus, given the results obtained in the physical health status, we expected to observe differences in the mentioned systems.

2.1. Body composition: Lck^{pr}-Bcl-X$_L$ mice preserve a youthful body composition during aging

In humans, lean body mass decreases whereas fat mass increases in old compared to young subjects (Harper, 1998). Similar changes occur in rodents and other animal models. In our mice, total body mass and fat mass increased with increasing age in wild-type mice, whereas these parameters remained constant in Lck^{pr}-Bcl-X$_L$ mice. These changes in body composition are typically seen when using dietary interventions, such as energy restriction with 55% of *ad libitum* energy intake (Colman *et al.*, 2007). Hence, the effect of BCL-XL could be comparable to that of caloric restriction in this regard. Curiously, no differences were found in daily food and drink consumption rates. Thus, the increase in body weight in B6 mice is due to an increased fat mass which may not be attributed to increased intake. Additionally, we found no differences in lean mass as it remained relatively uniform across the different ages in both strains. These results suggest that the decline of grip strength loss with age is not related to a loss of lean muscle mass. Although unexpected, this lack of relationship has been observed previously by other authors (Ge *et al.*, 2016).

2.2. Energy metabolism: Lck^{pr}-Bcl-X$_L$ mice do not show differences in intake, RQ or EE compared to B6 mice

Body weight and composition, food intake, and physical activity are major determinants of EE. In humans, total EE decreases with age as a result of changes in basal metabolic rate and EE associated with activity (Manini, 2010). The decline in basal metabolic rate with age is driven by the

relationship between the different changes in body composition (Rizzo *et al.*, 2005). Moreover, reduced physical activity and decreased basal metabolic rate are major drivers of age-related decline in the maintenance of energy requirements (Harper, 1998). Curiously, in our results, no differences in EE were found between strains despite the increased activity of Lck^{pr}-Bcl-X_L mice. Still, the values obtained were comparable to other studies in B6 mice of similar age (Fokin *et al.*, 2017). Similarly, no differences in RQ between Lck^{pr}-Bcl-X_L and B6 mice at 8-11 nor 17-20 mo either. Although some differences were expected due to the dissimilarities in body fat, these results could be explained by the fact that both strains had the same feeding conditions and exhibit a similar intake consumption rate.

2.3. Glucose tolerance: Lck^{pr}-Bcl-X_L mice prevent age-related glucose tolerance impairment

Glucose tolerance is known to decrease with age (Shimokata *et al.*, 1991) due to a decrease in insulin secretion and insulin sensitivity (Szoke *et al.*, 2008). Body fat mass and distribution, and physical fitness can additionally account for the decline in glucose tolerance. Indeed, maintaining physical health throughout life may protect against glucose intolerance and type 2 diabetes (Broughton and Taylor, 1991; Ryan, 2012). Similarly, interventions to promote healthy aging in animal models have been demonstrated to improve glucose tolerance (Paillasse and de Medina, 2015; Saraswat *et al.*, 2017; Zhou *et al.*, 2018), including caloric restriction (Ros and Carrascosa, 2020), and resveratrol treatment (Park *et al.*, 2012).

Given the prevention of frailty in Lck^{pr}-Bcl-X_L mice and the proposition of glucose metabolism impairment as a possible driver of frailty, we expected to find that Lck^{pr}-Bcl-X_L mice would also prevent age-related glucose intolerance. As we hypothesized, increased glucose intolerance was found in old B6 mice compared to Lck^{pr}-Bcl-X_L mice, which fits our previous findings in physical health status and body composition.

BCL-XL function regarding glucose metabolism has been associated with enhanced survival in other cell types, such as pancreatic progenitors from human pluripotent stem cells during differentiation (Loo *et al.*, 2020). Interestingly, studies in rats revealed that 2-to-3-fold BCL-XL overexpression in β-cells has no effect during intraperitoneal GTT in rats, whereas 10-fold overexpression produces glucose intolerance due to reduced insulin secretion (Zhou *et al.*, 2000). T cells have also been suggested as major mediators of β-cell apoptosis in insulin-dependent diabetes (Kurrer *et al.*, 1997). Likewise, other studies have found that B6 mice with induced diabetes exhibit impaired function of splenic T CD8$^+$ and tumor-infiltrating lymphocytes, which has been associated with enhanced tumor growth (Nojima *et al.*, 2020). Curiously, mice lacking natural killer T cells with high-fat diet-induced obesity exhibit improved glucose tolerance compared to control mice (Ohmura *et al.*, 2010). More recent studies show that the ablation of estrogen receptor α specifically in T cells causes glucose intolerance accompanied by reduced insulin secretion and increased chronic inflammation in a mouse model of gestational diabetes (Tanaka *et al.*, 2021). Thus, the protection against age-related glucose intolerance observed in Lck^{pr}-Bcl-X_L mice may be attributed to a T cell-dependent regulation of pancreatic cells due to the role of BCL-XL.

3. T CELL CHARACTERIZATION

As we already mentioned, our transgenic mice overexpress BCL-XL specifically in T cells. These cells can serve as an auxiliary function, primarily coordinating immune responses and activating humoral mechanisms (i.e., $CD4^+$ T cells) (Guimarães *et al.*, 2021), or can directly kill infected or tumor cells by direct interaction and cytotoxic proteins release (i.e., $CD8^+$ T cells) (Janeway *et al.*, 2001). Different changes occur in T cells during aging and ARDs. In this sense, Elisa Carrasco and collaborators recently reviewed the role of T cells in aging and ARDs, comprehensively describing the mechanism by which these cells contribute to chronic inflammation or inflammaging, cardiovascular disorders, metabolic dysfunction, and neurodegeneration (Carrasco *et al.*, 2022).

3.1. Lymphocyte count: Lck^{pr}-Bcl-X_L mice-derived splenic T cells are higher in number, with no differences in the total amount of splenic white cells

Mature T cells produced in the thymus are considered to be immunologically naïve until they encounter MHC-peptide complexes for which their T cell receptors (TCR) have high-affinity (Berard and Tough, 2002). Following the recognition of antigen, naïve T cells are activated to become effector T cells that help during the immune response. Effector T cells normally die by apoptosis after the acute immune response because they are no longer needed, but some of them survive (i.e., memory T cells) and are maintained in a lower state of activation.

As a general rule, T cell number and diversity decrease with age (Lian *et al.*, 2020). In humans, the most noticeable changes in the total T cell pool with age are the decline in the proportion of the naïve T cells, and with that shrinking of the TCR repertoire diversity (Thome *et al.*, 2016), and the expansion of the memory T cell pool (Berard and Tough, 2002). Our results show that the number of T cells was significantly higher in 2-5, 8-11, and 17-20 mo Lck^{pr}-Bcl-X$_L$ mice compared to B6 mice. This accumulation of T cells in the spleen could be attributed to the anti-apoptotic effect of BCL-XL promoting cell survival, although the reason why this effect is lost in 24-26 mo mice remains a mystery. Given that we kept our mice in a pathogen-free environment, we could assume that most of the circulating T cells are still immunologically naïve. Hence, this general decline in total T cells may be the consequence of a lower proportion of naïve T cells, probably due to thymic involution (Carrasco *et al.*, 2022).

3.2. Cell survival pathways: Lck^{pr}-Bcl-X$_L$ mice-derived T cells exhibit improved cell survival and stress response

Most physiological functions are reduced with advanced age, particularly the ability to maintain homeostasis during episodes of acute stress (Richardson and Holbrook, 1996). Similarly, the frailty syndrome has been associated with significantly reduced expression levels of several genes implicated in the cellular response to stress, including oxidative stress and hypoxia (El Assar *et al.*, 2017). Some of the cellular response mechanisms have been linked to enhanced survival, while others seem to lead to cell death (Martindale and Holbrook, 2002). There is also the possibility that some of these pathways can be implicated in both

extremes. This is the case of ROS, which can induce a complex signalling cascade, produce gene expression changes, and, ultimately, lead to cell death or survival. The immune system also declines with age accompanied by the deterioration of T cell function, leading to immunosenescence (McLeod, 2001). In this section, we will discuss the effect of BCL-XL observed in T cell senescence, autophagy, and apoptosis.

3.2.1. Apoptosis is differently modulated in Lck^{pr}-Bcl-X$_L$ mice-derived T cells in physiological and stressful conditions

Accumulating evidence suggests that the dysregulation of the apoptotic process may be involved in the aging process. Indeed, lymphocytes from the elderly are more susceptible to apoptosis and overexpress the apoptotic CD95/FAS antigen, which induces apoptosis in T cells in the presence of FAS ligand (Potestio *et al.*, 1998; Pollack and Leeuwenburgh, 2001; Gupta and Gollapudi, 2005). In contrast, exercise interventions have been demonstrated to reduce apoptosis in PBMCs from elderly subjects (Mejías-Peña *et al.*, 2017). Interestingly, some data suggest that the CD95 pathway is independent of cytochrome c-mediated apoptosis. In various cell types, the incidence of apoptosis correlates with the levels of accumulated damage in the cells (Higami and Shimokawa, 2000).

Contrary to our expectations, T cells from Lck^{pr}-Bcl-X$_L$ mice overexpressing BCL-XL, which is primarily an anti-apoptotic protein, exhibit increased apoptosis levels in 17-20 mo mice. No differences were found in the other age groups compared to T cells from B6 mice. Thus, BCL-XL is not preventing apoptosis in freshly isolated T cells.

Nonetheless, when cultured, T cells from young-adult (2-5 and 8-11 mo) Lck^{pr}-Bcl-X$_L$ mice were protected from apoptosis even in the presence of an apoptosis inducer. Previous research has shown that mature mouse spleen T cells die by apoptosis when cultured without any additional stimulus (Perandones *et al.*, 1993). Hence, our data suggest that BCL-XL lacks an anti-apoptotic effect under physiological conditions and only prevents T cell apoptosis under stressful circumstances in which this pathway is enhanced such as in *in vitro* culture. Still, BCL-XL's role in apoptosis is completely lost in 17-20 and 24-26 mo mice even though its overexpression is still maintained at old ages.

3.2.2. Autophagic response to starvation is enhanced in Lck^{pr}-Bcl-X$_L$ mice-derived T cells

Deregulation of autophagy and apoptosis are common hallmarks of the aging process (Cuervo *et al.*, 2005). Aging is generally associated with a decline in autophagy (Mejías-Peña *et al.*, 2017). However, increased but also decreased expression levels of proteins involved in this process (e.g., BECLIN-1, LC3, ATG5, and ATG7) have been reported in aged tissues (Fîlfan *et al.*, 2017).

We found that old Lck^{pr}-Bcl-X$_L$ mice-derived T cells exhibited an improved adaptation to starving conditions in comparison with B6-derived T cells. These results contradict the described function of BCL-XL as a suppressor of autophagy. Nevertheless, this contradictory effect of BCL-XL increasing autophagy has also been described under certain conditions, such as in response to etoposide and staurosporine treatment (Shimizu *et al.*, 2004). Moreover, BCL-XL also induces autophagy in cancer cells (Li *et al.*, 2020). Still, these differences could be attributed to

reduced basal autophagic activity in T cells from Lck^{pr}-Bcl-X$_L$ mice. Thus, even though the autophagic activity is similar in both strains, the increase would be greater in T cells overexpressing BCL-XL.

Autophagy is essential for T cell differentiation, activation, survival, and bioenergetics (Hubbard *et al.*, 2010; Puleston *et al.*, 2014; Macian, 2019). Indeed, these cells display basal autophagy levels to control organelle homeostasis (Cuervo and Macian, 2014). Human and murine models have shown a decreased autophagy in aged T cells, although the mechanisms responsible are not yet understood (Botbol, Guerrero-Ros and Macian, 2016; Macian, 2019). Taken together, our findings suggest that BCL-XL enhances autophagic response to starvation in T cells by maintaining a lower autophagic activity in basal conditions which allows a greater margin of action for the autophagic machinery.

3.2.3. Senescence is not altered in Lck^{pr}-Bcl-X$_L$ mice

Senescent cells accumulate in aged tissues from different species, secreting various inflammatory cytokines and chemokines, substantially affecting the organismal physiology (Nakagami, 2019). The increase of senescent cells with aging is normally accompanied by increased SA-β-GAL activity and the overexpression of P53, P16^{INK4a}, and PAI-1 (Mas-Bargues, Borrás and Viña, 2021). BCL-XL has been reported to be upregulated in tumoral and senescent cells, conferring cell death resistance, whereas BCL-XL inhibitors can cause these cells to undergo apoptosis (Trisciuoglio *et al.*, 2017; Ge *et al.*, 2021).

Despite the existing evidence of BCL-XL function in cellular senescence, no differences in senescence were found in splenic T cells from B6 and

Lck^{pr}-Bcl-X_L mice. This outcome could be due to a complete lack of BCL-XL effect or could be the result of two opposing roles (induction and suppression) resulting in a compensatory effect. This dual role of BCL-XL has been previously reported (Borrás *et al.*, 2020). On one hand, several studies have reported increased levels of BCL-XL associated with senescence. Indeed, the use of senolytics, some of which target BCL-XL and other BCL-2 family members (e.g., ABT-263 or ABT-737), efficiently delete senescent cells from aged tissues (He *et al.*, 2020; Ge *et al.*, 2021). On the other hand, BCL-XL protects centenarians from immune senescence (Borrás *et al.*, 2015). Additionally, BCL-XL overexpression decreases senescence and enhances proliferation in MEFs and centenarian-derived lymphocytes in primary culture (Borrás *et al.*, 2016).

In addition, although no statistical test was performed given the characteristics of the data, a remarkable increase in senescent T cells was observed in 24-26 mo mice from both strains compared to their younger homologs. This abrupt rise was caused by a clear differentiated group of T cells with high levels of SA-β-GAL activity rather than an increase in the overall population. In this regard, a subset of T cells exhibiting features of cellular senescence has been reported to increase gradually in number, reaching the 70% of the T cell population in aged mice (Fukushima, Minato and Hattori, 2018; Nakagami, 2019). These cells, known as senescence-associated T cells, do not proliferate in response to TCR stimulation and do not contribute to immune system maintenance. Curiously, senescent T cells exhibit reduced SA-β-GAL activity (Lian *et al.*, 2020).

In summary, although no effect was found in cellular senescence, BCL-XL overexpression enhances T cell survival under hostile conditions by preventing apoptosis in culture and boosting autophagic response to starvation. These results could be explained by the dissociation of BCL-XL and BECLIN-1 and its translocation to the mitochondrial membrane to block the formation of the transition membrane pore, which would promote autophagy and suppress cell death, promoting overall cell survival (Strozyk and Kulms, 2013).

Apoptosis and autophagy are two evolutionarily conserved processes that maintain homeostasis during stress (Kim *et al.*, 2014), and both are important regulator pathways in eukaryotic cells (M.C. Maiuri, LeToumelin, *et al.*, 2007). Crosstalk between these two mechanisms involving BCL-2 family members has been suggested recurrently (Nishida, Yamaguchi and Otsu, 2008; Zhou, Yang and Xing, 2011; Gordy and He, 2012; Su, Mei and Sinha, 2013; Chen *et al.*, 2019). Taken together, our findings suggest that BCL-XL plays an important pivotal role between apoptosis and autophagy to ultimately promote cell survival under stressful conditions.

3.3. Mitochondrial function: Lck^{pr}-Bcl-X_L mice-derived T cells have reduced mitochondrial respiration levels and improved proton leak

Mitochondrial dysfunction is a hallmark of aging in several cell types (Guimarães *et al.*, 2021; Rodrigues *et al.*, 2021; Zhang, Weyand and Goronzy, 2021). The decreased capacity to produce ATP by oxidative phosphorylation in aged rodents is accompanied by diminished electron

transfer, decreased membrane potential, and increased ROS production, consequently causing mitochondrial damage (Boveris and Navarro, 2008; Mammucari and Rizzuto, 2010). BCL-XL has been demonstrated to influence mitochondrial function by different mechanisms, including its interaction with the ATP synthase and the regulation of Ca^{2+} concentration (Michels *et al.*, 2013).

Our results show that overall O_2 uptake by young Lck^{pr}-Bcl-X_L mice-derived T cells was lower compared to B6-derived T cells during basal respiration and NMOC. At the same time, ATP production, maximal respiration, and spare respiratory capacity were similar in T cells from both strains. Hence, our data suggest that BCL-XL overexpressing T cells can maintain similar energy demands by consuming less oxygen. This hypothesis is reinforced by the reduced levels of proton leak observed in Lck^{pr}-Bcl-X_L mice-derived T cells. However, this effect is lost with increasing age, and the reason why this occurs is still unknown.

Similar results have been seen in other cell types. For instance, BCL-XL has been reported to decrease mitochondrial oxygen consumption in neurons, indicating an enhanced and more efficient coupling of ATP production to O_2 uptake (Alavian *et al.*, 2011; Jonas, 2014). BCL-XL has also been reported to prevent uncoupling and ADP-stimulated respiration inhibition by the effect of truncated Bid, a disruptor of mitochondrial homeostasis (Gonzalvez *et al.*, 2005). Given its effect on the proton gradient, proton leak reduces $\cdot O^{2-}$ production and is consequently involved in the regulation of ROS production (Muller *et al.*, 2019). In this sense, BCL-XL knockout MEFs exhibited reduced ATP and oxidative phosphorylation activity, had increased levels of ROS, and were more

susceptible to oxidative stress (Pfeiffer *et al.*, 2017). However, studies that link proton leak to ROS generation are still contradictory (Brookes, 2005; Cheng *et al.*, 2017).

Taken together, our findings suggest an improved mitochondrial respiratory efficiency in T cells from Lck^{pr}-Bcl-X$_L$ mice due to BCL-XL overexpression, which according to the rate-of-living theory of aging, could explain the healthier state of these mice in old age.

4. GENERAL PERSPECTIVE: BCL-XL AS A GENE IMPLICATED IN HEALTHY AGING

As the world's population ages, we are more aware that living longer does not imply living healthier. This scenario creates an urgent need to explain why some people enjoy a better quality of life during aging so that interventions to promote healthy aging could be designed. Since BCL-XL is physiologically upregulated in centenarians (Borrás *et al.*, 2016), considered models of healthy aging, it is interesting to test whether BCL-XL overexpression could promote healthy aging in other species.

Our group has tested BCL-XL overexpression in primary cells *in vitro*, nematodes, and flies. BCL-XL ortholog ced-9, increased mean and maximal lifespan in *C. elegans*. In *D. melanogaster*, BCL-XL overexpression increased flies' lifespan and enhanced response to light (i.e., phototaxis) and Earth's gravity (i.e., geotaxis) compared to wild-type flies, thus indicating a better locomotor behaviour (Gimeno-Mallench *et al.*, 2021).

In the present thesis, we studied the effect of BCL-XL overexpression during aging in a murine model (*M. musculus*). For that purpose, we evaluated healthy aging and frailty in our murine model with a battery of tests proposed by other authors, including grip strength, rotarod, GTT, body composition, and EE (Bellantuono *et al.*, 2020; Fried *et al.*, 2021). As a result, Lck^{pr}-Bcl-X_L mice overexpressing BCL-XL exhibited reduced frailty, which was accompanied by a general improvement in the physical health status in comparison with B6 mice. Additionally, Lck^{pr}-Bcl-X_L mice maintained a youthful body composition during aging and displayed an improved glucose tolerance in old age. Given that several studies imply a correlation between good physical health and immune function in older adults (Duggal *et al.*, 2019; Ciolac, da Silva and Vieira, 2020), we believe that these beneficial effects of BCL-XL may be attributed to an improved T cell function.

According to our hypothesis, splenic T cells from Lck^{pr}-Bcl-X_L mice are more abundant, exhibit enhanced stress response, and display an improved respiratory efficiency in comparison to B6 mice-derived T cells. Indeed, T cells display mitochondrial dysfunction with age (Zhang, Weyand and Goronzy, 2021; Carrasco *et al.*, 2022), which has been linked to impaired autophagy during immunosenescence (Bektas *et al.*, 2019). When this occurs, T cells become inefficient in senescence surveillance, hence losing their ability to efficiently clear damaged cells that become senescent (Prata *et al.*, 2018; Carrasco *et al.*, 2022). Thus, given the protective role of BCL-XL observed in our results, T cells from Lck^{pr}-Bcl-X_L mice are more likely to maintain a better immune function and, as a result, to better regulate overall homeostasis during aging.

Figure 55 summarises the role of BCL-XL in physical health and metabolism in Lck^{pr}-Bcl-X_L mice during aging and in T cell function.

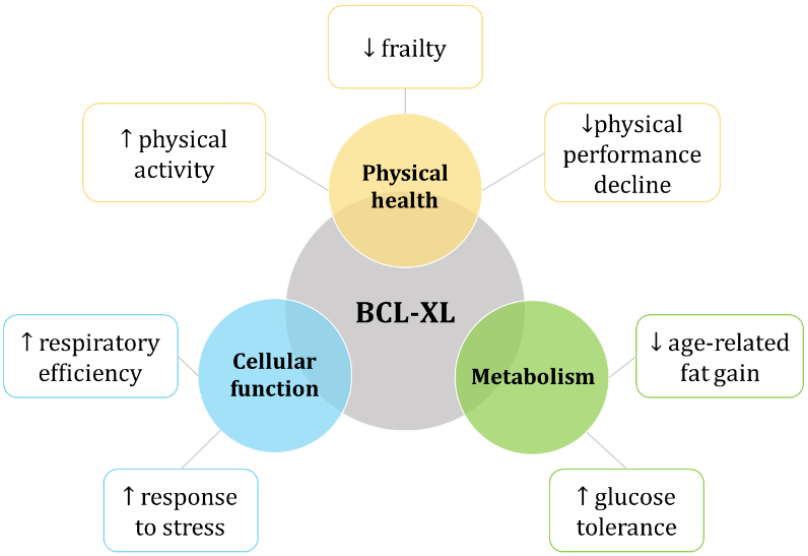

Figure 55. BCL-XL's role in physical health, metabolism, and cellular function.

Considering the theories of aging discussed in the introduction, our findings indicate that the aging process can be modulated genetically (longevity genes or programmed longevity theory) by enhancing immune cell function (immunological theory) in terms of improving respiratory efficiency by reducing oxygen consumption (rate of living theory), thus minimizing the probability to generate ROS (free radicals' theory), while maintaining mitochondrial function (mitochondrial theory).

Altogether, our results suggest that mice overexpressing BCL-XL in T cells enjoy better physical and metabolic conditions at advanced ages, probably due to an improved T cell function during the early stages of life. Figure 56 summarises this thesis background and results.

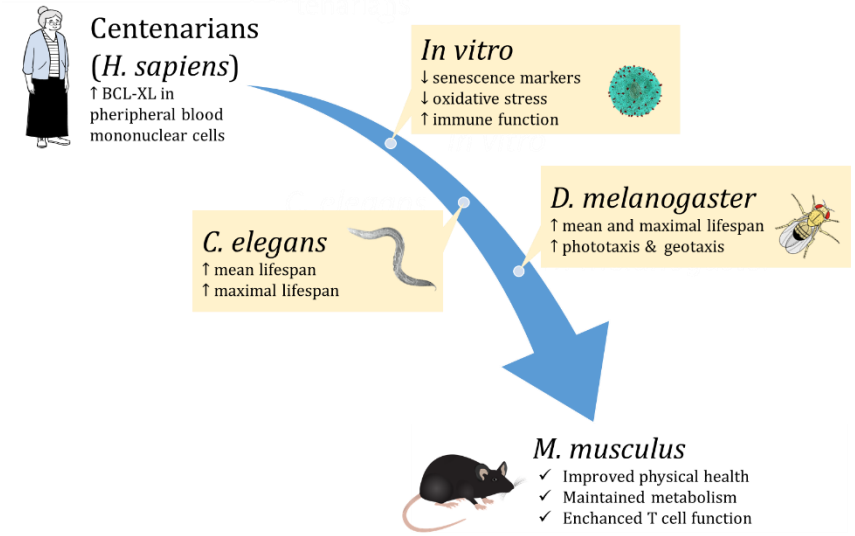

Figure 56. Thesis background and results summary.

5. STUDY LIMITATIONS

This study has potential limitations that need to be considered.

Firstly, given the characteristics of our data (i.e., non-normal distribution and non-equality of variances), the statistical analysis had to be simplified to a single factor (i.e., strain), and no further variables were included such as age and sex, which could have been interesting variables for the study.

Secondly, the two-hour acclimatization time used during metabolic monitoring and longer periods would almost certainly allow animals to better adapt to the new environment, possibly revealing previously unnoticed differences. The equipment availability was a limitation in this regard.

Thirdly, single markers were used to detect apoptosis, autophagy, and senescence. Normally, these pathways are measured as a battery of parameters, such as $P16^{INK4a}$, $P21^{CIP1}$, and lamin B1 for senescence; BECLIN-1, LAMP-1, P62, and overall autophagic flux for autophagy; and cytochrome c release and caspase-3/7 for apoptosis, in addition to the makers used for this thesis. Thus, the parameters used are probably not enough to demonstrate the activation or suppression of these pathways.

Finally, for mitochondrial measurements such as TMRM and OCR, the normalization method used may have induced some imprecision in our results. Other normalization methods such as mitochondrial mass measured by MitoTracker Green could have been more appropriate. Moreover, for optimal analysis of the mitochondrial respiratory function, all samples should have been measured in the same experiment. However, this condition was difficult to meet in terms of the logistics of the experiment since the animals had to be sacrificed and T cells had to be isolated.

Despite these limitations, we believe that the conclusions drawn from this study agree with the results obtained.

VI. CONCLUSIONS

The main conclusion of this thesis is that BCL-XL overexpression in T cells prevents frailty and improved overall health in Lck^{pr}-Bcl-X_L mice in comparison with the B6 mice.

The specific conclusions of the study are:

1) Lck^{pr}-Bcl-X_L mice were characterized by the presence of the human BCL-XL transgene and the overexpression of BCL-XL in the thymus, spleen, and T cells compared to B6 mice.

2) Lck^{pr}-Bcl-X_L mice exhibited improved physical health status:
    a. Physical performance decline in terms of body weight gain, grip strength loss, motor coordination loss, and physical endurance decline was attenuated in Lck^{pr}-Bcl-X_L mice compared to B6 mice during aging.
    b. Rearing behaviour was increased in Lck^{pr}-Bcl-X_L mice compared to B6 mice in middle age with no differences in activity.
    c. Prevalence of frailty and Valencia Frailty Score were reduced in Lck^{pr}-Bcl-X_L compared to B6 mice at advanced ages.

3) Lck^{pr}-Bcl-X_L mice maintained metabolism-related parameters:
    a. Total body weight and fat content were maintained in Lck^{pr}-Bcl-X_L mice whereas increased in B6 mice during aging.
    b. Respiratory quotient and energy expenditure did not change in Lck^{pr}-Bcl-X_L mice compared to B6 mice.

c. Glucose tolerance was improved in Lck^{pr}-Bcl-X_L mice compared to B6 mice in old age.

4) Lck^{pr}-Bcl-X_L mice-derived T cells exhibited improved function.
   a. The number of T cells obtained from Lck^{pr}-Bcl-X_L mice was higher compared to the number of T cells from B6 mice, with no differences in total white cells.
   b. Apoptosis resistance under stressful conditions and autophagic response to starvation was increased in Lck^{pr}-Bcl-X_L mice-derived T cells compared to B6 mice-derived T cells, with no differences in cellular senescence.
   c. Basal and non-mitochondrial respiration, and proton leak were reduced in Lck^{pr}-Bcl-X_L mice-derived T cells compared to B6 mice-derived T cells during the early stages of life, with no differences in mitochondrial $\Delta\Psi$, hydrogen peroxides, ATP production, maximal respiration, and spare respiratory capacity.

REFERENCES

Ackert-Bicknell, C. L. *et al.* (2015) 'Aging Research Using Mouse Models', *Current protocols in mouse biology*. NIH Public Access, 5(2), pp. 95–133. doi: 10.1002/9780470942390.mo140195.

Adams, J. M. and Cory, S. (2007) 'The Bcl-2 apoptotic switch in cancer development and therapy', *Oncogene 2007 26:9*. Nature Publishing Group, 26(9), pp. 1324–1337. doi: 10.1038/sj.onc.1210220.

Alavian, K. N. *et al.* (2011) 'Bcl-xL regulates metabolic efficiency of neurons through interaction with the mitochondrial F1FO ATP synthase', 13(10). Available at: https://www.nature.com/articles/ncb2330 (Accessed: 2 April 2019).

Allen, E. N. and Cavanaugh, J. E. (2014) 'Loss of motor coordination in an aging mouse model', *Behavioural Brain Research*. Elsevier, 267, pp. 119–125. doi: 10.1016/J.BBR.2014.03.032.

Alonso-Fernández, P. *et al.* (2008) 'Neutrophils of Centenarians Show Function Levels Similar to Those of Young Adults', *Journal of the American Geriatrics Society*. John Wiley & Sons, Ltd, 56(12), pp. 2244–2251. doi: 10.1111/J.1532-5415.2008.02018.X.

Aman, Y. *et al.* (2021) 'Autophagy in healthy aging and disease', *Nature Aging 2021 1:8*. Nature Publishing Group, 1(8), pp. 634–650. doi: 10.1038/s43587-021-00098-4.

Andersen, S. L. *et al.* (2012) 'Healthspan approximates life span among many supercentenarians: Compression of morbidity at the approximate limit of life span', *Journals of Gerontology - Series A Biological Sciences and Medical Sciences*. Oxford University Press, 67 A(4), pp. 395–405. doi: 10.1093/gerona/glr223.

Anisimov, V. N. and Bartke, A. (2013) 'The key role of growth hormone-insulin-IGF-1 signaling in aging and cancer', *Critical reviews in oncology/hematology*. Crit Rev Oncol Hematol, 87(3), pp. 201–223. doi: 10.1016/J.CRITREVONC.2013.01.005.

Antoch, M. P. *et al.* (2017) 'Physiological frailty index (PFI): Quantitative in-life estimate of individual biological age in mice', *Aging*. Impact Journals LLC, 9(3), pp. 615–626. doi: 10.18632/aging.101206.

Arc-Chagnaud, C. *et al.* (2021) 'Glucose 6-P dehydrogenase delays the onset of frailty by protecting against muscle damage', *Journal of Cachexia, Sarcopenia and Muscle*. Wiley-Blackwell, 12(6), p. 1879. doi: 10.1002/JCSM.12792.

El Assar, M. *et al.* (2017) 'Frailty Is Associated With Lower Expression of Genes Involved in Cellular Response to Stress: Results From the Toledo Study for Healthy Aging', *Journal of the American Medical Directors Association*. Elsevier, 18(8), pp. 734.e1-734.e7. doi: 10.1016/J.JAMDA.2017.04.019.

Azzu, V. and Valencak, T. G. (2017) 'Energy Metabolism and Ageing in the Mouse: A Mini-Review', *Gerontology*. Karger Publishers, 63(4), pp. 327–336. doi: 10.1159/000454924.

Baixauli, F. *et al.* (2015) 'Mitochondrial Respiration Controls Lysosomal Function during Inflammatory T cell Responses', *Cell Metabolism*. Cell Press, 22(3), pp. 485–498. doi: 10.1016/J.CMET.2015.07.020.

Banjara, S. *et al.* (2020) 'The Bcl-2 Family: Ancient Origins, Conserved Structures, and Divergent Mechanisms', *Biomolecules*. NLM (Medline). doi: 10.3390/biom10010128.

Bartke, A. *et al.* (2021) 'Energy Metabolism and Aging', *The World Journal of Men's Health*. Korean Society for Sexual Medicine and Andrology, 39(2), pp. 222–232. doi: 10.5534/WJMH.200112.

Bartling, B. *et al.* (2017) 'Sex-related differences in the wheel-running activity of mice decline with increasing age', *Experimental Gerontology*. Pergamon, 87, pp. 139–147. doi: 10.1016/J.EXGER.2016.04.011.

Basu, R. *et al.* (2003) 'Mechanisms of the age-associated deterioration in glucose tolerance: contribution of alterations in insulin secretion, action, and clearance', *Diabetes*. Diabetes, 52(7), pp. 1738–1748. doi: 10.2337/DIABETES.52.7.1738.

Baumann, C. W., Kwak, D. and Thompson, L. D. V. (2018) 'Assessing onset, prevalence and survival in mice using a frailty phenotype', *Aging*. Impact Journals LLC, 10(12), pp. 4042–4053. doi: 10.18632/aging.101692.

Baumann, C. W., Kwak, D. and Thompson, L. V. (2020) 'Phenotypic Frailty Assessment in Mice: Development, Discoveries, and Experimental Considerations', *Physiology*. American Physiological Society, 35(6), pp. 405–414. doi: 10.1152/physiol.00016.2020.

Bektas, A. *et al.* (2019) 'Age-associated changes in human CD4+ T cells point to mitochondrial dysfunction consequent to impaired autophagy', *Aging (Albany NY)*. Impact Journals, LLC, 11(21), p. 9234. doi: 10.18632/AGING.102438.

Bellantuono, I. *et al.* (2020) 'A toolbox for the longitudinal assessment of healthspan in aging mice', *Nature Protocols*. Springer US, pp. 1–35. doi: 10.1038/s41596-019-0256-1.

Belzacq, A.-S. *et al.* (2003) 'Bcl-2 and Bax Modulate Adenine Nucleotide Translocase Activity 1', *Cancer Research*, (63), pp. 541–546. Available at: http://aacrjournals.org/cancerres/article-pdf/63/2/541/2508531/ch0203000541.pdf (Accessed: 1 April 2022).

Berard, M. and Tough, D. F. (2002) 'Qualitative differences between naïve and memory T cells', *Immunology*. John Wiley & Sons, Ltd, 106(2), pp. 127–138. doi: 10.1046/J.1365-2567.2002.01447.X.

Berthelot, G. *et al.* (2019) 'The age-performance relationship in the general population and strategies to delay age related decline in performance', *Archives of Public Health 2019 77:1*. BioMed Central, 77(1), pp. 1–9. doi: 10.1186/S13690-019-0375-8.

Bharath, L. P. *et al.* (2020) 'Metformin Enhances Autophagy and Normalizes Mitochondrial Function to Alleviate Aging-Associated Inflammation', *Cell Metabolism*. Cell Press, 32(1), pp. 44-55.e6. doi: 10.1016/J.CMET.2020.04.015.

Billen, L. P. *et al.* (2008) 'Bcl-XL Inhibits Membrane Permeabilization by

Competing with Bax', *PLOS Biology*. Public Library of Science, 6(6), p. e147. doi: 10.1371/JOURNAL.PBIO.0060147.

Bisset, E. S. and Howlett, S. E. (2019) 'The biology of frailty in humans and animals: Understanding frailty and promoting translation', *AGING MEDICINE*. Wiley, 2(1), pp. 27–34. doi: 10.1002/agm2.12058.

Boise, L. H. *et al.* (1993) 'Bcl-X, a Bcl-2-Related Gene That Functions As a Dominant Regulator of Apoptotic Cell Death', *Cell*. Cell Press, 74(4), pp. 597–608. doi: 10.1016/0092-8674(93)90508-N.

Bondarev, D. *et al.* (2021) 'Associations of physical performance and physical activity with mental well-being in middle-aged women', *BMC Public Health*. BioMed Central Ltd, 21(1), pp. 1–11. doi: 10.1186/S12889-021-11485-2/TABLES/5.

Borrás, C. *et al.* (2015) 'Centenarians overexpress BCL-xL, which confers them a protection against apoptosis, oxidative stress and immunosenescence', *Free Radical Biology and Medicine*. Pergamon, 86, p. S11. doi: 10.1016/J.FREERADBIOMED.2015.07.051.

Borrás, C. *et al.* (2016) 'Human exceptional longevity: Transcriptome from centenarians is distinct from septuagenarians and reveals a role of Bcl-xL in successful aging', *Aging*. Impact Journals, LLC, 8(12), pp. 3185–3208. doi: 10.18632/aging.101078.

Borrás, Consuelo *et al.* (2020) 'BCL-xL, a mitochondrial protein involved in successful aging: From C. elegans to human centenarians', *International Journal of Molecular Sciences*. MDPI AG, 21(418). doi: 10.3390/ijms21020418.

Borrás, C. *et al.* (2020) 'Centenarians: An excellent example of resilience for successful ageing', *Mechanisms of Ageing and Development*. Elsevier, 186, p. 111199. doi: 10.1016/J.MAD.2019.111199.

Borrás, C. (2021) 'The Challenge of Unlocking the Biological Secrets of Aging', *Frontiers in Aging*. Frontiers, 0, p. 7. doi: 10.3389/FRAGI.2021.676573.

Botbol, Y., Guerrero-Ros, I. and Macian, F. (2016) 'Key roles of autophagy in regulating T cell function', *European Journal of Immunology*. John Wiley & Sons, Ltd, 46(6), pp. 1326–1334. doi: 10.1002/EJI.201545955.

Bou-Teen, D. *et al.* (2021) 'Mitochondrial ROS and mitochondria-targeted antioxidants in the aged heart', *Free Radical Biology and Medicine*. Pergamon, 167, pp. 109–124. doi: 10.1016/J.FREERADBIOMED.2021.02.043.

Boveris, A. and Navarro, A. (2008) 'Brain mitochondrial dysfunction in aging', *IUBMB Life*. John Wiley & Sons, Ltd, 60(5), pp. 308–314. doi: 10.1002/IUB.46.

Brand, M. D. and Nicholls, D. G. (2011) 'Assessing mitochondrial dysfunction in cells', *Biochemical Journal*. Portland Press, 435(2), pp. 297–312. doi: 10.1042/BJ20110162.

Breckenridge, D. G. and Xue, D. (2004) 'Regulation of mitochondrial membrane permeabilization by BCL-2 family proteins and caspases', *Current Opinion in Cell Biology*. Elsevier Current Trends, 16(6), pp. 647–652. doi: 10.1016/J.CEB.2004.09.009.

Brookes, P. S. (2005) 'Mitochondrial H+ leak and ROS generation: An odd couple', *Free Radical Biology and Medicine*. Pergamon, 38(1), pp. 12–23. doi: 10.1016/J.FREERADBIOMED.2004.10.016.

Broughton, D. L. and Taylor, R. (1991) 'Deterioration of Glucose Tolerance with Age: The Role of Insulin Resistance', *Age and Ageing*. Oxford Academic, 20(3), pp. 221–225. doi: 10.1093/AGEING/20.3.221.

Brown-Borg, H. M. *et al.* (1996) 'Dwarf mice and the ageing process', *Nature 1996 384:6604*. Nature Publishing Group, 384(6604), pp. 33–33. doi: 10.1038/384033a0.

Brys, K., Vanfleteren, J. R. and Braeckman, B. P. (2007) 'Testing the rate-of-living/oxidative damage theory of aging in the nematode model Caenorhabditis elegans', *Experimental gerontology*. Exp Gerontol, 42(9), pp. 845–851. doi: 10.1016/J.EXGER.2007.02.004.

Buchman, A. S. *et al.* (2007) 'Physical activity and motor decline in older persons', *Muscle & Nerve*. John Wiley & Sons, Ltd, 35(3), pp. 354–362. doi: 10.1002/MUS.20702.

Bullain, S. S. *et al.* (2013) 'Poor Physical Performance and Dementia in the Oldest Old: The 90+ Study', *JAMA neurology*. NIH Public Access, 70(1), p. 107. doi: 10.1001/JAMANEUROL.2013.583.

Burlacu, A. (2003) 'Regulation of apoptosis by Bcl-2 family proteins', *Journal of Cellular and Molecular Medicine*. John Wiley & Sons, Ltd, 7(3), pp. 249–257. doi: 10.1111/J.1582-4934.2003.TB00225.X.

Camicioli, R., Panzer, V. P. and Kaye, J. (1997) 'Balance in the Healthy Elderly: Posturography and Clinical Assessment', *Archives of Neurology*. American Medical Association, 54(8), pp. 976–981. doi: 10.1001/ARCHNEUR.1997.00550200040008.

Campisi, J. and D'Adda Di Fagagna, F. (2007) 'Cellular senescence: When bad things happen to good cells', *Nature Reviews Molecular Cell Biology*. Nature Publishing Group, 8(9), pp. 729–740. doi: 10.1038/nrm2233.

Caristia, S. *et al.* (2020) 'Is caloric restriction associated with better healthy aging outcomes? A systematic review and meta- analysis of randomized controlled trials', *Nutrients*. MDPI AG, pp. 1–19. doi: 10.3390/nu12082290.

Carpenter, D. G. (1968) 'An integrated theory of aging', *Journal of the American Geriatrics Society*, 16(12). doi: 10.1111/j.1532-5415.1963.tb00061.x.

Carrasco, E. *et al.* (2022) 'The role of T cells in age-related diseases', *Nature Reviews Immunology*, 22(2), pp. 97–111. doi: 10.1038/s41577-021-00557-4.

Carter, C. S. *et al.* (2002) 'Physical Performance and Longevity in Aged Rats', *The Journals of Gerontology: Series A*. Oxford Academic, 57(5), pp. B193–B197. doi: 10.1093/GERONA/57.5.B193.

Carter, R. J., Morton, J. and Dunnett, S. B. (2001) 'Motor Coordination and Balance in Rodents', *Current Protocols in Neuroscience*, 15(1), pp. 1–14. doi:

10.1002/0471142301.ns0812s15.

Carthy, C. M. *et al.* (2003) 'Bcl-2 and Bcl-xL overexpression inhibits cytochrome c release, activation of multiple caspases, and virus release following coxsackievirus B3 infection', *Virology*, 313(1), pp. 147–157. doi: 10.1016/S0042-6822(03)00242-3.

Caruso, C. *et al.* (2019) 'Genetic Signatures of Centenarians: Implications for Achieving Successful Aging', *Current Pharmaceutical Design*. Bentham Science Publishers Ltd., 25(39), pp. 4133–4138. doi: 10.2174/1381612825666191112094544.

Caspersen, C. J., Powell, K. E. and Christenson, G. M. (1985) 'Physical Activity, Exercise, and Physical Fitness: Definitions and Distinctions for Health-Related Research', *Public Health Reports*, 100(2), pp. 126–131. doi: 10.1093/nq/s9-IX.228.365-f.

Castelo-Branco, C. and Soveral, I. (2013) 'The immune system and aging: a review', *https://doi.org/10.3109/09513590.2013.852531*. Taylor & Francis, 30(1), pp. 16–22. doi: 10.3109/09513590.2013.852531.

Chang, A. Y. *et al.* (2019) 'Measuring population ageing: an analysis of the Global Burden of Disease Study 2017', *The Lancet. Public Health*. Elsevier, 4(3), p. e159. doi: 10.1016/S2468-2667(19)30019-2.

Chao, D. T. *et al.* (1995) 'Bcl-XL and Bcl-2 repress a common pathway of cell death.', *The Journal of experimental medicine*, 182(3), pp. 821–8. doi: 10.1084/jem.182.3.821.

Chazotte, B. (2011) 'Labeling Mitochondria with TMRM or TMRE', *Cold Spring Harbor Protocols*. Cold Spring Harbor Laboratory Press, 2011(7), p. pdb.prot5641. doi: 10.1101/PDB.PROT5641.

Chen, C. Y., Gan, P. and How, C. H. (2018) 'Approach to frailty in the elderly in primary care and the community', *Singapore Medical Journal*. Singapore Medical Association, 59(5), p. 240. doi: 10.11622/SMEDJ.2018052.

Chen, Y. *et al.* (2002) 'Constitutive expression of BCL-X(L) in the T lineage attenuates collagen-induced arthritis in Bcl-X(L) transgenic mice', *Arthritis Rheum*, 46(2), pp. 514–521. doi: 10.1002/art.10128.

Chen, Y. *et al.* (2019) 'The crosstalk between autophagy and apoptosis was mediated by phosphorylation of Bcl-2 and beclin1 in benzene-induced hematotoxicity', *Cell Death & Disease 2019 10:10*. Nature Publishing Group, 10(10), pp. 1–15. doi: 10.1038/s41419-019-2004-4.

Chen, Y. bei *et al.* (2011) 'Bcl-x L regulates mitochondrial energetics by stabilizing the inner membrane potential', *Journal of Cell Biology*. The Rockefeller University Press, 195(2), pp. 263–276. doi: 10.1083/jcb.201108059.

Cheng, J. *et al.* (2017) 'Mitochondrial Proton Leak Plays a Critical Role in Pathogenesis of Cardiovascular Diseases', *Advances in experimental medicine and biology*. NIH Public Access, 982, p. 359. doi: 10.1007/978-3-319-55330-6_20.

Cheon, S. Y. *et al.* (2019) 'Autophagy, Cellular Aging and Age-related Human Diseases', *Experimental Neurobiology*. Korean Society for Brain and Neural Science, 28(6), p. 643. doi: 10.5607/EN.2019.28.6.643.

Cherubini, A. *et al.* (1998) 'The Effects of Aging and Endurance Exercise on Cardiovascular Performance in Healthy Elderly: A Review of the Literature.', *The American Journal of Geriatric Cardiology*, 7(2), pp. 25–32. Available at: https://europepmc.org/article/med/11416449 (Accessed: 3 June 2022).

Chia, C. W., Egan, J. M. and Ferrucci, L. (2018) 'Age-Related Changes in Glucose Metabolism, Hyperglycemia, and Cardiovascular Risk', *Circulation Research*, 123(7), pp. 886–904. Available at: http://ahajournals.org (Accessed: 5 April 2022).

Childs, B. G. *et al.* (2014) 'Senescence and apoptosis: dueling or complementary cell fates?', *EMBO reports*. European Molecular Biology Organization, 15(11), pp. 1139–53. doi: 10.15252/embr.201439245.

Childs, B. G. *et al.* (2015) 'Cellular senescence in aging and age-related disease:

From mechanisms to therapy', *Nature Medicine*. doi: 10.1038/nm.4000.

Chipuk, J. E. *et al.* (2010) 'The BCL-2 Family Reunion', *Molecular Cell*. Elsevier Inc., 37(3), pp. 299–310. doi: 10.1016/j.molcel.2010.01.025.

Cho, H. J. and Eo, S. H. (2016) 'Outlier Detection for Mass Spectrometric Data', *Methods in Molecular Biology*. Humana Press, New York, NY, 1362, pp. 91–102. doi: 10.1007/978-1-4939-3106-4_5.

Ciolac, E. G., da Silva, J. M. R. and Vieira, R. P. (2020) 'Physical Exercise as an Immunomodulator of Chronic Diseases in Aging', *Journal of Physical Activity and Health*. Human Kinetics, 17(6), pp. 662–672. doi: 10.1123/JPAH.2019-0237.

Clegg, A. *et al.* (2013) 'Frailty in elderly people', in *The Lancet*. Elsevier B.V., pp. 752–762. doi: 10.1016/S0140-6736(12)62167-9.

Coin, D. (2007) 'Testing normality in the presence of outliers', *Statistical Methods and Applications 2007 17:1*. Springer, 17(1), pp. 3–12. doi: 10.1007/S10260-007-0046-8.

Colloca, G. *et al.* (2020) 'Biological and Functional Biomarkers of Aging: Definition, Characteristics, and How They Can Impact Everyday Cancer Treatment', *Current Oncology Reports*. Springer, 22(11), pp. 1–12. doi: 10.1007/S11912-020-00977-W/TABLES/3.

Colman, R. J. *et al.* (2007) 'Energy Restriction-Induced Changes in Body Composition Are Age Specific in Mice', *The Journal of Nutrition*. Oxford Academic, 137(10), pp. 2247–2251. doi: 10.1093/JN/137.10.2247.

Conley, K. E., Marcinek, D. J. and Villarin, J. (2007) 'Mitochondrial dysfunction and age', *Current Opinion in Clinical Nutrition and Metabolic Care*, 10(6), pp. 688–692. doi: 10.1097/MCO.0B013E3282F0DBFB.

Creed, S. and McKenzie, M. (2019) 'Measurement of Mitochondrial Membrane Potential with the Fluorescent Dye Tetramethylrhodamine Methyl Ester (TMRM)', *Methods in Molecular Biology*. Humana Press, New York, NY, 1928, pp. 69–76. doi: 10.1007/978-1-4939-9027-6_5.

Cuervo, A. M. *et al.* (2005) 'Autophagy and Aging: The Importance of Maintaining "Clean" Cells', *http://dx.doi.org/10.4161/auto.1.3.2017*. Taylor & Francis, 1(3), pp. 131–140. doi: 10.4161/AUTO.1.3.2017.

Cuervo, A. M. and Macian, F. (2014) 'Autophagy and the immune function in aging', *Current Opinion in Immunology*. Elsevier Current Trends, 29(1), pp. 97–104. doi: 10.1016/J.COI.2014.05.006.

Cui, H., Kong, Y. and Zhang, H. (2012) 'Oxidative stress, mitochondrial dysfunction, and aging.', *Journal of signal transduction*. Hindawi Limited, 2012, p. 646354. doi: 10.1155/2012/646354.

Cvecka, J. *et al.* (2015) 'Physical Activity in Elderly', *European journal of translational myology*. Eur J Transl Myol, 25(4), p. 249. doi: 10.4081/EJTM.2015.5280.

Das, K. R. and Rahmatullah Imon, A. H. M. (2016) 'A Brief Review of Tests for Normality', *American Journal of Theoretical and Applied Statistics*, 5(1), pp. 5–12. doi: 10.11648/j.ajtas.20160501.12.

Das, S. K. *et al.* (2001) 'An Underfeeding Study in Healthy Men and Women Provides Further Evidence of Impaired Regulation of Energy Expenditure in Old Age', *The Journal of Nutrition*. Oxford Academic, 131(6), pp. 1833–1838. doi: 10.1093/JN/131.6.1833.

Deacon, R. M. J. (2013) 'Measuring Motor Coordination in Mice', *Journal of Visualized Experiments : JoVE*. MyJoVE Corporation, (75), p. 2609. doi: 10.3791/2609.

Desdín-Micó, G., Soto-Heredero, G. and Mittelbrunn, M. (2018) 'Mitochondrial activity in T cells', *Mitochondrion*. Elsevier, 41, pp. 51–57. doi: 10.1016/J.MITO.2017.10.006.

Van Deursen, J. M., Deursen, J. M. Van and Van Deursen, J. M. (2014) 'The role of senescent cells in ageing', *Nature*. Nature Publishing Group, 509(7501), pp. 439–446. doi: 10.1038/nature13193.

Dickinson, B. C., Lin, V. S. and Chang, C. J. (2013) 'Preparation and use of MitoPY1 for imaging hydrogen peroxide in mitochondria of live cells', *Nature protocols*. NIH Public Access, 8(6), p. 1249. doi: 10.1038/NPROT.2013.064.

Dimri, G. P. *et al.* (1995) 'A biomarker that identifies senescent human cells in culture and in aging skin in vivo.', *Proceedings of the National Academy of Sciences of the United States of America*. National Academy of Sciences, 92(20), pp. 9363–7. Available at: http://www.ncbi.nlm.nih.gov/pubmed/7568133 (Accessed: 30 June 2018).

DiPietro, L. (2001) 'Physical Activity in AgingChanges in Patterns and Their Relationship to Health and Function', *The Journals of Gerontology: Series A*. Oxford Academic, 56(suppl_2), pp. 13–22. doi: 10.1093/GERONA/56.SUPPL_2.13.

Doherty, J. and Baehrecke, E. H. (2018) 'Life, death and autophagy', *Nature Cell Biology 2018 20:10*. Nature Publishing Group, 20(10), pp. 1110–1117. doi: 10.1038/s41556-018-0201-5.

Dou, Z. *et al.* (2021) 'Aberrant Bcl-x splicing in cancer: from molecular mechanism to therapeutic modulation', *Journal of Experimental & Clinical Cancer Research 2021 40:1*. BioMed Central, 40(1), pp. 1–18. doi: 10.1186/S13046-021-02001-W.

Duggal, N. A. *et al.* (2019) 'Can physical activity ameliorate immunosenescence and thereby reduce age-related multi-morbidity?', *Nature Reviews Immunology*. Springer US, 19(9), pp. 563–572. doi: 10.1038/s41577-019-0177-9.

Effros, R. B. (2005) 'Roy Walford and the immunologic theory of aging', *Immunity & Ageing 2005 2:1*. BioMed Central, 2(1), pp. 1–3. doi: 10.1186/1742-4933-2-7.

Elmore, S. (2007) 'Apoptosis: A Review of Programmed Cell Death', *Toxicologic pathology*. NIH Public Access, 35(4), p. 495. doi: 10.1080/01926230701320337.

Engberg, H. *et al.* (2009) 'Centenarians - A useful model for healthy aging? A 29-year follow-up of hospitalizations among 40000 Danes born in 1905', *Aging Cell*.

NIH Public Access, 8(3), pp. 270–276. doi: 10.1111/j.1474-9726.2009.00474.x.

Escobar, K. A. *et al.* (2019) 'Autophagy and aging: Maintaining the proteome through exercise and caloric restriction', *Aging Cell*. John Wiley & Sons, Ltd, 18(1), p. e12876. doi: 10.1111/ACEL.12876.

Ethisan, P. *et al.* (2017) 'Factors related to physical activity among the elderly population in rural Thailand', *Journal of Primary Care and Community Health*. SAGE Publications Inc., 8(2), pp. 71–76. doi: 10.1177/2150131916675899.

Evans, W. J. and Campbell, W. W. (1993) 'Sarcopenia and age-related changes in body composition and functional capacity.', *The Journal of Nutrition*, 123(2 Suppl), pp. 465–468. doi: 10.1093/JN/123.SUPPL_2.465.

Eyth, E., Basit, H. and Smith, C. J. (2022) 'Glucose Tolerance Test', *British Medical Journal*. StatPearls Publishing, 2(5145), pp. 191–192. doi: 10.1136/bmj.2.5145.191-b.

Fan, Y. *et al.* (2020) 'SenescenT cell Depletion Through Targeting BCL-Family Proteins and Mitochondria', *Frontiers in Physiology*. Frontiers Media SA, 11, p. 593630. doi: 10.3389/FPHYS.2020.593630.

Fan, Y. J. and Zong, W. X. (2013) 'The cellular decision between apoptosis and autophagy', *Chinese Journal of Cancer*. BioMed Central, 32(3), p. 121. doi: 10.5732/CJC.012.10106.

de Fátima Ribeiro Silva, C. I. *et al.* (2020) 'Dyspnea is associated with poor physical performance among community-dwelling older adults: a population-based cross-sectional study', *Sao Paulo Med J*, 138(2), pp. 112–119. doi: 10.1590/1516-3180.2019.0428.R1.09122019.

Favero, G. *et al.* (2015) 'Sirtuins, aging, and cardiovascular risks', *AGE 2015 37:4*. Springer, 37(4), pp. 1–19. doi: 10.1007/S11357-015-9804-Y.

Ferrannini, E. (1988) 'The theoretical bases of indirect calorimetry: A review', *Metabolism*. W.B. Saunders, 37(3), pp. 287–301. doi: 10.1016/0026-0495(88)90110-2.

Fîlfan, M. *et al.* (2017) 'Autophagy in aging and disease', *Rom J Morphol Embryol*, pp. 27–31. Available at: http://www.rjme.ro/ (Accessed: 8 June 2022).

Fisher, R. A. (1992) 'Statistical Methods for Research Workers'. Springer, New York, NY, pp. 66–70. doi: 10.1007/978-1-4612-4380-9_6.

Flack, K. D. *et al.* (2011) 'Aging, resistance training, and diabetes prevention', *Journal of Aging Research*, 2011. doi: 10.4061/2011/127315.

Fokin, A. *et al.* (2017) 'Metabolism Analysis in Mice With Reduced Citrate Synthase Activity', *Baltic Journal of Sport and Health Sciences*, 2(105), pp. 14–19. doi: 10.33607/bjshs.v2i105.20.

Folgueras, A. R. *et al.* (2018) 'Mouse models to disentangle the hallmarks of human aging', *Circulation Research*. Lippincott Williams and Wilkins, 123(7), pp. 905–924. doi: 10.1161/CIRCRESAHA.118.312204.

Forster, M. J. *et al.* (1996) 'Age-related losses of cognitive function and motor skills in mice are associated with oxidative protein damage in the brain (oxidative stress/brain function/memory/protein oxidative damage)', *Neurobiology Communicated by Earl R. Stadtman*, 93, pp. 4765–4769. Available at: https://www.pnas.org (Accessed: 19 March 2022).

Franceschi, C. *et al.* (2017) 'Inflammaging and "Garb-aging"', *Trends in Endocrinology and Metabolism*. Elsevier Current Trends, 28(3), pp. 199–212. doi: 10.1016/j.tem.2016.09.005.

Franceschi, C. and Bonafè, M. (2003) 'Centenarians as a model for healthy aging', *Biochemical Society Transactions*. Portland Press, 31(2), pp. 457–461. doi: 10.1042/BST0310457.

Fridovich, I. (1978) 'The Biology of Oxygen Radicals', *Science*. American Association for the Advancement of Science , 201(4359), pp. 875–880. doi: 10.1126/SCIENCE.210504.

Fried, L. P. *et al.* (2001) 'Frailty in Older Adults: Evidence for a Phenotype', *The Journals of Gerontology Series A: Biological Sciences and Medical Sciences*. Oxford

University Press, 56(3), pp. M146–M157. doi: 10.1093/gerona/56.3.M146.

Fried, L. P. *et al.* (2021) 'The physical frailty syndrome as a transition from homeostatic symphony to cacophony', *Nature Aging 2021 1:1*. Nature Publishing Group, 1(1), pp. 36–46. doi: 10.1038/s43587-020-00017-z.

de Fronzo, R. A. (1981) 'Glucose Intolerance and Aging', *CARE*, 4(4). Available at: http://diabetesjournals.org/care/article-pdf/4/4/493/547340/4-4-493.pdf (Accessed: 22 March 2022).

Fukushima, Y., Minato, N. and Hattori, M. (2018) 'The impact of senescence-associated T cells on immunosenescence and age-related disorders', *Inflammation and Regeneration*. BioMed Central Ltd., 38(1), pp. 1–6. doi: 10.1186/S41232-018-0082-9/FIGURES/3.

Fulop, T. *et al.* (2010) 'Aging, frailty and age-related diseases', *Biogerontology*. Biogerontology, 11(5), pp. 547–563. doi: 10.1007/S10522-010-9287-2.

Fulop, T. *et al.* (2014) 'On the Immunological Theory of Aging', *Aging: Facts and Theories*. Karger Publishers, 39, pp. 163–176. doi: 10.1159/000358904.

Furuya, N. *et al.* (2005) 'The Evolutionarily Conserved Domain of Beclin 1 is Required for Vps34 Binding, Autophagy, and Tumor Suppressor Function', *http://dx.doi.org/10.4161/auto.1.1.1542*. Taylor & Francis, 1(1), pp. 46–52. doi: 10.4161/AUTO.1.1.1542.

Gale, C. R. *et al.* (2007) 'Grip strength, body composition, and mortality', 36(1), pp. 228–235. Available at: https://academic.oup.com/ije/article/36/1/228/665601 (Accessed: 2 June 2022).

Galgani, J. and Ravussin, E. (2008) 'Energy metabolism, fuel selection and body weight regulation', *International Journal of Obesity*. Nature Publishing Group, 32(SUPPL. 7), pp. 109–119. doi: 10.1038/ijo.2008.246.

Galluzzi, L. *et al.* (2008) 'To Die or Not to Die: That is the Autophagic Question', *Current Molecular Medicine*, 8(2), pp. 78–91. doi:

10.2174/156652408783769616.

García-Giménez, J. L. *et al.* (2021) 'Implementing Precision Medicine in Human Frailty through Epigenetic Biomarkers', *International Journal of Environmental Research and Public Health*. Multidisciplinary Digital Publishing Institute (MDPI), 18(4), pp. 1–17. doi: 10.3390/IJERPH18041883.

Ge, M. *et al.* (2021) 'Senolytic targets and new strategies for clearing senescenT cells', *Mechanisms of Ageing and Development*. Elsevier, 195, p. 111468. doi: 10.1016/J.MAD.2021.111468.

Ge, X. *et al.* (2016) 'Grip strength is potentially an early indicator of age-related decline in mice', *https://doi.org/10.3402/pba.v6.32981*. Taylor & Francis, 6(1). doi: 10.3402/PBA.V6.32981.

Gellert, P. *et al.* (2018) 'Long-term Care Status in Centenarians and Younger Cohorts of Oldest Old in the Last 6 Years of Life: Trajectories and Potential Mechanisms', *Journal of the American Medical Directors Association*. J Am Med Dir Assoc, 19(6), pp. 535-540.e1. doi: 10.1016/J.JAMDA.2018.02.010.

Ghasemi, A. and Zahediasl, S. (2012) 'Normality tests for statistical analysis: A guide for non-statisticians', *International Journal of Endocrinology and Metabolism*. Kowsar Medical Institute, 10(2), pp. 486–489. doi: 10.5812/ijem.3505.

Gimeno-Mallench, L. *et al.* (2021) 'La sobreexpresión de los genes BCL-XL y FAS contribuyen al envejecimiento saludable de las moscas Drosophila', in *Sociedad Española de Geriatría y Gerontología (SEGG)*, p. 2021.

Ginaldi, L. *et al.* (2004) 'The immune system in the elderly', *Immunologic Research 2004 30:1*. Springer, 30(1), pp. 81–94. doi: 10.1385/IR:30:1:081.

Gladyshev, V. N. (2014) 'The Free Radical Theory of Aging Is Dead. Long Live the Damage Theory!', *Antioxidants & Redox Signaling*. Mary Ann Liebert, Inc., 20(4), p. 727. doi: 10.1089/ARS.2013.5228.

Glass, C. *et al.* (2013) 'Sarcopenia and a physiologically low respiratory quotient

in patients with cirrhosis: A prospective controlled study', *Journal of Applied Physiology*. American Physiological Society Bethesda, MD, 114(5), pp. 559–565. doi: 10.1152/JAPPLPHYSIOL.01042.2012/ASSET/IMAGES/LARGE/ZDG0051304840006.JPEG.

Glatt, V. *et al.* (2009) 'Age-Related Changes in Trabecular Architecture Differ in Female and Male C57BL/6J Mice', *Journal of Bone and Mineral Research*. John Wiley & Sons, Ltd, 22(8), pp. 1197–1207. doi: 10.1359/JBMR.070507.

Goldfeld, S. M. and Quandt, R. E. (1965) 'Some Tests for Homoscedasticity', *Journal of the American Statistical Association*, 60(310), pp. 539–547. doi: 10.1080/01621459.1965.10480811.

Gomez-Cabrera, M. C. *et al.* (2017) 'A New Frailty Score for Experimental Animals Based on the Clinical Phenotype: Inactivity as a Model of Frailty', *Journals of Gerontology - Series A Biological Sciences and Medical Sciences*. Oxford University Press, 72(7), pp. 885–891. doi: 10.1093/gerona/glw337.

Gonzalvez, F. *et al.* (2005) 'tBid interaction with cardiolipin primarily orchestrates mitochondrial dysfunctions and subsequently activates Bax and Bak', *Cell Death & Differentiation 2005 12:6*. Nature Publishing Group, 12(6), pp. 614–626. doi: 10.1038/sj.cdd.4401571.

Gordy, C. and He, Y. W. (2012) 'The crosstalk between autophagy and apoptosis: where does this lead?', *Protein & Cell 2012 3:1*. Springer, 3(1), pp. 17–27. doi: 10.1007/S13238-011-1127-X.

Graber, T. G. *et al.* (2021) 'Measuring Exercise Capacity and Physical Function in Adult and Older Mice', *The journals of gerontology. Series A, Biological sciences and medical sciences*. J Gerontol A Biol Sci Med Sci, 76(5), pp. 819–824. doi: 10.1093/GERONA/GLAA205.

Gregg, E. W., Engelgau, M. M. and Narayan, V. (2002) 'Complications of diabetes in elderly people', *BMJ*. British Medical Journal Publishing Group, 325(7370), pp.

916–917. doi: 10.1136/BMJ.325.7370.916.

Grevendonk, L. *et al.* (2021) 'Impact of aging and exercise on skeletal muscle mitochondrial capacity, energy metabolism, and physical function', *Nature Communications 2021 12:1*. Nature Publishing Group, 12(1), pp. 1–17. doi: 10.1038/s41467-021-24956-2.

Grillot, D. A. M., Merino, R. and Nunez, G. (1995) 'Bcl-xL Displays Restricted Distribution during T cell Development and Inhibits Multiple Forms of Apoptosis but Not Clonal Deletion in Transgenic Mice', *J. Exp. Med.*, 182(6), pp. 1973–1983. doi: https://doi.org/10.1084/jem.182.6.1973.

Gruver, A. L., Hudson, L. L. and Sempowski, G. D. (2007) 'Immunosenescence of ageing', *The Journal of Pathology*. John Wiley & Sons, Ltd, 211(2), pp. 144–156. doi: 10.1002/PATH.2104.

Guimarães, G. R. *et al.* (2021) 'Hallmarks of Aging in Macrophages: Consequences to Skin Inflammaging', *Cells*. Multidisciplinary Digital Publishing Institute, 10(6), p. 1323. doi: 10.3390/CELLS10061323.

Gupta, S. and Gollapudi, S. (2005) 'Molecular mechanisms of TNF-α-induced apoptosis in aging human T cell subsets', *The International Journal of Biochemistry & Cell Biology*. Pergamon, 37(5), pp. 1034–1042. doi: 10.1016/J.BIOCEL.2004.08.013.

Guralnik, J. M. *et al.* (1989) 'Physical performance measures in aging research', *Journals of Gerontology*, 44(5), pp. 141–146. doi: 10.1093/geronj/44.5.M141.

Guralnik, J. M. *et al.* (1994) 'A short physical performance battery assessing lower extremity function: association with self-reported disability and prediction of mortality and nursing home admission', *Journal of gerontology*. J Gerontol, 49(2). doi: 10.1093/GERONJ/49.2.M85.

Hahm, J. H. *et al.* (2015) 'C. elegans maximum velocity correlates with healthspan and is maintained in worms with an insulin receptor mutation', *Nature Communications 2015 6:1*. Nature Publishing Group, 6(1), pp. 1–7. doi:

10.1038/ncomms9919.

Hamrick, M. W. *et al.* (2006) 'Age-related loss of muscle mass and bone strength in mice is associated with a decline in physical activity and serum leptin', *Bone*. Elsevier, 39(4), pp. 845–853. doi: 10.1016/J.BONE.2006.04.011.

Harman, D. (1956) 'Aging: a theory based on free radical and radiation chemistry.', *Journal of gerontology*, 11(3), pp. 298–300. Available at: http://www.ncbi.nlm.nih.gov/pubmed/13332224 (Accessed: 14 May 2018).

Harman, D. (1981) 'The aging process.', *Proceedings of the National Academy of Sciences of the United States of America*. National Academy of Sciences, 78(11), pp. 7124–8. doi: 10.1073/PNAS.78.11.7124.

Harper, E. J. (1998) 'Changing Perspectives on Aging and Energy Requirements: Aging, Body Weight and Body Composition in Humans, Dogs and Cats', *The Journal of Nutrition*. Oxford Academic, 128(12), pp. 2627S-2631S. doi: 10.1093/JN/128.12.2627S.

Hatok, J. and Racay, P. (2016) 'Bcl-2 family proteins: Master regulators of cell survival', *Biomolecular Concepts*. Walter de Gruyter GmbH, 7(4), pp. 259–270. doi: 10.1515/BMC-2016-0015/XML.

He, C. and Levine, B. (2010) 'The Beclin 1 interactome', *Current Opinion in Cell Biology*. Elsevier Current Trends, 22(2), pp. 140–149. doi: 10.1016/J.CEB.2010.01.001.

He, Y. *et al.* (2020) 'Using proteolysis-targeting chimera technology to reduce navitoclax platelet toxicity and improve its senolytic activity', *Nature Communications 2020 11:1*. Nature Publishing Group, 11(1), pp. 1–14. doi: 10.1038/s41467-020-15838-0.

Hebert, S. L. *et al.* (2015) 'Mitochondrial Aging and Physical Decline: Insights From Three Generations of Women', *The Journals of Gerontology: Series A*. Oxford Academic, 70(11), pp. 1409–1417. doi: 10.1093/GERONA/GLV086.

Heinze-Milne, S. D. D., Banga, S. and Howlett, S. E. E. (2019) 'Frailty Assessment

in Animal Models', *Gerontology*. S. Karger AG, 65(6), pp. 610–619. doi: 10.1159/000501333.

Herndon, L. A. *et al.* (2002) 'Stochastic and genetic factors influence tissue-specific decline in ageing C. elegans', *Nature 2002 419:6909*. Nature Publishing Group, 419(6909), pp. 808–814. doi: 10.1038/nature01135.

Herranz, N. and Gil, J. (2018) 'Mechanisms and functions of cellular senescence', *The Journal of Clinical Investigation*. American Society for Clinical Investigation, 128(4), pp. 1238–1246. doi: 10.1172/JCI95148.

Herst, P. M. and Berridge, M. V. (2007) 'Cell surface oxygen consumption: a major contributor to cellular oxygen consumption in glycolytic cancer cell lines', *Biochimica et biophysica acta*. Biochim Biophys Acta, 1767(2), pp. 170–177. doi: 10.1016/J.BBABIO.2006.11.018.

Higami, Y. and Shimokawa, I. (2000) 'Apoptosis in the aging process', *Cell Tissue Res*, 301, pp. 125–132. doi: 10.1007/s004419900156.

Hirsch, C. H. *et al.* (2012) 'Predicting late-life disability and death by the rate of decline in physical performance measures', *Age and Ageing*. Oxford Academic, 41(2), pp. 155–161. doi: 10.1093/AGEING/AFR151.

Hollmann, W. *et al.* (2007) 'Physical activity and the elderly', *European journal of cardiovascular prevention and rehabilitation*. Oxford Academic, 14(6), pp. 730–739. doi: 10.1097/HJR.0B013E32828622F9.

Houtkooper, R. H. *et al.* (2011) 'The metabolic footprint of aging in mice', *Scientific Reports*. Nature Publishing Group, 1(1), p. 134. doi: 10.1038/srep00134.

Howlett, S. E. (2015) 'Assessment of Frailty in Animal Models', *Interdisciplinary Topics in Gerontology and Geriatrics*. S. Karger AG, 41, pp. 15–25. doi: 10.1159/000381131.

Hubbard, V. M. *et al.* (2010) 'Macroautophagy Regulates Energy Metabolism during Effector T cell Activation', *The Journal of Immunology*. American

Association of Immunologists, 185(12), pp. 7349–7357. doi: 10.4049/JIMMUNOL.1000576.

Huffman, D. M. *et al.* (2016) 'Evaluating Healthspan in Preclinical Models of Aging and Disease: Guidelines, Challenges, and Opportunities for Geroscience', *Journals of Gerontology - Series A Biological Sciences and Medical Sciences*. Oxford University Press, 71(11), pp. 1395–1406. doi: 10.1093/gerona/glw106.

Huska, J. D., Lamb, H. M. and Hardwick, J. M. (2019) 'Overview of BCL-2 Family Proteins and Therapeutic Potentials', *Methods in Molecular Biology*, 1877, pp. 1–21. doi: 10.1007/978-1-4939-8861-7_1.

Hyatt, H. W. and Powers, S. K. (2021) 'Mitochondrial Dysfunction Is a Common Denominator Linking Skeletal Muscle Wasting Due to Disease, Aging, and Prolonged Inactivity', *Antioxidants 2021, Vol. 10, Page 588*. Multidisciplinary Digital Publishing Institute, 10(4), p. 588. doi: 10.3390/ANTIOX10040588.

Ikezawa, K. *et al.* (2017) 'Increased Bcl-xL Expression in Pancreatic Neoplasia Promotes Carcinogenesis by Inhibiting Senescence and Apoptosis', *Cellular and Molecular Gastroenterology and Hepatology*. Elsevier, 4(1), pp. 185-200.e1. doi: 10.1016/J.JCMGH.2017.02.001.

Inglés, M. *et al.* (2018) 'Centenarian offspring: A model for understanding healthy aging', *Free Radical Biology and Medicine*. Pergamon, 120, pp. S77–S78. doi: 10.1016/J.FREERADBIOMED.2018.04.257.

Inglés, M. *et al.* (2019) 'Centenarians Overexpress Pluripotency-Related Genes', *The Journals of Gerontology: Series A*. Oxford Academic, 74(9), pp. 1391–1395. doi: 10.1093/GERONA/GLY168.

Ingram, D. K. (2000) 'Age-related decline in physical activity: generalization to nonhumans.', *Medicine and Science in Sports and Exercise*. American College of Sports Medicine, 32(9), pp. 1623–1629. doi: 10.1097/00005768-200009000-00016.

Jacotot, E. *et al.* (2006) 'Mitochondrial Membrane Permeabilization during the

Apoptotic Process', *Annals of the New York Academy of Sciences*. John Wiley & Sons, Ltd, 887(1), pp. 18–30. doi: 10.1111/J.1749-6632.1999.TB07919.X.

Janeway, C. A. *et al.* (2001) *Immunobiology: The Immune System in Health and Disease. T cell-mediated cytotoxicity*. 5th edn. Edited by G. Science. NCBI Bookshelf. Available at: https://www.ncbi.nlm.nih.gov/books/NBK27101/.

Jazwinski, S. M. (1996) 'Longevity, genes, and aging', *Science*. American Association for the Advancement of Science, 273(5271), pp. 54–59. doi: 10.1126/SCIENCE.273.5271.54.

Jeong, J. *et al.* (2017) 'Identifying outliers of non-Gaussian groundwater state data based on ensemble estimation for long-term trends', *Journal of Hydrology*. Elsevier, 548, pp. 135–144. doi: 10.1016/J.JHYDROL.2017.02.058.

Jeyapalan, J. C. *et al.* (2007) 'Accumulation of senescent cells in mitotic tissue of aging primates', *Mechanisms of Ageing and Development*. Elsevier, 128(1), pp. 36–44. doi: 10.1016/J.MAD.2006.11.008.

Jia, L. *et al.* (1999) 'Subcellular Distribution and Redistribution of Bcl-2 Family Proteins in Human Leukemia Cells Undergoing Apoptosis', *Blood*. Content Repository Only!, 93(7), pp. 2353–2359. doi: 10.1182/BLOOD.V93.7.2353.

Jin, K. (2010) 'Modern Biological Theories of Aging', *Aging and Disease*. JKL International LLC, 1(2), p. 72. doi: 10.1093/jn/119.6.952.

Jin, Z. and El-Deiry, W. S. (2005) 'Overview of cell death signaling pathways', *Cancer Biology and Therapy*, 4(2), pp. 147–171. doi: 10.4161/cbt.4.2.1508.

Joly-Amado, A. *et al.* (2016) 'Metabolic changes over the course of aging in a mouse model of tau deposition', *Neurobiology of aging*. NIH Public Access, 44, p. 62. doi: 10.1016/J.NEUROBIOLAGING.2016.04.013.

Jonas, E. (2014) 'Contributions of Bcl-xL to acute and long term changes in bioenergetics during neuronal plasticity', 154(11), pp. 2262–2265. doi: 10.1016/j.pain.2013.06.005.Re-Thinking.

Jonas, E. A., Porter, G. A. and Alavian, K. N. (2014) 'Bcl-xL in neuroprotection and

plasticity', *Frontiers in Physiology*, 5(September). doi: 10.3389/fphys.2014.00355.

Jones, D. M., Song, X. and Rockwood, K. (2004) 'Operationalizing a Frailty Index from a Standardized Comprehensive Geriatric Assessment', *Journal of the American Geriatrics Society*. John Wiley & Sons, Ltd, 52(11), pp. 1929–1933. doi: 10.1111/j.1532-5415.2004.52521.x.

Jung, M.-S. S. *et al.* (2004) 'Bcl-xL and E1B-19K Proteins Inhibit p53-induced Irreversible Growth Arrest and Senescence by Preventing Reactive Oxygen Species-dependent p38 Activation', *Journal of Biological Chemistry*. American Society for Biochemistry and Molecular Biology, 279(17), pp. 17765–17771. doi: 10.1074/jbc.M305015200.

Justice, J. N. *et al.* (2014) 'Battery of behavioral tests in mice that models age-associated changes in human motor function', *Age (Dordrecht, Netherlands)*. Age (Dordr), 36(2), pp. 583–595. doi: 10.1007/S11357-013-9589-9.

Kalyani, R. R. and Egan, J. M. (2013) 'Diabetes and Altered Glucose Metabolism with Aging', *Endocrinology and metabolism clinics of North America*. NIH Public Access, 42(2), p. 333. doi: 10.1016/J.ECL.2013.02.010.

Kaufman, R. J. and Malhotra, J. D. (2014) 'Calcium trafficking integrates endoplasmic reticulum function with mitochondrial bioenergetics', *Biochimica et Biophysica Acta (BBA) - Molecular Cell Research*. Elsevier, 1843(10), pp. 2233–2239. doi: 10.1016/J.BBAMCR.2014.03.022.

Kaushik, S. *et al.* (2008) 'Constitutive Activation of Chaperone-mediated Autophagy in Cells with Impaired Macroautophagy', *Molecular Biology of the Cell*. American Society for Cell Biology, 19(5), p. 2179. doi: 10.1091/MBC.E07-11-1155.

Kaushik, S. *et al.* (2021) 'Autophagy and the hallmarks of aging', *Ageing Research Reviews*. Elsevier, 72, p. 101468. doi: 10.1016/J.ARR.2021.101468.

Khaw, K. T. (1997) 'Healthy aging', *BMJ*. British Medical Journal Publishing Group,

315(7115), pp. 1090–1096. doi: 10.1136/BMJ.315.7115.1090.

Kida, Y. and Goligorsky, M. S. (2016) 'Sirtuins, Cell Senescence, and Vascular Aging', *The Canadian journal of cardiology*. Can J Cardiol, 32(5), pp. 634–641. doi: 10.1016/J.CJCA.2015.11.022.

Kim, S. Y. *et al.* (2014) 'Role of Bcl-xL/Beclin-1 in Interplay between Apoptosis and Autophagy in Oxaliplatin and Bortezomib-induced Cell Death', *Biochemical pharmacology*. NIH Public Access, 88(2), p. 178. doi: 10.1016/J.BCP.2014.01.027.

Kim, T. K. (2015) 'T test as a parametric statistic', *Korean Journal of Anesthesiology*. Korean Society of Anesthesiologists, 68(6), p. 540. doi: 10.4097/KJAE.2015.68.6.540.

Klionsky, D. J. *et al.* (2016) *Guidelines for the use and interpretation of assays for monitoring autophagy*. 3rd edn. Available at: https://www.tandfonline.com/loi/kaup20.

Kmetová, K. *et al.* (2022) 'Plasma DNA and deoxyribonuclease are associated with glucose metabolism in healthy mice', *PLOS ONE*. Edited by K.-H. Baek. Public Library of Science, 17(4), p. e0265099. doi: 10.1371/JOURNAL.PONE.0265099.

Koopman, G. *et al.* (1994) 'Annexin V for flow cytometric detection of phosphatidylserine expression on B cells undergoing apoptosis', *Blood*. American Society of Hematology, 84(5), pp. 1415–1420. doi: 10.1182/BLOOD.V84.5.1415.1415.

Krishnamurthy, J. and Sharpless, N. E. (2007) 'Stem Cells and the Rate of Living', *Cell Stem Cell*. Cell Press, 1(1), pp. 9–11. doi: 10.1016/J.STEM.2007.05.004.

Kumari, R. and Jat, P. (2021) 'Mechanisms of Cellular Senescence: Cell Cycle Arrest and Senescence Associated Secretory Phenotype', *Frontiers in Cell and Developmental Biology*. Frontiers Media S.A., 9, p. 485. doi: 10.3389/FCELL.2021.645593/BIBTEX.

Kuriyan, R. (2018) 'Body composition techniques', *The Indian Journal of Medical Research*. Wolters Kluwer -- Medknow Publications, 148(5), p. 648. doi:

10.4103/IJMR.IJMR_1777_18.

Kurrer, M. O. *et al.* (1997) 'β cell apoptosis in T cell-mediated autoimmune diabetes', *Proceedings of the National Academy of Sciences of the United States of America*. National Academy of Sciences, 94(1), pp. 213–218. doi: 10.1073/PNAS.94.1.213.

Kwak, D., Baumann, C. W. and Thompson, L. V (2019) 'Identifying Characteristics of Frailty in Female Mice Using a Phenotype Assessment Tool', *The Journals of Gerontology: Series A*, XX(Xx), pp. 1–7. doi: 10.1093/gerona/glz092.

Kyrana, E. *et al.* (2022) 'Sarcopenia and Fat Mass in Children With Chronic Liver Disease and Its Impact on Liver Transplantation', *JPGN Reports*, 3(2), p. e200. doi: 10.1097/PG9.0000000000000200.

Lam, Y. Y. and Ravussin, E. (2016) 'Analysis of energy metabolism in humans: A review of methodologies', *Molecular Metabolism*. Elsevier, 5(11), p. 1057. doi: 10.1016/J.MOLMET.2016.09.005.

Lara, B., Salinero, J. J. and Del Coso, J. (2014) 'The relationship between age and running time in elite marathoners is U-shaped', *Age*. Springer Science and Business Media Netherlands, 36(2), pp. 1003–1008. doi: 10.1007/S11357-013-9614-Z/FIGURES/2.

Layne, E. (1957) 'Spectrophotometric and turbidimetric methods for measuring proteins', *Methods in Enzymology*. Academic Press, 3(C), pp. 447–454. doi: 10.1016/S0076-6879(57)03413-8.

Lee, E. F. and Douglas Fairlie, W. (2019) 'The structural biology of Bcl-xL', *International Journal of Molecular Sciences*. MDPI AG, 20(9), p. 2234. doi: 10.3390/ijms20092234.

Leng, S., Chen, X. and Mao, G. (2014) 'Frailty syndrome: an overview', *Clinical Interventions in Aging*. Dove Medical Press Ltd., 9, p. 433. doi: 10.2147/cia.s45300.

Levine, J. A. (2022) 'Measurement of energy expenditure'. doi:

10.1079/PHN2005800.

Li, C. *et al.* (2006) 'Successful aging in Shanghai, China: Definition, distribution and related factors', *International Psychogeriatrics*, 18(3), pp. 551–563. doi: 10.1017/S1041610205002966.

Li, M. *et al.* (2020) 'Bcl-XL: A multifunctional anti-apoptotic protein', *Pharmacological Research*. Elsevier, 151(July 2019), p. 104547. doi: 10.1016/j.phrs.2019.104547.

Li, T. *et al.* (2016) 'Loss of p53-mediated cell-cycle arrest, senescence and apoptosis promotes genomic instability and premature aging', *Oncotarget*. Impact Journals LLC, 7(11), pp. 11838–11849. doi: 10.18632/oncotarget.7864.

Lian, J. *et al.* (2020) 'Immunosenescence: a key player in cancer development', *Journal of Hematology & Oncology 2020 13:1*. BioMed Central, 13(1), pp. 1–18. doi: 10.1186/S13045-020-00986-Z.

Liberale, L. *et al.* (2020) 'Ageing and longevity genes in cardiovascular diseases', *Basic & Clinical Pharmacology & Toxicology*. John Wiley & Sons, Ltd, 127(2), pp. 120–131. doi: 10.1111/BCPT.13426.

Lin, W. *et al.* (2015) 'Morphological change of CD4+ T cell during contact with DC modulates T cell activation by accumulation of F-actin in the immunology synapse', *BMC Immunology*. BioMed Central Ltd., 16(1), pp. 1–15. doi: 10.1186/S12865-015-0108-X/FIGURES/7.

Liu, H. *et al.* (2014) 'Clinically relevant Frailty Index for mice', *Journals of Gerontology - Series A Biological Sciences and Medical Sciences*. Oxford University Press, 69(12), pp. 1485–1491. doi: 10.1093/gerona/glt188.

Loo, L. S. W. *et al.* (2020) 'BCL-xL/BCL2L1 is a critical anti-apoptotic protein that promotes the survival of differentiating pancreatic cells from human pluripotent stem cells', *Cell Death & Disease 2020 11:5*. Nature Publishing Group, 11(5), pp. 1–18. doi: 10.1038/s41419-020-2589-7.

López-Otín, C. *et al.* (2013) 'The Hallmarks of Aging', *Cell*. Cell Press, 153(6), p.

1194. doi: 10.1016/J.CELL.2013.05.039.

Lowry, O. H. and Randall, R. J. (1951) 'Protein Measurement byt the Folin Reagent', *the Journal of Biological Chemistry*, 193(1), pp. 265–275. doi: 10.1016/0304-3894(92)87011-4.

Lu, B. *et al.* (2012) 'The relationship between apoptosis and aging', *Advances in Bioscience and Biotechnology*. Scientific Research Publishing, 3(6), pp. 705–711. doi: 10.4236/ABB.2012.326091.

Ludlow, A. T. and Roth, S. M. (2011) 'Physical activity and telomere biology: Exploring the link with aging-related disease prevention', *Journal of Aging Research*, 2011. doi: 10.4061/2011/790378.

Macian, F. (2019) 'Autophagy in T cell Function and Aging', *Frontiers in Cell and Developmental Biology*. Frontiers Media S.A., 7, p. 213. doi: 10.3389/FCELL.2019.00213/BIBTEX.

Maejima, Y. *et al.* (2013) 'Mst1 inhibits autophagy by promoting the interaction between Beclin1 and Bcl-2', *Nature Medicine 2013 19:11*. Nature Publishing Group, 19(11), pp. 1478–1488. doi: 10.1038/nm.3322.

Mahmood, T. and Yang, P. C. (2012) 'Western Blot: Technique, Theory, and Trouble Shooting', *North American Journal of Medical Sciences*. Wolters Kluwer -- Medknow Publications, 4(9), p. 429. doi: 10.4103/1947-2714.100998.

Maiuri, M.C., Criollo, A., *et al.* (2007) 'BH3-only proteins and BH3 mimetics induce autophagy by competitively disrupting the interaction between Beclin 1 and Bcl-2/Bcl-XL', *Autophagy*. Taylor & Francis, 3(4), pp. 374–376. doi: 10.4161/auto.4237.

Maiuri, M.C., LeToumelin, G., *et al.* (2007) 'Functional and physical interaction between Bcl-XL and a BH3-like domain in Beclin-1', *The EMBO Journal*. EMBO Press, 26(10), pp. 2527–2539. doi: 10.1038/sj.emboj.7601689.

Mammucari, C. and Rizzuto, R. (2010) 'Signaling pathways in mitochondrial dysfunction and aging', *Mechanisms of Ageing and Development*. Elsevier, 131(7–

8), pp. 536–543. doi: 10.1016/J.MAD.2010.07.003.

Manes, C. and Lai, N. C. (1995) 'Nonmitochondrial oxygen utilization by rabbit blastocysts and surface production of superoxide radicals', *Reproduction*. Bioscientifica Ltd, 104(1), pp. 69–75. doi: 10.1530/JRF.0.1040069.

Manini, T. M. (2010) 'Energy expenditure and aging', *Ageing Research Reviews*. Elsevier, 9(1), pp. 1–11. doi: 10.1016/J.ARR.2009.08.002.

Marcaletti, S., Thomas, C. and Feige, J. N. (2011) 'Exercise Performance Tests in Mice', *Current Protocols in Mouse Biology*, 1, pp. 141–154. doi: 10.1002/9780470942390.mo100160.

Martindale, J. L. and Holbrook, N. J. (2002) 'Cellular response to oxidative stress: Signaling for suicide and survival', *Journal of Cellular Physiology*. John Wiley & Sons, Ltd, 192(1), pp. 1–15. doi: 10.1002/JCP.10119.

Mas-Bargues, C. *et al.* (2020) 'Extracellular vesicles from healthy cells improves cell function and stemness in premature senescent stem cells by mir-302b and hif-1α activation', *Biomolecules*, 10(6), pp. 1–16. doi: 10.3390/biom10060957.

Mas-Bargues, C., Borrás, C. and Viña, J. (2021) 'Bcl-xL as a Modulator of Senescence and Aging', *International journal of molecular sciences*. Int J Mol Sci, 22(4), pp. 1–15. doi: 10.3390/IJMS22041527.

Matsumura, B. A. and Ambrose, A. F. (2006) 'Balance in the Elderly', *Clinics in Geriatric Medicine*, 22(2), pp. 395–412. doi: 10.1016/j.cger.2005.12.007.

Mayurasakorn, K. *et al.* (2018) 'Caloric restriction improves glucose homeostasis, yet increases cardiometabolic risk in caveolin-1-deficient mice', *Metabolism: clinical and experimental*. Metabolism, 83, pp. 92–101. doi: 10.1016/J.METABOL.2018.01.012.

Mazelin, L. *et al.* (2016) 'mTOR inactivation in myocardium from infant mice rapidly leads to dilated cardiomyopathy due to translation defects and p53/JNK-mediated apoptosis', *Journal of molecular and cellular cardiology*. J Mol Cell Cardiol, 97, pp. 213–225. doi: 10.1016/J.YJMCC.2016.04.011.

McClave, S. A. *et al.* (2003) 'Clinical use of the respiratory quotient obtained from indirect calorimetry', *JPEN. Journal of parenteral and enteral nutrition*. JPEN J Parenter Enteral Nutr, 27(1), pp. 21–26. doi: 10.1177/014860710302700121.

McDonald, S. D. *et al.* (2011) 'Adverse metabolic effects of a hypercaloric, high-fat diet in rodents precede observable changes in body weight', *Nutrition Research*. Elsevier, 31(9), pp. 707–714. doi: 10.1016/J.NUTRES.2011.08.009.

McKinley, M. J. *et al.* (2006) 'Differential effects of aging on fluid intake in response to hypovolemia, hypertonicity, and hormonal stimuli in Munich Wistar rats', *Proceedings of the National Academy of Sciences of the United States of America*, 103(9), pp. 3450–3455. doi: 10.1073/pnas.0511099103.

McKinnon, K. M. (2018) 'Flow Cytometry: An Overview', *Current Protocols in Immunology*. John Wiley & Sons, Ltd, 120(1), pp. 5.1.1-5.1.11. doi: 10.1002/CPIM.40.

McLeod, J. D. (2001) 'Apoptotic capability in ageing T cells', *Mechanisms of Ageing and Development*. Elsevier, 121(1–3), pp. 151–159. doi: 10.1016/S0047-6374(00)00206-2.

McMullan, R. C. *et al.* (2016) 'Long-term exercise in mice has sex-dependent benefits on body composition and metabolism during aging', *Physiological Reports*. John Wiley & Sons, Ltd, 4(21), p. e13011. doi: 10.14814/PHY2.13011.

McPhee, J. S. *et al.* (2016) 'Physical activity in older age: perspectives for healthy ageing and frailty', *Biogerontology*. Biogerontology, 17(3), pp. 567–580. doi: 10.1007/S10522-016-9641-0.

Meijer, E. P. *et al.* (2001) 'Physical inactivity as a determinant of the physical activity level in the elderly', *International Journal of Obesity*, 25(7), pp. 935–939. doi: 10.1038/sj.ijo.0801644.

Mejías-Peña, Y. *et al.* (2017) 'Impact of resistance training on the autophagy-inflammation-apoptosis crosstalk in elderly subjects', *Aging*. Impact Journals, LLC, 9(2), pp. 408–418. doi: 10.18632/aging.101167.

Meléndez, A. *et al.* (2003) 'Autophagy genes are essential for dauer development and life-span extension in C. elegans.', *Science (New York, N.Y.)*. American Association for the Advancement of Science, 301(5638), pp. 1387–91. doi: 10.1126/science.1087782.

Mendonca, G. V. *et al.* (2017) 'Impact of Aging on Endurance and Neuromuscular Physical Performance: The Role of Vascular Senescence', *Sports medicine (Auckland, N.Z.)*. Sports Med, 47(4), pp. 583–598. doi: 10.1007/S40279-016-0596-8.

Mesinovic, J. *et al.* (2019) 'Sarcopenia and type 2 diabetes mellitus: a bidirectional relationship', *Diabetes, Metabolic Syndrome and Obesity: Targets and Therapy*. Dove Press, 12, p. 1057. doi: 10.2147/DMSO.S186600.

Di Micco, R. *et al.* (no date) 'Cellular senescence in ageing: from mechanisms to therapeutic opportunities', 22(2). Available at: https://www.nature.com/articles/s41580-020-00314-w (Accessed: 22 April 2022).

Michel, J. P. and Sadana, R. (2017) '"Healthy Aging" Concepts and Measures', *Journal of the American Medical Directors Association*. Elsevier Inc., 18(6), pp. 460–464. doi: 10.1016/j.jamda.2017.03.008.

Michels, J. *et al.* (2013) 'Functions of BCL-XL at the interface between cell death and metabolism', *International Journal of Cell Biology*. doi: 10.1155/2013/705294.

Milanović, Z. *et al.* (2013) 'Age-related decrease in physical activity and functional fitness among elderly men and women', *Clinical Interventions in Aging*. Dove Press, 8, p. 549. doi: 10.2147/CIA.S44112.

Miller, R. A. *et al.* (2002) 'Big mice die young: early life body weight predicts longevity in genetically heterogeneous mice', *Aging Cell*. John Wiley & Sons, Ltd, 1(1), pp. 22–29. doi: 10.1046/J.1474-9728.2002.00006.X.

Miller, R. A., Chrisp, C. and Atchley, W. (2000) 'Differential longevity in mouse

stocks selected for early life growth trajectory', *The journals of gerontology. Series A, Biological sciences and medical sciences*. J Gerontol A Biol Sci Med Sci, 55(9). doi: 10.1093/GERONA/55.9.B455.

Mitnitski, A. B., Mogilner, A. J. and Rockwood, K. (2001) 'Accumulation of deficits as a proxy measure of aging.', *TheScientificWorldJournal*, 1, pp. 323–336. doi: 10.1100/tsw.2001.58.

Mohtashami, M., Zarin, P. and Zúñiga-Pflücker, J. C. (2016) 'Induction of T cell Development In Vitro by Delta-Like (Dll)-Expressing Stromal Cells', *Methods in molecular biology (Clifton, N.J.)*. Methods Mol Biol, 1323, pp. 159–167. doi: 10.1007/978-1-4939-2809-5_14.

Moretti, C. H. *et al.* (2020) 'Dietary nitrite extends lifespan and prevents age-related locomotor decline in the fruit fly', *Free Radical Biology and Medicine*. Pergamon, 160, pp. 860–870. doi: 10.1016/J.FREERADBIOMED.2020.09.018.

Moro, L. (2019) 'Mitochondrial Dysfunction in Aging and Cancer', *Journal of Clinical Medicine 2019, Vol. 8, Page 1983*. Multidisciplinary Digital Publishing Institute, 8(11), p. 1983. doi: 10.3390/JCM8111983.

Morris, J. L. *et al.* (2021) 'Bcl-2 Family of Proteins in the Control of Mitochondrial Calcium Signalling: An Old Chap with New Roles', *International Journal of Molecular Sciences 2021, Vol. 22, Page 3730*. Multidisciplinary Digital Publishing Institute, 22(7), p. 3730. doi: 10.3390/IJMS22073730.

Mousset, C. M. *et al.* (2019) 'Comprehensive Phenotyping of T cells Using Flow Cytometry', *Cytometry Part A*. John Wiley & Sons, Ltd, 95(6), pp. 647–654. doi: 10.1002/CYTO.A.23724.

Muchmore, S. W. *et al.* (1996) 'X-ray and NMR structure of human Bcl-xL, an inhibitor of programmed cell death'. Nature, p. Vol 281.

Muhammad, M. H. and Allam, M. M. (2018) 'Resveratrol and/or exercise training counteract aging-associated decline of physical endurance in aged mice; targeting mitochondrial biogenesis and function', *Journal of Physiological*

Sciences. Springer Tokyo, 68(5), pp. 681–688. doi: 10.1007/S12576-017-0582-4/TABLES/1.

Muller, B. *et al.* (2019) 'Application of extracellular flux analysis for determining mitochondrial function in mammalian oocytes and early embryos', *Scientific Reports 2019 9:1*. Nature Publishing Group, 9(1), pp. 1–14. doi: 10.1038/s41598-019-53066-9.

Muradian, K. and Schachtschabel, D. O. (2001) 'The role of apoptosis in aging and age-related disease: update', *Zeitschrift für Gerontologie und Geriatrie 2001 34:6*. Springer, 34(6), pp. 441–446. doi: 10.1007/S003910170015.

Nakagami, H. (2019) 'Cellular senescence and senescence-associated T cells as a potential therapeutic target', *Geriatrics & Gerontology International*. John Wiley & Sons, Ltd, 20(2), pp. 97–100. doi: 10.1111/GGI.13851.

Neideen, T. and Brasel, K. (2007) 'Understanding Statistical Tests'. doi: 10.1016/j.jsurg.2007.02.001.

Ni, L. *et al.* (2013) 'The protective effect of Bcl-xl overexpression against oxidative stress-induced vascular endothelial cell injury and the role of the Akt/eNOS pathway', *International Journal of Molecular Sciences*, 14(11), pp. 22149–22162. doi: 10.3390/ijms141122149.

Nicklas, B. J. and Brinkley, T. E. (2009) 'Exercise training as a treatment for chronic inflammation in the elderly', *Exercise and Sport Sciences Reviews*. NIH Public Access, 37(4), pp. 165–170. doi: 10.1097/JES.0b013e3181b7b3d9.

Nishida, K., Yamaguchi, O. and Otsu, K. (2008) 'Crosstalk between autophagy and apoptosis in heart disease', *Circulation Research*. Lippincott Williams & Wilkins, 103(4), pp. 343–351. doi: 10.1161/CIRCRESAHA.108.175448.

Nojima, I. *et al.* (2020) 'Dysfunction of CD8 + PD-1 + T cells in type 2 diabetes caused by the impairment of metabolism-immune axis', *Scientific Reports 2020 10:1*. Nature Publishing Group, 10(1), pp. 1–12. doi: 10.1038/s41598-020-71946-3.

O'Connor, T. P. *et al.* (2002) 'Prolonged longevity in naked mole-rats: age-related changes in metabolism, body composition and gastrointestinal function', *Comparative Biochemistry and Physiology Part A: Molecular & Integrative Physiology*. Pergamon, 133(3), pp. 835–842. doi: 10.1016/S1095-6433(02)00198-8.

Ohmura, K. *et al.* (2010) 'Natural killer T cells are involved in adipose tissues inflammation and glucose intolerance in diet-induced obese mice', *Arteriosclerosis, Thrombosis, and Vascular Biology*. Lippincott Williams and Wilkins, 30(2), pp. 193–199. doi: 10.1161/ATVBAHA.109.198614.

Okonkwo, O. C. *et al.* (2014) 'Physical activity attenuates age-related biomarker alterations in preclinical AD', *Neurology*. Wolters Kluwer Health, Inc. on behalf of the American Academy of Neurology, 83(19), pp. 1753–1760. doi: 10.1212/WNL.0000000000000964.

Ola, M. S., Nawaz, M. and Ahsan, H. (2011) 'Role of Bcl-2 family proteins and caspases in the regulation of apoptosis', *Molecular and Cellular Biochemistry*. Springer, 351(1–2), pp. 41–58. doi: 10.1007/S11010-010-0709-X/TABLES/2.

Olshansky, S. J. (2018) 'From Lifespan to Healthspan', *JAMA*. American Medical Association, 320(13), pp. 1323–1324. doi: 10.1001/JAMA.2018.12621.

Onder, G. *et al.* (2002) 'Change in Physical Performance Over Time in Older Women: The Women's Health and Aging Study', *Journal of Gerontology*, 57(5), pp. 289–293. Available at: https://academic.oup.com/biomedgerontology/article/57/5/M289/620579 (Accessed: 19 March 2022).

Orlikowsky, T. W. *et al.* (2005) 'Effect of Dexamethasone on B7 Regulation and T cell Activation in Neonates and Adults', *Pediatric Research 2005 57:5*. Nature Publishing Group, 57(5), pp. 656–661. doi: 10.1203/01.pdr.0000156211.48307.f5.

Ormerod, M. G. and Imrie, P. R. (1990) 'Flow Cytometry', *Animal Cell Culture*. New

Jersey: Humana Press, pp. 543–558. doi: 10.1385/0-89603-150-0:543.

Osborne, J. W. and Overbay, A. (2019) 'The power of outliers (and why researchers should ALWAYS check for them)', *Practical Assessment, Research, and Evaluation*, 9(1), p. 6. doi: https://doi.org/10.7275/qf69-7k43.

Paillasse, M. R. and de Medina, P. (2015) 'The NR4A nuclear receptors as potential targets for anti-aging interventions', *Medical Hypotheses*. Churchill Livingstone, 84(2), pp. 135–140. doi: 10.1016/J.MEHY.2014.12.003.

Palliyaguru, D. L. *et al.* (2019) 'Frailty index as a biomarker of lifespan and healthspan: Focus on pharmacological interventions', *Mechanisms of Ageing and Development*. Elsevier, 180, pp. 42–48. doi: 10.1016/J.MAD.2019.03.005.

Pan, J. *et al.* (2017) 'Inhibition of Bcl-2/xl With ABT-263 Selectively Kills Senescent Type II Pneumocytes and Reverses Persistent Pulmonary Fibrosis Induced by Ionizing Radiation in Mice', *International journal of radiation oncology, biology, physics*. NIH Public Access, 99(2), p. 353. doi: 10.1016/J.IJROBP.2017.02.216.

Pappas, L. E. and Nagy, T. R. (2019) 'The translation of age-related body composition findings from rodents to humans', *European journal of clinical nutrition*. NIH Public Access, 73(2), p. 172. doi: 10.1038/S41430-018-0324-6.

Park, H. A. *et al.* (2018) 'Nutritional regulators of Bcl-xL in the brain', *Molecules*. MDPI AG. doi: 10.3390/molecules23113019.

Park, S. J. *et al.* (2012) 'Resveratrol Ameliorates Aging-Related Metabolic Phenotypes by Inhibiting cAMP Phosphodiesterases', *Cell*. Cell Press, 148(3), pp. 421–433. doi: 10.1016/J.CELL.2012.01.017.

Pate, R. R. (1988) 'The evolving definition of physical fitness', *Quest*, 40(3), pp. 174–179. doi: 10.1080/00336297.1988.10483898.

Patel, H., Kerndt, C. C. and Bhardwaj, A. (2022) 'Physiology, Respiratory Quotient', *StatPearls*. StatPearls Publishing. Available at: https://www.ncbi.nlm.nih.gov/books/NBK531494/ (Accessed: 30 May 2022).

Pawelec, G. *et al.* (2002) 'T cells and aging', *Frontiers in bioscience : a journal and virtual library*, 7(June). doi: 10.2741/A831.

Pawlowska, E. *et al.* (2018) 'An Interplay between Senescence, Apoptosis and Autophagy in Glioblastoma Multiforme—Role in Pathogenesis and Therapeutic Perspective', *International Journal of Molecular Sciences*. Multidisciplinary Digital Publishing Institute (MDPI), 19(3). doi: 10.3390/IJMS19030889.

Pearl, R. (1928) 'The rate of living', *University of London Press LTD.*

Pedini, P. *et al.* (2019) 'Assessment of the Purity of Isolated Cd3+ T cell Populations by A New Molecular Biology Technology: Impact on the Quantification of Chimerism Monitoring After Hematopoietic Stem Cell Transplantation', *Biomedical Journal of Scientific & Technical Research*. Biomedical Research Network, LLC, 23(5). doi: 10.26717/BJSTR.2019.23.003972.

Pedrinelli, A., Garcez-Leme, L. E. and Nobre, R. do S. A. (2009) 'THE EFFECT OF PHYSICAL TRAINING ON THE LOCOMOTOR APPARATUS IN ELDERLY PEOPLE', *Revista Brasileira de Ortopedia*. Elsevier, 44(2), p. 96. doi: 10.1016/S2255-4971(15)30054-9.

Pedro, P. F., Tsakmaki, A. and Bewick, G. A. (2020) 'The Glucose Tolerance Test in Mice', *Methods in Molecular Biology*. Humana, New York, NY, 2128, pp. 207–216. doi: 10.1007/978-1-0716-0385-7_14.

Pellicciari, C., Bottone, M. and Biggiogera, M. (1997) 'Detection of apoptotic cells by annexin V labeling at electron microscopy - PubMed', *European journal of histochemistry*. Available at: https://pubmed.ncbi.nlm.nih.gov/9359032/ (Accessed: 19 April 2022).

Pence, B. D. and Yarbro, J. R. (2018) 'Aging impairs mitochondrial respiratory capacity in classical monocytes', *Experimental Gerontology*. Pergamon, 108, pp. 112–117. doi: 10.1016/J.EXGER.2018.04.008.

Peng, P. *et al.* (2021) 'Glucocorticoids induce femoral head necrosis in rats

through the ROS/JNK/c-Jun pathway', *FEBS Open Bio*. John Wiley & Sons, Ltd, 11(1), pp. 312–321. doi: 10.1002/2211-5463.13037.

Pera, A. *et al.* (2019) 'Immunosenescence and Its Hallmarks: How to Oppose Aging Strategically? A Review of Potential Options for Therapeutic Intervention', *Frontiers in Immunology | www.frontiersin.org*, 10, p. 2247. doi: 10.3389/fimmu.2019.02247.

Perandones, C. E. *et al.* (1993) 'Regulation of Apoptosis In Vitro in Mature Murine Spleen T cells'', *Printed in U.S.A. Journal of Immunology*, 151(7), p. 3521. Available at: http://www.jimmunol.org/ (Accessed: 8 June 2022).

Perillo, N. L. *et al.* (1989) 'Human T lymphocytes possess a limited in vitro life span', *Experimental Gerontology*. Pergamon, 24(3), pp. 177–187. doi: 10.1016/0531-5565(89)90009-0.

Perillo, N. L. *et al.* (1993) 'The in vitro senescence of human T lymphocytes: Failure to divide is not associated with a loss of cytolytic activity or memory T cell phenotype', *Mechanisms of Ageing and Development*. Elsevier, 67(1–2), pp. 173–185. doi: 10.1016/0047-6374(93)90121-7.

Pfeiffer, A. *et al.* (2017) 'Bcl-xLknockout attenuates mitochondrial respiration and causes oxidative stress that is compensated by pentose phosphate pathway activity', *Free Radical Biology and Medicine*, 112(March), pp. 350–359. doi: 10.1016/j.freeradbiomed.2017.08.007.

Picca, A. *et al.* (2019) 'Mitochondrial dysfunction and aging: Insights from the analysis of extracellular vesicles', *International Journal of Molecular Sciences*, 20(4), p. 2019. doi: 10.3390/ijms20040805.

Pietrobon, A. J., Teixeira, F. M. E. and Sato, M. N. (2020) 'Immunosenescence and Inflammaging: Risk Factors of Severe COVID-19 in Older People', *Frontiers in immunology*. Front Immunol, 11. doi: 10.3389/FIMMU.2020.579220.

Pillai, V. B., Sundaresan, N. R. and Gupta, M. P. (2014) 'Regulation of Akt signaling by sirtuins its implication in cardiac hypertrophy and aging', *Circulation*

Research. Lippincott Williams and Wilkins, 114(2), pp. 368–378. doi: 10.1161/CIRCRESAHA.113.300536.

Pimkina, J. *et al.* (2009) 'ARF induces autophagy by virtue of interaction with Bcl-xl', *Journal of Biological Chemistry*. Elsevier, 284(5), pp. 2803–2810. doi: 10.1074/JBC.M804705200/ATTACHMENT/1B951430-F934-4BD9-99D1-E36F721E972A/MMC1.PDF.

Poehlman, E. T. (1992) 'Critical Review Energy Expenditure Aging Humans1-2 and Requirements in', *World Health*, (August), pp. 2057–2065.

Pollack, M. and Leeuwenburgh, C. (2001) 'Apoptosis and Aging Role of the Mitochondria', *The Journals of Gerontology: Series A*. Oxford Academic, 56(11), pp. B475–B482. doi: 10.1093/GERONA/56.11.B475.

Polyak, K. *et al.* (1997) 'Less death in the dying', *Cell Death & Differentiation 1997 4:3*. Nature Publishing Group, 4(3), pp. 242–246. doi: 10.1038/sj.cdd.4400226.

Popgeorgiev, N., Jabbour, L. and Gillet, G. (2018) 'Subcellular Localization and Dynamics of the Bcl-2 Family of Proteins', *Frontiers in Cell and Developmental Biology*. Frontiers Media SA, 6(FEB). doi: 10.3389/FCELL.2018.00013.

Portegijs, E. *et al.* (2019) 'Assessing physical performance and physical activity in large population-based aging studies: Home-based assessments or visits to the research center?', *BMC Public Health*. BioMed Central Ltd., 19(1), pp. 1–16. doi: 10.1186/S12889-019-7869-8/TABLES/6.

Potestio, M. *et al.* (1998) 'Apoptosis and ageing', *Mechanisms of Ageing and Development*. Elsevier, 102(2–3), pp. 221–237. doi: 10.1016/S0047-6374(98)00020-7.

Powell, D. R. *et al.* (2022) 'Mice Lacking Gpr75 are Hypophagic and Thin', *Diabetes, Metabolic Syndrome and Obesity: Targets and Therapy*. Dove Press, 15, p. 45. doi: 10.2147/DMSO.S342799.

Pradas, I. *et al.* (2019) 'Exceptional human longevity is associated with a specific plasma phenotype of ether lipids', *Redox Biology*. Elsevier, 21, p. 101127. doi:

10.1016/J.REDOX.2019.101127.

Prata, L. G. P. L. *et al.* (2018) 'SenescenT cell clearance by the immune system: Emerging therapeutic opportunities', *Seminars in Immunology*. Academic Press, 40, p. 101275. doi: 10.1016/J.SMIM.2019.04.003.

Puleston, D. J. *et al.* (2014) 'Autophagy is a critical regulator of memory CD8+ T cell formation', *eLife*. eLife Sciences Publications Ltd, 3(November), pp. 1–21. doi: 10.7554/ELIFE.03706.

Ramanathan, A. and Schreiber, S. L. (2009) 'Direct control of mitochondrial function by mTOR', *Proceedings of the National Academy of Sciences of the United States of America*, 106(52), pp. 22229–22232. doi: 10.1073/PNAS.0912074106.

Raymond, M. and Rousset, F. (1995) 'An Exact Test for Population Differentiation', *Evolution*. JSTOR, 49(6), p. 1280. doi: 10.2307/2410454.

Rebelo-Marques, A. *et al.* (2018) 'Aging hallmarks: The benefits of physical exercise', *Frontiers in Endocrinology*. Frontiers Media S.A., 9(MAY), p. 258. doi: 10.3389/FENDO.2018.00258/BIBTEX.

Reula, A. *et al.* (2021) 'New Laboratory Protocol to Determine the Oxidative Stress Profile of Human Nasal Epithelial Cells Using Flow Cytometry', *J. Clin. Med*, 10, p. 1172. doi: 10.3390/jcm10061172.

Reynolds, T. H. *et al.* (2019) 'The impact of age and sex on body composition and glucose sensitivity in C57BL/6J mice', *Physiological Reports*. John Wiley & Sons, Ltd, 7(3), p. e13995. doi: 10.14814/PHY2.13995.

Richardson, A. and Holbrook, N. J. (1996) *Cellular Aging and Cell Death. Aging and the Cellular Rresponse to Stress: Reduction in the Heat Schok Response*. Wiley-Liss, Inc. Available at: https://books.google.es/books?hl=en&lr=&id=6Av-5HJUWrYC&oi=fnd&pg=PA67&dq=cellular+response+to+stress+with+aging&ots=9BHPh52T5H&sig=Pp9HPQ2OQJnCdOUd5bgNMg2Nnkw&redir_esc=y#v=onepage&q=cellular response to stress with aging&f=false (Accessed: 7 June 2022).

Ritz, P. and Berrut, G. (2005) 'Mitochondrial function, energy expenditure, aging and insulin resistance', *Diabetes and Metabolism*. Elsevier, 31(SPEC. ISS. 2), pp. 5S67-5S73. doi: 10.1016/s1262-3636(05)73654-5.

Rizzo, M. R. *et al.* (2005) 'Resting Metabolic Rate and Respiratory Quotient in Human Longevity'. doi: 10.1210/jc.2004-0390.

Robbins, P. D. *et al.* (2021) 'Senolytic Drugs: Reducing SenescenT cell Viability to Extend Healthspan', *https://doi.org/10.1146/annurev-pharmtox-050120-105018*. Annual Reviews , 61, pp. 779–803. doi: 10.1146/ANNUREV-PHARMTOX-050120-105018.

Roberts, S. B., Dallal, G. E. and Mayer, J. (2007) 'Energy requirements and aging', *Public Health Nutrition*. Cambridge University Press, 8(7a), pp. 1028–1036. doi: 10.1079/PHN2005794.

Roberts, S. B. and Rosenberg, I. (2006) 'Nutrition and aging: Changes in the regulation of energy metabolism with aging', *Physiological Reviews*. American Physiological Society, 86(2), pp. 651–667. doi: 10.1152/PHYSREV.00019.2005/ASSET/IMAGES/LARGE/Z9J0020624000005.JPEG.

Rockwood, K. and Mitnitski, A. (2007) 'Frailty in relation to the accumulation of deficits', *Journals of Gerontology - Series A Biological Sciences and Medical Sciences*. Gerontological Society of America, pp. 722–727. doi: 10.1093/gerona/62.7.722.

Rodrigues, L. P. *et al.* (2021) 'Hallmarks of aging and immunosenescence: Connecting the dots', *Cytokine & Growth Factor Reviews*. Pergamon, 59, pp. 9–21. doi: 10.1016/J.CYTOGFR.2021.01.006.

Ros, M. and Carrascosa, J. M. (2020) 'Current nutritional and pharmacological anti-aging interventions', *Biochimica et Biophysica Acta (BBA) - Molecular Basis of Disease*. Elsevier, 1866(3), p. 165612. doi: 10.1016/J.BBADIS.2019.165612.

Rostagno, A. *et al.* (2022) 'Sex Differences in Metabolic Indices and Chronic

Neuroinflammation in Response to Prolonged High-Fat Diet in ApoE4 Knock-In Mice', *International Journal of Molecular Sciences 2022, Vol. 23, Page 3921*. Multidisciplinary Digital Publishing Institute, 23(7), p. 3921. doi: 10.3390/IJMS23073921.

Rouabhi, Y., Guo, D. and Rahmouni, K. (2022) 'Investigation into the Role of the Skeletal Muscle BBSome in Insulin Sensitivity', *The FASEB journal*. The Federation of American Societies for Experimental Biology, 36. doi: 10.1096/FASEBJ.2022.36.S1.R4094.

Rowe, J. and Kahn, R. (1987) 'Human aging: usual and successful', *Science*. American Association for the Advancement of Science, 237(4811), pp. 143–149. doi: 10.1126/SCIENCE.3299702.

Rubinsztein, D. C., Mariño, G. and Kroemer, G. (2011) 'Autophagy and Aging', *Cell*. Cell Press, 146(5), pp. 682–695. doi: 10.1016/J.CELL.2011.07.030.

Rufini, A. *et al.* (2013) 'Senescence and aging: the critical roles of p53', *Oncogene*. Nature Publishing Group, 32(43), pp. 5129–5143. doi: 10.1038/onc.2012.640.

Runwal, G. *et al.* (2019) 'LC3-positive structures are prominent in autophagy-deficienT cells', *Scientific Reports*. Nature Publishing Group, 9(1). doi: 10.1038/S41598-019-46657-Z.

Russo, M., Bono, E. and Ghigo, A. (2021) 'The Interplay Between Autophagy and Senescence in Anthracycline Cardiotoxicity', *Current Heart Failure Reports*. Springer, 18(4), pp. 180–190. doi: 10.1007/S11897-021-00519-W/TABLES/1.

Russo, R. *et al.* (2018) 'Motor coordination and synaptic plasticity deficits are associated with increased cerebellar activity of NADPH oxidase, CAMKII, and PKC at preplaque stage in the TgCRND8 mouse model of Alzheimer's disease', *Neurobiology of Aging*. Elsevier, 68, pp. 123–133. doi: 10.1016/J.NEUROBIOLAGING.2018.02.025.

Ryan, A. S. (2012) 'Insulin Resistance with Aging', *Sports Medicine 2000 30:5*. Springer, 30(5), pp. 327–346. doi: 10.2165/00007256-200030050-00002.

Sallis, J. F. (1999) 'Age-related decline in physical activity: a synthesis of human and animal studies', *Med. Sci. Sports Exerc*, 32(9), pp. 1598–1600. Available at: http://www.msse.org (Accessed: 27 April 2022).

Salminen, A., Ojala, J. and Kaarniranta, K. (2010) 'Apoptosis and aging: increased resistance to apoptosis enhances the aging process', *Cellular and Molecular Life Sciences 2010 68:6*. Springer, 68(6), pp. 1021–1031. doi: 10.1007/S00018-010-0597-Y.

Sanz, C. *et al.* (2001) 'Antiapoptotic protein Bcl-xL is up-regulated during megakaryocytic differentiation of CD34+ progenitors but is absent from senescent megakaryocytes', *Experimental Hematology*. Elsevier, 29(6), pp. 728–735. doi: 10.1016/S0301-472X(01)00635-X.

Saraswat, K. *et al.* (2017) 'Novel strategies for anti-aging drug discovery', *http://dx.doi.org/10.1080/17460441.2017.1349750*. Taylor & Francis, 12(9), pp. 955–966. doi: 10.1080/17460441.2017.1349750.

Sasako, T. and Ueki, K. (2016) '[Insulin/IGF-1 signaling and aging]', *Nihon rinsho. Japanese journal of clinical medicine*. Nihon Rinsho, 74(9), pp. 1435–1440. Available at: https://pubmed.ncbi.nlm.nih.gov/30557473/ (Accessed: 30 May 2022).

Sastre, J. *et al.* (2002) *Mitochondrial Damage in Aging and Apoptosis*, *Ann. N.Y. Acad. Sci*.

Schlagheck, M. L. *et al.* (2020) 'Cellular immune response to acute exercise: Comparison of endurance and resistance exercise', *European Journal of Haematology*. John Wiley & Sons, Ltd, 105(1), pp. 75–84. doi: 10.1111/EJH.13412.

Schmidt, A. F. and Finan, C. (2018) 'Linear regression and the normality assumption', *Journal of Clinical Epidemiology*. Pergamon, 98, pp. 146–151. doi: 10.1016/J.JCLINEPI.2017.12.006.

Schmidt, S. *et al.* (2004) 'Glucocorticoid-induced apoptosis and glucocorticoid

resistance: molecular mechanisms and clinical relevance', *Cell Death & Differentiation 2004 11:1*. Nature Publishing Group, 11(1), pp. S45–S55. doi: 10.1038/sj.cdd.4401456.

Schultz, M. B. *et al.* (2020) 'Age and life expectancy clocks based on machine learning analysis of mouse frailty', *Nature Communications*. Nature Research, 11(1), pp. 1–12. doi: 10.1038/s41467-020-18446-0.

Seals, D. R., Justice, J. N. and Larocca, T. J. (2016) 'Physiological geroscience: targeting function to increase healthspan and achieve optimal longevity', *The Journal of Physiology*. John Wiley & Sons, Ltd, 594(8), pp. 2001–2024. doi: 10.1113/JPHYSIOL.2014.282665.

Sebastiani, P. and Perls, T. T. (2012) 'The genetics of extreme longevity: Lessons from the new england centenarian study', *Frontiers in Genetics*. Frontiers, 3(NOV), p. 277. doi: 10.3389/FGENE.2012.00277/BIBTEX.

Seidler, R. D. *et al.* (2010) 'Motor Control and Aging: Links to Age-Related Brain Structural, Functional, and Biochemical Effects', *Neuroscience and biobehavioral reviews*. NIH Public Access, 34(5), p. 721. doi: 10.1016/J.NEUBIOREV.2009.10.005.

Seldeen, K. L., Pang, M. and Troen, B. R. (2015) 'Mouse Models of Frailty: an Emerging Field', *Current Osteoporosis Reports*. Current Medicine Group LLC 1, pp. 280–286. doi: 10.1007/s11914-015-0283-y.

Sevilla, L. *et al.* (2001) 'Transcriptional regulation of the bcl-x gene encoding the anti-apoptotic Bcl-xL protein by Ets, Rel/NFκB, STAT and AP1 transcription factor families', *Histology and Histopathology*, 16(2), pp. 595–601.

Shen, C.-H. (2019) 'Quantification and Analysis of Proteins', *Diagnostic Molecular Biology*. Elsevier, pp. 187–214. doi: 10.1016/B978-0-12-802823-0.00008-0.

Shepherd, J. A. *et al.* (2017) 'Body Composition by DXA', *Bone*. NIH Public Access, 104, p. 101. doi: 10.1016/J.BONE.2017.06.010.

Sheth, K. A. *et al.* (2018) 'Muscle strength and size are associated with motor unit

connectivity in aged mice', *Neurobiology of Aging*. Elsevier, 67, pp. 128–136. doi: 10.1016/J.NEUROBIOLAGING.2018.03.016.

Shimizu, S. *et al.* (2004) 'Role of Bcl-2 family proteins in a non-apoptotic programmed cell death dependent on autophagy genes', *NATURE CELL BIOLOGY*, 6. doi: 10.1038/ncb1192.

Shimokata, H. *et al.* (1991) 'Age as Independent Determinant of Glucose Tolerance', *Diabetes*. American Diabetes Association, 40(1), pp. 44–51. doi: 10.2337/DIAB.40.1.44.

Shinkai, S. *et al.* (1995) 'Physical activity and immune senescence in men.', *Medicine and Science in Sports and Exercise*, 27(11), pp. 1516–1526. doi: 10.1249/00005768-199511000-00008.

Shoji, H. *et al.* (2016) 'Age-related changes in behavior in C57BL/6J mice from young adulthood to middle age', *Molecular Brain*. BioMed Central, 9(1), p. 11. doi: 10.1186/s13041-016-0191-9.

Siemasko, K. F. *et al.* (2008) 'In Vitro Expanded CD4+CD25+Foxp3+ Regulatory T cells Maintain a Normal Phenotype and Suppress Immune-Mediated Ocular Surface Inflammation', *Investigative Ophthalmology & Visual Science*. The Association for Research in Vision and Ophthalmology, 49(12), pp. 5434–5440. doi: 10.1167/IOVS.08-2075.

Simpson, R. J. (2010) 'Homogenization of Mammalian Tissue', *Cold Spring Harbor Protocols*. Cold Spring Harbor Laboratory Press, 2010(7), p. pdb.prot5455. doi: 10.1101/PDB.PROT5455.

Singh, R., Letai, A. and Sarosiek, K. (2019) 'Regulation of apoptosis in health and disease: the balancing act of BCL-2 family proteins', *Nature Reviews Molecular Cell Biology 2018 20:3*. Nature Publishing Group, 20(3), pp. 175–193. doi: 10.1038/s41580-018-0089-8.

Singhal, G. *et al.* (2020) 'Effects of aging on the motor, cognitive and affective behaviors, neuroimmune responses and hippocampal gene expression',

Behavioural Brain Research. Elsevier, 383, p. 112501. doi: 10.1016/J.BBR.2020.112501.

Smith, T. P., Kennedy, S. L. and Fleshner, M. (2004) 'Influence of age and physical activity on the primary in vivo antibody and T cell-mediated responses in men', *Journal of Applied Physiology*. American Physiological Society, 97(2), pp. 491–498. doi: 10.1152/JAPPLPHYSIOL.01404.2003/ASSET/IMAGES/LARGE/ZDG0080432380005.JPEG.

Al Snih, S. *et al.* (2002) *Handgrip Strength and Mortality in Older Mexican Americans*, *J Am Geriatr Soc*.

Song, Shuling *et al.* (2020) 'Targeting Senescent cells for a Healthier Aging: Challenges and Opportunities', *Advanced Science*. John Wiley & Sons, Ltd, 7(23), p. 2002611. doi: 10.1002/ADVS.202002611.

Soto-Gamez, A. and Demaria, M. (2017) 'Therapeutic interventions for aging: the case of cellular senescence', *Drug Discovery Today*. The Author(s), 22(5), pp. 786–795. doi: 10.1016/j.drudis.2017.01.004.

Speakman, J. R. *et al.* (2002) 'Living Fast, Dying When? The Link between Aging and Energetics', *The Journal of Nutrition*. Oxford Academic, 132(6), pp. 1583S-1597S. doi: 10.1093/JN/132.6.1583S.

Speakman, J. R., Acker, A. Van and Harper, E. J. (2003) 'Age-related changes in the metabolism and body composition of three dog breeds and their relationship to life expectancy', *Aging Cell*. John Wiley & Sons, Ltd, 2(5), pp. 265–275. doi: 10.1046/J.1474-9728.2003.00061.X.

St-Onge, M. P. and Gallagher, D. (2010) 'Body composition changes with aging: The cause or the result of alterations in metabolic rate and macronutrient oxidation?', 26(2). doi: 10.1016/J.NUT.2009.07.004.

Starkov, A. A. (2008) 'The role of mitochondria in reactive oxygen species metabolism and signaling', *Annals of the New York Academy of Sciences*. Blackwell

Publishing Inc., 1147, pp. 37–52. doi: 10.1196/ANNALS.1427.015.

Steen, B. (1988) 'Body Composition and Aging Bertil', *Nutrition Reviews*, 46(2). doi: 10.1111/j.1753-4887.1988.tb05386.x.

Stevens, M. and Oltean, S. (2019) 'Modulation of the Apoptosis Gene Bcl-x Function Through Alternative Splicing', *Frontiers in Genetics*. Frontiers Media SA, 10(September), pp. 1–9. doi: 10.3389/fgene.2019.00804.

Stevic, R. *et al.* (2007) 'Oral glucose tolerance test in the assessment of glucose-tolerance in the elderly people', *Age and Ageing*. Oxford Academic, 36(4), pp. 459–462. doi: 10.1093/AGEING/AFM076.

Stewart, K. J. (2006) 'Physical Activity and Aging', *Annals of the New York Academy of Sciences*. John Wiley & Sons, Ltd, pp. 193–206. doi: 10.1196/ANNALS.1323.029.

Strozyk, E. and Kulms, D. (2013) 'The Role of AKT/mTOR Pathway in Stress Response to UV-Irradiation: Implication in Skin Carcinogenesis by Regulation of Apoptosis, Autophagy and Senescence', *OPEN ACCESS Int. J. Mol. Sci*, 14, p. 14. doi: 10.3390/ijms140815260.

Strzyz, P. (2017) 'Pulling the apoptotic trigger for necrosis', *Nature Reviews Molecular Cell Biology*. Nature Publishing Group, 18(2), pp. 72–72. doi: 10.1038/nrm.2017.1.

Su, M., Mei, Y. and Sinha, S. (2013) 'Role of the crosstalk between autophagy and apoptosis in cancer', *Journal of Oncology*. doi: 10.1155/2013/102735.

Suh, Y. *et al.* (2002) 'Aging alters the apoptotic response to genotoxic stress', *Nature Medicine 2002 8:1*. Nature Publishing Group, 8(1), pp. 3–4. doi: 10.1038/nm0102-3.

Szoke, E. *et al.* (2008) 'Effect of Aging on Glucose HomeostasisAccelerated deterioration of β-cell function in individuals with impaired glucose tolerance', *Diabetes Care*. American Diabetes Association, 31(3), pp. 539–543. doi: 10.2337/DC07-1443.

Takeshita, H. *et al.* (2017) 'Modified forelimb grip strength test detects aging-associated physiological decline in skeletal muscle function in male mice', *Scientific Reports 2017 7:1*. Nature Publishing Group, 7(1), pp. 1–9. doi: 10.1038/srep42323.

Tamura, I. *et al.* (2021) 'Long-term melatonin treatment attenuates body weight gain with aging in female mice', *Journal of Endocrinology*. Bioscientifica Ltd, 251(1), pp. 15–25. doi: 10.1530/JOE-20-0462.

Tanaka, H. and Seals, D. R. (2008) 'Endurance exercise performance in Masters athletes: age-associated changes and underlying physiological mechanisms', *The Journal of Physiology*. John Wiley & Sons, Ltd, 586(1), pp. 55–63. doi: 10.1113/JPHYSIOL.2007.141879.

Tanaka, T. *et al.* (2021) 'Oestrogen receptor α in T cells controls the T cell immune profile and glucose metabolism in mouse models of gestational diabetes mellitus', *Diabetologia*. Springer Science and Business Media Deutschland GmbH, 64(7), pp. 1660–1673. doi: 10.1007/S00125-021-05447-X/FIGURES/7.

Tanida, I., Ueno, T. and Kominami, E. (2008) 'LC3 and Autophagy', *Methods in molecular biology (Clifton, N.J.)*. Methods Mol Biol, 445, pp. 77–88. doi: 10.1007/978-1-59745-157-4_4.

Tarantini, S. *et al.* (2021) 'Treatment with the BCL-2/BCL-xL inhibitor senolytic drug ABT263/Navitoclax improves functional hyperemia in aged mice', *GeroScience*. Springer Science and Business Media Deutschland GmbH, 43(5), pp. 2427–2440. doi: 10.1007/S11357-021-00440-Z/FIGURES/3.

Tarazona-Santabalbina, F. J. *et al.* (2016) 'A Multicomponent Exercise Intervention that Reverses Frailty and Improves Cognition, Emotion, and Social Networking in the Community-Dwelling Frail Elderly: A Randomized Clinical Trial', *Journal of the American Medical Directors Association*. Elsevier, 17(5), pp. 426–433. doi: 10.1016/J.JAMDA.2016.01.019.

Tasnim, H. *et al.* (2018) 'Quantitative measurement of naïve T cell association

with dendritic cells, FRCs, and blood vessels in lymph nodes', *Frontiers in Immunology*. Frontiers Media S.A., 9(JUL), p. 1571. doi: 10.3389/FIMMU.2018.01571/BIBTEX.

Teixeira, J. *et al.* (2021) 'Mitochondria-targeted phenolic antioxidants induce ROS-protective pathways in primary human skin fibroblasts', *Free Radical Biology and Medicine*. Pergamon, 163, pp. 314–324. doi: 10.1016/J.FREERADBIOMED.2020.12.023.

Thome, J. J. C. *et al.* (2016) 'Long-term maintenance of human naïve T cells through in situ homeostasis in lymphoid tissue sites', *Science Immunology*, 1(6), pp. 1–12. doi: 10.1126/sciimmunol.aah6506.

Thornton, J. S. *et al.* (2016) 'Physical activity prescription: A critical opportunity to address a modifiable risk factor for the prevention and management of chronic disease: A position statement by the Canadian Academy of Sport and Exercise Medicine', *British Journal of Sports Medicine*, 50(18), pp. 1109–1114. doi: 10.1136/bjsports-2016-096291.

Tian, S. *et al.* (2010) 'Beclin 1-independent autophagy induced by a Bcl-XL/Bcl-2 targeting compound, Z18', *https://doi.org/10.4161/auto.6.8.13336*. Taylor & Francis, 6(8), pp. 1032–1041. doi: 10.4161/AUTO.6.8.13336.

Tian, Y. *et al.* (2013) 'Adaptor complex AP2/PICALM, through interaction with LC3, targets Alzheimer's APP-CTF for terminal degradation via autophagy', *Proceedings of the National Academy of Sciences of the United States of America*. National Academy of Sciences, 110(42), pp. 17071–17076. doi: 10.1073/pnas.1315110110.

Tornero, D., Posadas, I. and Ceña, V. (2011) 'Bcl-xL Blocks a Mitochondrial Inner Membrane Channel and Prevents Ca2+ Overload-Mediated Cell Death', *PLOS ONE*. Public Library of Science, 6(6), p. e20423. doi: 10.1371/JOURNAL.PONE.0020423.

Tower, J. (2015) 'Programmed cell death in aging', *Ageing research reviews*. NIH

Public Access, 23(Pt A), p. 90. doi: 10.1016/J.ARR.2015.04.002.

Trisciuoglio, D. *et al.* (2017) 'BCL-XL overexpression promotes tumor progression-associated properties', *Cell Death & Disease 2017 8:12*. Nature Publishing Group, 8(12), pp. 1–15. doi: 10.1038/s41419-017-0055-y.

Troen, B. R. (2003) 'The Biology of aging', *Article in Mount Sinai Journal of Medicine A Journal of Translational and Personalized Medicine*. Available at: https://www.researchgate.net/publication/10961016 (Accessed: 18 May 2022).

Tsujimoto, Y. (1998) 'Role of Bcl-2 family proteins in apoptosis: apoptosomes or mitochondria?', *Genes to cells : devoted to molecular & cellular mechanisms*. Genes Cells, 3(11), pp. 697–707. doi: 10.1046/J.1365-2443.1998.00223.X.

Ueda, H. *et al.* (2000) 'Age-dependent changes in phenotypes and candidate gene analysis in a polygenic animal model of Type II diabetes mellitus; NSY mouse', *Diabetologia*. Diabetologia, 43(7), pp. 932–938. doi: 10.1007/S001250051472.

Vaanholt, L. M. *et al.* (2015) 'Metabolism and Aging: Effects of Cold Exposure on Metabolic Rate, Body Composition, and Longevity in Mice', *https://doi.org/10.1086/589727*. The University of Chicago Press, 82(4), pp. 314–324. doi: 10.1086/589727.

Vaughan, L., Zurlo, F. and Ravussin, E. (1991) 'Aging and energy expenditure', *The American Journal of Clinical Nutrition*. Oxford Academic, 53(4), pp. 821–825. doi: 10.1093/AJCN/53.4.821.

Veas-Perez de Tudela, M. *et al.* (2015) 'Regulation of Bcl-xL-ATP Synthase Interaction by Mitochondrial Cyclin B1-Cyclin-Dependent Kinase-1 Determines Neuronal Survival', *Journal of Neuroscience*, 35(25), pp. 9287–9301. doi: 10.1523/jneurosci.4712-14.2015.

Vella, A. T. *et al.* (1998) 'Cytokine-induced survival of activated T cells in vitro and in vivo', *Proceedings of the National Academy of Sciences of the United States of America*. National Academy of Sciences, 95(7), p. 3810. doi:

10.1073/PNAS.95.7.3810.

Vicencio, J. M. *et al.* (2008) 'Senescence, apoptosis or autophagy? When a damaged cell must decide its path - A mini-review', *Gerontology*. Karger Publishers, 54(2), pp. 92–99. doi: 10.1159/000129697.

Viña, J. *et al.* (2013) 'The free radical theory of aging revisited: the cell signaling disruption theory of aging.', *Antioxidants & redox signaling*. Mary Ann Liebert, Inc., 19(8), pp. 779–87. doi: 10.1089/ars.2012.5111.

Viña, J., Tarazona-Santabalbina, F. J., *et al.* (2016) 'Biology of frailty: Modulation of ageing genes and its importance to prevent age-associated loss of function', *Molecular Aspects of Medicine*. Elsevier Ltd, 50, pp. 88–108. doi: 10.1016/j.mam.2016.04.005.

Viña, J., Rodriguez-Mañas, L., *et al.* (2016) 'Exercise: The lifelong supplement for healthy ageing and slowing down the onset of frailty', *Journal of Physiology*. Wiley-Blackwell, 594(8), pp. 1989–1999. doi: 10.1113/JP270536.

Viña, J., Borrás, C. and Miquel, J. (2007) 'Theories of ageing', *IUBMB Life*. Wiley-Blackwell, 59(4), pp. 249–254. doi: 10.1080/15216540601178067.

Vitale, G. *et al.* (2017) 'GH/IGF-I/insulin system in centenarians', *Mechanisms of Ageing and Development*. Elsevier, 165, pp. 107–114. doi: 10.1016/J.MAD.2016.12.001.

Walford, R. L. (1964) 'the Immunologic Theory of Aging', *Immunological Reviews*, 2(1), pp. 171–171. doi: 10.1111/j.1600-065X.1969.tb00210.x.

Walston, J. D. (2012) 'Sarcopenia in older adults', *Current opinion in rheumatology*. NIH Public Access, 24(6), p. 623. doi: 10.1097/BOR.0B013E328358D59B.

Warburton, D. E. R., Nicol, C. W. and Bredin, S. S. D. (2006) 'Health benefits of physical activity: The evidence', *CMAJ*, 174(6), pp. 801–809. doi: 10.1503/CMAJ.051351.

Warnes, G. (2014) 'Measurement of autophagy by flow cytometry', *Current*

protocols in cytometry. Curr Protoc Cytom, 68(SUPPL.68). doi: 10.1002/0471142956.CY0945S68.

Warren, C. F. A., Wong-Brown, M. W. and Bowden, N. A. (2019) 'BCL-2 family isoforms in apoptosis and cancer', *Cell Death & Disease 2019 10:3*. Nature Publishing Group, 10(3), pp. 1–12. doi: 10.1038/s41419-019-1407-6.

Waterborg, J. H. and Matthews, H. R. (1994) 'The Lowry Method for Protein Quantitation', *Methods in molecular biology (Clifton, N.J.)*. Humana Press, 32, pp. 1–4. doi: 10.1385/0-89603-268-X:1.

Weiss, R. *et al.* (2021) 'Comparison of Three CD3-Specific Separation Methods Leading to Labeled and Label-Free T cells', *Cells 2021, Vol. 10, Page 2824*. Multidisciplinary Digital Publishing Institute, 10(11), p. 2824. doi: 10.3390/CELLS10112824.

Westerterp, K. R. and Meijer, E. P. (2001) *Physical Activity and Parameters of Aging: A Physiological Perspective*, *Special Issue II*. Available at: https://academic.oup.com/biomedgerontology/article/56/suppl_2/7/581098.

Whitehead, J. C. *et al.* (2014) 'A clinical frailty index in aging mice: Comparisons with frailty index data in humans', *Journals of Gerontology - Series A Biological Sciences and Medical Sciences*. Oxford University Press, 69(6), pp. 621–632. doi: 10.1093/gerona/glt136.

Wickramasinghe, K. *et al.* (2020) 'From lifespan to healthspan: the role of nutrition in healthy ageing', *Journal of nutritional science*. J Nutr Sci, 9. doi: 10.1017/JNS.2020.26.

Wilcox, R. R. (2016) 'Adjusting for Unequal Variances When Comparing Means in One-Way and Two-Way Fixed Effects ANOVA Models':, *http://dx.doi.org/10.3102/10769986014003269*. SAGE PublicationsSage CA: Los Angeles, CA, 14(3), pp. 269–278. doi: 10.3102/10769986014003269.

Williams, A. *et al.* (2016) 'The non-apoptotic action of Bcl-xL: regulating Ca2+ signaling and bioenergetics at the ER-mitochondrion interface', *Journal of*

Bioenergetics and Biomembranes. Journal of Bioenergetics and Biomembranes, 48(3), pp. 211–225. doi: 10.1007/s10863-016-9664-x.

Wlodkowic, D., Skommer, J. and Darzynkiewicz, Z. (2009) 'Flow Cytometry-Based Apoptosis Detection', *Methods in molecular biology (Clifton, N.J.)*. Humana Press, Totowa, NJ, 559, pp. 19–32. doi: 10.1007/978-1-60327-017-5_2.

Wong, S. Q. *et al.* (2020) 'Autophagy in aging and longevity', *Human Genetics*. Springer, 139(3), pp. 277–290. doi: 10.1007/S00439-019-02031-7/FIGURES/1.

Xie, W. qing *et al.* (2021) 'Mouse models of sarcopenia: classification and evaluation', *Journal of Cachexia, Sarcopenia and Muscle*. Springer Nature, 12(3), pp. 538–554. doi: 10.1002/JCSM.12709.

Xing, K. *et al.* (2015) 'Dexamethasone enhances programmed cell death 1 (PD-1) expression during T cell activation: An insight into the optimum application of glucocorticoids in anti-cancer therapy', *BMC Immunology*. BioMed Central Ltd., 16(1), pp. 1–9. doi: 10.1186/S12865-015-0103-2/FIGURES/6.

Xue, Q. L. (2011) 'The Frailty Syndrome: Definition and Natural History', *Clinics in geriatric medicine*. NIH Public Access, 27(1), p. 1. doi: 10.1016/J.CGER.2010.08.009.

Yaffe, K. *et al.* (2001) 'A Prospective Study of Physical Activity and Cognitive Decline in Elderly Women: Women Who Walk', *Archives of Internal Medicine*. American Medical Association, 161(14), pp. 1703–1708. doi: 10.1001/ARCHINTE.161.14.1703.

Yanai, S. and Endo, S. (2021) 'Functional Aging in Male C57BL/6J Mice Across the Life-Span: A Systematic Behavioral Analysis of Motor, Emotional, and Memory Function to Define an Aging Phenotype', *Frontiers in Aging Neuroscience*. Frontiers Media S.A., 13, p. 457. doi: 10.3389/FNAGI.2021.697621/BIBTEX.

Yang, K., Tu, J. and Chen, T. (2019) 'Homoscedasticity: an overlooked critical assumption for linear regression', *General Psychiatry*. Shanghai Mental Health Center, 32(5), p. 100148. doi: 10.1136/GPSYCH-2019-100148.

Yeh, C.-K. (2016) 'Cellular senescence and aging', *Oral Diseases*. Wiley/Blackwell (10.1111), 22(7), pp. 587–590. doi: 10.1111/odi.12483.

Yépez, V. A. *et al.* (2018) 'OCR-Stats: Robust estimation and statistical testing of mitochondrial respiration activities using Seahorse XF Analyzer', *PLOS ONE*. Edited by J. Zhang. Public Library of Science, 13(7), p. e0199938. doi: 10.1371/journal.pone.0199938.

Yosef, R. *et al.* (2016) 'Directed elimination of senescent cells by inhibition of BCL-W and BCL-XL', *Nature Communications*. Nature Publishing Group, 7(1), p. 11190. doi: 10.1038/ncomms11190.

Zamboni, M. *et al.* (2005) 'Health consequences of obesity in the elderly: a review of four unresolved questions', *International Journal of Obesity 2005 29:9*. Nature Publishing Group, 29(9), pp. 1011–1029. doi: 10.1038/sj.ijo.0803005.

von Zglinicki, T. *et al.* (2016) 'Frailty in mouse ageing: A conceptual approach', *Mechanisms of Ageing and Development*. Elsevier Ireland Ltd, 160, pp. 34–40. doi: 10.1016/j.mad.2016.07.004.

Zhang, H. *et al.* (2020) 'Reduction of elevated proton leak rejuvenates mitochondria in the aged cardiomyocyte', *eLife*. eLife Sciences Publications Ltd, 9, pp. 1–18. doi: 10.7554/ELIFE.60827.

Zhang, H., Weyand, C. M. and Goronzy, J. J. (2021) 'Hallmarks of the aging T cell system', *The FEBS Journal*. John Wiley & Sons, Ltd. doi: 10.1111/FEBS.15770.

Zhang, Y. and Herman, B. (2002) 'Ageing and apoptosis', *Mechanisms of Ageing and Development*. Elsevier, 123(4), pp. 245–260. doi: 10.1016/S0047-6374(01)00349-9.

Zhou, F., Yang, Y. and Xing, D. (2011) 'Bcl-2 and Bcl-xL play important roles in the crosstalk between autophagy and apoptosis', *FEBS Journal*. Wiley/Blackwell (10.1111), 278(3), pp. 403–413. doi: 10.1111/j.1742-4658.2010.07965.x.

Zhou, Q. *et al.* (2018) 'Apelin/APJ system: A novel promising target for anti-aging intervention', *Clinica Chimica Acta*. Elsevier, 487, pp. 233–240. doi:

10.1016/J.CCA.2018.10.011.

Zhou, Y. P. *et al.* (2000) 'Overexpression of Bcl-X(L) in β-cells prevents cell death but impairs mitochondrial signal for insulin secretion', *American Journal of Physiology - Endocrinology and Metabolism*. American Physiological Society, 278(2 41-2). doi: 10.1152/AJPENDO.2000.278.2.E340/ASSET/IMAGES/LARGE/AEND10208010X.JPEG.

Zhu, Y. *et al.* (2015) 'The Achilles' heel of senescenT cells: from transcriptome to senolytic drugs', *Aging cell*. Wiley-Blackwell, 14(4), pp. 644–658. doi: 10.1111/acel.12344.

Zhu, Y. *et al.* (2016) 'Identification of a novel senolytic agent, navitoclax, targeting the Bcl-2 family of anti-apoptotic factors', *Aging Cell*. John Wiley & Sons, Ltd (10.1111), 15(3), pp. 428–435. doi: 10.1111/acel.12445.

Zhu, Y. *et al.* (2017) 'New agents that target senescent cells the flavone,fisetin, and the BCL-X-L inhibitors', *Aging*. Impact Journals, LLC, 9(3), pp. 955–963. Available at: http://www.ncbi.nlm.nih.gov/pubmed/28273655 (Accessed: 15 February 2019).

Zorova, L. D. *et al.* (2018) 'Mitochondrial membrane potential', *Analytical Biochemistry*. Academic Press, 552, pp. 50–59. doi: 10.1016/J.AB.2017.07.009.

Zupin, L. *et al.* (2021) 'In vitro effects of photobiomodulation therapy on 50B11 sensory neurons: evaluation of cell metabolism, oxidative stress, mitochondrial membrane potential (MMP), and capsaicin-induced calcium flow', *Journal of Biophotonics*. John Wiley & Sons, Ltd, 14(2), p. e202000347. doi: 10.1002/JBIO.202000347.

ANNEXES

1. ANNEX I: ETHICAL COMMITTEES

1.1. Authorization for the creation and maintenance of the colony

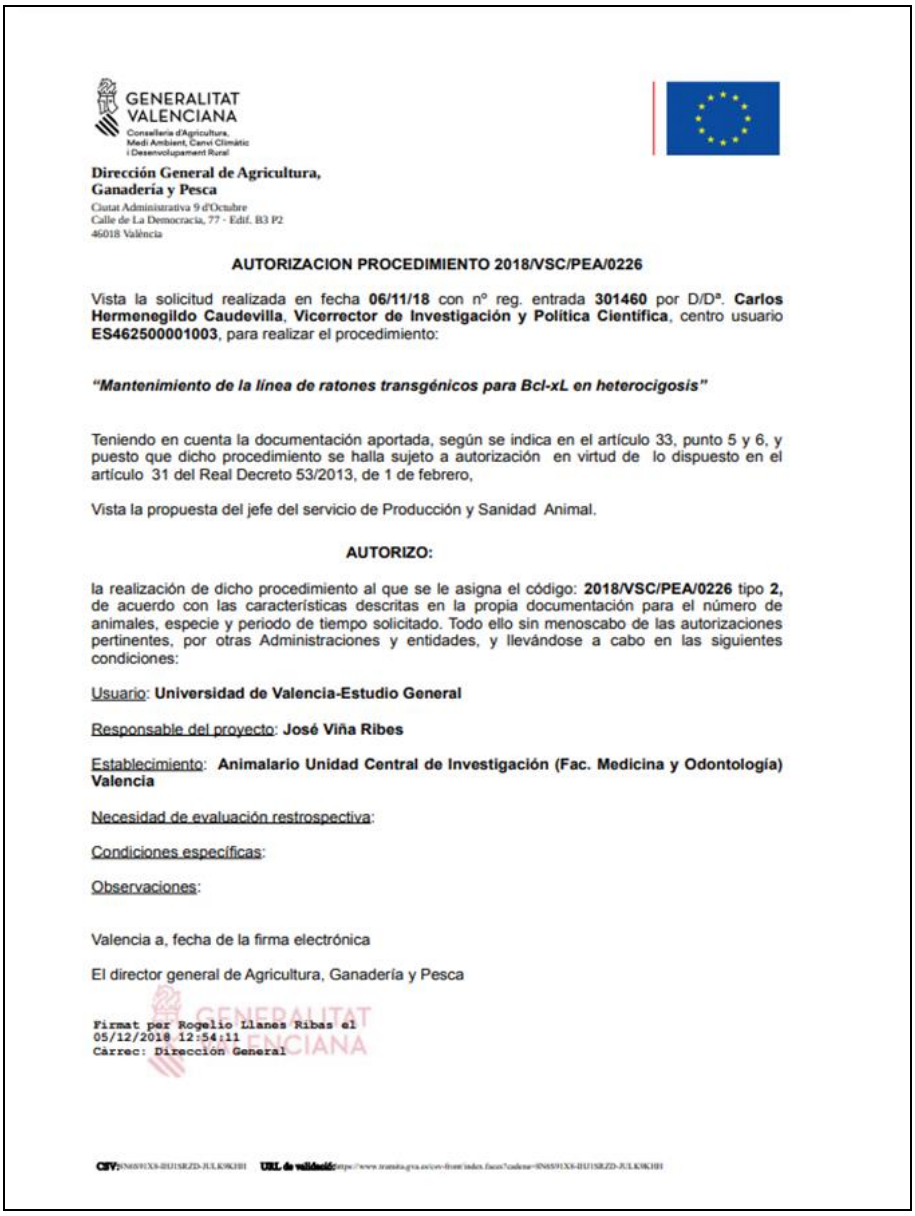

GENERALITAT VALENCIANA
Conselleria d'Agricultura, Medi Ambient, Canvi Climàtic i Desenvolupament Rural

Dirección General de Agricultura, Ganadería y Pesca
Ciutat Administrativa 9 d'Octubre
Calle de La Democracia, 77 - Edif. B3 P2
46018 València

AUTORIZACION PROCEDIMIENTO 2018/VSC/PEA/0226

Vista la solicitud realizada en fecha **06/11/18** con nº reg. entrada **301460** por D/Dª. **Carlos Hermenegildo Caudevilla**, **Vicerrector de Investigación y Política Científica**, centro usuario **ES462500001003**, para realizar el procedimiento:

"Mantenimiento de la línea de ratones transgénicos para Bcl-xL en heterocigosis"

Teniendo en cuenta la documentación aportada, según se indica en el artículo 33, punto 5 y 6, y puesto que dicho procedimiento se halla sujeto a autorización en virtud de lo dispuesto en el artículo 31 del Real Decreto 53/2013, de 1 de febrero,

Vista la propuesta del jefe del servicio de Producción y Sanidad Animal.

AUTORIZO:

la realización de dicho procedimiento al que se le asigna el código: **2018/VSC/PEA/0226** tipo **2,** de acuerdo con las características descritas en la propia documentación para el número de animales, especie y periodo de tiempo solicitado. Todo ello sin menoscabo de las autorizaciones pertinentes, por otras Administraciones y entidades, y llevándose a cabo en las siguientes condiciones:

Usuario: **Universidad de Valencia-Estudio General**

Responsable del proyecto: **José Viña Ribes**

Establecimiento: **Animalario Unidad Central de Investigación (Fac. Medicina y Odontología) Valencia**

Necesidad de evaluación restrospectiva:

Condiciones específicas:

Observaciones:

Valencia a, fecha de la firma electrónica

El director general de Agricultura, Ganadería y Pesca

Firmat per Rogelio Llanes Ribas el 05/12/2018 12:54:11
Càrrec: Dirección General

CSV: [illegible] URL de validació: [illegible]

1.2. Authorization for animal experimentation

GENERALITAT VALENCIANA
Conselleria d'Agricultura, Medi Ambient, Canvi Climàtic i Desenvolupament Rural

Dirección General de Agricultura, Ganadería y Pesca
Ciutat Administrativa 9 d'Octubre
Calle de La Democracia, 77 · Edif. B3 P2
46018 València

AUTORIZACION PROCEDIMIENTO 2018/VSC/PEA/0220

Vista la solicitud realizada en fecha **18/10/18** con nº reg. entrada **276273** por D/Dª. **Carlos Hermenegildo Caudevilla**, **Vicerrector de Investigación y Política Científica**, centro usuario **ES462500001003**, para realizar el procedimiento:

"Estudio del papel de Bcl-xL en el envejecimiento saludable y en la prevención de la fragilidad."

Teniendo en cuenta la documentación aportada, según se indica en el artículo 33, punto 5 y 6, y puesto que dicho procedimiento se halla sujeto a autorización en virtud de lo dispuesto en el artículo 31 del Real Decreto 53/2013, de 1 de febrero,

Vista la propuesta del jefe del servicio de Producción y Sanidad Animal.

AUTORIZO:

la realización de dicho procedimiento al que se le asigna el código: **2018/VSC/PEA/0220** tipo **2,** de acuerdo con las características descritas en la propia documentación para el número de animales, especie y periodo de tiempo solicitado. Todo ello sin menoscabo de las autorizaciones pertinentes, por otras Administraciones y entidades, y llevándose a cabo en las siguientes condiciones:

Usuario: **Universidad de Valencia-Estudio General**

Responsable del proyecto: **José Viña Ribes**

Establecimiento: **Animalario Unidad Central de Investigación (Fac. Medicina y Odontología) Valencia**

Necesidad de evaluación restrospectiva:

Condiciones específicas:

Observaciones:

Valencia a, fecha de la firma electrónica

El director general de Agricultura, Ganadería y Pesca

Firmado por Rogelio Llanes Ribas el 24/10/2018 20:52:12
Cargo: Dirección General

GENERALITAT VALENCIANA

CSV:8R271P96-BQM9SCAS-B8TH8HV6 URL de validación: https://www.tramita.gva.es/csv-front/index.faces?codesu=8R271P96-BQM9SCAS-B8TH8HV6

2. ANNEX II: SUPPLEMENTARY DATA

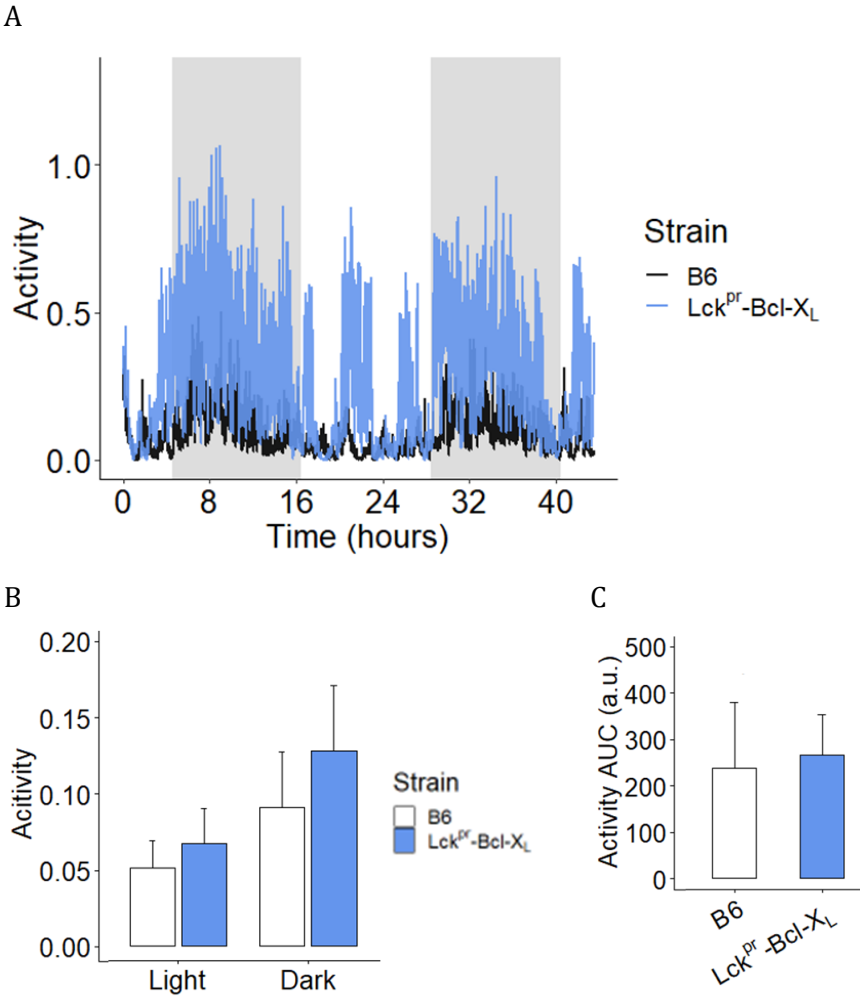

Supplementary figure 1. Spontaneous activity in 17-20 mo B6 and Lck^{pr}-Bcl-X$_L$ mice. Activity measured as horizontal activity over 42h (A), average data from the light and dark cycles (B), and area under curve (AUC) analysis (C) in 17-20 mo B6 (n=7) and Lckpr-Bcl-XL mice (n=7). Data are presented as mean ± sd, and p values were calculated with the T-test.

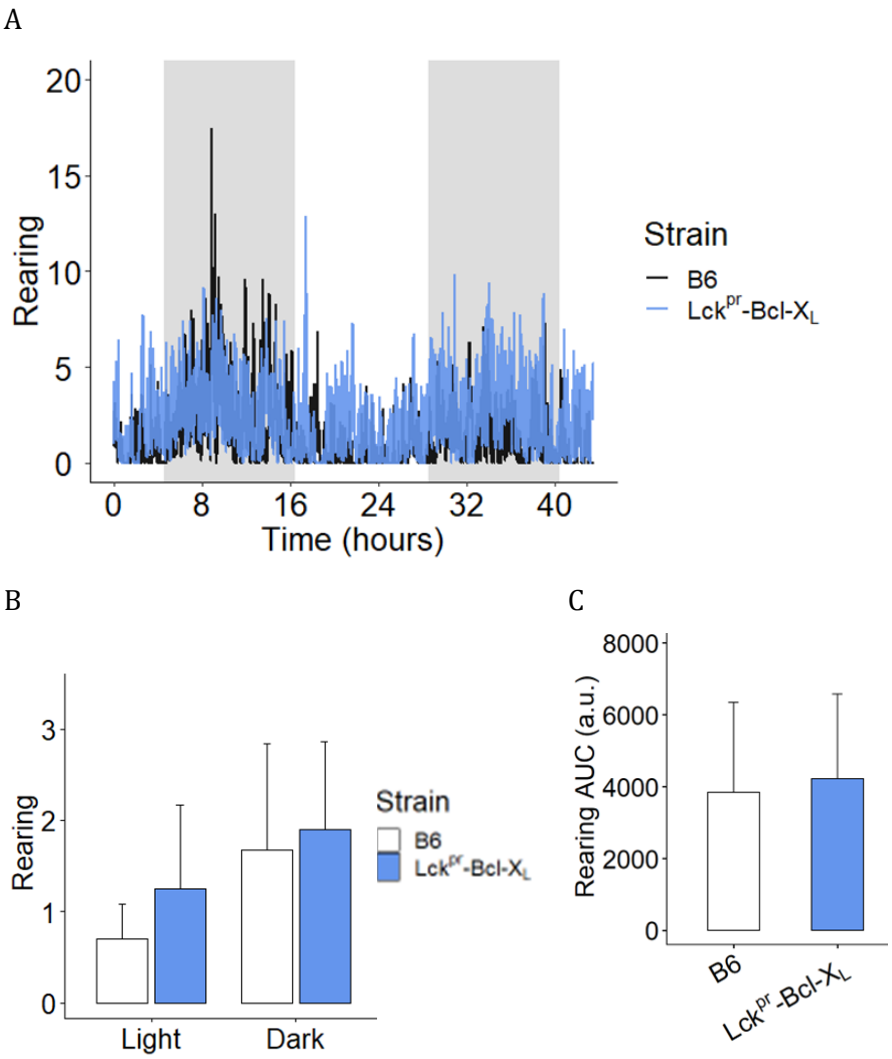

Supplementary figure 2. Rearing events in 17-20 mo B6 and Lckpr-Bcl-XL mice. Rearing measured as vertical activity over 42h (A), average data from the light and dark cycles (B) and area under curve (AUC) analysis (C) in 17-20 mo B6 (n=7) and Lck^{pr}-$Bcl\text{-}X_L$ mice (n=7). Data are presented as mean ± sd, and p values were calculated with the T-test.

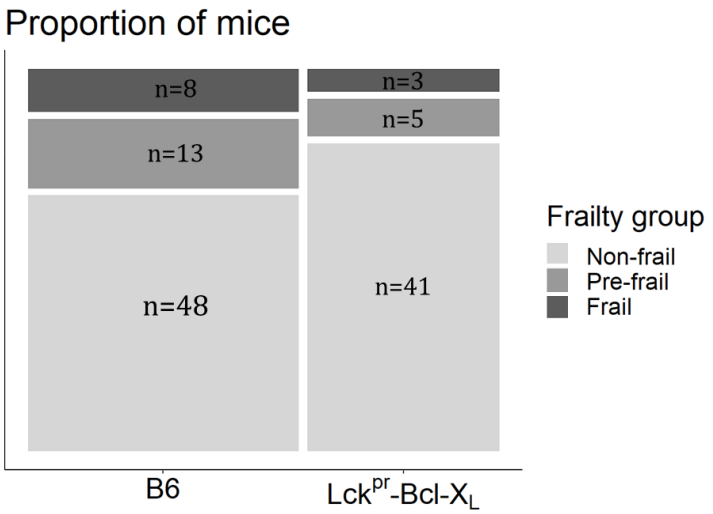

Supplementary figure 3. Prevalence of frailty in 17-20 mo B6 and Lck^{pr}-Bcl-X$_L$ mice.

The proportion of 17-20 mo B6 (n=69) and Lck^{pr}-Bcl-X$_L$ (n=41) mice for each frail group (non-frail, pre-frail, and frail). The number of mice is indicated for each group. Data are presented as mosaic plots and a p-value = 0.2425 was calculated with Fisher's exact test.

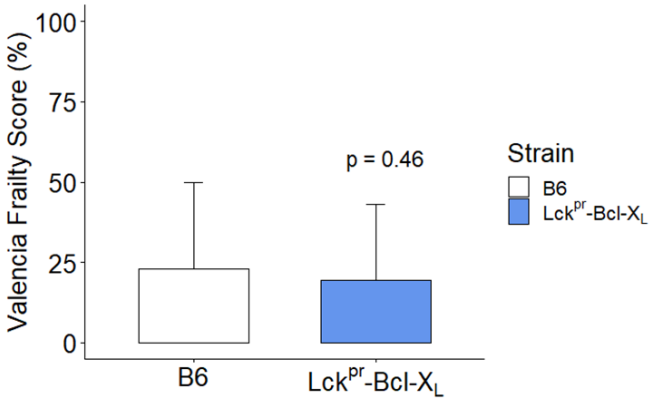

Supplementary figure 4. Valencia Frailty Score in 17-20 mo B6 and Lck^{pr}-Bcl-X$_L$ mice.

Valencia frailty score in 17-20 mo B6 (n=69) and Lck^{pr}-Bcl-X$_L$ (n=41). Data are presented as mean ± sd, and the p-value was calculated with the unpaired two-samples T-test.

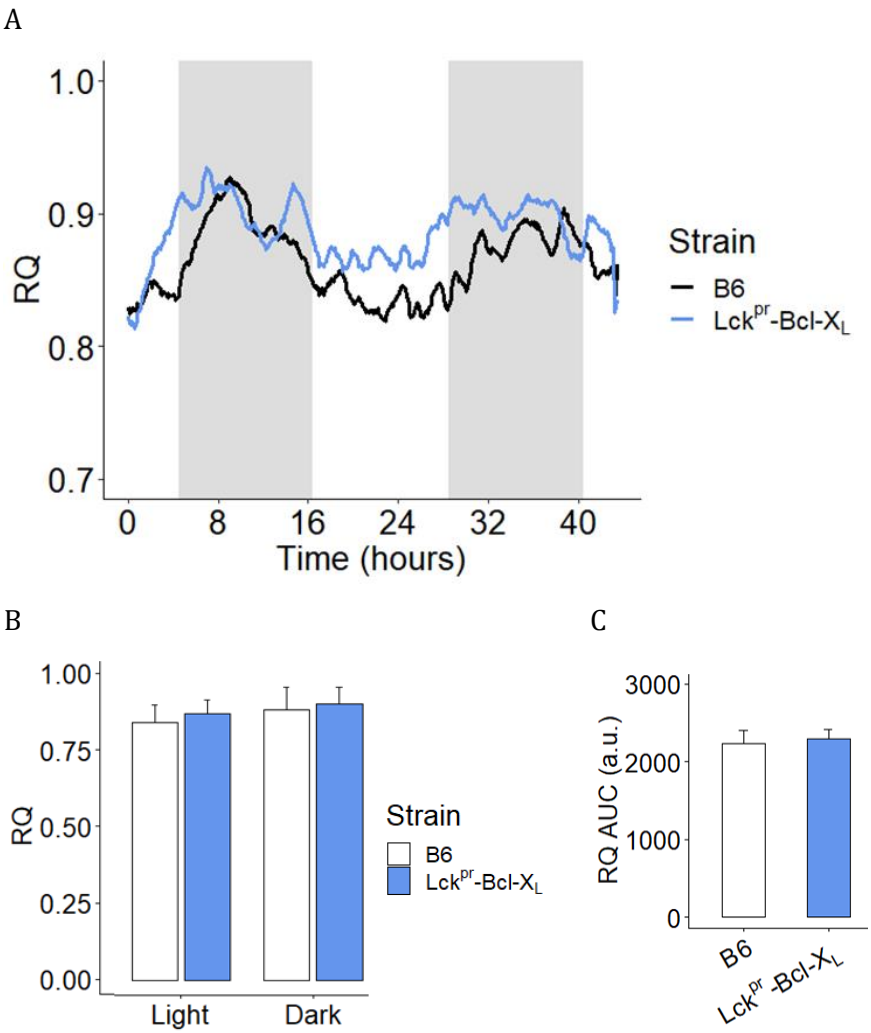

Supplementary figure 5. Respiratory quotient in 17-20 mo B6 and Lck^{pr}-Bcl-X$_L$ mice.

Respiratory quotient (RQ) over 42h (A), average data from the light and dark cycles (B), and area under curve (AUC) analysis (C) in 17-20 mo B6 (n=7) and Lck^{pr}-Bcl-X$_L$ (n=7) mice.

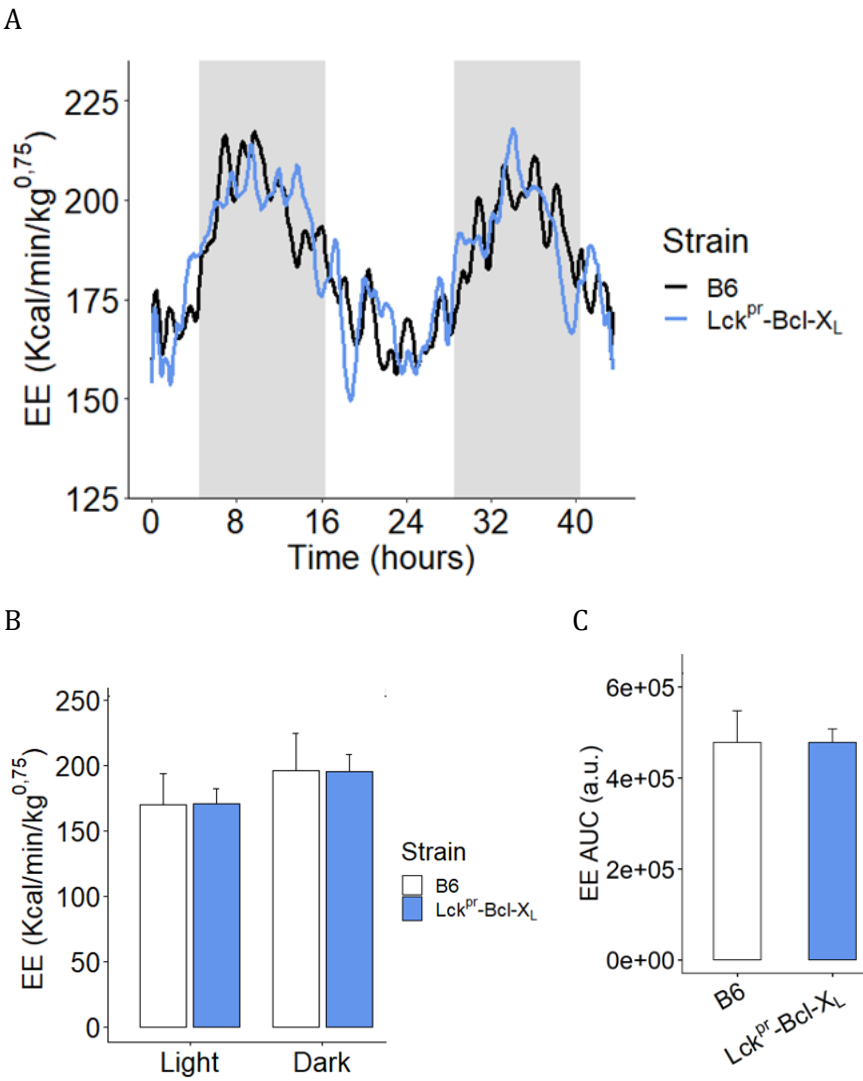

Supplementary figure 6. Energy expenditure in 17-20 mo B6 and Lck^{pr}-Bcl-X$_L$ mice.

Energy expenditure (EE) over 42h (A), average data from the light and dark cycles (B), and area under curve (AUC) analysis (C) in 17-20 mo B6 (n=6) and Lck^{pr}-Bcl-X$_L$ (n=9) mice.

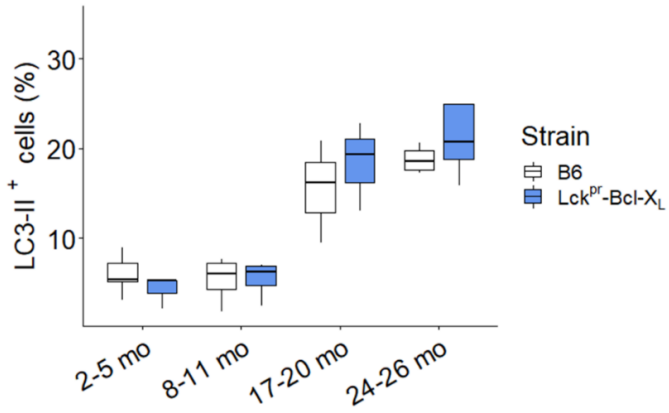

Supplementary figure 7. Autophagy in T cells from B6 and Lck^{pr}-Bcl-X$_L$ mice.
Percentage of LC3-II positive T cells from 2-5 (n=10), 8-11 (n=10), 17-20 (n=6) and 24-26 mo (n=8) B6 and Lck^{pr}-Bcl-X$_L$ mice after 4h of culture under starving conditions. Data are represented as box plots and p values were calculated with the two-sample Wilcox test.

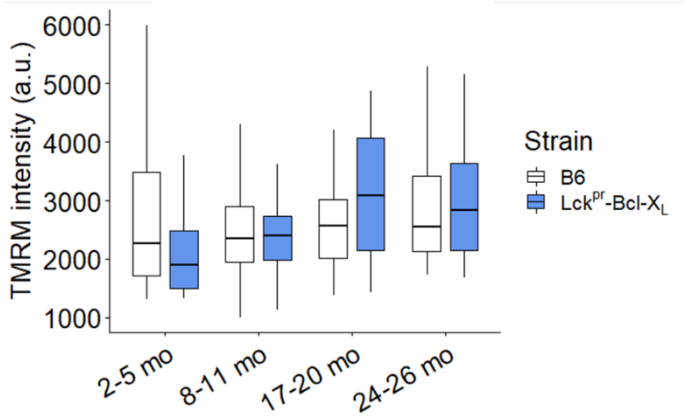

Supplementary figure 8. Mitochondrial ΔΨ in T cells from B6 and Lck^{pr}-Bcl-X$_L$ mice.
Mitochondrial membrane potential measured as tetramethylrhodamine methyl ester (TMRM) intensity in T cells from 2-5 (n=27), 8-11 (n=29), 17-20 (n=31) and 24-26 mo (n=28) B6 and Lck^{pr}-Bcl-X$_L$ mice. Data are represented as box plots and p values were calculated with the two-sample Wilcox test.

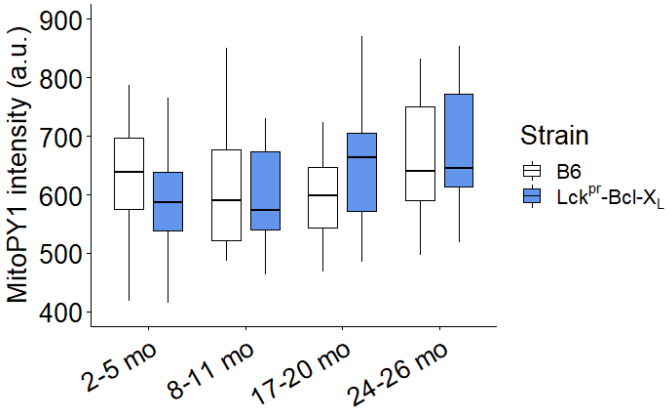

Supplementary figure 9. Mitochondrial hydrogen peroxides in T cells from B6 and Lck^{pr}-Bcl-X$_L$ mice.

Mitochondrial hydrogen peroxides (H_2O_2) measured as MitoPY1 intensity in T cells from 2-5 (n=27), 8-11 (n=29), 17-20 (n=31) and 24-26 mo (n=28) B6 and Lck^{pr}-Bcl-X$_L$ mice. Data are represented as box plots and p values were calculated with the two-sample Wilcox test.

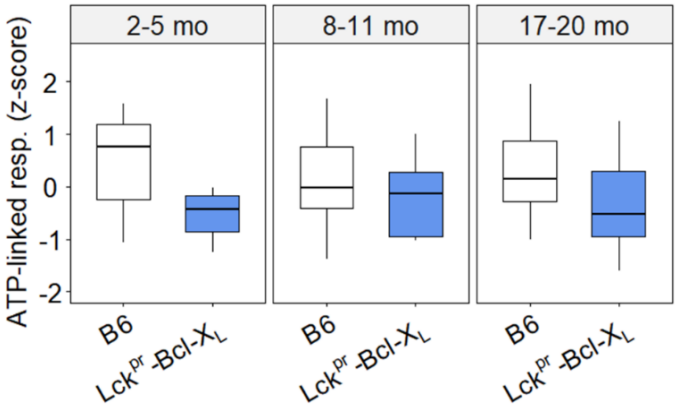

Supplementary figure 10. ATP-linked respiration in T cells from B6 and Lck^{pr}-Bcl-X$_L$ mice.

ATP-linked respiration measured by extracellular flux analyzer in T cells from 2-5 (n=15), 8-11 (n=17) and 17-20 mo (n=21) B6 and Lck^{pr}-Bcl-X$_L$ mice. Data was relativized to total protein content and normalized with the z-score. Data is represented as boxplot and p values were calculated with the Wilcox t-test.

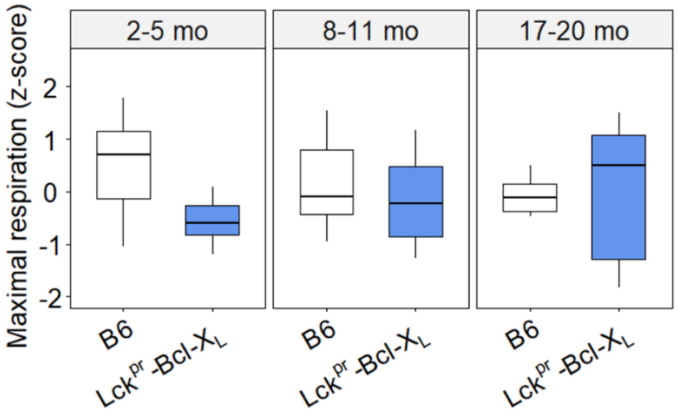

Supplementary figure 11. Maximal respiration in T cells from B6 and Lck^{pr}-Bcl-X$_L$ mice.

Maximal respiration measured by extracellular flux analyzer in T cells from 2-5 (n=15), 8-11 (n=17) and 17-20 mo (n=21) B6 and Lck^{pr}-Bcl-X$_L$ mice. Data was relativized to total protein content and normalized with the z-score. Data is represented as boxplot and p values were calculated with the Wilcox t-test.

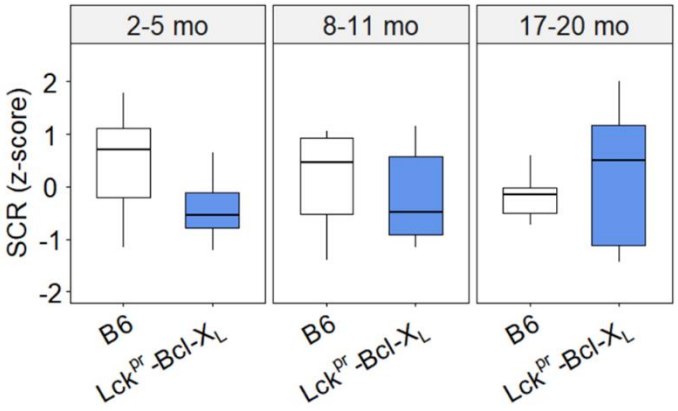

Supplementary figure 12. Spare respiratory capacity in T cells from B6 and Lck^{pr}-Bcl-X$_L$ mice.

Spare respiratory capacity (SRC) measured by extracellular flux analyzer in T cells from 2-5 (n=15), 8-11 (n=17) and 17-20 mo (n=21) B6 and Lck^{pr}-Bcl-X$_L$ mice. Data was relativized to total protein content and normalized with the z-score. Data is represented as boxplot and p values were calculated with the Wilcox t-test.